Proceedings of the 4th International Circular Packaging Conference

4 CIRCULAR PACKAGING CONFERENCE

Ljubljana and online
16th and 17th October 2025

PROCEEDINGS OF THE 4TH INTERNATIONAL CIRCULAR PACKAGING CONFERENCE

4TH CPC 2025

The Proceedings contain peer reviewed scientific, professional papers and abstracts.

Publishers

Pulp and Paper Institute, Bogišićeva 8, 1000 Ljubljana, Slovenia
Faculty of Polymer Technology, Ozare 19, Slovenj Gradec, Slovenia

For the publishers

Gregor Lavrič, PhD
Blaž Nardin, PhD

Editors

Urška Kavčič, PhD
Gregor Lavrič, PhD

Layout and design

Katja Premru

Place and date

Ljubljana, 2025

Kataložni zapis o publikaciji (CIP) pripravili v Narodni in univerzitetni knjižnici v Ljubljani
COBISS.SI-ID 252953603
ISBN 978-961-97167-0-0 (Inštitut za celulozo in papir, PDF)

PROCEEDINGS OF THE

4TH INTERNATIONAL CIRCULAR PACKAGING CONFERENCE

Ljubljana and online, 16th and 17th October 2025

ORGANIZED BY

Pulp and Paper Institute, Ljubljana, Slovenia

Faculty of Polymer Technology, Slovenj Gradec, Slovenia

SCIENTIFIC COMMITTEE

PROF. DR. MILICA BALABAN
FACULTY OF NATURAL SCIENCES AND MATHEMATICS, UNIVERSITY OF BANJA LUKA, BOSNIA AND HERZEGOVINA

PROF. DR. JÖRG FISCHER
INSTITUTE OF POLYMERIC MATERIALS AND TESTING, JOHANNES KEPLER UNIVERSITY OF LINZ, AUSTRIA

PROF. DR. NEMANJA KAŠIKOVIĆ
FACULTY OF TECHNICAL SCIENCES, UNIVERSITY OF NOVI SAD, SERBIA

DR. URŠKA KAVČIČ
PULP AND PAPER INSTITUTE, SLOVENIA

PROF. DR. VANJA KOKOL
FACULTY OF MECHANICAL ENGINEERING, UNIVERSITY OF MARIBOR, SLOVENIA

ASSIST. PROF. DR. KAJA KUPNIK
FACULTY OF POLYMER TECHNOLOGY, SLOVENIA

DR. GREGOR LAVRIČ
PULP AND PAPER INSTITUTE, SLOVENIA

PROF. DR. SANJA MAHOVIĆ POLJAČEK
FACULTY OF GRAPHIC ARTS, UNIVERSITY OF ZAGREB, CROATIA

ASSIST. PROF. DR. UROŠ NOVAK
NATIONAL INSTITUTE OF CHEMISTRY, SLOVENIA

PROF. DR. FÁTIMA POÇAS
FACULTY OF BIOTECHNOLOGY, CATHOLIC UNIVERSITY OF PORTUGAL, PORTUGAL

ASSOC. PROF. DR. IRENA PULKO
FACULTY OF POLYMER TECHNOLOGY, SLOVENIA

PROF. DR. GREGOR RADONJIČ
FACULTY OF ECONOMICS AND BUSINESS, UNIVERSITY OF MARIBOR, SLOVENIA

ASSOC. PROF. DR. URŠKA VRABIČ BRODNJAK
FACULTY OF NATURAL SCIENCES AND ENGINEERING, UNIVERSITY OF LJUBLJANA, SLOVENIA

REVIEWING COMMITTEE

DR. DAMJAN BALABANIČ, KOMUNALA NOVO MESTO D.O.O. (SI)

PROF. DR. GREGOR ČEPON, LADISK, FACULTY OF MECHANICAL ENGINEERING, UNIVERSITY OF LJUBLJANA (SI)

PROF. DR. DIANA GREGOR SVETEC, FACULTY OF NATURAL SCIENCES AND ENGINEERING, UNIVERSITY OF LJUBLJANA (SI)

DR. TEA KAPUN, PULP AND PAPER INSTITUTE (SI)

DR. IGOR KARLOVITS, DANFOSS TRATA D.O.O. (SI)

DR. URŠKA KAVČIČ, PULP AND PAPER INSTITUTE (SI)

PROF. DR. VANJA KOKOL, FACULTY OF MECHANICAL ENGINEERING, UNIVERSITY OF MARIBOR (SI)

ASSIST. PROF. DR. KAJA KUPNIK, FACULTY OF POLYMER TECHNOLOGY (SI)

DR. GREGOR LAVRIČ, PULP AND PAPER INSTITUTE (SI)

PROF. DR. SANJA MAHOVIĆ POLJAČEK, FACULTY OF GRAPHIC ARTS, UNIVERSITY OF ZAGREB (HR)

ASSIST. PROF. DR. ALEKSANDRA NESIĆ, FACULTY OF TECHNOLOGY, UNIVERSITY OF NOVI SAD (RS)

DR. ŽIGA NOSE, PAPIRNICA VEVČE D.O.O. (SI)

ASSIST. PROF. DR. UROŠ NOVAK, NATIONAL INSTITUTE OF CHEMISTRY (SI)

PROF. DR. FÁTIMA POÇAS, FACULTY OF BIOTECHNOLOGY, CATHOLIC UNIVERSITY OF PORTUGAL (PT)

PROF. DR. GREGOR RADONJIČ, FACULTY OF ECONOMICS AND BUSINESS, UNIVERSITY OF MARIBOR (SI)

DR. MIJA SEŽUN, COBIK (SI)

DR. ANDRIJANA SEVER ŠKAPIN, SLOVENIAN NATIONAL BUILDING AND CIVIL ENGINEERING INSTITUTE – ZAG (SI)

DR. ANJA VERBIČ, NATIONAL INSTITUTE OF CHEMISTRY (SI)

ASSOC. PROF. DR. URŠKA VRABIČ BRODNJAK, FACULTY OF NATURAL SCIENCES AND ENGINEERING, UNIVERSITY OF LJUBLJANA (SI)

ORGANIZED BY

FTPO
Faculty of
Polymer Technology

PULP AND PAPER
INSTITUTE, LJUBLJANA
Innovative Cellulose Products

GENERAL SPONSOR

DS Smith

SILVER SPONSORS

ECHO
INSTRUMENTS

MM

tesa®

SPONSOR

Saubermacher

TABLE OF CONTENTS

ADVANCED (BIO)-BASED FILMS

STARCH/BNC COMPOSITE FILMS ENRICHED WITH ANTHOCYANINS: SURFACE, WATER VAPOR PERMEABILITY AND COLORIMETRIC PROPERTIES

Sanja Mahović Poljaček [1], Tamara Tomašegović [1], Urška Kavčič [2], Gregor Lavrič [2], Igor Karlovits [3,4]

[1] University of Zagreb Faculty of Graphic Arts, Zagreb, Croatia
[2] Pulp and Paper Institute, Ljubljana, Slovenia
[3] Danfoss Trata d.o.o., Šentvid, Slovenia
[4] National Institute of Chemistry, Ljubljana, Slovenia

doi: 10.5281/zenodo.17293628
sanja.mahovic.poljacek@grf.unizg.hr

Abstract: *In this research, colorimetric pH indicators based on biomaterials were produced. Potato, maize and wheat starch with the addition of bacterial nanocellulose were used as polymeric matrices for the production of indicators. Bacterial nanocellulose and natural pigments, anthocyanins extracted from red cabbage leaves, were added to film-forming solutions. Anthocyanins are water-soluble color pigments that are known for their color sensitivity to different pH values. This property is of great importance for the production of pH indicators, as food spoilage is often associated with changes in the natural pH value of fresh food, which can be detected on the food surface or in the packaging atmosphere. By using pH indicators, these changes can be easily monitored and visually detected. In this study, pH indicators were produced and their surface properties, water vapour permeability, transmission density and colorimetric properties of films immersed in different pH buffers were observed. The results have shown that different starch types and different amounts of bacterial nanocellulose lead to different surface and water vapor permeability properties as well as different colorimetric responses in an atmosphere with variable pH.*

Keywords: smart packaging, colorimetric indicators, biodegradable composite films

1 INTRODUCTION

The growing demand for food safety and extended shelf life has accelerated the development of smart packaging technologies. One of the most interesting innovations in this area is the integration of chromogenic indicators, materials that change color in response to certain stimuli, into packaging systems. Chromogenic indicators serve as visual sensors that provide real-time and non-destructive information about the condition of the packaged product or its storage. Among the different types of chromogenic indicators, pH-sensitive indicators are particularly effective for monitoring the freshness of perishable foods such as fish, meat and dairy products (Brockgreitens & Abbas, 2016; Thirupathi Vasuki et al., 2023). As microbial activity increases during spoilage, it often leads to the release of basic compounds such as ammonia or amines, resulting in a measurable shift in pH. PH indicators incorporated into the packaging can visibly change color in response to these chemical changes and thus serve as freshness indicators without having to open the packaging. One promising system for this application is composite films made from starch and bacterial nanocellulose (BNC), which are

enriched with anthocyanins. Starch is a natural, biodegradable polymer with good film-forming properties, while BNC, which is produced by certain bacterial strains, has excellent mechanical strength and barrier properties. In combination, these biopolymers form a bio-based matrix that can be used to produce a pH indicator. Anthocyanins, naturally occurring pigments found in fruits such as red cabbage, blueberries and blackberries, are known for their pH-sensitive chromogenic properties. When incorporated into starch/BNC films, anthocyanins enable the production of bio-based, colorimetric indicators that can visually indicate changes in pH and therefore food spoilage. Produced indicators can change color over a wide pH range, typically from red in an acidic environment to green or yellow in an alkaline environment and are therefore very effective for monitoring food freshness.

In this research, potato, maize and wheat starch were used as polymeric matrices to produce pH indicators. Anthocyanins were extracted from red cabbage and different amounts of BNC were added to film-forming solutions. The influence of BNC on the surface properties, water vapour permeability, transmission density and colorimetric properties of films was observed.

2 MATERIALS AND METHODS

2.1 Preparation of the samples

Three types of starch were used for the production of pH indicators: potato starch (PS) (extra pure, CAS: 9005-25-8), maize starch (MS) (extra pure, CAS: 9005-25-8) and wheat starch (WS) (extra pure, CAS: 9005-25-8). Bacterial nanocellulose was prepared from the cellulose-rich biofilm formed after acetic acid fermentation of apple juice according to the previously published method (Mahović Poljaček et al., 2024). The prepared BNC was obtained in a suspension containing 2 % of the dry mass of the BNC (according to ISO 638-2:2022). The anthocyanins were extracted from red cabbage (Brassica oleracea L.). The extraction method and the calculation of the total content of monomeric anthocyanin pigments in red cabbage were carried out according to the previously published procedure (Mahović Poljaček et al., 2024).

The concentration of anthocyanins added to the film-forming solutions was 12 % (v/v) for the PS film solution, 14 % (v/v) for the MS film solution and 12 % (v/v) for the WS film solution. The films were prepared by dissolving starch in distilled water along with varying amounts of bacterial nanocellulose (BNC) (0 %, 30 % and 60 % (v/v)). This mixture was then placed on a temperature-controlled hotplate (Tehtnica, Rotamix 550 MMH, Slovenia) while stirring with a DLS Digital Overhead Stirrer (Velp Scientifica Srl, Italy). Glacial acetic acid (CAS: 64-19-7) (1 % v/v) was added to the film-forming solution under stirring at a concentration of 5 % (v/v) for PS-based films, 3 % (v/v) for MS-based films and 5 % (v/v) for WS-based films. Glycerol (purity 99.5 %, CAS: 56-81-5) was added to the potato, maize and wheat solutions at a concentration of 20 % (v/v), 15 % (v/v) and 20 % (v/v), respectively. After mixing for about 30 minutes, the film-forming solutions of a certain volume were poured into Petri dishes to obtain a constant film thickness, dried and stored for ten days in a ventilated climate chamber at 23 °C and 50 % relative humidity (RH). Depending on the type of starch used and the BNC concentration added, the films were labelled PS, MS or WS, i.e. 0BNC for films without BNC and 30BNC or 60BNC for films with different BNC concentrations.

2.2 Measurement and analysis methods

The optical density of the produced pH indicators was measured with the film transmission densitometer (Techkon Dens, TECHKON GmbH, Germany) to determine the influence of different starch types and different BNC concentrations on the film transparency. The colorimetric measurements of dried films and films immersed in different buffers were carried out with the Techkon SpectroDens (Techkon GmbH, Germany) with a D50 illuminant and a viewing angle of 2° using the M1 filter. The CIE L*a*b* values were calculated and the relative CIE L*a*b* values were displayed with paper as the white point. The results presented are the average values of ten measurements. The

contact angles of water on the prepared films were measured using a DataPhysics OCA 30 goniometer (DataPhysics Instruments GmbH, Filderstadt, Germany) using a sessile drop method with a drop volume of 1 µl. Ten measurements were taken on each film sample. Due to the rapid absorption of water on some films, the contact angles were recorded one second after contact of the water with the solid phase. It was measured to determine the wettability of pH indicators, which is important for understanding and controlling their surface properties. The calculation of water vapour transmission rate (WVTR) was determined according to the principles of ISO 2528:2018 and ASTM E96 at 23 °C and 50 % relative humidity. The gravimetric method was used and the WVTR values were calculated from the slope of weight change versus time (Song et al., 2014). This was used to evaluate the influence of the addition of BNC to the film-forming solution on the water vapor transmission rate.

3 RESULTS AND DISCUSSION

3.1 Optical properties of dry films

Figure 1 shows the results of the lightness and optical transmission density of the dry film samples. The results of the relative lightness differ depending on the type of the starch and due to the addition of BNC. It lies between 57 (measured on WS_60BNC) and 77 (measured on PS_20BNC) units. The films containing BNC generally show a slight increase in lightness values compared to the films without BNC. The reason for this is probably the BNC itself, as it is not optically transparent but has a slightly yellowish color. An exception is the WS_60BNC sample, which has the lowest lightness value, which is probably due to the uneven homogenisation process of the components. It can also be seen that the type of thickness has a minor influence on the optical transmission density of the films produced. In general, films based on potato and maize starch had a higher optical density than films based on wheat starch. It should be noted that the addition of BNC slightly increases the density of all samples, which is probably due to its own colouring (BNC has a slightly yellowish color).

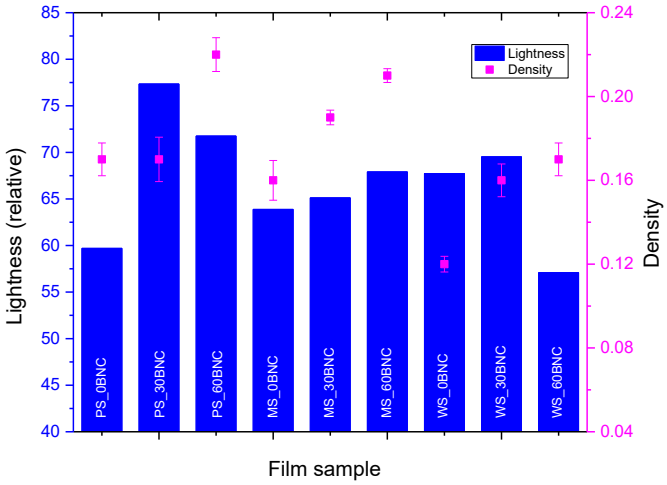

Figure 1: Optical density and lightness of the starch-based films

3.2 Contact angle of water

The water contact angle is useful for characterizing the surface properties of starch-based films with BNC by evaluating their hydrophilicity when using different starch types. Figure 2 displays the water contact angles of films made from various starches and different concentrations of BNC.

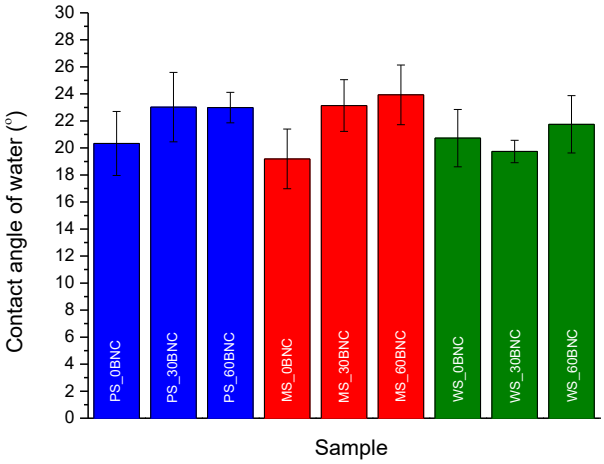

Figure 2: Contact angle of water on starch-based films with different BNC portions

The addition of BNC to the film compositions generally increased the water contact angle, with a more pronounced effect observed in films based on potato starch and maize starch. Although cellulose is made up of β-D-glucopyranose units that contribute to its hydrophilic nature, the electrostatic interactions and hydrogen bonding between BNC and starch can enhance the hydrophobicity of the surface (Lavrič et al., 2021; Bangar & Whiteside, 2021). The slightly different effects of BNC addition on the water contact angle of films made from wheat starch may be attributed to structural differences compared to maize starch and potato starch, such as the size of the starch molecules and the amylose content (Żołek-Tryznowska & Kałuża, 2021).

3.3 Water vapour transmission rate

The WVTR values of the starch-based films without and with the addition of BNC are listed in Table 1. The WVTR test was carried out at 23 °C and 50 % RH. For potato-based films, it was not possible to measure the WVTR as the samples were too fragile, so this test was not performed. The results showed that wheat starch-based films had higher total WVTR than maize starch-based films. The measured WVTR values were 23.84 and 20.88 g m^{-2} h^{-1} for samples without BNC, maize and wheat, respectively. In both cases, the addition of BNC resulted in a small increase in WVTR, indicating a negative effect on water vapour permeability. Although it was expected that the addition of BNC would decrease WVTR, it appears that BNC causes an increase in WVTR. According to Gitari et al. (2019), a high BNC content in nanocomposite films could be the reason for the decrease in WVTR. BNC consists of a network of fibres that make it porous and have a large surface area. With a high BNC content in the starch-based films, the fibres begin to form agglomerations (Sardjono et al., 2025; Zong et al., 2014), which can promote the transport of water vapour through the produced films. It can be said that a lower amount of BNC should be further tested in order to obtain a lower WVTR property, as a high fibre content can deteriorate the barrier properties.

Table 1: Water vapor transmission rate (WVTR)

WVTR ***(g m^{-2} h^{-1})***	***MS_0BNC***	***MS_60BNC***	***WS_0BNC***	***WS_60BNC***
	23.84	*27.01*	*20.88*	*21.80*

3.4 Colorimetric analysis

Figures 3.a-3.c present the changes in CIE a* and b* values of the produced films. To highlight and compare the trends in CIE a*/b* shifts across different pH environments, a B-spline trendline was added to the plots.

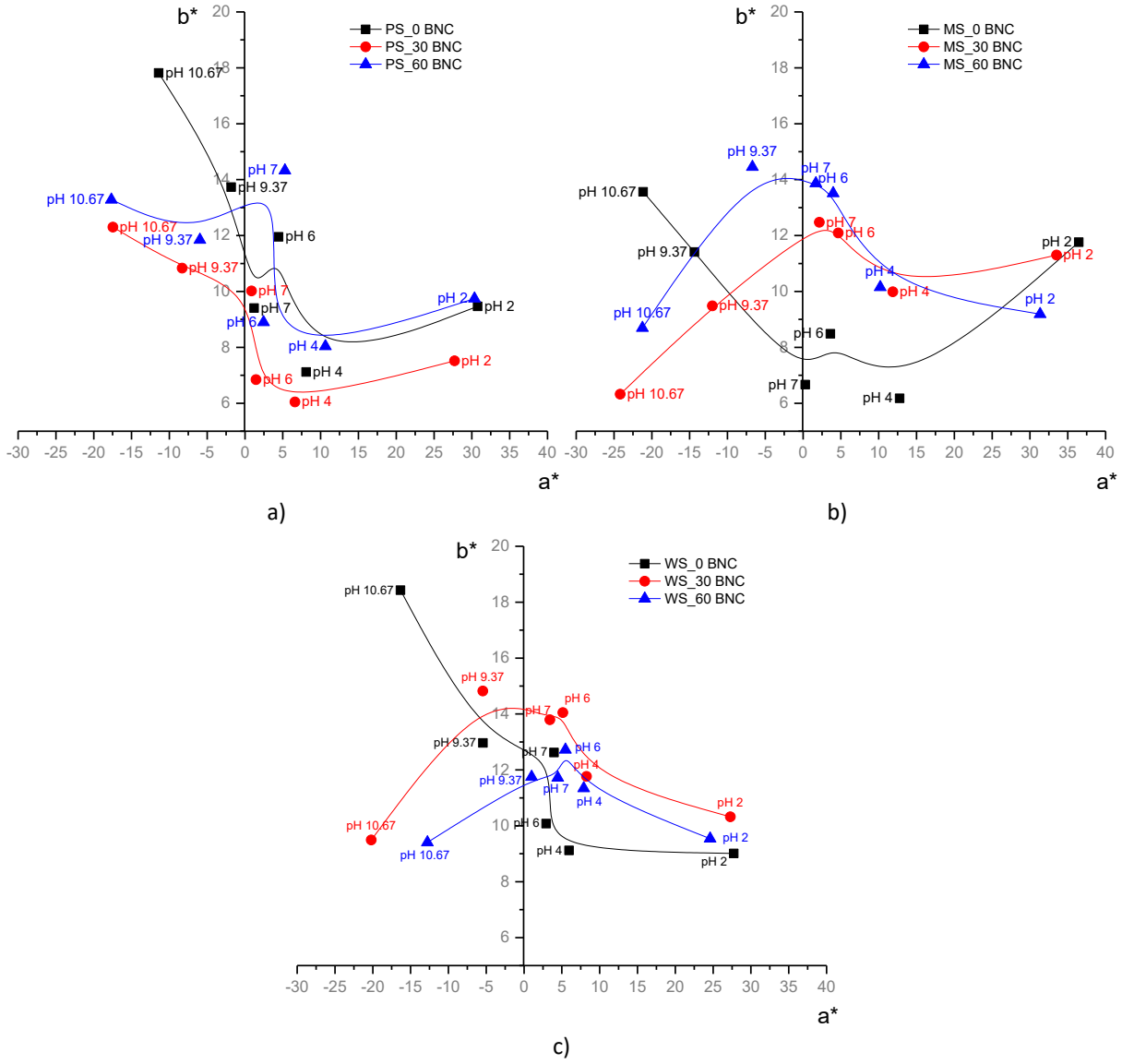

Figure 3: CIE a/b* diagrams for films at different pH values: a) PS-based, b) MS-based, c) WS-based*

The pH-dependent variations in a* and b* values of the films were influenced by both the type of starch used and the concentration of BNC. The trendlines for the CIE a*/b* data points for potato and wheat starch showed a noticeable shift towards +b* values as the concentration of BNC increased in mildly acidic, neutral, and mildly basic environments. This shift can be attributed to the hue of the BNC used and its interaction with anthocyanins, affecting their structural changes. As the pH changed, the color of the films transitioned from pink hues at acidic pH to nearly colourless hues at neutral pH, and finally to green-yellow hues at alkaline pH. While the addition of BNC did not significantly impact the +a*/-a* color shift, the type of starch did have a notable effect. Films based on maize starch exhibited the widest range of a* values when immersed in buffers with varying pH levels, whereas films based on wheat starch showed the narrowest range on the a* axis. This suggests that the type of starch affects the degree of color change in the films. Furthermore, the changes in a*/b* plots indicate that BNC can stabilize anthocyanins when exposed to different pH levels, which is consistent with previous research (Mahović Poljaček et al., 2024). BNC creates a network that protects anthocyanins from their breakdown, which is visible in the lower b* value (i.e., yellow hues) at highly alkaline pH for the samples with BNC, pointing to the decreased presence of the chalcone structure (Ohno et al., 2021). However, the type of starch used can influence the colorimetric changes observed in the films when they are exposed to varying pH environments. Therefore, careful selection of the starch for film production is

essential to optimize both the functional properties (such as barrier and mechanical properties) and the colorimetric response of the produced films.

4 CONCLUSIONS

In this study, pH-sensitive starch-based films containing bacterial nanocellulose (BNC) and anthocyanins from red cabbage were used to observe their potential for the production of pH indicators. Potato, maize and wheat starch were used as polymeric matrices. Different amounts of BNC were added to the film-forming solutions to observe their influence on the surface properties, water vapour permeability, transmission density and colorimetric properties of the produced films. The results showed that the interactions between the main components of the films and the resulting property changes were significantly influenced by the BNC concentration and the type of starch. It was found that films containing BNC generally showed a slight increase in lightness values compared to the films without BNC and a slight decrease in transmission density. The addition of BNC to the film compositions generally increased the water contact angle, with a stronger effect observed in films based on potato and maize starch based films. The results showed that wheat starch-based films had an overall higher WVTR than maize starch-based films and that the high BNC content in the nanocomposite films could cause the decrease in the WVTR property. The results of the colorimetric measurement showed that maize starch-based films exhibited the widest range of changes in the red and green color directions when immersed in buffers with different pH values, while wheat starch-based films exhibited the narrowest range within the same color range. This indicates that the type of starch has a significant influence on the extent of color change in the films.

The results obtained in this study show that the addition of a small amount of BNC to starch-based films, particularly when MS and WS films are involved, provides a potentially significant advantage for the production of pH indicators for smart packaging applications.

5 REFERENCES

Bangar, S.P. & Whiteside, W.S. (2021) Nano-cellulose reinforced starch bio composite films- A review on green composites. International Journal of Biological Macromolecules. [Online] 185, 849–860. Available from: doi:10.1016/J.IJBIOMAC.2021.07.017.

Brockgreitens, J., Abbas, A. (2016) Responsive Food Packaging: Recent Progress and Technological Prospects. Compr. Rev. Food Sci. Food. Saf. [Online], 15, 3–15. Available from: https://doi.org/10.1111/1541-4337.12174

Gitari, B., Chang, B. P., Misra, M., Navabi, A., and Mohanty, A. K. (2019) A comparative study on the mechanical, thermal, and water barrier properties of PLA nanocomposite films prepared with bacterial nanocellulose and cellulose nanofibrils. BioRes. [Online] 14 (1), 1867-1889. Available from: 10.15376/biores.14.1.1867-1889

Lavrič, G., Oberlintner, A., Filipova, I., Novak, U., et al. (2021) Functional nanocellulose, alginate and chitosan nanocomposites designed as active film packaging materials. Polymers. [Online] 13 (15), 2523. Available from: doi:10.3390/POLYM13152523/S1

Mahović Poljaček, S., Tomašegović, T., Strižić Jakovljević, M., Jamnicki Hanzer, S., et al. (2024) Starch-Based Functional Films Enhanced with Bacterial Nanocellulose for Smart Packaging: Physicochemical Properties, pH Sensitivity and Colorimetric Response. Polymers. [Online] Vol. 16, Page 2259. [Online] 16 (16), 2259. Available from: doi:10.3390/POLYM16162259

Ohno, S., Yokota, M., Yamada, H., Tatsuzawa, F., et al. (2021) Identification of Chalcones and their Contribution to Yellow Coloration in Dahlia (Dahlia variabilis) Ray Florets. The Horticulture Journal. [Online] 90 (4), 450–459. Available from: doi:10.2503/HORTJ.UTD-305.

Susanto Arif Sardjono, Heru Suryanto, Aminnudin, Muhamad Muhajir (2019) Crystallinity and morphology of the bacterial nanocellulose membrane extracted from pineapple peel waste using high-pressure homogenizer. AIP Conf. Proc. 3 July 2019; 2120 (1): 080015. Available from: https://doi.org/10.1063/1.5115753

Song, Z., Xiao, H., & Zhao, Y. (2014) Hydrophobic-Modified Nano-Cellulose Fiber/PLA Biodegradable Composites for lowering Water Vapour Transmission Rate (WVTR) of Paper. Carbohydrate Polymers. [Online] 111, 442-448. Available from: http://dx.doi.org/10.1016/j.carbpol.2014.04.049

Thirupathi Vasuki, M., Kadirvel, V., Pejavara Narayana, G. (2023) Smart packaging - An overview of concepts and applications in various food industries. Food Bioeng. [Online] 2, 25-41. Available from: https://doi.org/10.1002/fbe2.12038

Żołek-Tryznowska, Z. & Kałuża, A. (2021) The Influence of Starch Origin on the Properties of Starch Films: Packaging Performance. Materials 2021, Vol. 14, Page 1146. [Online] 14 (5), 1146. Available from: doi:10.3390/MA14051146

MANGO PEEL-DERIVED PECTIN FILMS FOR SUSTAINABLE ANTIBACTERIAL PACKAGING APPLICATIONS

Patricija Skrivarnik, Kaja Kupnik

Faculty of Polymer Technology, Ozare 19, 2380 Slovenj Gradec, Slovenia

doi: 10.5281/zenodo.17293718
patricija.skrivarnik@ftpo.eu

Abstract: *The increasing demand for sustainable packaging solutions has driven research toward biodegradable materials derived from agricultural waste. This study explores the valorization of mango peels, a prevalent fruit processing by-product, through a dual-extraction methodology to recover bioactive compounds and pectin. The optimized extraction protocols enabled the efficient isolation of pectin from the residual biomass, enhancing the economic and environmental value of the original feedstock. Biopolymer films were fabricated via solution casting using isolated pectin and bioactive extracts from mango peels, resulting in uniform, biodegradable materials suitable for scalable production. Structural and thermal characterizations using FTIR spectroscopy and thermogravimetric analysis (TGA) confirmed the successful incorporation of functional bioactive compounds within the film matrix. Notably, the mango peel extracts and the resulting pectin films exhibited strong antibacterial activity against selected bacteria, as demonstrated by agar diffusion assays. When applied to fresh produce, the films effectively inhibited microbial growth and extended shelf life, demonstrating direct functional benefits beyond material sustainability. These results underscore a promising circular economy strategy, in which fruit processing waste is transformed into high-value packaging materials with built-in antimicrobial functionality. By leveraging the intrinsic bioactivity of mango peel-derived compounds, the developed films offer a biodegradable packaging solution that actively contributes to food preservation. This integrated approach addresses both environmental and food safety challenges, reinforcing the potential of agricultural waste valorization in advancing sustainable packaging technologies.*

Keywords: antibacterial activity, extraction, food waste valorization, mango peel, pectin, sustainable packaging

1 INTRODUCTION

The environmental impact of non-biodegradable plastic waste has intensified global efforts to seek sustainable alternatives, with global plastic consumption for packaging expected to nearly triple by 2060 (Stoica et al., 2024). Consequently, biopolymers have attracted significant attention as food packaging materials owing to their advantageous properties including non-toxicity, renewable sourcing, biocompatibility, and biodegradability (Dirpan et al., 2023). Agricultural waste offers promising feedstocks for developing biopolymer-based packaging materials (Khanashyam et al., 2023).

Mango (Mangifera indica L.), being one of the most cultivated tropical fruits worldwide, generates substantial quantities of processing waste, with peels constituting approximately 7-24% of the total fruit weight (García-Mahecha et al., 2023). These peels are rich in pectin, a naturally occurring polysaccharide with excellent film-forming properties, as well as bioactive compounds including

phenolic acids, flavonoids, and antioxidants that remain largely underutilized in conventional waste management practices (Chaiwarit et al., 2020; García-Mahecha et al., 2023).

Pectin-based films have gained great attention as sustainable packaging materials due to their biodegradability, biocompatibility, and barrier properties. However, the mechanical and functional limitations of pure pectin films often restrict their practical applications (Singaram et al., 2024). The incorporation of bioactive compounds derived from the same raw material source presents an innovative approach to enhance film functionality while maintaining the principles of circular economy and waste valorization. Additionally, the integration of plant-derived antimicrobial agents into biopolymer matrices addresses critical food safety concerns while extending product shelf-life through active packaging mechanisms.

The outcomes of this research contribute to the advancement of sustainable packaging technologies by demonstrating the feasibility of transforming agricultural waste into functional packaging materials with enhanced preservation properties, supporting both environmental sustainability and food security objectives.

2 MATERIALS AND METHODS

2.1 Sample preparation

Bioactive extracts were obtained from mango peels using Soxhlet extraction. Dried mango peels (15 g) were placed in a cellulose thimble and extracted with 150 mL of ethanol under reflux for 5 h until the condensate became colorless. The solvent was removed under reduced pressure using a rotary evaporator (Heidolph Laborota 4000 efficient, Schwabach, Germany). Mango ethanol extracts (MEE) were stored at -20°C until further use.

Pectin extraction from mango peels was performed using an acid-catalyzed process. The dried and crushed peels were extracted in acidified water (pH 1.5–2.0, citric acid) at 80–90 °C, then filtered. Pectin was precipitated from the filtrate by ethanol addition, washed with ethanol, and dried to constant weight.

For mango pectin film (MPF), dry pectin (2 g) was dissolved in deionized water at 80 °C. Glycerol (2 mL) was added, followed by dropwise addition of 0.2 M calcium chloride ($CaCl_2$) solution under continuous stirring until gel formation occurred. The gel was cast into petri dishes and dried at 50 °C for 24 h to obtain the final film. For MPF enriched with MEE (MPF_MEE), the procedure was identical with the addition of 10% w/w MEE during the dissolution step.

2.2 Characterization

Fourier transform infrared spectroscopy (FT-IR) spectra were recorded using a Spectrum 65 (Perkin Elmer, Waltham, MA, USA) in attenuated total reflection (ATR) mode, with 4 cm^{-1} resolution over the range 4000–600 cm^{-1}, averaging 16 scans.

Termogravimetric analysis (TGA) was performed using a TGA/DSC 3+ (Mettler Toledo, Greifensee, Switzerland). Samples were heated from 25 to 550 °C at a heating rate of 10 K/min under N2 atmosphere (20 mL/min), followed by a 10-minute isothermal hold under O2 atmosphere (20 mL/min).

Mechanical properties were evaluated using a universal testing machine (Shimadzu, AG-X plus 10 kN) according to ISO 527-1 standard. Tensile testing was performed with a gauge length of 50 mm, a preload of 0.03 N, and variable testing speeds (10 mm/min until 0.05% strain, then 100 mm/min until failure).

Optical microscopy was performed on MPF and MPF_MEE using a Keyence VHX-7000 digital microscope at 150x magnification.

The antibacterial activity of MPF_MEE films was evaluated qualitatively against Gram-negative (Escherichia coli) and Gram-positive (Staphylococcus aureus) bacteria using the agar diffusion method. Briefly, agar plates were inoculated with prepared bacterial solution (1–5 × 10^6 CFU/mL), MEE and MPF_MEE were placed directly on the inoculated agar plates and incubated for 24 h at 37 ± 1 °C.

Furthermore, fresh strawberries of uniform size and ripeness were selected for shelf-life evaluation. The first group of strawberries was wrapped in MPF, the second group was wrapped in MPF_MEE, and the third group was left unwrapped as a control. All samples were stored at ambient conditions (25 ± 3 °C, ambient humidity) and monitored for 14 days. Daily visual assessment evaluated surface appearance, decay progression, and overall preservation quality.

3 RESULTS AND DISCUSSION

The FTIR spectrum (Figure 1) of MP shows characteristic polysaccharide absorption bands, including O–H stretching at 3400 cm^{-1} (hydroxyl groups and hydrogen bonds), C–H stretching at 2920 cm^{-1} (aliphatic bonds), C=O stretching at 1730-1600 cm^{-1} (carbonyl groups in esters and carboxylates), and C-O-C vibrations at 1200-1000 cm^{-1} (glycosidic bonds). The MPF spectrum shows preserved polysaccharide bands with enhanced intensity at 3400 cm^{-1} due to glycerol and water interactions. The band at 1600 cm^{-1} exhibits slight shifts attributed to Ca^{2+}-carboxylate crosslinking, confirming network formation. For MPF_MEE, minimal spectral changes occur in the 1700-1500 and 1200-1000 cm^{-1} regions, attributed to phenolic compounds, flavonoids, and other bioactive components containing carbonyl, aromatic C=C, and C–O functional groups. However, due to the low extract concentration (10% w/w), spectral changes are subtle, with higher concentrations expected to produce more distinct absorption band modifications (Demir et al., 2021).

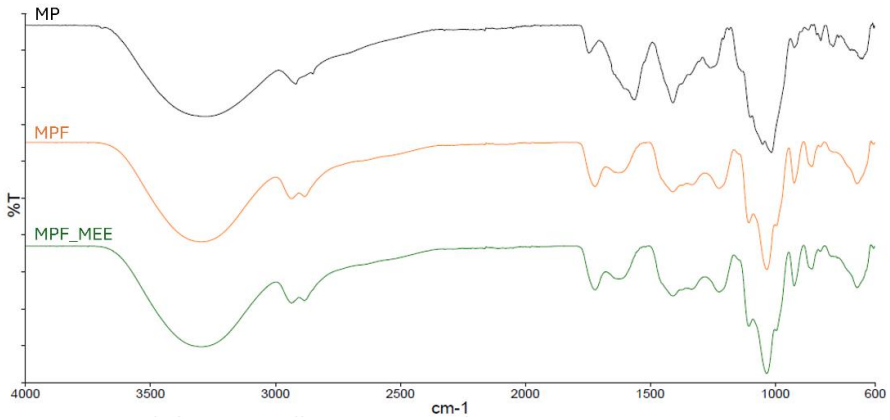

Figure 1: Comparative FTIR spectra of MP, MPF, MPF_MEE

To further evaluate the thermal stability and degradation behaviour of synthesised MP-derived pectin films, TGA was conducted. TGA profile (Figure 2) demonstrated a multistage thermal decomposition. Initial mass loss occurred at 67 °C (2.1 % mass loss) corresponding to desorption of free or weakly bound water.

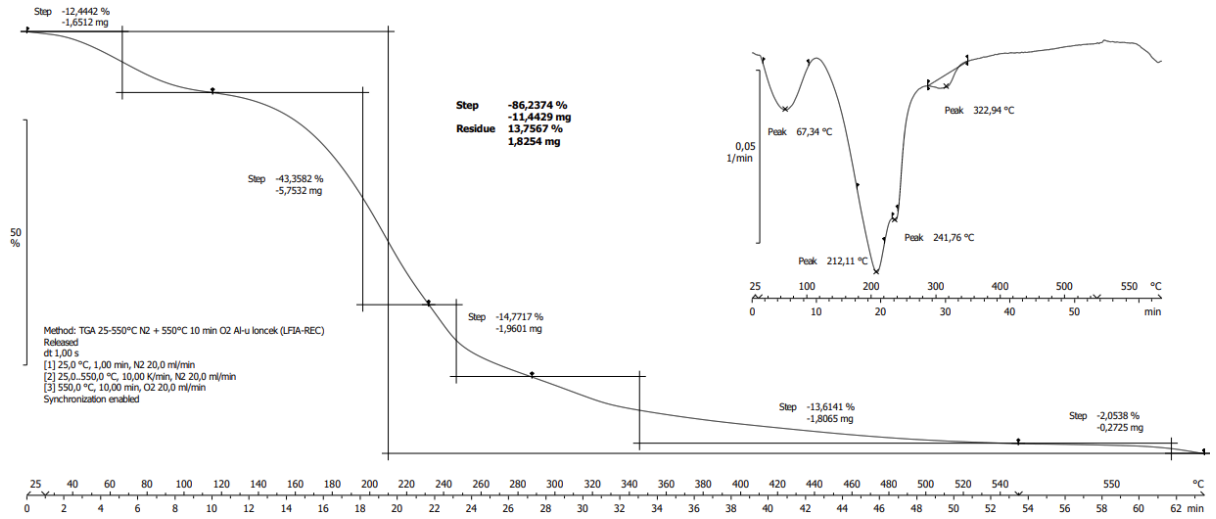

Figure 2: Thermal degradation profile of the MPF obtained by TGA

Primary decomposition of the polysaccharide chain initiated at 212-242 °C through dehydration and decarboxylation reactions. The main decomposition occurred at 323 °C with the highest mass loss (43.4%), attributed to complete polymer chain breakdown. Heating to 550 °C under nitrogen resulted in an additional 12.4% mass loss, while subsequent oxidative treatment yielded a total mass loss of 86.2%, leaving 13.8% inorganic residue. The results indicate thermal stability up to approximately 200 °C, beyond which rapid degradation occurs. The relatively high ash content (13.8%) suggests significant mineral content, likely from inherent pectin constituents or processing residues, which could potentially be reduced through enhanced purification procedures or modified film preparation methods.

Beyond thermal stability, the mechanical properties of the films are crucial for packaging applications. The stress-strain curve (Figure 3) demonstrates the typical behavior of a flexible, low-strength material characteristic of MPF. Low Young's modulus (0.38 ± 0.3 MPa) indicates high flexibility and easy deformation, while tensile strength (0.19 ± 0.03 MPa) reflects limited load-bearing capacity. However, the films exhibit exceptional elongation at break (29.4 ± 2.2%), exceeding values reported for comparable biopolymer films in the literature (Pereira et al., 2021; Syarifuddin et al., 2025). The combination of low stiffness and strength with high extensibility suggests potential applications requiring flexibility and deformability rather than structural rigidity. The mechanical behavior is influenced by film thickness (0.35 ± 0.05 mm), which contributes to the overall performance characteristics. These properties position the material favorably for packaging applications where conformability and stretch capacity are prioritized over mechanical strength.

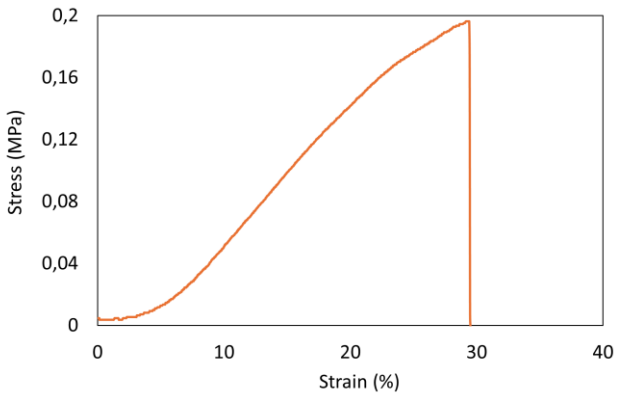

Figure 3: Stress-strain curve of MPF

The mechanical behavior observed was further investigated through surface morphological analysis. Optical microscopy analysis (Figure 4) reveals differences in surface morphology between the film samples. The MPF film exhibits a relatively homogeneous surface with smooth topography, indicating uniform pectin matrix formation. In contrast, the MPF_MEE film displays increased surface roughness and heterogeneous microstructure. The incorporation of MEE (10% w/w) altered the pectin matrix organization, resulting in morphological changes that reflect the interaction between bioactive compounds and the polymer network.

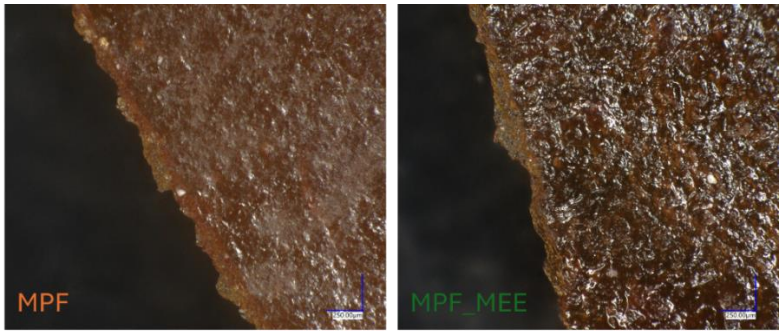

Figure 4: Optical micrographs (150× magnification) of MPF (left) and MPF_MEE (right)

In addition to structural characterization, the functional properties of the films were assessed, particularly their antibacterial activity. The agar diffusion assay (Figure 5) demonstrates the antibacterial efficacy of MEE and MPF_MEE against selected bacteria. Clear inhibition zones are observed around both MEE and MPF_MEE samples when tested against E. coli and S. aureus. The MPF_MEE films exhibit notable inhibition zones, indicating antibacterial activity attributed to the incorporated bioactive compounds from mango peel ethanol extract. The phenolic compounds, flavonoids, and other bioactive substances present in the extract contribute to the antibacterial properties through mechanisms such as cell membrane disruption and enzyme inhibition (Liu et al., 2025). The results demonstrate effectiveness against both Gram-negative and Gram-positive bacterial strains, highlighting the broad-spectrum antibacterial potential of the bioactive compounds, which supports the application of bioactive extract-enriched films in food packaging, where microbial growth inhibition is crucial for food safety and extension of shelf-life.

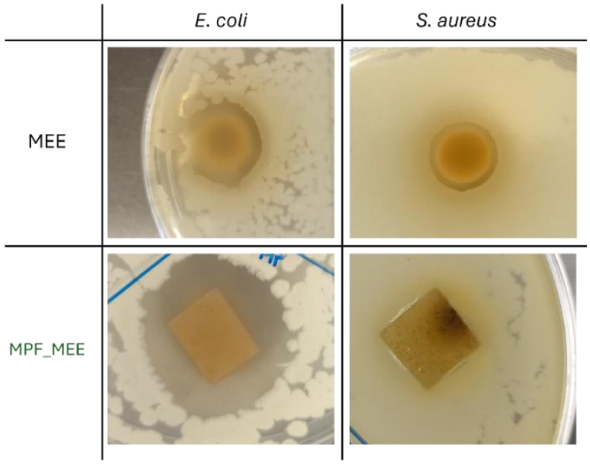

Figure 5: Inhibition zones of MEE and MPF_MEE against E. coli and S. aureus

Furthermore, to validate the practical application potential, the films were evaluated for their effectiveness in food preservation. Figure 6 demonstrates the preservation efficacy of different pectin films on strawberry quality over 14 days at ambient temperature.

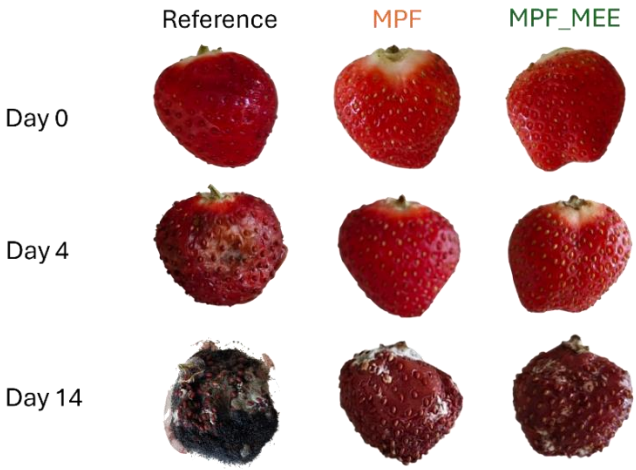

Figure 6: Visual assessment of strawberry preservation showing reference (unwrapped), MPF, and MPF_MEE treatments over 14 days of storage at ambient conditions (25 °C)

The unwrapped control strawberry exhibited rapid deterioration, showing visible decay after 4 days with extensive mold growth and complete degradation by day 14. Strawberries wrapped in MPF films displayed delayed spoilage compared to the control, though signs of decay including color changes, surface wrinkling, and mold development were evident after 14 days. The MPF_MEE films provided superior preservation performance, with wrapped strawberries maintaining better color retention, structural integrity, and significantly reduced mold growth throughout the storage period. The enhanced protective effect demonstrates that incorporation of bioactive compounds from MEE improves the antimicrobial and antioxidant properties of the pectin matrix, effectively extending fruit shelf-life. These results indicate the potential of bioactive extract-enriched pectin films as sustainable packaging materials for perishable produce preservation.

4 CONCLUSIONS

Mango peel-derived pectin films were successfully prepared and characterized, demonstrating suitable properties for food packaging applications. The films demonstrated thermal stability up to 200 °C, high flexibility (29.4% elongation), and high antibacterial activity against both Gram-positive and Gram-negative bacteria. Shelf-life evaluation showed superior preservation of strawberries wrapped in bioactive-enriched films compared to controls over 14 days. These results indicate that synthesized films represent a promising sustainable packaging solution for extending the shelf-life of perishable produce through combined barrier and antibacterial properties.

5 REFERENCES

Chaiwarit, T., Masavang, S., Mahe, J., Sommano, S., Ruksiriwanich, W., Brachais, C. H., Chambin, O., & Jantrawut, P. (2020). Mango (cv. Nam Dokmai) peel as a source of pectin and its potential use as a film-forming polymer. Food Hydrocolloids, 102, 105611.

Demir, D., Ceylan, S., Göktürk, D., & Bölgen, N. (2021). Extraction of pectin from albedo of lemon peels for preparation of tissue engineering scaffolds. Polymer Bulletin, 78(4), 2211–2226.

Dirpan, A., Ainani, A. F., & Djalal, M. (2023). A Review on Biopolymer-Based Biodegradable Film for Food Packaging: Trends over the Last Decade and Future Research. Polymers 2023, Vol. 15, Page 2781, 15(13), 2781.

García-Mahecha, M., Soto-Valdez, H., Carvajal-Millan, E., Madera-Santana, T. J., Lomelí-Ramírez, M. G., & Colín-Chávez, C. (2023). Bioactive Compounds in Extracts from the Agro-Industrial Waste of Mango. Molecules 2023, Vol. 28, Page 458, 28(1), 458.

Khanashyam, A. P. , Mundanat, A. P. , Mundanat, A. S., Shah, K., Babu, K. S., Thorakkattu, P., Al-Asmari, F., Pandiselvam, R., Prakash Nirmal, N., Khanashyam, A. C., Mundanat, A. S., Shah, K., Sajith Babu, K., Thorakkattu, P., Al-Asmari, F., & Pandiselvam, R. (2023). Valorization of Fruit Waste for Bioactive Compounds and Their Applications in the Food Industry. Foods 2023, Vol. 12, Page 556, 12(3), 556.

Liu, Y., Zhu, J., Liu, Z., Zhi, Y., Mei, C., & Wang, H. (2025). Flavonoids as Promising Natural Compounds for Combating Bacterial Infections. International Journal of Molecular Sciences 2025, Vol. 26, Page 2455, 26(6), 2455.

Pereira, D. G. M., Vieira, J. M., Vicente, A. A., & Cruz, R. M. S. (2021). Development and Characterization of Pectin Films with Salicornia ramosissima: Biodegradation in Soil and Seawater. Polymers, 13(16), 2632.

Singaram, A. J. V., Guruchandran, S., & Ganesan, N. D. (2024). Review on functionalized pectin films for active food packaging. Packaging Technology and Science, 37(4), 237–262.

Stoica, M., Bichescu, C. I., Crețu, C. M., Dragomir, M., Ivan, A. S., Podaru, G. M., Stoica, D., & Stuparu-Crețu, M. (2024). Review of Bio-Based Biodegradable Polymers: Smart Solutions for Sustainable Food Packaging. Foods 2024, Vol. 13, Page 3027, 13(19), 3027.

Syarifuddin, A., Muflih, M. H., Izzah, N., Fadillah, U., Ainani, A. F., & Dirpan, A. (2025). Pectin-based edible films and coatings: From extraction to application on food packaging towards circular economy-A review. Carbohydrate Polymer Technologies and Applications, 9, 100680.

CLOSING THE LOOP: SUSTAINABLE COMPOSITE MATERIALS FROM POST-CONSUMER AGRICULTURAL FILMS AS A REPLACEMENT FOR CONVENTIONAL RAW MATERIALS

Silvester Bolka, Marko Verčkovnik, Sebastjan Zaverla, Rajko Bobovnik, Blaž Nardin

Faculty of Polymer Technology, Slovenj Gradec, Slovenia

doi: 10.5281/zenodo.17294083
silvester.bolka@ftpo.eu

Abstract: *The depletion of natural resources and growing environmental concerns have intensified the search for sustainable material solutions. Agricultural waste, traditionally landfilled or incinerated, presents a major opportunity for recycling within circular economies. Recent advancements show that such waste can be transformed into valuable secondary raw materials, reducing reliance on virgin resources and minimizing ecological harm. A particularly promising approach combines waste agricultural polyethylene (PE) films with natural fibers like corn husks to create high-performance composite materials. This method not only diverts waste from landfills but also enhances the mechanical and thermal properties of recycled plastics. Mechanical recycling has emerged as a viable solution for processing these materials, offering a cost-effective and eco-friendly alternative to conventional disposal methods. This study examines the challenges of mechanically recycling waste PE films and corn husks while proposing optimization strategies. The research demonstrates that corn husk content significantly influences composite performance—higher fiber proportions improve stiffness but may reduce ductility. Key processing techniques, including thermoplastic compounding and injection molding, enable efficient material production while supporting localized circular value chains. The resulting composites exhibit balanced strength, thermal stability, and sustainability, making them suitable for applications in packaging, automotive components, and construction. By closing the loop on agricultural waste, this approach reduces pollution and creates new economic opportunities for farming communities. In conclusion, mechanical recycling of PE-corn husk composites offers a scalable pathway toward resource efficiency. The findings contribute to broader efforts in sustainable material development, aligning with global environmental goals. Further research could refine processing methods and expand applications, reinforcing the role of agricultural waste in the circular economy.*

Keywords: PE films, corn husk, compatibilizer, recycling, mechanical recycling.

1 INTRODUCTION

The growing use of agricultural plastics—such as silage films, mulch sheets, and bale wraps—has led to significant environmental concerns due to their low recycling rates and persistence in ecosystems. Globally, only 30–40% of agricultural plastic waste is collected for recycling, while the rest is either incinerated, landfilled, or left to degrade in soils, contributing to microplastic pollution (European Commission, 2021; UNEP, 2023). In Europe alone, over 2 million tonnes of agricultural plastics are consumed annually, with films accounting for a substantial portion (Plastics Europe, 2022). Given their contamination with soil, organic residues, and UV degradation, conventional mechanical

recycling methods often yield low-quality materials, limiting their economic viability (Picuno et al., 2020).

To address these challenges, upcycling agricultural plastic waste into value-added thermoplastic composites presents a promising circular economy solution. Thermoplastic composites, reinforced with natural fibers or mineral fillers, have gained attention for their lightweight, durable, and reprocessable properties, making them suitable for construction, automotive, and packaging applications (La Mantia & Morreale, 2011; Faruk et al., 2014). Recent studies demonstrate that post-consumer polyolefins (e.g., LDPE from agricultural films) can be effectively blended with reinforcing agents (e.g., wood flour, talc, or recycled fibers) to enhance mechanical properties while maintaining recyclability (Bahlouli et al., 2022). For instance, Azizi et al. (2020) showed that incorporating 30% wheat straw fibers into recycled LDPE improved stiffness by 50%, offering a viable pathway for waste valorization.

However, critical barriers remain in the development of agricultural plastic waste-based composites, primarily due to material heterogeneity, as degraded agricultural films exhibit significant variations in polymer composition and contamination levels, necessitating robust pre-processing steps to ensure consistent feedstock quality (Garcia & Robertson, 2017). Another major challenge lies in achieving adequate fiber-matrix compatibility, since poor interfacial adhesion between natural fibers and recycled plastics frequently requires the use of compatibilizers such as maleic anhydride-grafted polyolefins to enhance mechanical performance (Srebrenkoska et al., 2014). Furthermore, while laboratory-scale studies have demonstrated the technical feasibility of such composites, there remains a significant gap in industrial scalability, with most research failing to address practical considerations like large-scale processing, cost-effectiveness, and long-term durability under real-world conditions (George et al., 2021). These limitations collectively hinder the widespread adoption of agricultural plastic waste in high-value composite applications, underscoring the need for integrated solutions that address both material and processing challenges.

This study addresses the challenge by developing a prototype to upcycle agricultural plastics waste films into thermoplastic composites.

2 MATERIALS AND METHODS

2.1 Sample

The agricultural plastics waste film (rPE) was provided by farms from Slovenia. The corn husk (CH) was provided by Žipo d.o.o., Slovenia. Commercially available PE-HD–g-MA (C) with the trade name Exxelor PE 1040 was purchased from Exxon Mobil, Italy. Commercially available antioxidant (A) with the trade name AT10 was purchased from Amik Italia S.p.A., Italy. The composition of the samples is listed in Table 1.

Table 1: Composition of the samples of the third series and number of comounding cycles

Sample	***rPE (wt.%)***	***C (wt.%)***	***A (wt.%)***	***CH (wt.%)***
rPE	*99.6*	*0*	*0*	*0*
rPE CA	*94.6*	*5*	*0.4*	*0*
rPE CA CH10	*84.6*	*5*	*0.4*	*10*
rPE CA CH20	*74.6*	*5*	*0.4*	*20*
rPE CA CH30	*64.6*	*5*	*0.4*	*30*

2.2 Compounding

For the compounding, the materials were mixed separately and extruded on the Labtech LTE 20-44 twin screw extruder. The screw diameter was 20 mm, the L/D ratio was 44:1 and the screw speed was 600 rpm. The temperature profile for the samples increased from the hopper (155 °C) to the die (190 °C). Vacuum extraction was performed during reactive extrusion to remove the volatile gaseous products of reactive extrusion. The vacuum was set to 50 mbar. After compounding, the two produced filaments with a diameter of 3 mm were cooled in a water bath and formed into pellets with a length of about 5 mm and a diameter of 3 mm.

2.3 Injection moulding

The injection moulding was carried out on a Krauss Maffei 50-180 CX injection moulding machine with a screw diameter of 30 mm and a clamping force of 500 kN. The cold runner mould was used to produce the samples. The mould had two cavities, one with a dumbbell-shaped mould of type 1BA (ISO 527-1), the second with a cuboid-shaped mould (ISO 178/ ISO 179). The temperature was increased from the hopper (175 °C) to the die (190 °C), the injection speed was set to 50 mm/min and the mould temperature to 25 °C, and the cooling time was set to 10 s. During plasticising, the back pressure was set to 15 bar and the screw speed to 60 rpm. The low screw speed was used to prevent thermal degradation of the corn husk and to minimise shear during processing due to the higher processing temperature.

2.4 Methods for characteriaztion of the samples

The tensile tests were carried out with the Shimadzu AG -X plus according to ISO 527-1. Five measurements were taken for each sample. In the tensile tests, tensile stiffness (E_t), tensile strength (σ_m) and elongation at break (ε_{tb}) were determined. Bending tests were conducted according to ISO 178 on the Shimadzu AG-X plus equipped with a load cell of maximum 10 kN, at a crosshead speed of 2 mm/min and span width of 64 mm. Five replicates for each sample were tested. Samples were 10 mm wide and 4 mm thick. During bending, the bending stiffness (E_f), the bending strength (σ_{fM}) and the elongation at yield (ε_{fM}) were evaluated. Thermal measurements were performed with a differential scanning calorimeter (DSC 2, Mettler Toledo) under a nitrogen atmosphere (20 mL/min). The temperature of the samples was raised from 0 to 180 °C at a heating rate of 10 °C/min and held in the molten state for 5 minutes to quench the thermal history. After cooling at 10 °C/min, the samples were reheated to 180 °C at 10 °C/min. The crystallisation temperature (T_c), crystallisation enthalpy (ΔH_c), melting temperature (T_m) and melting enthalpy (ΔH_m) were determined from the cooling scan and the second heating scan. Thermogravimetric analysis was carried out using the Mettler Toledo TGA/DSC 3+. About 5 mg of the sample was heated from 40 °C to 550 °C in Al_2O_3 crucible in a nitrogen atmosphere with a gas flow of 20 mL/min at 10 °C/min, followed by isothermal heating 30 min. at 550 °C in an oxygen atmosphere with a gas flow of 20 mL/min.

3 RESULTS AND DISCUSSION

3. 1 Mechanical properties

A comparison of the results for Et in Table 2 indicates that the stiffness of the samples is not significantly influenced by the addition of the compatibilizer and antioxidant. However, an increase in the amount of added corn husk was observed to elevate the stiffness.

The σm was found to increase upon the incorporation of both the compatibilizer and the antioxidant. Consistent with the trend in stiffness, the tensile strength was also increased by raising the amount of added corn husk. In contrast, the elongation at break was reduced with an increasing amount of corn

husk. A decrease in elongation at break was also noted with the addition of the compatibilizer and antioxidant.

The simultaneous increase in stiffness and strength is attributed to enhanced interfacial interactions between the corn husk surface and the rPE matrix, facilitated by the added compatibilizer. Based on the results presented in Table 2, the amount of compatibilizer used appears to be sufficient to wet the entire surface of the corn husk, thereby promoting effective interactions between the husk and the rPE matrix.

Table 2: Summarized results from the tensile tests

	Tensile test results		
Sample	***E_t (GPa)***	***σ_m (MPa)***	***ε_{tb} (%)***
rPE	*0.18 ± 0.02*	*10.5 ± 0.1*	*194 ± 16*
rPE CA	*0.18 ± 0.01*	*11.4 ± 0.2*	*174 ± 20*
rPE CA CH10	*0.24 ± 0.02*	*13.4 ± 0.2*	*50 ± 13*
rPE CA CH20	*0.33 ± 0.03*	*14.5 ± 0.2*	*28 ± 4*
rPE CA CH30	*0.46 ± 0.11*	*16.2 ± 0.3*	*15 ± 4*

The flexural test results presented in Table 3 are consistent with the tensile test results. Furthermore, in the flexural tests, the addition of the compatibilizer and antioxidant was found to increase the stiffness and strength, while the elongation remained unchanged.

An increase in the amount of added corn husk resulted in elevated stiffness and strength, whereas a decrease in elongation was observed.

Table 3: Summarized results from the flaxural tests

	Flexural test results		
Sample	***E_f (GPa)***	***σ_{fM} (MPa)***	***ε_{fM} (%)***
rPE	*0.15 ± 0.01*	*7.2 ± 0.1*	*8.2 ± 0.3*
rPE CA	*0.17 ± 0.06*	*7.8 ± 0.1*	*8.2 ± 0.3*
rPE CA CH10	*0.20 ± 0.02*	*8.7 ± 0.2*	*8.1 ± 0.1*
rPE CA CH20	*0.26 ± 0.06*	*10.0 ± 0.2*	*7.9 ± 0.1*
rPE CA CH30	*0.35 ± 0.03*	*11.6 ± 0.5*	*7.2 ± 0.3*

The flexural test results confirm the good interfacial interactions between the corn husk surface and the rPE matrix, facilitated by the compatibilizer, as was previously concluded from the tensile test data.

The thermal properties of the samples are presented in Table 4. In all samples, three melting points are observed during the second heating. The first is observed at a temperature of 112 °C for LD-PE, the second at 126 °C for LLDPE, and the third at 161 °C for PP. This result indicates the clear presence of a small fraction of PP in the rPE matrix. As expected, the melting enthalpy for the rPE matrix is decreased by increasing the amount of added corn husk; similarly, the melting enthalpy for PP is also reduced.

The amount of added corn husk does not affect the melting points for either PE or PP. During cooling, the crystallization temperature for PE is 112 °C and is independent of the amount of added corn husk. However, the crystallization of the PP component was not observed due to its excessively low content. As anticipated, the crystallization enthalpy for PE is decreased with an increasing amount of added corn husk.

Table 4: Summarized results from the 2nd heating and cooling from DSC tests

Sample	2nd heating				cooling	
Sample	T_{mPE} (°C)	ΔH_{mPE} (J/g)	T_{mPP} (°C)	ΔH_{mPP} (J/g)	T_c (°C)	ΔH_c (J/g)
rPE	111 & 124	86.7	161	0.9	111	85.9
rPE CA	112 & 126	89.8	161	1.1	112	88.1
rPE CA CH10	112 & 125	82.0	161	0.9	112	81.5
rPE CA CH20	112 & 126	46.4	161	0.4	112	45.4
rPE CA CH30	112 & 126	32.7	161	0.3	112	32.1

In accordance with the results of the mechanical tests, which led to the conclusion that the compatibilizer wets the entire surface of the corn husk, it can also be concluded from the DSC tests that the wetting of the corn husk by the compatibilizer prevents the smaller corn husk particles from acting as nucleation sites and causing heterogeneous crystallization, due to the identical crystallization temperature.

The TGA results are presented in Table 5. The degradation of rPE and rPE CA was single-step. The degradation temperature of the rPE matrix was significantly lowered by the addition of a compatibilizer and an antioxidant. The inorganic residue was found to be 0.5 wt%. A two-step degradation process was observed for the samples containing corn husk. First, the corn husk was degraded at a temperature of approximately 340 °C.

With an increasing amount of added corn husk, the degradation temperature of the matrix was reduced, while the amount of carbon black, which decomposes in an O_2 atmosphere, was increased. Similarly, the quantity of the inorganic residue was also increased.

Table 5: Summarized results from TGA tests

Sample	T_{d1} (°C)	Decomposition1 (%)	T_{d2} (°C)	Decomposition2 (%)	Ash (%)	Residue (%)
rPE	-	4.0	498	96.0	0.0	0.0
rPE CA	-	1.3	477	98.0	0.2	0.5
rPE CA CH10	339	7.9	477	89.1	2.6	0.4
rPE CA CH20	338	19.7	476	72.2	7.6	0.5
rPE CA CH30	337	31.9	472	54.4	12.9	0.8

As expected, the degradation temperature of the composites relative to the rPE matrix was decreased by increasing the corn husk content. Nevertheless, it remained relatively high even at 30% corn husk content, measuring 470 °C.

4 CONCLUSIONS

In this study, which involved the incorporation of corn husk into recycled agricultural film alongside a compatibilizer and an antioxidant, the addition of 30 wt% corn husk resulted in an increase in tensile and flexural modulus by 156% and 133%, respectively, and in tensile and flexural strength by 54% and 61%, respectively. As anticipated, a considerable reduction in elongation at break by 179%, and in elongation at yield by 12%, was also observed. An increasing amount of added corn husk was found to lower the degradation temperature of the PE matrix, while the amount of inorganic residue was increased, albeit remaining within the range observed for the inorganic residue of the rPE matrix. Furthermore, the addition of corn husk resulted in a two-step degradation process, with an additional degradation step occurring at 340 °C due to the corn husk additive. It can be concluded that corn husk does not affect the thermal properties of the rPE matrix, as both the melting temperature and the crystallization temperature are independent of the amount of added corn husk.

The addition of a suitable compatibilizer to the rPE matrix containing corn husk was observed to increase both the stiffness and the strength. It can therefore be concluded that good interfacial interactions between the corn husk surface and the rPE matrix are enabled by the compatibilizer. Since the increase in strength is substantial, and since the thermal properties of the rPE matrix are not affected by the corn husk addition, it can also be concluded that the corn husk surface is thoroughly wetted, thereby allowing for the successful incorporation of corn husk as an effective reinforcing filler.

The results presented in this contribution provide an excellent foundation for further research, including towards the development of packaging films, as the complete wetting of the corn husk surface was successfully achieved by the use of a compatibilizer. As a proof of concept, a film was produced and transformed into pots for the hydroponic cultivation of vegetables using thermoforming technology.

Acknowledgments: *This work largely builds on findings, developed within the project »Circular technological concepts and business models in Slovenian agriculture« (V4-2208), financed jointly by the Slovenian Research and Innovation Agency, and Ministry for Agriculture, Forestry and Food.*

5 REFERENCES

Bahlouli N., Sari A., Aymard A., Ziane S., Kriker A., Benderradji A. (2022) Recycling of post-consumer polyolefins for sustainable composites: A review. Waste Manag., 139, pp. 208-222.

European Commission. (2021) Assessment of the options to improve the management of agricultural plastic waste in the EU.

Faruk O., Bledzki A.K., Fink H.P., Sain M. (2012) Biocomposites reinforced with natural fibres: 2000–2010. Prog. Polym. Sci. 2012, 37, pp. 1565-1596.

Garcia J. M., & Robertson M. L. (2017) The future of plastics recycling. Sci., 358, 6365, pp. 870-872.

La Mantia F. P., Morreale M. (2011) Green composites: A brief review. Compos. - A: Appl. Sci. Manuf., 42, 6, pp. 579-588.

UNEP. (2023) Turning off the Tap: How the world can end plastic pollution and create a circular economy.

TOWARDS ENGINEERING SMART ECO-PACKAGING FROM FOOD SYSTEM WASTE

Fideline Tchuenbou-Magaia[1], Siting Guo[1], Constance Ojo[1], Evgeni Ivanov[2], Vladimir Georgiev[2], Iza Radecka[3]

[1]School of Engineering, Computing and Mathematical Sciences, Centre for Engineering Innovation, Research Faculty of Science and Engineering, University of Wolverhampton, United Kingdom;

[2]Open Laboratory on Experimental Micro and Nano Mechanics (OLEM), Institute of Mechanics, Bulgarian Academy of Sciences, Sofia, Bulgaria;

[3]School of Pharmacy & Life Sciences, Research Institute of Healthcare Sciences, Faculty of Science and Engi-neering, University of Wolverhampton, United Kingdom

doi: 10.5281/zenodo.17294211
f.tchuenbou-magaia@wlv.ac.uk

Abstract: *Our study investigates the development of smart, sustainable food packaging materials derived from agricultural and household food waste. This includes, the production of bacterial cellulose from food waste-based culture media and resulting nanocrystal (BCN) used in packing formulations, the production of composite filaments of polylactic acid, BCN and graphene for smart 3D printed packaging and active packaging films made from starch extracted cassava peels and loaded with plant extracts.*

THE INFLUENCE OF SOLAR SPECTRUM ON OPTICAL PROPERTIES OF PRINTED EFFECT PIGMENTS

Mirica Karlovits, Ivan Jerman, Blaž Likozar, Uroš Novak

National Insitute of Chemistry, Ljubljana, Slovenia

doi: 10.5281/zenodo.17294242
mirica.karlovits@ki.si

Abstract: *In this study, the influence of the entire solar spectrum, including the ultraviolet (UV), visible (VIS), and near infrared (NIR) regions, on the transmission and reflectance of printed effect pigments on OPP film was investigated. Five different commercially available effect pigments from Merck (Germany) were used, which differ in their pigment shape, chemical composition, pigment color and particle size. The results show that all the pigments analysed have the lowest transmission in the UV region, which then gradually increases with increasing wavelength, meanin that the values in the NIR region were the highest. In addition, the largest deviations in the reflectance spectra were found for the pigments EP1 and EP5 in the UV region. In the VIS region, the reflectance increased for all pigments and fell slowly in the NIR region. Among the pigments analyzed, pigment EP3 achieved the lowest overall transmission, whereas EP2 exhibited the lowest reflectance across the entire solar spectrum.*

Keywords: effect pigments, solar spectrum, transmission, reflectance

1 INTRODUCTION

In space, the solar spectrum is more like the radiation of a black body and covers different wavelengths. On the Earth, Sunlight is scattered in specific infrared, visible, and ultraviolet (UV) light rays. The composition of the solar spectrum includes 52% NIR radiation (700-2500 nm), 43% visible (VIS) light (400-700 nm), and 5% ultraviolet (UV) radiation (100-400 nm). The infrared radiations account for more than half of the solar radiations (Mansour et al., 2025, La Notte et al., 2020). The UV radiation is further divided into: UV-C (100-280 nm, which is generally created from artificial light sources), UV-B (280-315 nm, being the most energetic component of natural UV light), UV-A (315-400 nm, which accounts for the lowest energy of UV light) (Roy et al., 2023).

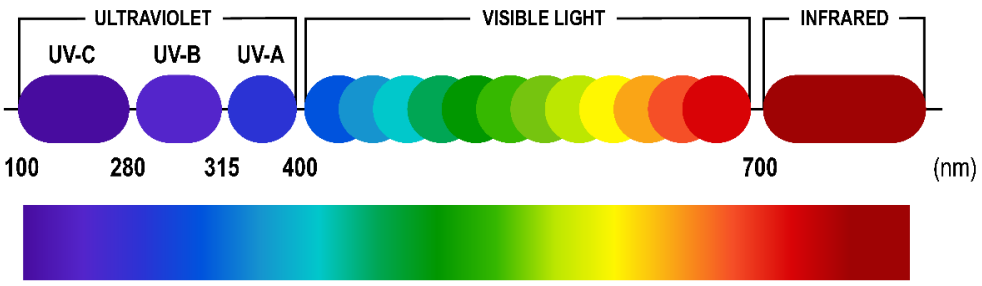

Figure 1: The solar spectrum.

UV-light is known for its negative impact on human health. It causes sun burns, eye damages, accelerated skin ageing and skin cancer. Beside these health issues, the protection against UV-light is often also required for material protection, e.g. for improvement of the light fastness. IR-light is also named as heat radiation and for this the protection against IR-light is often related to heat regulation and heat management (Greiler et al., 2021).

In cases of surfaces exposed to Sunlight, solar energy can be transmitted, reflected, or absorbed. When the frequency of the incoming light is near to the electron energy levels of a sun-exposed material, the electrons will absorb the light wave energy and the electrons' energy state changes. In other words, the absorbed light is converted into thermal energy. The absorption of light depends on the nucleus and on electrons. In its transmission, light moves through a substrate, and at the reflection of different wavelengths, the angle of incidence of the light is equal to that of the reflection on smooth surfaces; consequently, the light bounces back from the surface (Mara et al., 2023).

Apart from the visible region, effect pigments also interact with other wavelengths of light in the electromagnetic spectrum (Bendiganavale et al., 2008). The class of effect pigments (luster pigments) comprises the two main groups of special effect pigments including pearl luster pigments (pearlescent pigments, nacreous pigments, interference pigments) and metal effect pigments (Buxbaum et al., 2005). All these pigments consist of small thin platelets that show strong lustrous effects when oriented in parallel alignment in application systems (e.g. in paints, plastics, printing inks, etc.) (Klein, 2010, Rossi et al., 2020). Pearlescent pigment is a kind of optical effect pigment invented by imitating the principle of pearl formation. The core is a micron-sized mica sheet or other substrates, and the surface can be coated with multi-layer nano-scale metal or non-metal oxide film. The pigment is colored on the base of light interference effect. As the white light shines on the surface of the pearlescent pigment sheet, it exhibits a variety of bright colors through multiple reflection and refraction of light (Yang et al., 2024).

Figure 2 shows the various optical principles of conventional pigments (absorption pigments), metallic pigments, natural pearl as well as pearl lustre pigments.

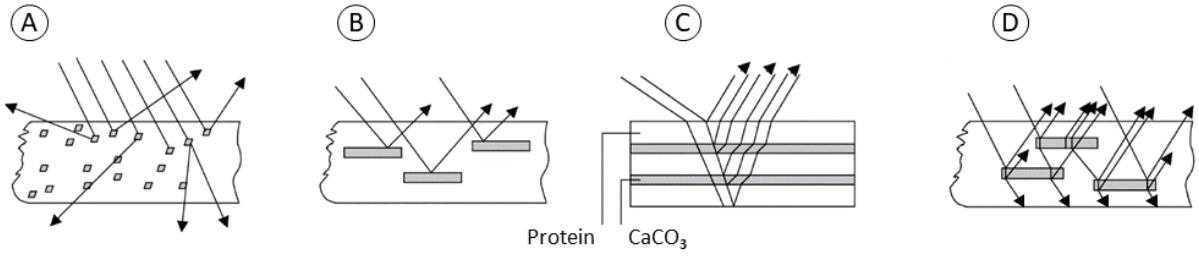

Figure 2: Optical properties of A) absorption pigments; B) metal effect pigments; C) natural pearl; D) pearl lustre pigments.

In the case of absorption pigments, the interaction with light is based upon absorption and/or diffuse scattering. A completely different optical behaviour can be observed with the group of effect pigments including pearl lustre and metal effect pigments. Metal effect pigments consists of small metal platelets (for example aluminium, titanium, copper) which operate like mirrors and almost completely reflect the incident light. Pearl lustre pigments are natural or synthetic pigments and the visual impression develops by reflection and scattering of light on thin multiple layers. The visual impression develops by reflection and scattering of light on thin multiple layers (Fig. 2D) (Buxbaum et al., 2005, Glausch et al., 1998).

In recent years, there have been several studies on solar spectral optical properties of pigments. Yang et al. investigate VO_2 nano-rod coated mica composites pearlesecnt pigment for temperature control packaging (Yang et al., 2024). In the study conducted by Alkan et al., iron oxide particles with promising energy storage properties were investigated as new solar heat absorber and storage medium candidates (Alkan et al, 2023). Furthermore, in the study conducted by Toy, E. et al., the effect of particle size on color and NIR reflectivity of $(Fe,Cr)_2O_3$ black pigment was investigated (Toy, E. et al., 2025).

2 MATERIALS AND METHODS

In this study, five different commercially available effect pigments from Merck (Germany) were used, which were printed on transparent OPP film using the gravure printing process. The pigments differed in their pigment shape, chemical composition, pigment's color and particle size. Three pigments (EP1, EP2, EP3) are mica-based pigments, two pigments (EP4, EP5) are silica-based pigments (Table 1). Oriented polypropylene (OPP) is a polypropylene plastic film that is oriented in two directions for added strength.

Table 1: Properties of effect pigments

Pigment label	***Trade name***	***Form***	***Chemical composition***	***Pigment color***	***Particle size***
EP1	*Iriodin® 123*	*Powder*	*Mica: 60-68 %* *Titanium Dioxide: 32-39 %* *Tin Oxide: < 1 %*	*White*	*5 - 25 µm*
EP2	*Iriodin® 305*	*Powder*	*Mica + Silicon Dioxide: 45-66 %* *Titanium Dioxide: 19-29 %* *Iron Oxide: 15-25 %* *Tin Oxide: 1 %*	*Yellow*	*10 - 60 µm*
EP3	*Iriodin ®520*	*Powder*	*Mica: 53-58 %* *Iron Oxide: 42-47 %*	*Orange*	*5 - 25 µm*
EP4	*Colorstream® T10-02*	*Powder*	*Silicon Dioxide: 57-68 %* *Titanium Dioxide: 30-39 %* *Tin Oxide: 2-4 %*	*Turquoise / Silver / Red / Gold*	*5 - 50 µm*
EP5	*Colorstream® T10-04*	*Powder*	*Silicon Dioxide: 72-84 %* *Titanium Dioxide: 14-24 %* *Tin Oxide: 2-4 %*	*Gold / Silver / Green / Blue*	*5 - 50 µm*

A Scanning Electron Microscope - SEM (JSM-5610JOEL) was used to evaluate the pigment particles. The transmission (T) and reflectance (R) spectra of the printed pigments were obtained with Lambda 950 UV-VIS-NIR spectrometer (PerkinElmer, USA) in the range of wavelengths from 250 nm to 2000 nm, at 10-nm intervals.

3 RESULTS AND DISCUSSION

Figure 3 shows a scanning electron microscope (SEM) micrographs of pigments based on a) mica flakes (EP1) and b) silica flakes (EP4) at 1000x magnification. In both pigments examined (EP1 and EP4), the "corn flake" morphology is clearly recognisable, in which the particles appear as thin, irregular flakes with sharp edges and relatively smooth surfaces.

a) 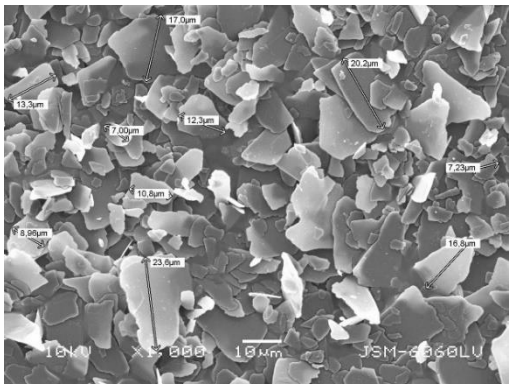 b) 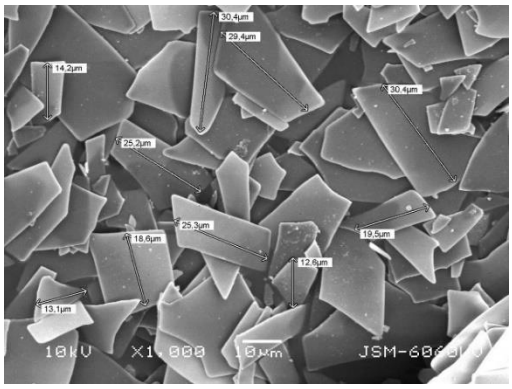

Figure 3: Scanning electron micrographs of pigments based on mica flakes (EP1) and b) silica flakes (EP4).

The transparent mica flakes are coated on all sides with a thin layer of metal oxide, mostly titanium dioxide. The presence of a highly refractive and reflective surface layer covering the less refractive support material results in a significant pearlescent effect and provides colours resulting from light interference. The carrier material of Colorstream® multicolor effect pigments (EP4, EP5) is synthetically produced silicon dioxide (SiO_2). Coated with highly refractive metal oxides, the wafer-thin and smooth platelets reflect the light and create extraordinary, changing interference colours (Maile et al., 2005). The transmission through a coating containing effect pigments is influenced by two effects the absorption of the pigment and interference effects (Greiler, 2021).

The Figure 4 shows the optical transmission spectra of five printed pigments (EP1-EP5) on transparent film, measured with a UV-VIS-NIR spectrophotometer across the wavelength range from 250 to 2000 nm. The spectra are divided into three main regions: UV (250-400 nm), VIS (400-700 nm), NIR (700-2000 nm). All pigments show the lowest transmission in the UV region compared to VIS and NIR regions, indicating strong absorption or scattering, which provides UV-shielding properties. In the visible region, the transmission spectra vary strongly among the pigments, with pigments EP4 and EP5, having a higher transmittance, while pigment EP3 has the lowest. In the NIR region, most pigments tend toward higher transmission (>70%), suggesting they allow infrared light to pass through while still modifying visible appearance. The pigment EP3 exhibits the lowest transmittance in the entire solar spectrum.

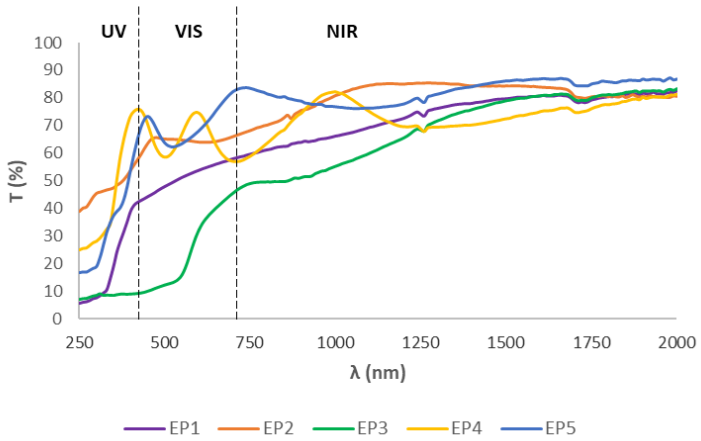

Figure 4: Transmission spectra of printed pigments on OPP film in the UV-VIS-NIR regions.

Infrared reflective pigments, such as titanium dioxide (TiO_2) powder, exhibit significant visible opacity This means such pigments primarily scatter or transmit the infrared radiation. On the other hand, thin

films are not proficient in scattering or reflecting all infrared radiation, which allows a portion of this radiation to penetrate to the substrate (Mansour et al., 2025).

The Figure 5 presents in more detail the transmission spectra in UV region (the wavelength range from 250 to 400 nm).

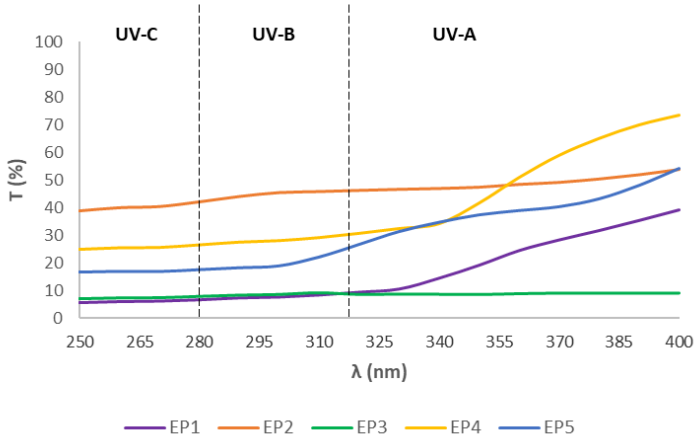

Figure 5: Transmission spectra of printed pigments on OPP film in the UV-A, UV-B and UV-C regions.

The pigment EP3 shows high UV-shielding properties in whole UV region with <10 % transmission. As shown in Table 1, the pigment EP3 contains 53-58 % mica and 42-47 % iron oxide. Silica or mica are almost transparent materials for light. However, metal oxide like titania or iron oxide absorb UV-light and can for this decrease the transmission in the spectral area of UV-light (Greiler, 2021). Similar values was noticed for pigment EP1, except in the UV-A region, where the transmission increased. The highest transmitance was noticed for pigment EP2 (chemical composition: mica + silicon dioxide: 45-66 %, titanium dioxide: 19-29 %, iron oxide: 15-25 %, tin oxide: 1 %), where the values was higher than 40%.

Figure 6 shows that the reflectance is relatively different between the pigments. The pigments EP2, EP3 and EP4 have a low reflectance in the UV range, which indicates a high UV absorption. The pigments EP1 and EP5 have a higher reflectance compared to the others. For the pigment EP1, the peak value R at 285 nm is around 75 % and decreases in the VIS and NIR range. In the visible range (400-700 nm), the highest R values were found for pigment EP1, where the peak value R at 420 nm was 67 %. In the NIR range, pigment EP3 has the highest reflectance.

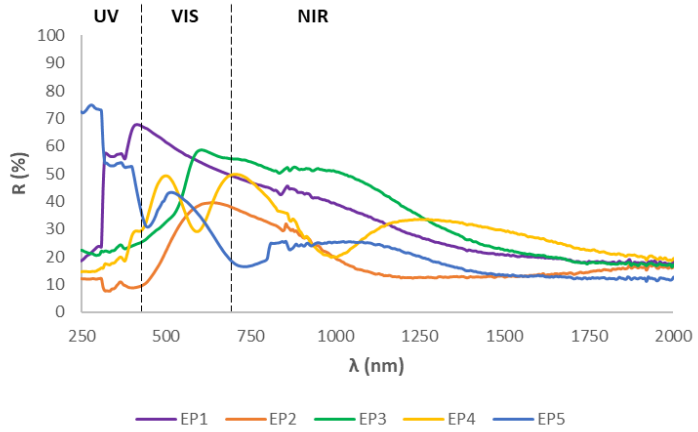

Figure 6: Reflectance spectra of printed pigments on OPP film in the UV-VIS-NIR regions.

As shown in Figure 7, the pigments EP2, EP3, and EP4 exhibit low reflectance (<25%) in the entire UV region, indicating strong UV absorption in the deep UV region. The pigment EP5 has the highest reflectance (~73%) in UV-C and UV-B regions, while the pigment EP1 in the UV-A region (~57%).

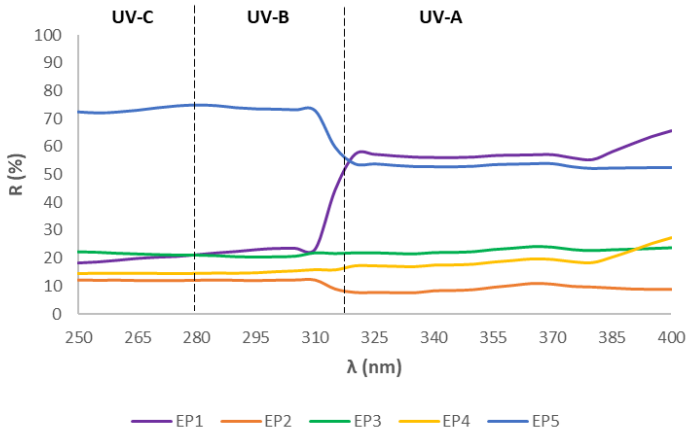

Figure 7: Reflectance spectra of printed pigments on OPP film in the UV-A, UV-B and UV-C regions.

4 CONCLUSIONS

This study demonstrated that the transmittance and reflectance of printed effect pigments on OPP film are strongly dependent on wavelength of light and pigment characteristics. All pigments exhibited the lowest transmission in the UV region, which increased toward the NIR region, while reflectance showed a rising trend in the VIS region and a gradual decline in the NIR region. Among the pigments analyzed, pigment EP3 achieved the lowest overall transmittance, whereas EP2 exhibited the lowest reflectance across the entire solar spectrum. These findings provide valuable insights for optimizing pigment selection in applications requiring controlled optical properties under entire spectrum solar exposure.

Acknowledgments: *The authors would like to acknowledge the financial support of Horizon Europe project UPSTREAM (GA 101112877).*

5 REFERENCES

Alkan, G., Mechnich, P. and Johannes Pernpeintner (2023) Using an Al-Incorporated Deep Black Pigment Coating to Enhance the Solar Absorptance of Iron Oxide-Rich Particles, Coatings, 13(11), pp. 1925-1925.

Bendiganavale A.K et al. (2008) Infrared Reflective Inorganic Pigments. Recent Patents and Chemical Engineering, 1, pp. 67-79.

Buxbaum, G. in Pfaff, G. (2005) Industrial Inorganic Pigments. 3rd Revised Edition.WILEY-VCH Verlag GmbH & Co KGaA, Weinheim, pp. 230-235.

Glausch, R. et al. (1998) Special Effect Pigments. Hannover: Vincentz, pp. 13-15.

Greiler, L.C. and Mahltig, B. (2021) Pearlescent Effect Pigments for Coatings on Textiles -Part I: Protective Materials Against UV Light and IR Light. World Journal of Textile Engineering and Technology, 7, pp. 73-83.

Kehren, K. (2013) Optical properties and Visual Appearance of Printed Special Effect Colors. PH diss., Technischen Universität Darmstadt, pp. 23-50.

Klein G. A. (2010) Industrial Color Physics. 1st ed. Springer Series in Optical Sciences, pp. 63-92.

La Notte, L. et al. (2020) Hybrid and organic photovoltaics for greenhouse applications, Applied Energy, 278, p. 115582.

Maile, F.J., Pfaff, G. and Reynders, P. (2005) Effect pigments - past, present and future, Progress in Organic Coatings, 54(3), pp. 150–163.

Mansour, S.A. and Farha, A.H. (2025) A Review of Near - Infrared Reflective Nanopigments: Aesthetic and Cooling Properties, Crystals, 15(3), pp. 271–271

Mara, J. et al. (2023) Development of Effective Infrared Reflective Coatings. Applied sciences, 13(23), pp. 12903–12903.

Rossi, S., Russo, F. and Bouchakour Rahmani, L. (2020) 'Study of the Durability and Aesthetical Properties of Powder Coatings Admixed with Pearlescent Pigments', Coatings, 10(3), p. 229

Roy, Swarup, et al. (2023) Recent Progress on UV-Light Barrier Food Packaging Films - a Systematic Review. Innovative Food Science & Emerging Technologies, Vol. 91, Elsevier BV, pp. 103550–50.

Toy, E. et al. (2025) Effect of particle size on color and NIR reflectivity of (Fe,Cr)2O3 black pigment, Inorganic Chemistry Communications, 175, p. 114132.

Yang, J. et al. (2024) VO2 nano-rod coated mica composite pearlescent pigment for temperature control packaging. Surfaces and Interfaces, 48, p. 104157.

COATINGS AND BARRIER SOLUTIONS

INFLUENCE OF RELATIVE HUMIDITY ON CARRAGEENAN-BASED FILMS FOR IMPROVED BIO-BASED AND BIODEGRADABLE PACKAGING

Lilou Avidos [1,2], Petra Babić [3], Mia Kurek [3], Nasreddine Benbettaieb [1,2] and Frédéric Debeaufort [1,2]

[1]Institution Joint research unit UMR PAM, Université Bourgogne Europe, Institut Agro, INRAE, Dijon, France.

[2] Department of BioEngineering, IUT-Dijon-Auxerre, Université de Bourgogne Europe, 7 blvd Docteur Petitjean, Dijon, France

[3] Faculty of Food Technology and Biotechnology, University of Zagreb, Zagreb, Croatia

doi: 10.5281/zenodo.17294312
frederic.debeaufort@ube.fr

Abstract: *Fresh fish products are sensitive food to oxidation and microbial spoilage. They consequently require performing packaging materials for their preservation. However, most of the biobased and biodegradable materials developed and available on the market (PLA, paper-based, etc.) have too poor oxygen barrier performance. One of the strategies to compensate these performance lacks is to apply active coatings based on natural hydrocolloids that meet food contact regulations, which can enhance the oxygen barrier effectiveness and release bioactive compounds. Carrageenan-based coatings crosslinked by Cacl2 or mixed with alginate exhibit good oxygen barrier properties, but they are very sensitive to moisture. This study focuses on behaviour and mobility of water in such films.*

Keywords: crosslinked carrageenan films, moisture sorption isotherms, water diffusivity, surface water behaviour.

1 INTRODUCTION

Films based on carrageenan and alginate, two polysaccharides derived from seaweed, are attracting growing interest in the fields of eco-friendly food packaging and edible films for their low cost, food contact ability and commercially availability. Carrageenans, extracted from red algae, are linear sulphated polysaccharides, mainly divided into three types: κ-, ι- and λ-carrageenans. κ-Carrageenan forms solid gels in the presence of potassium ions and binds well with food proteins. ι-carrageenan, in the presence of calcium, produces elastic and transparent gels, while λ-carrageenan does not gel but greatly increases the viscosity of solutions (Kocira et al., 2021). Unlike alginate, films based solely on carrageenan are often fragile. To overcome these limitations, combinations with plasticisers, other polymers, or active substances (such as essential oils, nanofillers, etc.) improve their mechanical, barrier and hydrophobic properties (Cheng et al., 2022; Kokkuvayil Ramadas et al., 2024). Alginate, a salt of alginic acid derived from brown seaweed, is distinguished by its excellent film-forming properties, transparency, low oxygen permeability, flexibility, and good mechanical strengthms (Kocira et al., 2021). In the presence of divalent ions—particularly Ca^{2+} from calcium chloride, lactate or gluconate—alginate undergoes ionic cross-linking, forming a denser three-dimensional network, increasing mechanical strength and reducing susceptibility to swelling and consequently the moisture and gases transfers (Jabeen et al., 2025). The alginate–carrageenan combination offers an interesting

compromise: it combines flexibility, transparency and improved cohesion, particularly in the presence of Ca^{2+}, thanks to the formation of a more regular ionic network that creates greater film crystallinity (from 28.7% to 43.6% with $CaCl_2$), which improves mechanical properties (Prasetyaningrum et al., 2021).

Hydrocolloid-based films exhibit relatively good barrier properties gaianst oxygen transfers when isolated from moisture. For instance, gelatine-base coating applied onto Pla could reduce the oxygen permeability from 40 to 600 times according composition and exposure to moisture (Debeaufort et al., 2022). Compared to conventional plastic like or commercially available biopolymer films, which oxygen transfer rates (OTR) are respectively 2100 $cm^3.m^{-2}.day^{-1}$ for PE and 900 $cm^3.m^{-2}.day^{-1}$ for PLA, those of hydrocolloids in dry conditions range between 0.01 $cm^3.m^{-2}.day^{-1}$ (chitosan, sodium alginate...) and 100 $cm^3.m^{-2}.day^{-1}$ (starch, carrageenan, cellulosic, etc.) for 25µm thick (Debeaufort et al., 2025; Wu et al., 2021). However, the moisture exposure of hydrocolloid-based films and coatings could have a detrimental impact on their barrier properties (Song et al., 2025). For instance, OTR of carrageenan films rises from 0.23 $cm^3.m^{-2}.day^{-1}$ at 0%RH (Guo et al., 2022), 0.5 $cm^3.m^{-2}.day^{-1}$ at 50% RH and 75 $cm^3.m^{-2}.day^{-1}$ at 80% RH or from 0.02 $cm^3.m^{-2}.day^{-1}$ to 0.55 $cm^3.m^{-2}.day^{-1}$ for sodium alginate films (Song et al., 2025; Ureña et al., 2023).

The aim of this study is to better understand how the moisture could affect the structural and molecular dynamics of seaweed-based films that could be used for optimising active coatings to be applied onto biodegradable packaging, as previous works has shown their potential as effective oxygen barrier coatings.

2 MATERIALS AND METHODS

2.1 Sample materials

Iota carrageenan (Car) (commercial grade, Louis François, Croissy Beaubourg, France) and sodium alginate (Alg) (high viscosity, Fisher Scientific, Waltham, US) were used as a film-forming matrix. Calcium chloride ($CaCl_2$, MW = 110.98 $g.mol^{-1}$, Prolabo, Croissy Beaubourg, France) was used as a crosslinker. Anhydrous glycerol (98% purity, Fluka Chemical, Seelze, Germany) was used as a plasticizer during films making. Distilled water was used for film surface characterisations.

2.2 Film making

Films (3%, w/v) were prepared from iota carrageenan (Car) or sodium alginate (Alg) powder by dissolution at 65 °C in distilled water for 30 min under stirring at 8000 rpm. Once the solutions were homogeneous, glycerol (15% w/w db) was added to the film-forming solution (FFS) under a continuous stirring at 8000 rpm. The carrageenan–sodium alginate (Car–Alg) solution was prepared by mixing equal volumes (50:50, v/v) of the individual Car and Alg dispersions under the same conditions. The pH of each solution was adjusted to 6 using a lactic acid solution (10%, v/v). Once the active film-forming solutions (FFS) were fully dissolved, 40 mL aliquots of each solution were poured into square plastic Petri dishes (12.2 × 12.2 cm^2). A 20g/L solution of calcium chloride ($CaCl_2$), used as a crosslinking agent for the carrageenan solutions, was sprayed onto cast FFS to reach a ratio of about 1.6% $CaCl_2$ to the weight of dry biopolymer. The FFS were dried for 18 to 24 hours at about 35% RH and 30°C using a fan heater. After drying, the films were carefully peeled from the Petri dish surfaces and stored between aluminum foils at 25 °C until further analysis.

2.3 Film characterisations

The film thickness was measured at 5 locations of each film sample after peeling from Petri dish, using a micrometer electronic gauge (F50, Hans Schmidt & Co GmbH; Germany) with a resolution of 1 µm.

The water vapour absorption kinetics of the film samples was demonstrated by dynamic water vapor adsorption instrument (ProUmid, Germany) at a constant temperature of 25°C, within a humidity range of 0-85% RH. About 250 mg of each film sample, in triplicate, were dried for 8 days at prior doing absorption kinetics experiments. Kinetics were stopped when mass variation was lower than 0.01%/h. moisture content at equilibrium was used for sorption isotherm plots and weight variation kinetics used for water diffusivity calculation using the second Fick's law according to Crank's modelling (Crank, 1975). The GAB model (Guggenheim–Anderson–de Boer) was used for estimation of the monomolecular water content of film M_0, and to the determination of moisture binding energy of the water monolayer (C) and subsequent layers of water absorbed (K) (Anderson, 1946; Poulain et al., 2024).

Surface water wettability and absorption by the film was assessed using a goniometer (DSA30, Kruss GmbH, Germany). Kinetics of wetting (angles, volume, dimension of the droplet measured every second) were recorded during 5 minutes. The water absorption rate (WAR) was determined using the Krüss Advance software, using recorded data (Debeaufort et al., 2022). Film surface behaviour (swelling, absorption, dissolution) was also observed from recorded video.

3 RESULTS AND DISCUSSION

The sorption kinetics measurements gave information on the behaviours at equilibrium and during absorption kinetics of the bulk structure of the films. The equilibrium in the sorption of water vapour by the films was achieved over fairly long periods (150-170 hours). Once equilibrium was reached, sorption isotherms could be plotted, representing the water content (% of water to dry basis) at equilibrium as a function of relative humidity (Figure 1). Neat carrageenan film (CAR) exhibits a little less water absorption compared to films when either $CaCl_2$ or alginate was added in the formulation. The shape of the isotherms obtained with the sorption analysis, corresponds to type II according to the IUPAC international classification of sorption isotherms, and it is characteristic of hygroscopic products (Sing et al., 2014). The shape of the isotherm is very similar to those obtained by other authors for carrageenan and alginate based films, having also very similar values within the studied water activity range (Jabeen et al., 2025; Montes et al., 2022). Modelling of the sorption isotherms using the GAB model display changes mainly in the monolayer adsboprtion water content and related energy (= C parameter), whereas the energy for the subsequent layers was not modified by the addition of $CaCl_2$ nor alginate (Table1). However, calcium chloride increases the amount of the first layer water molecule absorbed (bound water for structural networking of carrageenan) without requiring more energy, whereas alginate-carrageenan network require the same amount of bound water, but alginate requires twice more energy for settling the network by hydrogen bonding with water. This was also demonstrated by authors using other techniques (Anugrah et al., 2022; Qiao et al., 2025). The apparent diffusion coefficient calculated from the sorption kinetic display a strong effet of the relative humidity (figure 2). Both $CaCl_2$ and sodium alginate allowed to slightly reduce the diffusivity in carrageenan films, by 10-20% according to the RH. Diffusivity of water initially increased up to about 30% RH, subsequently up to 60%RH a plateau is observed, and finally a decrease occurs. This "3-steps" behaviour is explained as follows: during the initial absorption stages, water induces a slight swelling of the network by forming hydrogen bonding at specific sites, inducing a plasticization. Once plasticized, the diffusion remained almost constant, and finally, the diffusivity decreases as no more sites were available for water fixation. Subsequently at high RH, hydrophobic interactions induced clustering of water molecules as dimers and tetramers mainly. Consequently, water cluster radius and molecular volume increase and require more space to diffuse. This behaviour was also observed for other soluble biopolymers with gelling properties, whereas bonding occured mainly through hydrogen bonds with some hydrophobic interactions occurring in swelled/plasticized networks (Anugrah et al., 2022; De Kort et al., 2018).

Table 1: GAB parameters of films, initial water contact angle and surface water absorption rate (WAR)

Film type	**M_O (% db)**	**C**	**K**	**Contact angle (°)**	**WAR (10^{-6} g.m^{-2}.s^{-1})**
CAR	*11.56 [a]*	*1.99 [a]*	*0.996 [a]*	*91.9±2.3 [c]*	*2.339±0.319 [b,c]*
CAR-$CaCl_2$	*13.80 [b]*	*1.75 [a]*	*0.992 [a]*	*82.7±1.4 [b]*	*1.514±0.538 [a,b]*
CAR-Alg	*11.56 [a]*	*3.14 [b]*	*0.996 [a]*	*67.5±0.7 [a]*	*0.971±0.049 [a]*

[a,b,c] Means with the same letter in the same column are not significantly different at p<0.05.

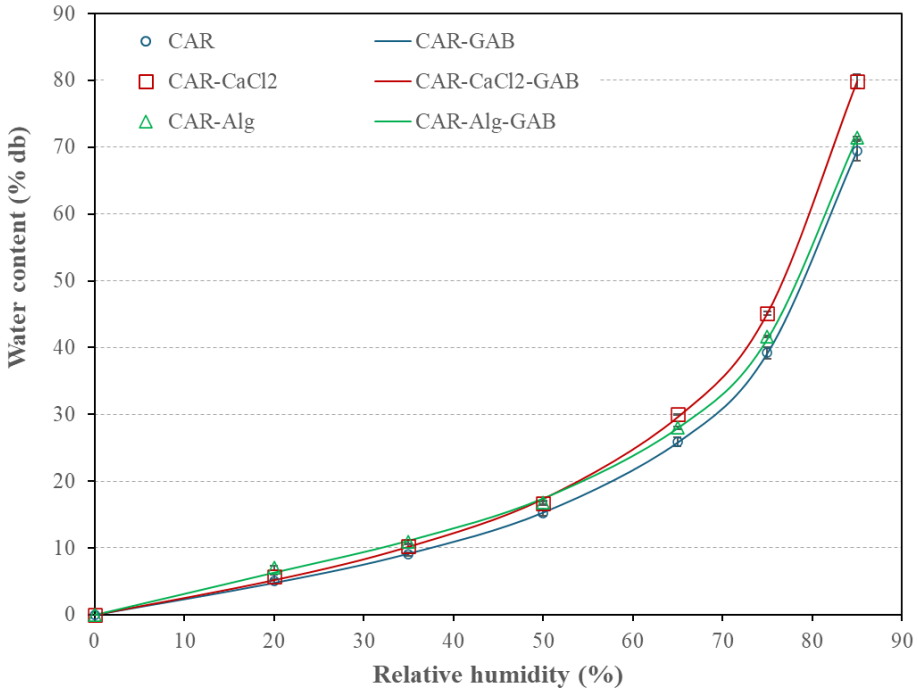

Figure 1: Water vapour sorption isotherm of films at 25°C (symbols are experimental values and lines are GAB fitted values)

Contrarily to sorption experiments, contact angle measurement allowed to better understand the surface behaviour, which is of key importance for barrier properties as it conditions the affinity and thus the wettability and absorption of moisture within the films. The surface of films became more hydrophilic when both $CaCl_2$ or alginate have been added. However, the initial contact angle of carraghenan films showed real hydrophobic value (>90°) as displays the table 1. In contrast to the behaviour of films exposed to water vapour, the surface liquid water absorption (WAR) confirms that water diffusion at elevated RH or in the presence of liquid water is significantly reduced with the incorporation of $CaCl_2$ or alginate, as evidenced by the diffusion coefficients observed (figure 2).

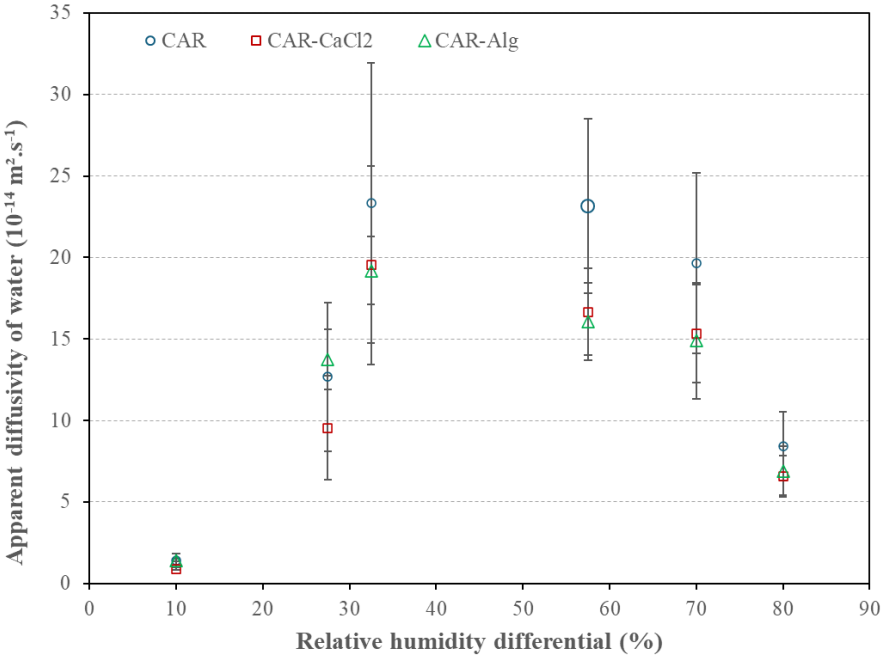

Figure 2: Water diffusivity in films at 25°C as a function of the median relative humidity

4 CONCLUSIONS

In conclusion, the study of water vapour sorption by carrageenan films reveals typical hygroscopic behaviour, characterised by type II isotherms. The addition of $CaCl_2$ or alginate modifies the structure of the networks and their interaction with water: calcium chloride promotes the adsorption of the first layer of water molecules without additional energy costs, while alginate increases the energy required for hydrogen bonding. These additions also reduce the diffusivity and absorption of liquid water, making the films more hydrophilic on the surface but more resistant to water penetration. In further works, it would be of interest to verify if oxygen transfer increase are more related to the absorption behaviour or to the diffusivity of water acting as a co-permeant more than as a plasticizer in such systems.

Acknowledgments: *The authors address a particular thanks to Bernadette Rollin and Agathe Pissis, for their technical support in some experiments. This work was supported by the Croatian Science Foundation under the project number HRZZ-IP-2022-10-1837, Sustainable concept in ACTive edible COatings development for shelf-life extension of fresh Adriatic FISH"- ActCoFISH. For the French partner, this work was partly supported by the Conseil Régional de Bourgogne Franche-Comté and the European Union through the PO FEDER-FSE Bourgogne 2021-2027 programs who invest in lab equipment.*

5 REFERENCES

Anderson, R. B. (1946). Modifications of the Brunauer, Emmett and Teller Equation1. Journal of the American Chemical Society, 68(4), 686-691. https://doi.org/10.1021/ja01208a049

Anugrah, D. S. B., Darmalim, L. V., Polanen, M. R. I., Putro, P. A., Sasongko, N. A., Siahaan, P., & Ramadhan, Z. R. (2022). Quantum Chemical Calculation for Intermolecular Interactions of Alginate Dimer-Water Molecules. Gels, 8(11), 703. https://doi.org/10.3390/gels8110703

Bajpai, S. K., & Pradeep, T. (2013). Studies on equilibrium moisture absorption of kappa carrageenan. 20(5), 2183-2191.

Bozović, A., Tomašević, K., Benbettaieb, N., & Debeaufort, F. (2023). Influence of Surface Corona Discharge Process on Functional and Antioxidant Properties of Bio-Active Coating Applied onto PLA Films. Antioxidants, 12(4), Article 4. https://doi.org/10.3390/antiox12040859

Cheng, C., Chen, S., Su, J., Zhu, M., Zhou, M., Chen, T., & Han, Y. (2022). Recent advances in carrageenan-based films for food packaging applications. Frontiers in Nutrition, 9, 1004588. https://doi.org/10.3389/fnut.2022.1004588

Crank, J. (1975). The Mathematics of Diffusion (Second Edition). Clarendon Press, Oxford University Press.

De Kort, D. W., Schuster, E., Hoeben, F. J. M., Barnes, R., Emondts, M., Janssen, H. M., Lorén, N., Han, S., Van As, H., & Van Duynhoven, J. P. M. (2018). Heterogeneity of Network Structures and Water Dynamics in κ-Carrageenan Gels Probed by Nanoparticle Diffusometry. Langmuir, 34(37), 11110-11120. https://doi.org/10.1021/acs.langmuir.8b01052

Debeaufort, F., Riondet, J., Brachais, C.-H., & Benbettaieb, N. (2022). Influence of Gelatin-Based Coatings Crosslinked with Phenolic Acids on PLA Film Barrier Properties. Coatings, 12(7), 993. https://doi.org/10.3390/coatings12070993

Debeaufort, F., Voilley, A., & Meares, P. (1994). Water vapor permeability and diffusivity through methylcellulose edible films. Journal of Membrane Science, 91(1-2), 125-133. https://doi.org/10.1016/0376-7388(94)00024-7

Derkach, S. R., Voron'ko, N. G., Kuchina, Yu. A., Kolotova, D. S., Gordeeva, A. M., Faizullin, D. A., Gusev, Yu. A., Zuev, Yu. F., & Makshakova, O. N. (2018). Molecular structure and properties of κ-carrageenan-gelatin gels. Carbohydrate Polymers, 197, 66-74. https://doi.org/10.1016/j.carbpol.2018.05.063

Hecht, H., & Srebnik, S. (2016). Structural Characterization of Sodium Alginate and Calcium Alginate. Biomacromolecules, 17(6), 2160-2167. https://doi.org/10.1021/acs.biomac.6b00378

Jabeen, F., Zil-e-Aimen, Ahmad, R., Mir, S., Awwad, N. S., & Ibrahium, H. A. (2025). Carrageenan : Structure, properties and applications with special emphasis on food science. RSC Advances, 15(27), 22035-22062. https://doi.org/10.1039/D5RA03296B

Kocira, A., Kozłowicz, K., Panasiewicz, K., Staniak, M., Szpunar-Krok, E., & Hortyńska, P. (2021). Polysaccharides as Edible Films and Coatings : Characteristics and Influence on Fruit and Vegetable Quality—A Review. Agronomy, 11(5), 813. https://doi.org/10.3390/agronomy11050813

Kokkuvayil Ramadas, B., Rhim, J.-W., & Roy, S. (2024). Recent Progress of Carrageenan-Based Composite Films in Active and Intelligent Food Packaging Applications. Polymers, 16(7), 1001. https://doi.org/10.3390/polym16071001

Montes, L., Gisbert, M., & Moreira, R. (2022). Water sorption isotherms of different sodium alginates : Thermodynamic evaluation and influence of mannuronate-guluronate copolymers. Journal of Food Processing and Preservation, 46(12), e17179. https://doi.org/10.1111/jfpp.17179

Moreira, R., Chenlo, F., Sineiro, J., Sánchez, M., & Arufe, S. (2016). Water sorption isotherms and air drying kinetics modelling of the brown seaweed Bifurcaria bifurcata. Journal of Applied Phycology, 28(1), 609-618. https://doi.org/10.1007/s10811-015-0553-1

Olivas, G. I., & Barbosa-Cánovas, G. V. (2008). Alginate–calcium films : Water vapor permeability and mechanical properties as affected by plasticizer and relative humidity. LWT - Food Science and Technology, 41(2), 359-366. https://doi.org/10.1016/j.lwt.2007.02.015

Poulain, C., Brachais, C.-H., Krystianiak, A., Heintz, O., Léonard, M.-L., Benbettaieb, N., & Debeaufort, F. (2024). Changes in the structure and barrier properties induced by corona atmospheric plasma process applied on wet gelatin layers for packaging film applications. Food Hydrocolloids, 110858. https://doi.org/10.1016/j.foodhyd.2024.110858

Prasetyaningrum, A., Utomo, D. P., Raemas, A. F. A., Kusworo, T. D., Jos, B., & Djaeni, M. (2021). Alginate/κ-Carrageenan-Based Edible Films Incorporated with Clove Essential Oil : Physico-Chemical Characterization and Antioxidant-Antimicrobial Activity. Polymers, 13(3), 354. https://doi.org/10.3390/polym13030354

Qiao, D., Zhang, Y., Sun, F., Yoo, M., Zhao, G., & Zhang, B. (2025). Enhancement mechanism of ι-carrageenan on the network structure and gel-related properties of soy protein isolate/λ-carrageenan system. Food Chemistry, 468, 142476. https://doi.org/10.1016/j.foodchem.2024.142476

Senturk Parreidt, T., Müller, K., & Schmid, M. (2018). Alginate-Based Edible Films and Coatings for Food Packaging Applications. Foods, 7(10), 170. https://doi.org/10.3390/foods7100170

Sing, K. S. W., Rouquerol, F., & Rouquerol, J. (2014). 5—Classical Interpretation of Physisorption Isotherms at the Gas–Solid Interface. In F. Rouquerol, J. Rouquerol, K. S. W. Sing, P. Llewellyn, & G. Maurin (Éds.), Adsorption by Powders and Porous Solids (2nd Edition, p. 159-189). Academic Press. https://doi.org/10.1016/B978-0-08-097035-6.00005-X

Stortz, C. A. (2005). Carrageenans : Structural and Conformational Studies. In Handbook of Carbohydrate Engineering. CRC Press.

Zhang, Y., Man, J., Li, J., Xing, Z., Zhao, B., Ji, M., Xia, H., & Li, J. (2022). Preparation of the alginate/carrageenan/shellac films reinforced with cellulose nanocrystals obtained from enteromorpha for food packaging. International Journal of Biological Macromolecules, 218, 519-532. https://doi.org/10.1016/j.ijbiomac.2022.07.145

PHA AND PLA DISPERSIONS AS BIODEGRADABLE SEALING LACQUERS FOR PAPER-BASED BARRIER PACKAGING

Kerstin Müller[1], Felix Fischbeck[1], Christoph Bantz[2], Anna Musyanovych[2]

[1]Materials Development, Fraunhofer Institute for Process Engineering and Packaging IVV, Giggenhauser Str. 35, 85354 Freising, Germany

[2]Micro- and Nanoparticle Engineering Group, Chemistry Division, Fraunhofer Institute for Microengineering and Microsystems IMM, Carl-Zeiss-Str. 18-20, 55129 Mainz, Germany

doi: 10.5281/zenodo.17294351
kerstin.mueller@ivv.fraunhofer.de

Abstract: *The shortage of biodegradable options for sealing lacquers for paper-based packaging has led to research on biopolyesters like PLA and PHA, though both pose challenges due to their high crystallinity and melting temperatures, complicating film formation at lower coating temperatures. In our research, we addressed these challenges by using low crystalline polymer grades in an emulsification/solvent evaporation process, resulting in dispersions characterised by small particle sizes in the range of 220-510 nm and effective film formation at reduced temperatures of maximum 150 °C. Coated papers showed strong barrier performance, with WVTR and oxygen permeance values below 20 g/m²·d and 1 cm³/m²·d·bar, respectively. While PLA-based coatings achieved acceptable seal strengths, PHA coatings require further optimization. The potential for use in food packaging applications was confirmed by overall migration below regulatory limits and sensory tests on chocolate showing no differences to the conventional packaging over the given shelf-life.*

Keywords: paper packaging, biopolymer, polymer dispersion, barrier coating, sealing

1 INTRODUCTION

The shift towards sustainable packaging is a crucial endeavour for our society today, particularly in the transition from plastic to paper packaging. One of the main challenges lies in developing reliable barriers that can effectively protect the contents of the package. Conventional coatings like polyolefins and acrylates are petroleum-based, non-biodegradable, and difficult to recycle (Kunam et al. 2022), making them poorly suitable for single-use applications. Biobased materials such as proteins and polysaccharides offer good oxygen barriers, but struggle with moisture resistance and sealability. Thermoplastic biopolymers like PLA and PHAs are promising alternatives.

For practical use in paper coatings, water-based formulations are preferred due to easier handling and lower emissions. However, formulating these biopolymers into dispersions presents additional challenges. The film-forming temperature for dispersion lacquers typically falls between the glass transition and melting temperatures of the polymer, indicating that the amorphous parts of the polymer form the closed barrier layer. Standard PLA and PHA grades exhibit high crystallinities that limit film formation, often requiring processing temperatures above their melting point, which is not economically feasible. In particular, the crystalline nature of the PHB copolymers available on the market, such as PHBV, of almost 60% with a low hydroxy valerate content has disadvantages such as high melting points between 160-180 °C, inherent brittleness and a narrow processing window, which limit their large-scale application (Wu et al. 2021). Thus, it is essential to explore alternative grades and

formulation techniques to achieve efficient film formation at temperatures at least below 150 °C that can be processed more easily on paper coating lines.

To address this, we developed water-based dispersions using an emulsification/solvent evaporation process with low-crystallinity polymer grades. This paper presents the preparation and upscaling of PLA and PHA dispersions in a multilayer coating approach, along with packaging-relevant characterizations.

2 MATERIALS AND METHODS

2.1 Materials

Paper substrates were the one-side coated packaging paper PackPro 7.0 at a grammage of 80 gsm and the barrier paper NiklaBarr Base at a grammage of 88 gsm, both from Brigl & Bergmeister GmbH. Polymers used for dispersion preparation were the amorphous PLA Luminy® LX930 and LX975 from TotalEnergies Corbion and a PHB-copolymer PHBHHx provided by HPX Polymers. Other PHAs tested for their film formation were the Green Planet™ X331N PHBH by Kaneka Belgium and the PHI 003 PHBV from Natureplast. The polyvinyl alcohol (PVOH) used as a 10 wt% aqueous solution for precoating was the Exceval AQ-4104 from Kuraray. During the formulation process, chloroform and ethyl acetate from VWR chemicals were used as solvents for the polymers, and 0.5 wt% aqueous solution of polyvinyl alcohol (M_w = 9000-10000 g/mol, Sigma Aldrich) was used for stabilization of droplets/particles.

2.2 Dispersion preparation

Polymer particles were obtained by the solvent evaporation method combined with the miniemulsion technique using the adapted procedure described in Musyanovych et al. 2008. Briefly, 0.4 g of polymer was dissolved in 10 g of chloroform (or 8 g ethyl acetate in the case of PLA Luminy® LX930 and LX975). The macroemulsion was prepared by adding 24 g of an 0.5 wt% PVA solution to the organic phase, and subsequent magnetic stirring of the mixture at 900 rpm for 60 min. Afterwards, the macroemulsion was subjected to ultrasonication under ice cooling for 180 s at 70% amplitude in a pulse regime (30 s sonication, 10 s pause) using a Branson 450 W sonifier and ¼" tip. The obtained miniemulsion was transferred to the 50 ml reaction flask with a large size neck and left overnight at 40 °C for a complete evaporation of the organic solvent. This general procedure was realized in various project phases using different batch sizes, depending on the individual requirements in each project phase. For Roll-to-Roll trials the obtained aqueous dispersions were concentrated up to 30 wt% solid content by removing water in a rotary evaporator at 40 °C.

2.3 Paper Coating

Sheet coating. Preliminary tests on film formation and barrier properties were conducted using a lab-scale coating unit (CUF 5, Sumet Messtechnik) with a convection dryer and k-bar technique. To achieve dry coating thicknesses of 4–8 µm, k-bars with varying wet layer thicknesses were selected based on each dispersion's solid content. Minimum film formation temperature (MFFT) was evaluated on transparent oPET (Hostaphan, 23 µm) by assessing coating transparency and scratch resistance across temperatures from 90–160 °C. The same parameters were applied to paper substrates.

Multilayer approach. To combine functionalities, a PVOH precoat was applied for planarization and oxygen barrier, followed by a PLA or PHA topcoat for water vapor barrier and sealability.

Roll-to-roll coating. Multilayer structures were produced on a pilot-scale lacquering line (Fraunhofer IVV, Freising) using a slot-die system (FMP Technology). The die had a width of 260 mm, gap length of

45 mm, and shim thickness of 100 µm. Wet layer thicknesses were adjusted to achieve target dry coating weights of 4 gsm (precoat) and 7 gsm (topcoat).

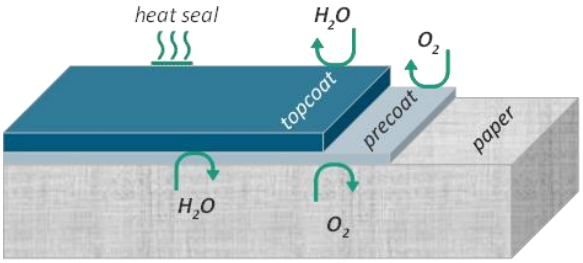

Figure 1: Multilayer barrier concept

2.4 Sample characterization

Particle Morphology. The morphology of produced particles was studied by scanning electron microscopy (zeiss leo 1550 vp, acceleration voltage 1 kv). A drop of diluted sample was dried on a silicon wafer at room temperature and sputtered with gold to enhance electron density contrast.

Particle Size. Dynamic light scattering was conducted on water diluted samples using a Malvern Zetasizer Ultra-Red at 173° (backscattering option); analysed based on cumulants analysis (Malvern General Purpose Algorithm).

Oxygen Permeance. Measured per DIN 53380-3 using an OX-TRAN 2/21 OTR Analyzer (Ametek Mocon) at 23 °C, 50% RH. Measurements were taken until permeation stabilized for at least 10 h; duplicates were performed.

Water Vapor Transmission Rate. Determined gravimetrically per DIN 53122-1. Samples were weighed initially and stored at 23 °C, 85% RH in a climate chamber. Weight gain was tracked four times in 48 h until it stagnated; four replicates per specimen were tested.

Heat Sealability. Packaging was sealed using a Brugger HSG-C. Sealing parameters (temperature, pressure and time) differed depending on the dispersion coating as indicated in the results section. Sealed-seam strength was tested per DIN 55 529 at 90° pull-off, 50 N, 100 mm/min on 15 mm strips.

Migration Testing. Total migration was tested using Tenax® (food simulant E) for dry foods. 1 dm² coated paper from roll-to-roll trials was exposed to 4 g Tenax® for 10 days at 40 °C (coating = food contact side). After 3-fold extracted with diethyl ether; the residue was weighed to determine overall migration (mg/dm²).

Sensory Testing. Chocolate bars were re-packed in coated paper from the roll-to-roll trials and heat-sealed (sachet packaging). Both originally and re-packed samples were stored at 23 °C, 50% RH. Repeated triangle tests (DIN EN ISO 4120-2007) with a non-trained panel (n=16) were performed to assess perceptual sensory differences.

3 RESULTS AND DISCUSSION

3.1 Dispersion characteristics

The particle sizes and respective PDI values obtained by DLS measurements for representative dispersion samples are summarized in Table 1. The morphology of the particles obtained was analysed using SEM. The selected representative images are shown in Figure 2. All produced particles are spherical in shape, except PHBV nanoparticles. Due to the high crystallinity of PHBV, the obtained particles have irregular shape. The average diameter varies in the range between 220 and 510 nm.

Compared to PHBHHx particles, the surface of PLA particles is smoother and looks harder, which is mainly due to the difference in T_g values for both polymers. The dispersions produced from ethyl acetate as solvent possess smaller particle size in comparison to those obtained from chloroform.

Table 1: DLS measurement results of produced biopolymer particle dispersions

Polymer	Grade	Solvent	Particle size [nm]	PDI
PLA	Luminy® LX975	Chloroform	434	0.21
PLA	Luminy® LX930	Chloroform	510	0.18
PHBV	PHI 003	Chloroform	413	0.25
PHBH	Green Planet™ X331N	Chloroform	423	0.24
PHBHHx	-	Chloroform	369	0.26
PLA	Luminy® LX975	Ethyl acetate	325	0.39
PLA	Luminy® LX930	Ethyl acetate	223	0.23

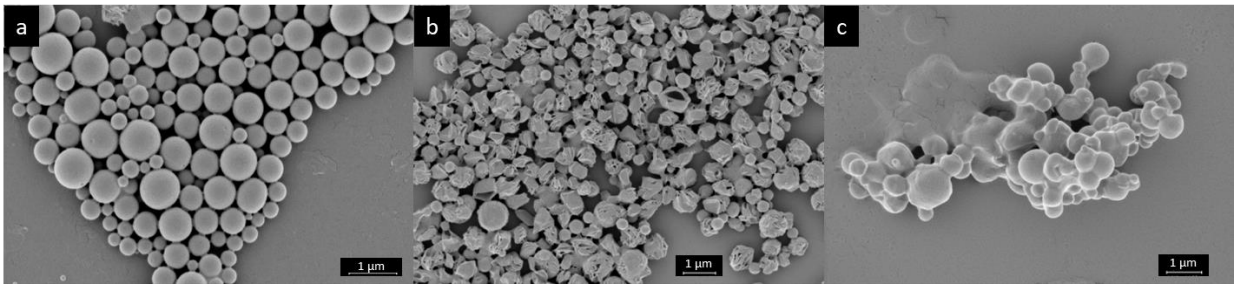

Figure 2: Representative SEM images of selected biopolymer particle dispersions; PLA Luminy® LX975 (a), PHBV (b) and PHBHHx (c)

3.2 Preliminary studies on film formation

To find suitable polymer grades that offer film formation at temperatures <150 °C, different PLA and PHA types (Table 2) were screened. Only low-crystallinity grades enabled successful film formation below their melting points. According to latex film formation theory, the MFFT is closely related to the T_g and usually lies closely above it (Keddie und Routh 2010). For the semi-crystalline standard polymer grades used in this study, film formation only in the amorphous regions was not sufficient to obtain particle deformation and film formation to obtain a continuous polymer layer. Therefore, we prefer grades with low crystallinity and lower molecular weights. This choice is also beneficial regarding the dispersion preparation step, since less toxic solvents than chloroform such as ethyl acetate can be used.

Table 2: Tested polymers and their properties. MFFT = Minimum film forming temperature. Information on biodegradability is provided by the manufacturer.

Polymer	Grade	Biodegradability	M_w [kg/mol]	T_g [°C]	T_m [°C]	X_c [%]	MFFT [°C]
PLA	LX930	Industrially Compostable[1]	160	60	130**	0	90
PLA	LX975	Industrially Compostable[1]	180	60	130**	0	90
PHBV	PHI 003	Industrially Compostable[2]	315	0	165	64*	>160***
PHBH	X331N	Industrially[1] and Home[3] Compostable, Marine[4] and Soil[5] Biodegradable	260	0	135 / 150	40*	160
PHBHHx	-	no data available, comparable to PHBH based on chemical similarity	185	0	63 / 105	15*	90

*ΔH_{ref} (PHB) = 146 J/g (Barham et al. 1984), **Flow point, ***no film formation after convectional drying, but with hot press at 170 °C
[1]certified by TÜV Austria (OK Compost INDUSTRIAL), [2]according to manufacturer information on https://natureplast.eu/de/produit/pha/, [3]certified by TÜV Austria (OK Compost HOME), [4]according to manufacturer information on https://kanekagreenplanet.com/, [5]certified by TÜV Austria (OK Compost SOIL)

3.3 Barrier and sealing properties of coated papers

To estimate the theoretical barrier potential of our dispersion coatings, ideal WVTR values were calculated based on known permeation rates for PLA and PHBHHx films. For PHBHHx, a WVTR of ~9 g/m²·d at 100 µm thickness suggests a theoretical value of ~90 g/m²·d for a 10 µm coating. Similarly, PLA with ~25 g/m²·d at 100 µm would yield ~250 g/m²·d at 10 µm. These values represent defect-free coatings and do not account for substrate or precoat effects, coating imperfections or other interactions during water vapour permeation.

Table 3: Overview of coated samples, their barrier and sealing properties.

	Sample description		WVTR 23 °C, 85 % RH	OP 23 °C, 50% RH		Grammage (approx. coating weight)	Medium Force	Maximum Force	Application
	Layer structure	Substrate	g/(m²·d)	cm³/(m²·d·bar)		gsm	N/15mm	N/15mm	
1	PP7/PLA	PP7 80 gsm	140 ± 3.40	-	-	86.6 (8)	1.68 ± 0.28[1]	2.83 ± 0.51[1]	sheet
2	PP7/PVOH/PLA	PP7 80 gsm	150 ± 0.5	0.144	0.761	91.92 (4.5+7.5)	1.78 ± 0.19[1]	2.52 ± 0.39[1]	roll-to-roll
3	NB/PVOH/PLA	NB 88 gsm	19.5 ± 1.23	<ML	0.694	101.29 (4.5+8)	-	3.39 ± 0.30[1]	roll-to-roll
4	PP7/PHBHHx	PP7 80 gsm	151 ± 2.5	136	130	95.5 (15.5)	1.40 ± 0.29[3]	2.06 ± 0.44[3]	sheet
5	NB/PHBHHx	NB 88 gsm	24.1 ± 0.57	590	661	96.35 (8)	0.83 ± 0.61[2]	1.17 ± 0.15[2]	sheet
6	PP7/PVOH/PHBHHx	PP7 80 gsm	90.3 ± 6.02	161	164	85.84 (2+6)	1.38 ± 0.03[2]	1.98 ± 0.16[2]	sheet
7	PP7/PVOH/PHBHHx	PP7 80 gsm	119 ± 1.5	0.616	2495	85.17 (4+3)	0.50 ± 0.23[4]	0.75 ± 0.29[4]	sheet
8	NB/PVOH/PHBHHx	NB 88 gsm	17.6 ± 0.15	1.02	1.3	96.21 (4+4)	0.14 ± 0.04[4]	0.20 ± 0.05[4]	roll-to-roll

[1] 150 °C / 5 bar / 2 sec; paper tear; [2] 130 °C / 5 bar / 0.5 sec; partial delamination from substrate/precoat; [3] 130 °C / 5 bar / 0.5 sec; paper tear; [4] 150 °C / 5 bar / 2 sec, delamination from substrate/precoat

Table 3 shows the barrier values as well as sealing strengths achieved for our samples. All dispersion tested were produced using chloroform and PLA dispersion refer to the LX930 grade. Both barrier and sealing performances vary with coating quality and thickness.

Measured WVTR values approached these theoretical limits, with PLA reaching 140 g/m²·d and PHBHHx 90 g/m²·d on PP7. Using the precoated substrate NB, significantly lower WVTRs (< 20 g/m²·d) were achieved (structures 3 and 8), although the substrate itself contributes ~40 g/m²·d.

A recent study by Nissinen et al. 2025 using PLA dispersion (PLAX) and bioORMOCER® reported WVTRs of 260 g/m²·d for similar multilayer structures. Our best values (~150 g/m²·d on PP7) compare favourably. For oxygen permeance (OP), PVOH outperformed bioORMOCER®, achieving values < 1 cm³/m²·d·bar, indicating nearly defect-free coatings. In contrast, OP values in the hundreds suggest coating defects and thus rather free diffusion of oxygen, likely caused by mechanical stress during multilayer application or sample handling. PHBHHx also showed moderate oxygen barrier properties, with structure 4 reaching ~130 cm³/m²·d·bar.

Beyond barrier properties, biopolyester coatings also offer grease resistance (Basak et al. 2024) and enable heat sealing. PLA's low flow point allowed effective sealing at 120 °C, with optimal results at 150 °C. Structure 3 achieved a maximum seal strength of ~3.4 N/15 mm, with paper tear observed in all samples. PHBHHx coatings showed lower seal strengths (≤ 2 N/15 mm), often accompanied by delamination, indicating a need for improved adhesion and optimized sealing parameters.

A minimum of 5 gsm coating is recommended to ensure acceptable performance, as demonstrated by structures 9 and 10, which differ only in PHBHHx coating weight but show significant variation, although mentioned delamination effects have a great influence on the measured values.

Compared to conventional PE-based sealing lacquers (> 6 N/25 mm; Merabtene et al. 2023), our seal strengths are lower. The S-POP structure discussed by Nissinen et al. 2025 achieved 4.1 N/25 mm under optimized conditions (170 °C, 2 s, 800 N), comparable to our results when accounting for sample size differences. They attributed reduced sealability to foaming and bubble formation during coating. Despite degassing, residual bubbles may have affected our results as well. To improve seal seam strength, further reduction of foaming—via defoaming agents and optimized degassing—is recommended, along with refinement of sealing parameters.

3.4 Food contact evaluation and migration testing

Materials and articles intended for food contact must comply with the general safety requirements outlined in Article 3 of Framework Regulation (EC) No. 1935/2004, which ensures that substances do not endanger human health, alter food composition, or impair sensory properties. Plastic materials are further regulated under Commission Regulation (EU) No. 10/2011, which includes a Union list of authorized substances and sets specific migration limits (SMLs) and an overall migration limit (OML) of 10 mg/dm² of food contact surface. This limit represents the maximum allowable release of non-volatile substances from packaging into food. For non-plastic materials, such as paper or coatings, national recommendations from the German Federal Institute for Risk Assessment (BfR) can apply.

All biopolyesters used in this study—PLA, PHBV, and PHBH—are authorized for food contact under Regulation (EU) No. 10/2011. For PHBH oligomers (M_w < 1000 Da), a specific migration limit (SML) of 5 mg/kg food must not be exceeded. Furthermore, the SML of 0.05 mg/kg food for crotonic acid must be considered (Silano et al. 2019), which also applies for degradation products of PHBV. In the case of polyvinyl alcohol (PVOH), vinyl acetate—its monomer—is subject to an SML of 12 mg/kg food.

In this study, overall migration testing was conducted prior to sensory evaluation. Using Tenax® as a food simulant, measured migration values were consistently below 1 mg/dm², significantly under the regulatory limit of 10 mg/dm². These results confirm the suitability of the tested coatings for food contact applications.

3.4 Sensorical testing

To assess whether chocolate bars packed in the paper-based packaging differed perceptibly from those in the original metallized film, triangle tests were conducted at 3, 7, 11, 15, and 20 weeks—covering the product's shelf life. With n = 16, a minimum of 8 correct identifications is required to confirm a perceptible difference (α > 0.20). A correct answer corresponds to an identified difference between the original and paper packed product. Panellists indicated whether their choice was based on certainty or guessing. Table 4 shows correct answers given for each test. Based on this, no perceptible differences were determined, and there is also no trend indicating that product differences arise due to the respective packaging over the storage period.

Table 4: Results of the triangle test

Layer structure		***3 Weeks***	***7 Weeks***	***11 Weeks***	***16 Weeks***	***20 Weeks***
2	*PP7/PVOH/PLA*	*7/16* *3 guesses*	*3/16* *1 guess*	*5/16* *4 guesses*	*6/16* *1 guess*	*5/16* *1 guess*
3	*NB/PVOH/PLA*	*5/16* *3 guesses*	*4/16* *4 guesses*	*5/16* *3 guesses*	*6/16* *3 guesses*	*5/16* *1 guess*

Even though the WVTR values between structure 3 (< 20 g/(m2·d)) and structure 2 (150 g/(m2·d)) vary greatly, no sensory differences were detected. For chocolate products, internal results showed that especially light and aroma barrier is needed to maintain food quality (ChocoPack 2022-2024), while moderate water vapor and oxygen barriers might be sufficient to prevent texture changes or sugar bloom as well as oxidation of fats. Although often claimed as being closely related, aroma and oxygen

concentrations showed complicated relationships regarding oxygen dependence when investigated for rapeseed oil (Andersson und Lingnert 1999). They observed that storage at lower oxygen levels could even lead to more off-flavour in the product, especially during very early stages of oxidation. However, these small differences between samples when oxidation proceeds very slowly may not be detected by sensory evaluation. Compared to rapeseed oil, oxidation processes on the surface of chocolate bars should even be more slowly and therefore sensory differences are unlikely to occur during the product's shelf life.

In terms of aroma barrier properties, PLA could offer notable advantages in aroma protection compared to conventional polyolefins. Due to its low diffusivity for organic molecules, PLA acts as a low-permeability polymer, effectively limiting the migration of volatile compounds into or out of the packaging (Ewender et al. 2025). As Ducruet et al. 2011 further highlight, PLA displays promising barrier properties especially towards hydrophobic aroma compounds.

4 CONCLUSIONS

This study confirms the potential of water-based PLA and PHA dispersions for sustainable paper packaging. Low-crystallinity polymer grades enabled film formation below 150 °C and allow the potential use of less harmful solvents, which can also be beneficial for processing at higher scale. Multilayer structures significantly improved oxygen water vapor barrier properties, achieving values close to theoretical limits given by the polyesters. While PLA-based coatings showed moderate seal strength, PHA samples used in this study require further optimization, especially regarding the adhesion on substrate and precoating. Sensory results indicate that PLA coatings are particularly suitable for aroma-sensitive products like chocolate, helping preserve flavour integrity throughout the shelf life. Overall, the approach offers a biodegradable food packaging alternative, though improvements in sealing performance and process stability are still needed for industrial application.

Acknowledgments: *We would like to thank the Fachagentur Nachwachsende Rohstoffe on behalf of the German Federal Ministry of Agriculture, Food and Home Affairs (BMLEH) for funding the project "BioPack", FKZ 221NR040A-D. We further want to acknowledge our project partners Dr. Dr. Uwe Bölz from HPX Polymers, Dr. Sebastian Brück from Naturhaus Naturfarben GmbH and colleagues from Pilot Pflanzenöltechnologie Magdeburg PPM e.V. for their support during the project.*

5 REFERENCES

Andersson, K.; Lingnert, H. (1999): Kinetic Studies of Oxygen Dependence During Initial Lipid Oxidation in Rapeseed Oil. In: Journal of Food Science 64 (2), S. 262–266. DOI: 10.1111/j.1365-2621.1999.tb15879.x.

Barham, P. J.; Keller, A.; Otun, E. L.; Holmes, P. A. (1984): Crystallization and morphology of a bacterial thermoplastic: poly-3-hydroxybutyrate. In: J Mater Sci 19 (9), S. 2781–2794. DOI: 10.1007/BF01026954.

Basak, Sumanta; Dangate, Milind Shrinivas; Samy, Shanmugha (2024): Oil- and water-resistant paper coatings: A review. In: Progress in Organic Coatings 186, S. 107938. DOI: 10.1016/j.porgcoat.2023.107938.

ChocoPack 2022-2024: Bio-Based Barrier Coating for Sustainable Chocolate Packaging. Cornet Projekt, IGF Number 340 EN, 2022-2024. Available online: https://cornet.online/EN/SuccessStories/cornet-projects/Chocopack/Chocopack.html.

Ducruet, Violette; Domenek, Sandra; Guinault, Alain; Courgneau, Cecile; Bernasconi, Marta; Plessis, Cedric (2011): Barrier properties of PLA towards oxygen and aroma compounds. In: Italian Journal of Food Science 23, S. 59–62. Available online: https://hal.science/hal-01019105v1.

Ewender, Johann; Auras, Rafael; Sonchaeng, Uruchaya; Welle, Frank (2025): Diffusion Coefficients and Activation Energies of Diffusion of Organic Molecules in Poly(lactic acid) Films. In: Molecules 30 (9), S. 2064. DOI: 10.3390/molecules30092064.

Keddie, Joseph L.; Routh, Alexander F. (2010): Fundamentals of Latex Film Formation. Dordrecht: Springer Netherlands.

Kunam, Praveen Kumar; Ramakanth, Dakuri; Akhila, Konala; Gaikwad, Kirtiraj K. (2022): Bio-based materials for barrier coatings on paper packaging. In: Biomass Conv. Bioref. 14 (12), S. 1–16. DOI: 10.1007/s13399-022-03241-2.

Merabtene, Mahdi; Tanninen, Panu; Wolf, Johanna; Kayatz, Fabian; Hauptmann, Marek; Saukkonen, Esa et al. (2023): Heat-sealing and microscopic evaluation of paper-based coated materials using various seal bar geometries in vertical form fill seal machine. In: Packag Technol Sci 36 (8), S. 667–679. DOI: 10.1002/pts.2735.

Musyanovych, Anna; Schmitz-Wienke, Julia; Mailänder, Volker; Walther, Paul; Landfester, Katharina (2008): Preparation of biodegradable polymer nanoparticles by miniemulsion technique and their cell interactions. In: Macromolecular bioscience 8 (2), S. 127–139. DOI: 10.1002/mabi.200700241.

Nissinen, Eetu; Anghelescu-Hakala, Adina; Hämäläinen, Roosa; Kivinen, Pauliina; Somorowsky, Ferdinand; Avellan, Jani; Koppolu, Rajesh (2025): Upscaled Multilayer Dispersion Coating Application for Barrier Packaging: PLAX and bioORMOCER®. In: Coatings 15 (2), S. 214. DOI: 10.3390/coatings15020214.

Silano, Vittorio; Barat Baviera, José Manuel; Bolognesi, Claudia; Brüschweiler, Beat Johannes; Chesson, Andrew; Cocconcelli, Pier Sandro et al. (2019): Safety assessment of the substance poly((R)-3-hydroxybutyrate-co-(R)-3-hydroxyhexanoate) for use in food contact materials. In: EFSA Journal 17 (1), e05551. DOI: 10.2903/j.efsa.2019.5551.

Wu, Feng; Misra, Manjusri; Mohanty, Amar K. (2021): Challenges and new opportunities on barrier performance of biodegradable polymers for sustainable packaging. In: Progress in Polymer Science 117, S. 101395. DOI: 10.1016/j.progpolymsci.2021.101395.

VALORISATION OF FOOD LOSS INTO SUSTAINABLE ACTIVE PACKAGING: POLYLACTIC ACID COATING WITH ARTICHOKE LEAF EXTRACT AND CARBOXYMETHYL CELLULOSE

Zeinab Qazanfarzadeh and Amparo Jiménez-Quero

Division of Industrial Biotechnology, Department of Life Sciences, Chalmers University of Technology, Gothenburg, Sweden

doi: 10.5281/zenodo.17294465
zeinabq@chalmers.se

Abstract: *Food loss and waste is a major global problem, yet it contains valuable compounds with aintioxiand and antimicrobial properties that can be sustainably valorized. Incorporating such compouns into an active packaging system offers a dual benefit: reducing waste while extending food shelf life. In this study we developed and characterized polylactic acid (PLA) coated packaging using artichoke leaves extract (ALE) and carboxymethyl cellulose (CMC) for enhanced antioxidant and antibacterial properties. ALE was obtained through subcritical water extraction, and PLA clamshell surfaces were first modified with spray-coating PLA-polyethylene glycol (PEG) solution to improve coating adherence. Coating solutions of CMC and ALE at different ratios (70:30, 60:40, and 50:50 w/w) were then applied in multiple layers. Surface modification with PLA-PEG increased wettability and facilitate uniform coating formation. Incorporation of ALE altered packaging color, increasing red and yellow hues proportionally to its concentration. SEM imaging confirmed a smooth, pore-free coating on modified surfaces, while unmodified or CMC-only were uneven. Functional testing showed that PLA-PEG modification reduced water vapor permeability by 36%, although the hydrophilic CMC-ALE coatings increased moisture uptake. Antioxidant activity, measured by DPPH assay, reached 40–44% scavenging after 15 min, and increased to 54–67% after 45 min, indicating sustained release of phenolic and flavonoid compounds. Antibacterial assays revealed concentration-dependent inhibition of E. coli (0.9–2.1 log reduction) and moderate reduction of S. aureus (~1 log), likely due to polyphenol-mediated disruption of bacterial membranes. Overall, the results demostrate the potential of ALE-based coatings in PLA packaging to extend shelf-life and preserve food quality through combined antioxidant and antibacterial effects.*

Keywords: active packaging, coating, artichoke leaf, polylactic acid, antioxidant activity, antibacterial activity

1 INTRODUCTION

Food loss and waste across the food supply chain pose serious global challenges, contributing significantly to environmental degradation and greenhouse gas emissions (Read et al., 2020). According to the FAO, nearly one-third of all food produced worldwide is lost or wasted each year (FAO, 2011), with approximately 58 million tonnes generated annually in the European Union (Eurostat, 2022). Among these, fruits and vegetables account for the highest proportion of losses around 41% and 46%, respectively at various stages including primary production, processing, distribution, and consumption (Caldeira et al., 2019). To address this issue, it is essential to shift from

the traditional linear economy model of “take, make, and dispose” towards a circular economy approach. For instance, plant residues such as artichoke leaves are largely discarded during harvesting and preparation. The global artichoke production reaching 1,978 kton annually, of which 70–80% is wasted as leaves, stems, and roots (Bittencourt et al., 2023). Notably, artichoke leaves are rich in bioactive compounds such as polysaccharides and phenolics with promising functional potential.

Meanwhile, the food packaging industry is increasingly seeking sustainable active packaging materials that can extend shelf life, maintain food quality, and reduce food waste at the retail and consumption stages (Momtaz et al., 2024). Valorizing food losses generated during raw material production, processing, and distribution for such applications further enhances the environmental and economic impact of active packaging innovations (Bhargava et al., 2020; Riaz et al., 2024).

Active packaging can be developed by adding active agents to the material or applying them as surface coatings. These agents provide specific functions, such as absorbing or scavenging substances like moisture, flavors, gases, or UV light, releasing compounds such as antioxidants and antibacterials (John et al., 2023). Surface coating is preferable for heat-sensitive natural compounds, as it preserves their functionality, maintains the material’s properties, and allows better food contact and controlled release of actives (Bastarrachea et al., 2015; John et al., 2023). Several techniques including spraying, electrospraying, dipping, cast coating, chemical vapor deposition, physical vapor deposition, roll-to-roll, and screen printing have been used for coating applications (Vasile, 2018). For example, natural plant polyphenol proanthocyanidins and layered clays were incorporated into poly (vinyl alcohol)-based coatings applied to corona-treated polylactic acid (PLA) films using an automatic wire-bar coater, which significantly improved both active functions and gas barrier properties (Wang et al., 2023). In another study, cellulose nanocrystals modified with methacrylamide, cetyltrimethylammonium bromide, or zinc oxide were spray-coated onto PLA films, resulting in excellent antibacterial activity against S. aureus and E. coli, improved mechanical properties, reduced gas permeability, faster compostability, and extended pork shelf life (Huang et al., 2023).

Therfore, the present study aimes to develop a bioactive coating based on artichoke leaf extract (ALE), a valorized food loss stream, combined with carboxymethyl cellulose (CMC), applied to PLA-based food containers. The functional and physical properties of the coated packaging were then evaluated.

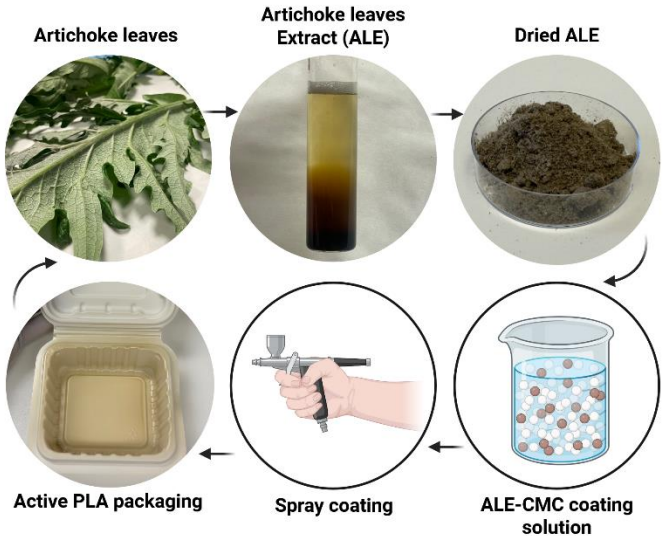

Figure 1: Circular valorization of artichoke leaves extract in active food packaging

2 MATERIALS AND METHODS

2.1 Prepartion of active packaging

ALE was obtained using subcritical water extraction technique at 150 °C and biomass to water ratio of 1:10 (g:mL) at two cycles of 20 min (1500 psi). The freeze-dried fraction obtained from second cycle was utilized in this research. In order to enhance the surface activity of the PLA-based clamshells before applying the active coating, it was modified by spraying the solution of 1 % (w/v) of PLA containing 20 % (w/w) of polyethylene glycol (PEG) on the surface of PLA clamshells using an airbrush connected to a vacuum air pump. Then, the coating solutions were prepared by mixing different ratios of CMC and ALE (e.i. 100:00, 70:30, 60:40, 50:50 w/w) and 30% (w/w) glycerol. The coating soultion was spayed at several layers on the modified PLA surface at distance of 15 cm and pressure of 2.5 bar (Figure 2).

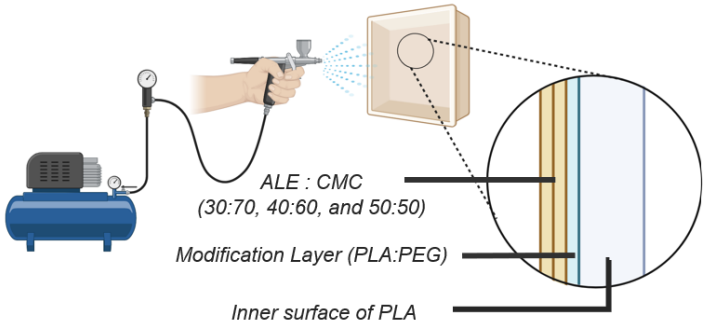

Figure 2: Development of active layers composing of ALE and CMC on PLA based packaging using spary coating

2.2 Characterization of active packaging

The contact angle measurement was carried out using a tensiometer to investigate how surface modification affected the surface hydrophilicity of PLA-based clamshells. The surface microstructure and the morphology of the cross-section of the PLA-based clamshells before and after coating was observed by scanning electron microscopy (SEM). Active packaging were then charactirized for their color, hygroscopicity, water vapor permeability (WVP), antioxidant activity, and antibacterial activities.

3 RESULTS AND DISCUSSION

Surface modification of PLA packaging by sparying PLA-PEG prior to applying active layer enhanced the wettability of the container surface to interact with the active coating layer. PLA-PEG modifying solution was compatible with the beneath PLA surface and including the PEG as shown in Figure 3 enhanced the surface hydrophilicity compared to the control samples by decreasing the contact angle.

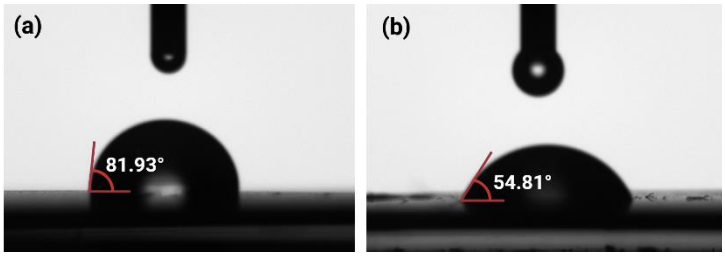

Figure 3: Water contact angle of PLA based packaging (a) before and (b) after surface modification

The inclusion of ALE in the coating solutions changed the color parameters of packaging surface as shown in Table 1. ALE significantly reduced the brightness of packaging. The a* factor showed all the films surface color were in greenish hue while the b* factor showed yellowish hue in all samples. Increasing the ALE content in the coating enhanced both reddish and yellowish color which might be due to the contribution of phenolic compounds in ALE to the coloration of coatings. The overall color change (ΔE) of samples compared to the uncoated PLA showed enhancing the differences by increasing the ALE concentration as it was also observed in visual appearance of the corresponding coated packaging.

Table 1: Color parameters and colour differences of uncoated and coated PLA packagings

Samples	***L****	***a****	***b****	***ΔE***
PLA-C	*84.98 ± 0.04 [a]*	*-1.83 ± 0.01[c]*	*3.26 ± 0.03 [f]*	*reference*
C:E (70:30)	*77.84 ± 0.50 [c]*	*-0.86 ± 0.05 [b]*	*14.41 ± 0.12 [c]*	*13.28 ± 0.30 [b]*
C:E (60:40)	*76.16 ± 0.30 [d]*	*-0.63 ± 0.05 [a]*	*16.29 ± 0.33 [b]*	*15.79 ± 0.28 [a]*
C:E (50:50)	*76.31 ± 0.77 [d]*	*-0.66 ± 0.12 [a]*	*16.70 ± 0.31 [a]*	*16.05 ± 0.56 [a]*

As shown in SEM images of uncoated and coated packaging (Figure 4), plain PLA presented a rough surface. CMC solution alone was not able to cover the whole surface (Figure 4e) due to higher viscosity and lower flowability. Substitution of ALE with CMC made a uniform and smooth coating covering the whole surface without any pores or cracks (Figure 4f). As shown in the cross-sectional SEM image, modification with PLA-PEG partially dissolved the underlying surface, and the thickness of the active layer was approximately 5 µm (Figure 4g).

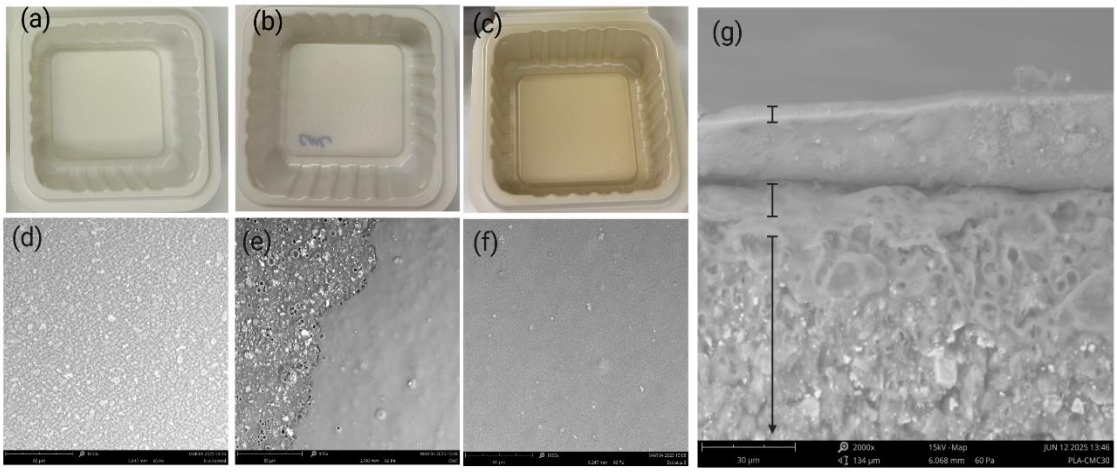

Figure 4. Photographs (top) and SEM images of surface morphology (down, magnification × 1000) of PLA-based packaging: (a,d) uncoated PLA, (b, e) coated with C:E (100:00), (c, f) coated with C:E (60:40), and (g) cross-sectional SEM image of coated PLA with C:E (70:30) representing different layers.

Regarding the WVP barrier, the uncoated PLA packaging showed the highest WVP values, while the surface modified PLA decreased the WVP significantly by 36%. Introduction of additional layers using CMC containing ALE could not reduce the WVP further due to the hydrophilic nature of active coating compound. The moisture absorption behavior of various coated and uncoated PLA samples exposed to 100% relative humidity over 10 days is presented in Figure 5. All samples exhibited an increasing trend in moisture uptake over time. The uncoated PLA sample demonstrated the lowest moisture absorption, reaching only 1.75% after 10 days. This limited uptake is due to the hydrophobic nature of PLA and the absence of sufficient polar functional groups capable of interacting with water molecules. In contrast, the active coated samples absorbed and retained significantly more moisture. This is attributed to the hydrophilic nature of both CMC and ALE. The presence of polar groups in these materials enhances water binding within the matrix. Substituting higher amounts of ALE with CMC led

to even greater moisture absorption, likely due to the combined effects of increased hydrophilicity and structural characteristics.

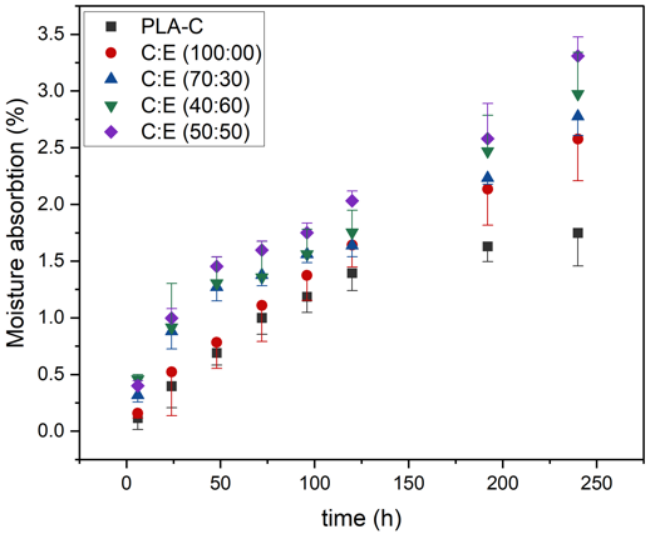

Figure 5. Moisture absorption behavior of various coated and uncoated PLA samples exposed to 100% relative humidity over 10 days

Antioxidant and antibacterial activity are crucial features of active packaging, helping preserve nutrients and food quality, while also inhibiting microbial growth to extend the shelf life and safety of food products. The coated packaging was tested over time by additional free radicals. After 15 min incubation in the presence of DDPH radicals, only ALE-coated samples showed 40–44% scavenging. Increasing the incubation time to 45 min in presence of additional radicals, showed higher antioxidant scavenging activity (54–67%), attributed to gradual ALE release and its phenolic and flavonoid content. Active packaging also combated microbial contamination. Uncoated PLA and CMC-only coatings had negligible antibacterial effects, while ALE coatings exhibited concentration-dependent inhibition of E. coli (0.9–2.1 log reduction) and moderate reduction of S. aureus (~1 log). ALE polyphenols likely cause bacterial cell death by disrupting membranes.

4 CONCLUSIONS

This study demonstrate the successful development of active packaging by coating PLA material with ALE. Surface modification of PLA improved the adhesion of active layers and enhanced the water vapor barrier properties. Coating with CMC/ALE solutions produced uniform, defect-free layers that provided sustained antioxidant activity and concentration-dependent antibacterial effects. These bioactive properties underline the potential of valorizing food loss into sustainable active packaging solutions that preserves food quality and extends shelf life.

Acknowledgments: *This project was supported by funding from the European Union's Horizon 2020 research and innovation programme under Grant Agreement No. 101037796.*

5 REFERENCES

Bastarrachea, L.J., Wong, D.E., Roman, M.J., Lin, Z., Goddard, J.M., 2015. Active packaging coatings. Coatings 5, 771–791.

Bhargava, N., Sharanagat, V.S., Mor, R.S., Kumar, K., 2020. Active and intelligent biodegradable packaging films using food and food waste-derived bioactive compounds: A review. Trends Food Sci Technol 105, 385–401.

Bittencourt, G.M., dos Reis Simprônio, M., Mothé, I.R., Ferreira, G.R., de Oliveira, A.L., 2023. Globe artichoke leaf extracts and production of phytotherapeutic solid lipid particles using high pressure technologies. J Supercrit Fluids 201, 106028.

Caldeira, C., De Laurentiis, V., Corrado, S., van Holsteijn, F., Sala, S., 2019. Quantification of food waste per product group along the food supply chain in the European Union: a mass flow analysis. Resour Conserv Recycl 149, 479–488.

Eurostat, 2022. First EU-wide monitoring of food waste: 127 kg per inhabitant in the EU in 2020 .

FAO, G., 2011. Global food losses and food waste–Extent, causes and prevention. SAVE FOOD: An initiative on food loss and waste reduction 9, 2011.

Huang, S., Zou, S., Wang, Y., 2023. Construction of compostable packaging with antibacterial property and improved performance using sprayed coatings of modified cellulose nanocrystals. Carbohydr Polym 305, 120539.

John, A., Črešnar, K.P., Bikiaris, D.N., Zemljič, L.F., 2023. Colloidal solutions as advanced coatings for active packaging development: Focus on PLA systems. Polymers (Basel) 15, 273.

Momtaz, M., Momtaz, E., Mehrgardi, M.A., Momtaz, F., Narimani, T., Poursina, F., 2024. Preparation and characterization of gelatin/chitosan nanocomposite reinforced by NiO nanoparticles as an active food packaging. Sci Rep 14, 519.

Read, Q.D., Brown, S., Cuéllar, A.D., Finn, S.M., Gephart, J.A., Marston, L.T., Meyer, E., Weitz, K.A., Muth, M.K., 2020. Assessing the environmental impacts of halving food loss and waste along the food supply chain. Science of the Total Environment 712, 136255.

Riaz, S., Maan, A.A., Butt, M.S., Khan, M.K.I., 2024. Valorization of agricultural residues in the development of biodegradable active packaging films. Ind Crops Prod 215, 118587.

Vasile, C., 2018. Polymeric nanocomposites and nanocoatings for food packaging: A review. Materials 11, 1834.

Wang, C., Mao, L., Yao, J., Zhu, H., 2023. Improving the active food packaging function of poly (lactic acid) film coated by poly (vinyl alcohol) based on proanthocyanidin functionalized layered clay. LWT 174, 114407.

OPTIMIZATION OF FILMS FOR ENHANCED BARRIER PROPERTIES OF BIODEGRADABLE PACKAGING

Yasaman Ghasemi[1], Mia Kurek [2], Maria-Jose Fabra [3], Nasreddine Benbettaieb [1,4] and Frédéric Debeaufort [1,4]

[1]Joint research unit UMR PAM, Université Bourgogne Europe, Institut Agro, INRAE, Dijon, France.
[2] Faculty of Food Technology and Biotechnology, University of Zagreb, Zagreb, Croatia
[3] Instituto de Agroquímica y Tecnología de Alimentos (IATA), Consejo Superior de Investigaciones Cientificas, C/ Catedrático Agustín Escardino 7, Paterna (Valencia), Spain.
[4] Department of BioEngineering, IUT-Dijon-Auxerre, Université Bourgogne Europe, Dijon, France

doi: 10.5281/zenodo.17294500
frederic.debeaufort@ube.fr

Abstract: *Fresh foods are sensitive to oxidation and spoilage. If sustainable biopackaging are wished, these require performing barrier properties that need to be optimized for instance by coating applications. Blending of hydrocolloids and other biopolymers to form interpenetrated network coatings is one of the strategies to improve oxygen and moisture barrier efficacy of cellulosic or biodegradable materials. Gelatin, psyllium, and zein have been associated to reach the permeability value targetted.*

Keywords: biodegradable packaging, barrier properties, oxygen permeability, water vapour permeability, surface wettability

1 INTRODUCTION

The environmental issue of plastic pollution has led the scientific community to explore sustainable alternatives, including edible films and coatings. These materials, made from natural biopolymers, have the advantage of being biodegradable, renewable, and sometimes functional, actively contributing to food preservation (Azeredo & Waldron, 2016; Pavlath & Orts, 2009). Among them, films based on gelatin, zein, and psyllium are attracting growing interest, each offering specific properties that are useful in the field of active and intelligent packaging.

Gelatin, derived from collagen, is widely studied for film manufacturing due to its good gelation properties and ability to form homogeneous polymer networks. It provides excellent transparency and good retention capacity for active additives (antioxidants, antimicrobials, freshness indicators (Chen et al., 2023; Sobral et al., 2001). However, its hydrophilic nature limits its mechanical strength and stability in humid conditions (Kchaou et al., 2018; Krishna et al., 2012). To overcome these limitations, gelatin is often combined with other more resistant or hydrophobic biopolymers. It is in this context that zein and psyllium are of strategic interest: the former for its barrier and rigidity properties, the latter for its fibrous and functional characteristics (Coltelli et al., 2016).

Zein is a prolamin protein derived from corn, characterized by a high content of non-polar amino acids (Lawton, 2002). This structure gives it a natural hydrophobicity that is rare among proteins, making it a major asset for food packaging. Unlike gelatin, zein forms films that are less sensitive to moisture

and provide an effective barrier against oxygen and fats (Ghanbarzadeh & Almasi, 2013). In addition, zein films are distinguished by their rigidity and good adhesion to food surfaces, making them suitable as protective coatings on fruit, confectionery, or meat (Lan et al., 2023). Their compatibility with aqueous-alcoholic solvents also facilitates the incorporation of lipophilic bioactive molecules (essential oils, polyphenols) into a stable matrix. Studies have shown that incorporating antioxidant-rich plant extracts (e.g., pomegranate or green tea) into zein films allows for controlled and prolonged release of the active compounds, helping to delay lipid oxidation in meat products (Figueroa-Lopez, Enescu, et al., 2020; Figueroa-Lopez, Torres-Giner, et al., 2020; Wang et al., 2022). It is therefore regularly considered as a coating solution for materials with very low barrier properties (Kansal et al., 2020). Another advantage is zein's ability to form nanoparticles and nanofibers via electrospinning, paving the way for smart, active films that can, for example, incorporate freshness indicators or encapsulated antimicrobials (Cheng et al., 2024).

Psyllium (Plantago ovata, Plantago psyllium) is a source of mucilage rich in soluble and insoluble polysaccharides. These polysaccharides, particularly arabinoxylan, form viscoelastic gels capable of retaining large amounts of water (Ahmadi et al., 2012). This property gives psyllium a remarkable ability to produce flexible films and improve the mechanical texture of composite films when combined with other polymers. The most distinctive contribution of psyllium is its ability to form fibrous networks that reinforce the cohesion and tensile strength of films (Krystyjan et al., 2017; Niknam et al., 2019). Recent work has explored the use of psyllium in synbiotic films, where it plays a dual role: film-forming matrix and prebiotic. For example, the combination of psyllium and other hydrocolloids has made it possible to develop edible films that can encapsulate live probiotics while maintaining their viability for fruit, meat or dairy products applications without sensory alteration (Aslan Kaya et al., 2025a, 2025b).

The combination of gelatin with zein and psyllium offers interesting prospects. Zein compensates for gelatin's low moisture resistance with its hydrophobic properties. Psyllium strengthens the mechanical structure and adds nutritional value to the films. Together, these biopolymers can be used to design multifunctional films (barrier, active, smart, nutritional) suitable for various food products.

The objective of our work is to evaluate the functional properties of gelatin-based coatings combined with zein or psyllium for paper impregnation.

2 MATERIALS AND METHODS

2.1 Sample materials

Fish gelatin (Louis François, France), psyllium fiber (Louis François, France), glycerol (>99%, Sigma-Aldrich), ethanol (>99.7%, Sigma-Aldrich), acetic acid (>99.5%, Sigma-Aldrich), and zein (Sigma-Aldrich) were used for the preparation of biopolymer films. All reagents were of analytical grade and used without further purification.

2.2 Film making

A film-forming solution was prepared by dissolving 7.4 g of gelatin and 0.8 g of zein in 100 mL of 60% (v/v) aqueous acetic acid under continuous stirring until complete solubilization of the proteins. After dissolution, 1 g of glycerol was added as a plasticizer and thoroughly mixed into the solution.

For gelatin-psyllium films, 7.4 g of gelatin and 0.8 g of psyllium were dissolved in 100 mL of distilled water preheated to 60 °C. A few drops of acetic acid were added to adjust the pH, and the mixture was stirred until complete dispersion. Glycerol (1 g) was then incorporated under constant agitation.

Both film-forming solutions were cast onto non-stick square Petri dishes (12 × 12 cm) and left to dry under ambient conditions until complete solvent evaporation. The resulting films were carefully peeled off the casting surfaces and stored in desiccators for subsequent characterization. The average film thicknesses was measured using a digital caliper and values were for gelatin–zein 0.25±0.03 mm, for gelatin–psyllium 0.15±0.02 mm, and for gelatin 0.07±0.03 mm.

2.3 Film characterizations

All the characterizations have been done at 25°C and 50% RH as they refers to EU standards (ISO) and allow to mimic ambiant conditions, and not to the US methods (ASTM).

The surface morphology of the films was examined after gold coating by sputtering using a scanning electron microscope using 5-15 kV and max 0.1Pa (SU1510, Hitachi, Japan) to observe structural features and homogeneity.

Mechanical properties were determined with a universal traction testing machine (TA.HD plus, Stable MicroSystems, England) equipped with a 300 N load cell, following the ISO 527-3. Rectangular specimens (2.5 × 8 cm^2) were prepared with a precision cutter, equilibrated for two weeks at 25 °C and 50% RH, and stretched uniaxially at 50 mm/min until rupture; tensile strength (TS) and Young's modulus (YM) were calculated from the stress – strain curves, with five replicates per formulation tested at 25 ± 2 °C.

Water vapor permeability (WVP) was measured gravimetrically according to the standard method (ISO 2528 - International Standard Organisation, 2017) using a relative humidity gradient of 33–84% at 25 °C according to the method adapted for hydrophilic polymers (Debeaufort et al., 1993). The values were obtained by recording the weight loss of test cells sealed with the films and corrected for film thickness and vapor pressure difference.

Contact angle measurements were carried out with a DSA30 goniometer (Kruss, Germany) using eleven liquids of different polarities, including water, glycerol, ethylene glycol, ethanol (96% v/v), and selected binary mixtures (water–ethanol, water–ethylene glycol, and glycerol–ethanol) at varying ratios. Initial contact angles and their kinetics were recorded, and the surface free energy (SFE) of the films, including its polar and dispersive components, was calculated using the Owens–Wendt–Rabel–Kaelble (OWRK) method (Owens & Wendt, 1969). The critical surface tension (CST) of wetting was estimated according to Zisman's extrapolation method (Zisman, 1964).

3 RESULTS AND DISCUSSION

As shown in Figure 1, the gelatin–psyllium forming solution exhibited markedly higher viscosity than the gelatin–zein system. This suggests that psyllium incorporation enhances solution thickness due to stronger intermolecular interactions and greater water-binding capacity compared to zein.

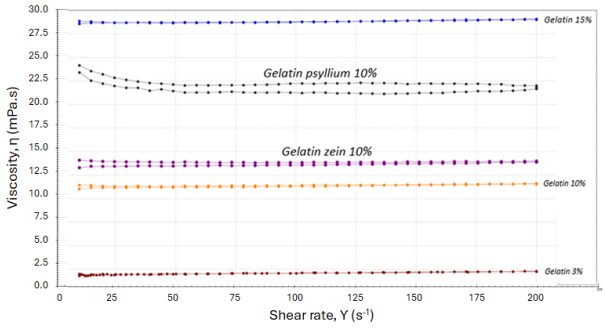

Figure 1: Viscosity of gelatin and gelatin based systems with additives (MPa·s)

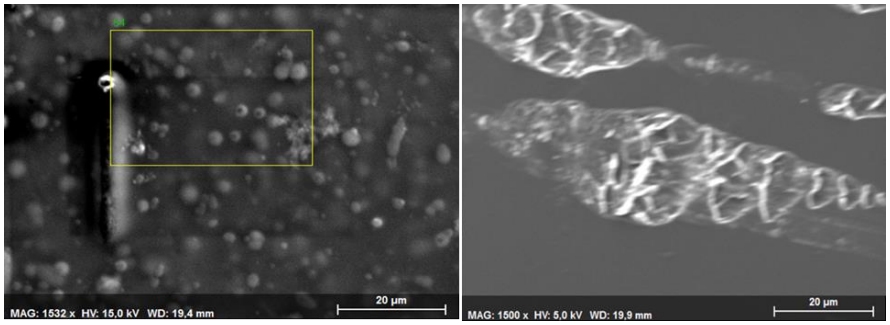

Figure 2: SEM micrographs of gelatin–zein (left) and gelatin–psyllium (right) films at 1500× magnification

The SEM micrographs showed clear differences in surface morphology between the films. Gelatin–psyllium displayed a fibrous network structure, indicating that some psyllium fibers were not fully dissolved, with fibers measuring about 20 µm in width and 80 µm in length. In contrast, gelatin–zein presented dot-like domains, likely caused by phase separation due to the limited miscibility between hydrophilic gelatin and hydrophobic zein, resulting in small, precipitated particles of about 2–5 µm (Figure 2).

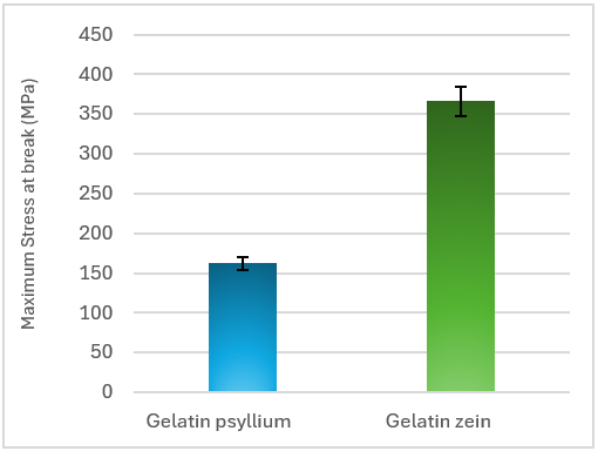

Figure 3: Tensile strength of gelatin–zein and gelatin–psyllium films

As shown in Figure 3, the mechanical properties of the films were strongly influenced by composition. Gelatin–zein films exhibited a much higher tensile strength (maximum stress at break = 366 MPa). For comparison, fish gelatin films without additional components have been reported to exhibit a tensile strength of only 4.3±0.5 MPa, highlighting the reinforcing effect of both zein (>350 MPa) and psyllium (>150 Mpa). Even if psyllium was less efficient than zein to increase tensile strength, it allowed to rise by almost 35 times gelatine-based films mechanical resistance to break. This suggests gelatin–zein films are better suited for applications requiring high mechanical durability, whereas gelatin–psyllium films, despite lower strength, may provide greater flexibility, which is beneficial where elasticity is desired.

The oxygen permeability of the films clearly depended on the film composition and structure. Gelatin–zein films showed the lowest oxygen permeability (0.98×10^{-12} $cm^3 \cdot m.m^{-2} \cdot s^{-1} \cdot Pa^{-1}$), indicating the best oxygen barrier, while gelatin –psyllium films were more permeable (2.46×10^{-12}). For comparison, pure gelatin had an even lower oxygen permeability of 0.148×10^{-12}. These results show that adding zein improves oxygen resistance compared to psyllium, making gelatin–zein films more suitable for protecting oxygen-sensitive foods (Figure 4). The water vapor permeability (WVP) values indicate that gelatin-zein films (9.6×10^{-11} $g.m.m^{-2}.s^{-1}.Pa^{-1}$) have the lowest barrier to moisture transfer, followed by gelatin-psyllium (3.3×10^{-11}) and pure gelatin films (2.6×10^{-11}). It is most probable the particle dispersion of zein, thought it is hydrophobic, does not affect the moisture transfer throught the

continuous layer of gelatine, explaining why it is worst as a barrier. Moreover, psyllium also favoured the moisture transfer, maybe acting s a moisture absorbent. Overall, the results demonstrate that the choice of zein or psyllium addition in gelatin films cannot effectively modulate in the expected trend their moisture barrier properties.

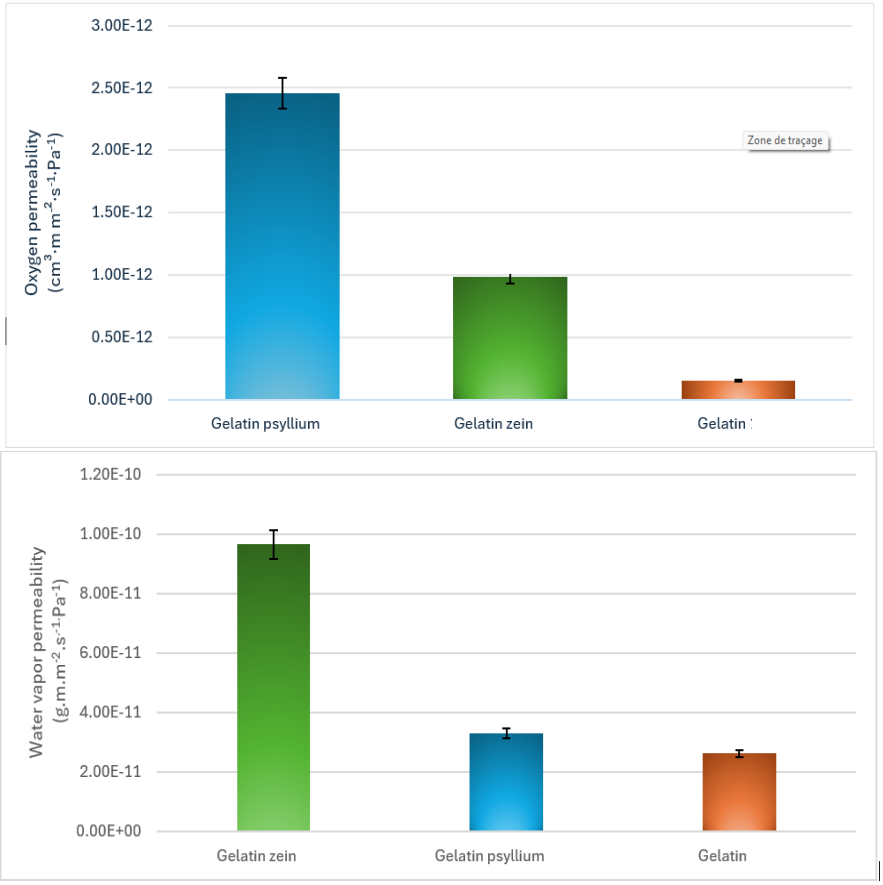

Figure 4: Oxygen and water vapour permeability of films

Table 1: surface properties of films

Film name	***Initial contact angle °***	***critical surface tension (mN.m^{-1})***	***Polar/dispersive ratio***
Gelatin–Psyllium 10%	*117*	*25.51*	*0.22*
Gelatin–Zein 10%	*124*	*18.77*	*0.06*
Gelatin 10%	*120*	*28.95*	*0.00*

The surface properties of the films were also influenced by the incorporation of Psyllium or zein. Contact angle measurements, surface free energy (SFT), and the polar/dispersive component ratio indicated significant differences in wettability and surface characteristics. The higher critical surface tension of gelatin–psyllium (25.5 mN.m^{-1}) compared to gelatin–zein (18.9) suggests that gelatin–psyllium films are more hydrophilic, exhibiting higher water wettability, whereas gelatin–zein films seems slightly hydrophobic (Figure 5). Indeed, the highe the critical surface tension means liquids of about 30 mN.m^{-1} are most suitable to spread and wet surface of films, and for instance, ethanol which value is 22 mN.m^{-1} is most probable adapted to gelatin zein that is more hydrophobic. This is consistent with the observed contact angle and surface energy values, where the increased polar component in gelatin–psyllium enhances interactions with water, while the higher dispersive component in gelatin–zein reduces surface affinity toward polar liquids (Table 1).

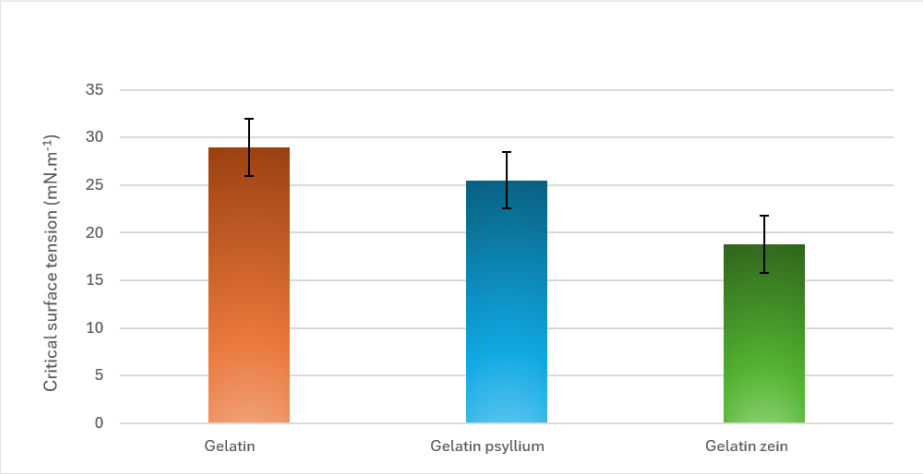

Figure 5: critical surface tension of films

4 CONCLUSIONS

In summary, the incorporation of psyllium and zein into gelatin films produced distinct effects on their structural, mechanical, and barrier properties. Psyllium increased viscosity and generated a fibrous surface morphology, resulting in more flexible and hydrophilic films with greater water wettability, though at the expense of tensile strength and oxygen resistance. Conversely, zein enhanced mechanical strength and oxygen barrier properties, forming a more homogeneous but slightly hydrophobic structure. However, neither additive improved water vapor permeability in the expected manner, as both facilitated moisture transfer through the gelatin matrix. Overall, the choice between psyllium and zein depends on the intended application: gelatin–zein films are better suited for high-strength, oxygen-sensitive packaging, while gelatin–psyllium films may be advantageous where flexibility and hydrophilicity are desired.

Acknowledgments: *The authors address a particular thanks to Adrien Lerbret, for their technical support in some experiments. For the French partner, this work was mansily supported by the Horizon Europe Prima project EVOLVEPACK (PCI2024-153409 funded by MICIU/AEI/10.13039/501100011033) and by the French National Reaserch Agency (ANR-24-P013-0008-04) and partly supported by the Conseil Régional de Bourgogne Franche-Comté and the European Union through the PO FEDER-FSE Bourgogne 2021-2027 programs who invest in lab equipment.*

5 REFERENCES

Ahmadi, R., Kalbasi-Ashtari, A., Oromiehie, A., Yarmand, M.-S., & Jahandideh, F. (2012). Development and characterization of a novel biodegradable edible film obtained from psyllium seed (Plantago ovata Forsk). Journal of Food Engineering, 109(4), 745-751. https://doi.org/10.1016/j.jfoodeng.2011.11.010

Aslan Kaya, D., Ceylan, H. G., & Atasoy, A. F. (2025a). Probiotic Edible Films Supplemented with Psyllium (Plantago ovata) Mucilage Containing Lacticaseibacillus rhamnosus GG : Coating for Fresh Apple Slices. Food and Bioprocess Technology, 18(2), 1692-1706. https://doi.org/10.1007/s11947-024-03556-0

Aslan Kaya, D., Ceylan, H. G., & Atasoy, A. F. (2025b). Probiotic Edible Films Supplemented with Psyllium (Plantago ovata) Mucilage Containing Lacticaseibacillus rhamnosus GG : Coating for Fresh Apple Slices. Food and Bioprocess Technology, 18(2), 1692-1706. https://doi.org/10.1007/s11947-024-03556-0

Azeredo, H. M. C., & Waldron, K. W. (2016). Crosslinking in polysaccharide and protein films and coatings for food contact – A review. Trends in Food Science & Technology, 52, 109-122. https://doi.org/10.1016/j.tifs.2016.04.008

Chen, L., Qiang, T., Ren, W., Tian, Q., Zhang, X., & Zhang, H. J. (2023). Strong, water-repellent, and recyclable gelatin-based bioplastic film as sustainable express packaging film. Journal of Cleaner Production, 385, 135705. https://doi.org/10.1016/j.jclepro.2022.135705

Cheng, E., Zhang, M., Xiang, L., Xiang, A., & Zhou, H. (2024). Edible antibacterial gelatin/zein fiber films loaded with cinnamaldehyde for extending the shelf life of strawberries by electrospinning approach. Food Bioscience, 60, 104329. https://doi.org/10.1016/j.fbio.2024.104329

Coltelli, M.-B., Wild, F., Bugnicourt, E., Cinelli, P., Lindner, M., Schmid, M., Weckel, V., Müller, K., Rodriguez, P., Staebler, A., Rodríguez-Turienzo, L., & Lazzeri, A. (2016). State of the Art in the Development and Properties of Protein-Based Films and Coatings and Their Applicability to Cellulose Based Products : An Extensive Review. Coatings, 6(1), 1. https://doi.org/10.3390/coatings6010001

Debeaufort, F., Martin-Polo, M., & Voilley, A. (1993). Polarity Homogeneity and Structure Affect Water Vapor Permeability of Model Edible Films. Journal of Food Science, 58(2), Article 2. https://doi.org/10.1111/j.1365-2621.1993.tb04290.x

Figueroa-Lopez, K. J., Enescu, D., Torres-Giner, S., Cabedo, L., Cerqueira, M. A., Pastrana, L., Fuciños, P., & Lagaron, J. M. (2020). Development of electrospun active films of poly(3-hydroxybutyrate-co-3-hydroxyvalerate) by the incorporation of cyclodextrin inclusion complexes containing oregano essential oil. Food Hydrocolloids, 108, 106013. https://doi.org/10.1016/j.foodhyd.2020.106013

Figueroa-Lopez, K. J., Torres-Giner, S., Angulo, I., Pardo-Figuerez, M., Escuin, J. M., Bourbon, A. I., Cabedo, L., Nevo, Y., Cerqueira, M. A., & Lagaron, J. M. (2020). Development of Active Barrier Multilayer Films Based on Electrospun Antimicrobial Hot-Tack Food Waste Derived Poly(3-hydroxybutyrate-co-3-hydroxyvalerate) and Cellulose Nanocrystal Interlayers. Nanomaterials, 10(12), 2356. https://doi.org/10.3390/nano10122356

Ghanbarzadeh, B., & Almasi, H. (2013). Biodegradable Polymers. In R. Chamy (Éd.), Biodegradation—Life of Science. InTech. https://doi.org/10.5772/56230

ISO 2528 - International Standard Organisation. (2017). ISO 2528:2017 Sheet materials—Determination of water vapour transmission rate (WVTR)—Gravimetric (dish) method. ISO. https://www.iso.org/cms/render/live/en/sites/isoorg/contents/data/standard/07/23/72382.html

Kansal, D., Hamdani, S. S., Ping, R., Sirinakbumrung, N., & Rabnawaz, M. (2020). Food-Safe Chitosan–Zein Dual-Layer Coating for Water- and Oil-Repellent Paper Substrates. ACS Sustainable Chemistry & Engineering, 8(17), 6887-6897. https://doi.org/10.1021/acssuschemeng.0c02216

Kchaou, H., Benbettaïeb, N., Jridi, M., Abdelhedi, O., Karbowiak, T., Brachais, C.-H., Léonard, M.-L., Debeaufort, F., & Nasri, M. (2018). Enhancement of structural, functional and antioxidant properties of fish gelatin films using Maillard reactions. Food Hydrocolloids, 83, 326-339. https://doi.org/10.1016/j.foodhyd.2018.05.011

Krishna, M., Nindo, C. I., & Min, S. C. (2012). Development of fish gelatin edible films using extrusion and compression molding. Journal of Food Engineering, 108(2), 337-344. https://doi.org/10.1016/j.jfoodeng.2011.08.002

Krystyjan, M., Khachatryan, G., Ciesielski, W., Buksa, K., & Sikora, M. (2017). Preparation and characteristics of mechanical and functional properties of starch/Plantago psyllium seeds mucilage films. Starch - Stärke, 69(11-12), 1700014. https://doi.org/10.1002/star.201700014

Lan, X., Zhang, X., Wang, L., Wang, H., Hu, Z., Ju, X., & Yuan, Y. (2023). A review of food preservation based on zein : The perspective from application types of coating and film. Food Chemistry, 424, 136403. https://doi.org/10.1016/j.foodchem.2023.136403

Lawton, J. W. (2002). Zein : A History of Processing and Use. Cereal Chemistry, 79(1), 1-18. https://doi.org/10.1094/CCHEM.2002.79.1.1

Niknam, R., Ghanbarzadeh, B., Ayaseh, A., & Hamishehkar, H. (2019). Plantago major seed gum based biodegradable films : Effects of various plant oils on microstructure and physicochemical properties of emulsified films. Polymer Testing, 77, 105868. https://doi.org/10.1016/j.polymertesting.2019.04.015

Owens, D. K., & Wendt, R. C. (1969). Estimation of the surface free energy of polymers. Journal of Applied Polymer Science, 13(8), 1741-1747. https://doi.org/10.1002/app.1969.070130815

Pavlath, A. E., & Orts, W. (2009). Edible Films and Coatings : Why, What, and How? In K. C. Huber & M. E. Embuscado (Éds.), Edible Films and Coatings for Food Applications (p. 1-23). Springer New York. https://doi.org/10.1007/978-0-387-92824-1_1

Sobral, P. J. A., Menegalli, F. C., Hubinger, M. D., & Roques, M. A. (2001). Mechanical, water vapor barrier and thermal properties of gelatin based edible films. Food Hydrocolloids, 15(4), 423-432. https://doi.org/10.1016/S0268-005X(01)00061-3

Wang, D., Sun, J., Li, J., Sun, Z., Liu, F., Du, L., & Wang, D. (2022). Preparation and characterization of gelatin/zein nanofiber films loaded with perillaldehyde, thymol, or ε-polylysine and evaluation of their effects on the preservation of chilled chicken breast. Food Chemistry, 373, 131439. https://doi.org/10.1016/j.foodchem.2021.131439

Zisman, W. A. (1964). Relation of the Equilibrium Contact Angle to Liquid and Solid Constitution. In F. M. Fowkes, Contact Angle, Wettability, and Adhesion (Vol. 43). American Chemical Society. https://doi.org/10.1021/ba-1964-0043

BIOWAX IMPREGNATION OF FLEXIBLE PACKAGING PAPERS WITH HIGH TRANSPARENCY AND RECYCLABILITY

Pieter Samyn[1], Dave Stappaerts[2], Jef Van Dun[2]

[1]SIRRIS – Department Innovations in Circular Economy and Renewable Materials, Gaston Geenslaan 8, B-3001 Leuven, Belgium

[2]ACE Packaging and Technologies – Industrieterrein, Diest, Belgium

doi: 10.5281/zenodo.17294552
pieter.samyn@sirris.be

Abstract: *Papers are preferably used as renewable materials for flexible packaging where barrier resistance, transparency, and recyclability are required. In replacement of traditional transparent packaging papers with integrated window of a polymer film, a new method has been optimized by local impregnation of the paper with biowax in an industrial roll-to-roll process. In this study, a range of biowaxes was screened in relation with their processing conditions to improve transparency of impregnated papers. However, the paper structures impregnated with a hydrophobic biowax and intimate interaction between cellulose fibers, might pose challenges in the recycling: the fiber clogging and permanent deposition of wax during repulping may possibly interfere with the recycling process. Following the Harmonised European laboratory test method to generate parameters enabling the assessment of the recyclability of paper and board products in recycling mills with conventional process (Part I)", version February 2024, it has been successfully demonstrated that impregnated biowaxes papers give positive technical recyclability scores (T = 91 to 98), with extremely high total fiber yield (> 99 %). In parallel with optimizing impregnation and recycling processes, the intrinsic properties of selected biowax types remain critical for best performance.*

Keywords: paper, packaging, transparent, recyclable, impregnation, biowax.

1 INTRODUCTION

The European Union's Single-Use Plastics Directive represents a landmark policy aimed at reducing the environmental impact of plastic waste, particularly from items designed for single use (EU 2019/904). While the directive primarily targets plastic products, it also addresses plastic-coated papers by encouraging the development and adoption of sustainable alternatives, while their functionalities as a flexible packaging material should remain (Lin et al., 2012). In this context, recyclable transparent papers are emerging as a promising substitute for conventional plastic films used in packaging, labelling, and wrapping, or flexible electronics, sensors and light-emitting devices (Ling et al., 2020). The use of innovative materials from cellulose and renewable sources may offer transparency and barrier properties while being compatible with paper recycling streams and promoting circular material flows.

As the opacity of conventional papers originates from the interaction of light with the heterogeneous structure of a porous fiber network causing scattering effects at the fiber-air interface, the micro-voids between the fibers may be reduced by calandering (Vernhes et al., 2009), internal crosslinking (He et al., 2024), or impregnation with substances of comparable refractive index (Asayama et al., 2024), such

as cellulose nanofibers (Huang et al., 2023), vitrimer polymers (Zhang et al., 2022), glycerol (Wang et al., 2022), polyvinyl alcohol (Zhao et al., 2023), or alternative thermosetting resins, such as limonene acrylates, and epoxy (Song et al., 2025). The ecological packaging papers trough impregnation with bio-waxes were still less explored (Jasiolek et al., 2021). As a replacement for traditional multimaterial papers with integrated transparent window of a polymer film, they can be developed at industrial scale for practical applications with preferential recyclability (Figure 1).

Figure 1: Illustration for application of biowax-impregnated paper as flexible bread bag with high transparency.

2 MATERIALS AND METHODS

2.1 Samples

An overview of reference materials and impregnated paper samples evaluated in this study is given in Table 1. A standard packaging grade paper (Flexpack Smooth, Starkraft, Pöls, Austria) with base grammage 35 g/m^2 was utilized as reference material of bleached kraft paper from 100% virgin fibers (sample 1). The glassine paper typically used as transparent paper grade (Crystal^{TM} Flexible, Ahlstrom-Munksjö, Espoo, Finland) with available base grammage of 32 g/m^2 is used as an industrial reference material available for transparent packaging applications (sample 2).

The standard papers were impregnated with either *(i)* a single type of synthetic "paraffin" wax (sample 3), and *(ii)* different types of biowax (samples 3 to 9), either covering one or two sides of the paper. The impregnation of a paper roll was done on an industrial pilot-scale roll-to-roll set-up under confidential conditions of temperature, pressure and contact times that were internally optimized in order to achieve maximized transparency. The non-disclosure of detailed processing conditions and wax compositions does not interfere with further implementation of the test results in this study, focusing on characterization of optical properties and recyclability of the impregnated papers.

Table 1: Sample characterization of impregnated papers with different types of biowax

Sample number	***Side 1***		***Side 2***	
1	*Reference non-impregnated paper*			
2	*Glassine paper*			
3	*Synthetic wax*	*8.0 g/m2*	-	
4	*Palm wax*	*8.0 g/m2*	-	
5	*Sunflower wax*	*8.0 g/m2*	-	
6	*Rapeseed wax*	*8.0 g/m2*	-	
7	*Castor wax*	*8.0 g/m2*	-	
8	*Castor wax*	*4.5 g/m2*	-	
9	*Castor wax*	*4.5 g/m2*	*Castor wax*	*3.5 g/m2*

2.2 Testing Methods

The optical properties of the paper samples were evaluated in terms of standard transparency measurements (ISO 2471:2008 Paper and board — Determination of opacity (paper backing)), and gloss measurements (ISO 8254-1:2009 Paper and board — Measurement of specular gloss). The transparency was determined on a UV-2450 spectrophotometer (Shimadzu, Kyoto, Japan), reporting the transmission value (%) in relation to a reference measurement on a fully transparent polymer film. The paper samples were measured with the incident light beam directed towards the impregnated

side of the paper. After recording the UV/VIS spectra in the wavelength region between 200 to 900 nm, the transmission value was determined at selected wavelength of 600 nm. The gloss was measured with a microgloss meter (BYK-Gardener Instruments, Geretsried, Germany) at an incident light angle of 80° normal to the paper surface, after calibration on a black reference sample. All transparency and gloss measurements were repeated at five places over an A4-size paper surface and reported as average values.

The recyclability was evaluated following the "Harmonised European laboratory test method to generate parameters enabling the assessment of the recyclability of paper and board products in recycling mills with conventional process (Part I)", version Febraury 2024. In short, the repulping of a 50 ± 1 g dry sample at a stock consistency of 2.5 % (total volume 2 liter) was done in a disintegrator (TLS TechLab Systems, Lezo, Spain) compliant with ISO 5263-1 at temperature = 40 ± 1°C , pH = 7 and number of revolutions = 30,000 corresponding to a minimum required time of 10 min. The screening was done for a pulp stock sample of 1.5 liter poured on a Somerville screen (TLS TechLab Systems, Lezo, Spain) without addition of a thickener. The coarse screening was performed while using a perforated plate containing holes with 5 mm diameter and a water flow of 8.6 l/min for 5 minutes. The fine screening was performed while using a plate with slots of 150 µm width and a water flow of 8.6 l/min for 20 minutes. The weight fractions of coarse rejects (CR) and fine rejects (FR) were determined after filtration and drying and reported as a percentage with respect to the dry weight of the sample. The results are expressed as a technical recyclability score (T) calculated according to the protocol from the total screening yield score (TSY), visual impurity score (VI) and sheet adhesion score (SA). A schematic summary of the operations for disintegration, screening and sheet formation is shown in Figure 2.

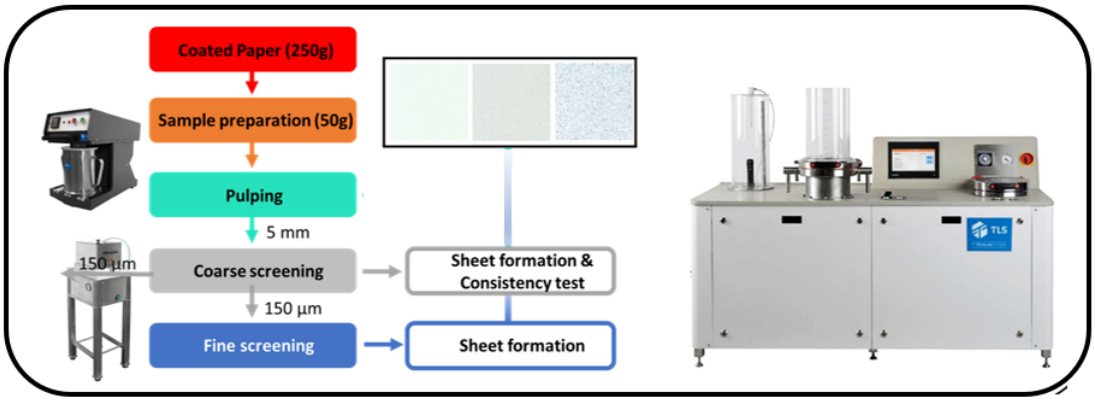

Figure 2: Flow diagram for recyclability assessment and evaluation of coated paper samples.

The microscopic images of impregnated paper samples and laboratory handsheets made from coarse accepts (CA) and fine accepts (FA) were made on a confocal laser scanning microscope at objective magnifications of 20x and 50x.

3 RESULTS AND DISCUSSION

3.1 Paper sample evaluation

The surface morphology of wax-impregnated papers is visualized in Figure 3, with various coverage of the surface and interfiber pores depending on the wax type and grammage. In contrast with traditional coatings processes, the impregnated papers do not have a continuous surface coating owing to the relatively low amounts of applied wax. The concentration of waxes corresponding to the required filling grade of the pores at both paper sides was calculated from a theoretical model for mesoporous

paper (Zhu et al., 2015) in line with the practically applied grammage of 8 g/m^2. The further analysis for chemical compatibility between the wax and fibers did not indicate chemical interactions.

The resulting transparency and values of surface gloss for the different wax-impregnated papers are summarized in Figure 4, indicating favorable increase in transparency relatively to the non-impregnated base paper (Figure 4a) and highest transparency for selected biowax types with either one- or two-sided impregnation (sample 7) approaching the values of 80 % for industrial transparent paper grades (sample 2). The latter confirms a good saturation of the pores in the paper structure though impregnation of the biowax at given concentration. The maximized gloss value (Figure 4b) for biowax impregnated papers exceeds industrial reference samples and confirms the formation of a homogeneous smooth surface after one-sided impregnation at highest wax concentration (sample 7).

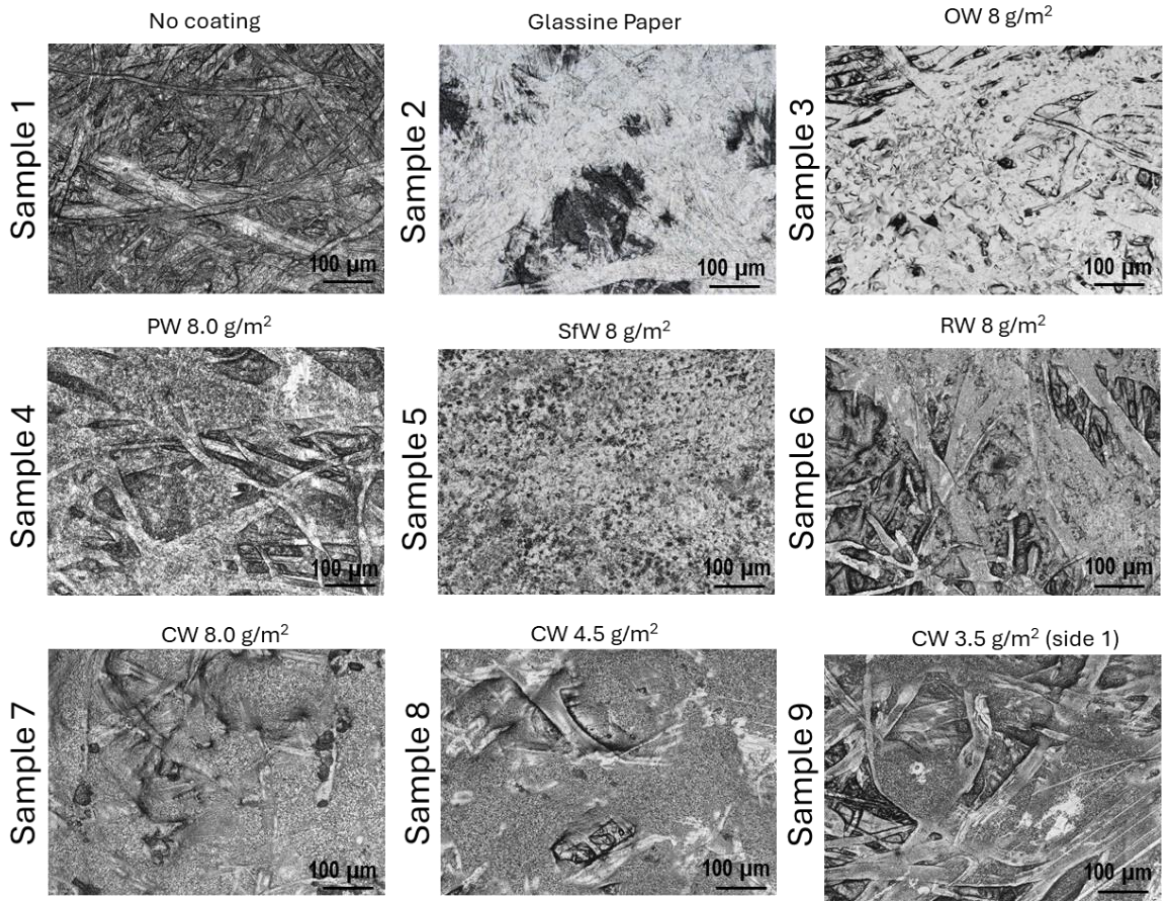

Figure 3: Microscopic evaluation of surfaces for reference papers and wax-impregnated paper samples.

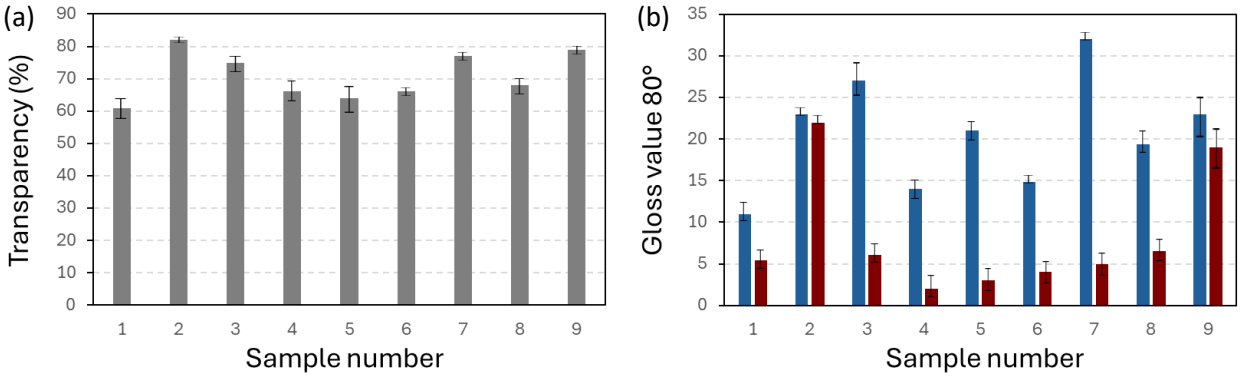

Figure 4: Optical evaluations of wax-impregnated paper samples, with (a) transparency (%) determined from UV/VIS spectroscopy, (b) gloss measurements with microgloss meter on side 1 (blue bars), side 2 (brown bar).

3.2 Recyclability assessment

The different parameters resulting from the recyclability assessment are given in Table 2. The total fiber yields are high (TSY > 98.5%) for best performing biowax impregnated papers (sample 5, 6, 7, 8, 9), as compared to synthetic wax (sample 3, TSY = 98.1 %) and industrial transparent paper (sample 2, TSI = 97.0 %). The main differences are seen in a strong reduction of coarse fiber rejects for biowax impreg-nated papers due to the absence of fiber clogging during repulping in contrast with poor recyclability of traditional wax-coated papers (Yadav et al., 2024). The sheet adhesion tests did not reveal any tackiness for all samples (SA level 1 corresponding to SA score 0): the handsheet can be separated completely from the carrier board and cover sheet without any damage or breakages.

As a result, the total recyclability scores T = 91 to 98 (samples 4, 5, 6, 7) for biowax impregnated papers exceed the acceptance limit T > 80, and perform better than papers with synthetic wax with (sample 3, T = 83). The recycling of papers with synthetic wax was also complicated by the deposition of a thick wax slurry in the water effluent after repulping. Main differences in T scores are observed by the influences of wax grammage and single/double sided impregnation (samples 7, 8, 9). The reduction in fine rejects for biowax impregnated papers is visually confirmed by the residues on the screen (Figure 5a, 5b), including single fibers and partly disintegrated sample material. The quality of the handsheets from coarse accepts and fine accepts (Figure 5c, 5d) indicates non-fibrous material impurities for samples 2, 3, 4 and high fiber qualities for samples 5, 6, 7 and 8. The visual impurities (VI score) can mainly be related to presence of few small translucent particles, according to a general overview of the quality of handsheets made from fine accepts with different VI scores (Figure 6).

Table 2: Test results of recyclability assessment

Sample number	***CR (%)***	***FR (%)***	***TSY (%)***	***VI score***	***SA score***	***T score***
1	*0.00*	*0.00*	*100*	*0*	*0*	*100*
2	*2.10*	*0.90*	*97.0*	*-5*	*0*	*80*
3	*1.02*	*0.85*	*98.1*	*-15*	*0*	*83*
4	*1.10*	*0.80*	*98.1*	*-5*	*0*	*91*
5	*0.53*	*0.78*	*98.7*	*-5*	*0*	*91*
6	*0.42*	*0.65*	*98.9*	*0*	*0*	*98*
7	*0.00*	*0.30*	*99.7*	*-5*	*0*	*94*
8	*0.20*	*0.30*	*99.5*	*-15*	*0*	*84*
9	*0.20*	*0.50*	*99.3*	*-15*	*0*	*84*

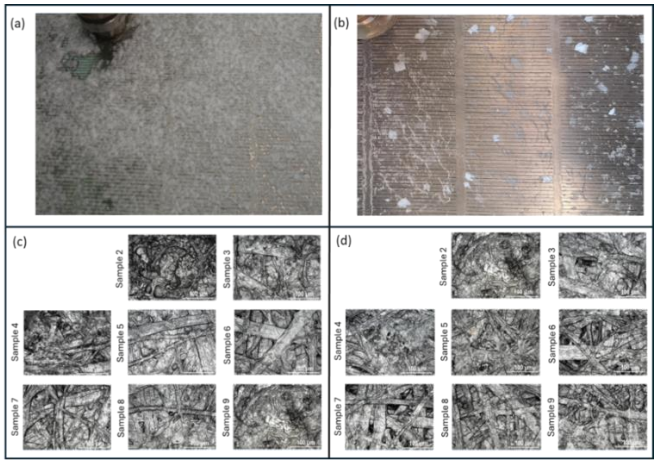

Figure 5: Evaluation of different fiber fractions after screening of the repulped fibers, (a) fine rejects (RF) on the 150 µm screen collected from sample 2 (synthetic wax), (b) fine rejects (RF) on the 150 µm screen collected from sample 7 (biowax), (c) microscopic evaluation of handsheets made from coarse accepts (AC), (d) microscopic evaluation of handsheets made from fine accepts (AF).

(a) (b) (c)

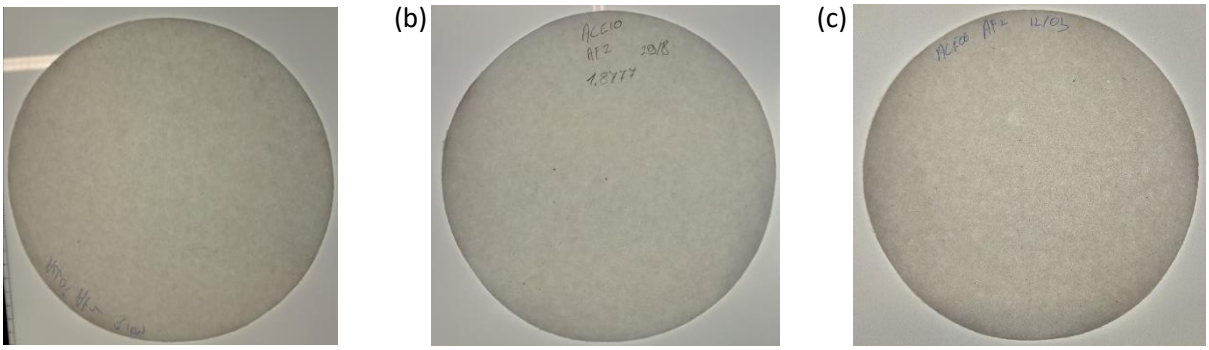

Figure 6: Illustration of handsheets from fine accepts with different VI scores, (a) VI level 1 (VI score 0, e.g. sample 6), (b) VI level 2 (VI score -5, e.g. sample 4), (c) VI level 3 (VI score -15, e.g. sample 8).

4 CONCLUSIONS

The biowax-impregnated papers provide a valuable alternative for flexible packaging papers with local insertion of transparent areas. Depending on the processing parameters and selection of appropriate biowax types, competitive transparency with industrial paper grades is demonstrated in parallel with superior recyclability scores. The technology can be upscaled for roll-to-roll processing in industry.

Acknowledgement: *This work was financially supported by the Flanders Innovation & Entrepreneurship Agency (VLAIO) in frame of the Nada-project (HBC.2022.0944).*

5 REFERENCES

EU2019/940 (2019): Directive of the european parliament and of the council on the reduction of the impact of certain plastic products on the environment, European Directive.

Asayama Y., Enomae T. (2024) Paper transparency technology and research on improving visual transparency. J. Imag. Soc. Japan 63, 44-56.

He Y., Ye H., Li H., Cui F., Xu F., You T. (2024) Multifunctional films with superior mechanical performance, transparency, antibacterial properties enabled by a physical and chemical dual crosslinking network construction. Chem. Eng. J. 479, 147546.

Huang Y., Kasuga T., Nogi M., Koga H. (2023) Clearly transparent and air-permeable nanopaper with porous structures consisting of TEMPO-oxidized cellulose nanofibers. RSC Adv. 13, 21494-21501.

Jasiolek A., Latka J., Brzezicki M. (2021) Biodegradable methods of impregnating paperboard for its use as a building material. Int. J. Sus. Eng. 14, 1081-1089.

Lin X., Fang Z., Zhao S., Zhang D., Liu Y., Qiu X. (2024) Super foldable transparent paper by regulating the multi-scale structure of cellulose fibers. Carbohydr. Polym., 346, 122610.

Ling H., Chen R., Huang Q., Shen F., Wang Y., Wang X. (2020) Transparent, flexible and recyclable nanopaper-based touch sensors fabricated via inkjet-printing. Green Chem., 22, 3208-3215.

Song Z., Liu G., Wang T., Wu J., Liu H., Li Z. (2025) Fabrication of flexible transparent paper substrate via epoxy resin impregnation and luminescence enhancement through synergistic action of high transparency and desirable haze of substrate for LEC devices. Mater. Today Phys. 54, 101738.

Vernhes P., Bloch J.F., Blayo A., Pineoux B. (2009) Effect of calendering on paper surface micro-structure: A multi-scale analysis. J Mater. Proc. Technol. 209, 11, 5204-5210.

Wang W., Wang X., Zhao X., Ren X., Jiang W., Zhang Z. (2022) Two-sided, flexible, durable, highly transparent and hazy plastic-paper for green optoelectronics. Cellulose 29, 3311-3322.

Yadav S., Khan A., Hamdani S.S., Rabnawaz M. (2024) Degradable polymeric waxes for paper coating applications. ACS Appl. Polym. Mater. 6, 6, 3263-3272.

Zhang T., Yuan T., Xiao X., Peng H., Fang X., Wang K., Liu X., Li Y. (2022) Transparent and shape-memory cellulose paper reinforced by vitrimer polymer for efficient light management and sustainability. Cellulose 29, 8781-8795.

Zhao C., Gong X., Lin X., Zhang C., Wang Y. (2023) Regenerated cellulose/polyvinyl alcohol composite films with high transparency and ultrahigh haze for multifunctional light management. Carbohydr. Polym., 321, 121303.

Zhu H., Fang Z., Wang Z., Dai J., Yao Y., Shen F., Preston C., Wu W., Peng P., et al. (2015) Extreme light management in mesoporous wood cellulose paper for optoelectronics. ACS Nano 10, 1, 1369-1377.

CELLULOSE NANOFIBRILS AS FUNCTIONAL ADDITIVES IN BIO-BASED BARRIER COATINGS FOR PAPER PACKAGING

Patricija Pevec[1], Urška Kavčič[1], Janja Juhant Grkman[2], Panu Lahtinen[3], Urban Svoljšak[4]

[1]Pulp and Paper Institute, Ljubljana, Slovenia
[2]KANSAI HELIOS Kemostik d.o.o., Kamnik, Slovenia
[3]VTT, Espoo, Finland
[4]Goričane d.d., Medvode, Slovenia

doi: 10.5281/zenodo.17294678
patricija.pevec@icp-lj.si

Abstract: *Sustainable fiber-based packaging materials are primarily produced from renewable materials that have high recyclability. Nevertheless, to achieve barrier properties required for food packaging applications, paper and cardboards are often laminated or coated. Conventional barrier coatings that are currently in use are still mostly fossil-based, highlighting the need to develop sustainable coating solutions for fiber-based materials. Cellulose nanofibrils (CNF) that has large specific area and ability to form strong network structures via hydrogen bonding is a promising material for improvement of mechanical as well as barrier properties. While CNF can be obtained also from alternative biomass sources, in the SuperBark project we aim to produce CNF from bark and use it in bio-based coatings to achieve barrier properties for food packaging papers. To evaluate the bark-based CNF used in these kinds of applications, the barrier coating solutions with starch and bleached or unbleached bark-based CNF were developed and applied on three different base papers. Barrier properties of rod coated samples were evaluated regarding water vapour transition rate (WVTR) and grease resistance. Subsequent mechanical evaluation of the coated samples was performed. The research has confirmed that the starch coating increase barrier as well as mechanical properties on all three paper samples. However, the addition of bark-based CNF into starch coating increased the water vapour barrier at 85% relative humidity and was crucial to achieve the highest KIT 12 grease resistance and better mechanical properties on Paper 3.*

Keywords: barrier coating development, barrier packaging material, CNF, sustainable packaging

1 INTRODUCTION

Food packaging manufacturers often utilize fossil-based materials or fiber-based materials that are (extrusion) coated or laminated, typically with materials which are neither non-biodegradable nor biobased, to increase their barrier properties. The pressure on packaging manufacturers to replace non-biodegradable plastics has become a global trend at both academic and industrial level. To overachieve these unsustainable practices, greener and more renewable solutions and materials could be developed and used for barrier packaging materials. Enhancing papers resistance to moisture, grease and air by aqueous coating suspensions presents one of the possibilities. (Mazega et al., 2022) Besides that, utilization of environmentally more acceptable and biodegradable materials like cellulose and its derivates could be an option. The challenge of attaining paper-based materials with barrier properties comparable to those obtained by plastic remains ongoing, despite the latest efforts of researchers. A key limitation is that most biopolymers are hydrophilic in nature and thus the performance is highly affected by the relative humidity of the environment. (Hamdani et al., 2020) To

improve the water barrier property and mechanical stability of cellulose materials, hydrophobic modification strategies provide a barrier to wettability and offer low permeability to moisture. (Asim et al., 2022) Recent advancements highlight nanocellulose, especially CNF, as a biocompatible and biodegradable coating that enhances paper's density, mechanical strength, resistance to moisture and air permeability, making it suitable for food contact and thermal processing conditions. (Lengowski et al., 2023) CNF can improve aqueous suspensions encompassing water-insoluble components both as rheology modifier and as stabilizer. (Zheng et al., 2022) They have also been used as coating components and are well-known to increase the air resistance of paper by esterification with sizing agents (Alkyl Ketene Dimer (AKD), Alkenyl Succinic Anhydride (ASA)) commonly used in papermaking. (Mazega et al., 2022) Mazega et al. discovered, that coating paper sheets with CNF effectively decreased papers oil-wicking ability and increased KIT rating. The air resistance was also improved by two orders of magnitude. Anyway, the surface became more hydrophilic. (Mazega et al., 2022) In the study of Lengowski et al., CNF was produced from bleached eucalyptus pulp and applied in two wet thicknesses (1 mm and 2 mm) onto unbleached Pinus-based kraft paper. They prepared and analysed coated paper and standalone CNF films, examining their morphological, physical, mechanical, and thermal properties. CNF effectively filled the pores in the kraft paper surface, resulting in a denser, smoother, and less permeable structure. Water absorption and air permeance were significantly reduced on the coated side, while mechanical properties (particularly bursting and tensile strength) increased markedly with CNF application. Although films alone had high tensile strength, they lacked tearing resistance due to fibril morphology. All materials, including coated papers, met thermal stability requirements for food contact. (Lengowski et al., 2023) Lyytikäinen et al. explored the barrier performance of multilayered cellulose-based coatings (specifically methyl nanocellulose (MeNC), microfibrillated cellulose (MFC), and hydrophobically modified cellulose (HM-EHEC)). The study systematically evaluated the effects of varying coat weights and layering strategies on key properties such as surface morphology, wettability, oil and grease resistance (OGR), and oxygen transmission rate (OTR) under diverse temperature and humidity conditions. The inclusion of HM-EHEC enhanced hydrophobicity, particularly under elevated humidity. Notably, coating structures that combined all three components achieved complete surface sealing and high barrier performance, even at high temperatures and relative humidities, suggesting their strong potential in replacing synthetic barriers for food packaging applications. (Lyytikäinen et al., 2025)

While CNF offer many possibilities and advantageous in the field of fiber-based packaging materials, in the presented research, coating solutions with starch and starch with addition of bleached as well as unbleached bark-based CNF were prepared and applied on three different base papers. The aim of the study was to investigate the influence of bark-based CNF on barrier (water vapour, grease) and mechanical properties of all (un)coated samples.

2 MATERIALS AND METHODS

In the scope of this research different base papers were firstly analysed, then coated with different coating solutions containing starch and bark-based CNF. Finally, barrier properties of the coated samples were determined.

As a base papers, three papers (Paper 1, Paper 2, Paper 3) produced by Goričane d.d. papermill were selected and evaluated regarding grammage (ISO 536), thickness (ISO 534), filler content (ISO 1762), Bendtsen smoothness (ISO 8791-2) and Bendtsen porosity (ISO 5636-3). Beside basic properties also the surfaces of the base papers were evaluated using scanning electron microscope (SEM) Jeol 6060 LV (Jeol, Japan).

To evaluate the influence of coating on barrier properties of the coated papers, three different coating formulations were prepared and applied on the surfaces of the papers. The base of the coating formulations was thermally modified, commercially available starch (Stabilys EVO 280, Roquette) to

which two different bleached and unbleached bark-based CNFs (VTT, Finland) were added to analyse the influence of CNF type on barrier properties.

2.1 Samples preparation

Firstly, (1) thermally modified starch coating with 20% concentration was prepared. The dry starch was mixed with water and cooked for 30 minutes, then allowed to cool down to 30–40 °C. After cooling, nanocellulose was incorporated into the mixture. To determine the influence of unbleached and bleached bark-based CNF on the barrier properties, two additional coating solutions were prepared. Initially (2) starch-based coating with addition of 3% bleached bark-based CNF VTT24 was prepared and finally, (3) starch-based coating with addition of 3% unbleached bark-based CNF VTT20. The final concentration of coating solutions with bark-based CNF was 20%.

One layer (10 g/m^2) of the developed coating solutions were applied on the surfaces of the base papers with laboratory rod coater (RK Print Coater, UK) and dried 1 minute at 105°C in ventilation oven.

The coated samples were evaluated regarding water vapour and grease resistance. The water vapour transition rate (WVTR) was analysed according to ISO 2528 standard at two different conditions (50% RH at 23°C and 85% RH at 23°C). Grease resistance was assessed using the KIT test according to TAPPI T559 cm.

Besides barrier properties, all the samples were evaluated also regarding mechanical properties. Tensile strength was determined in accordance with ISO 1924-2 standard using Zwick/Roell Z010 multi testing device (Zwick/Roell, Germany).

3 RESULTS AND DISCUSSION

All three selected base papers were firstly analysed regarding basic paper properties. As can be seen from *Table 1*, all samples have similar grammage (around 50 g/m^2), Paper 1 and Paper 2 have almost the same thickness (67 and 68 µm) while Paper 3 is thinner (57 µm). The main difference between the papers is in filler content (Paper 1 is without filler, Paper 2 and Paper 3 have 7% filler content). Additionally, Paper 3 also has a precoat, that decreases smoothness as well as porosity of the paper.

Table 1: Basic properties of selected base papers

Paper property	***Paper 1***	***Paper 2***	***Paper 3***
Grammage (g/m²)	*50.7*	*50.3*	*51.2*
Thickness (µm)	*67*	*68*	*57*
Filler at 500°C (%)	*/*	*7*	*7*
Smoothness Bendtsen (ml/min)	*280*	*235*	*90*
Porosity Bendtsen (ml/min)	*125*	*310*	*90*
Type of sizing agent	*AKD*	*Rosin sizing agent*	*Rosin sizing agent*

The evaluation of the base papers with scanning electron microscope (SEM) provides a clear demonstration of the base paper's surfaces with visible filler in Paper 2 and precoating on the surface of Paper 3 (Figure 1:*1*).

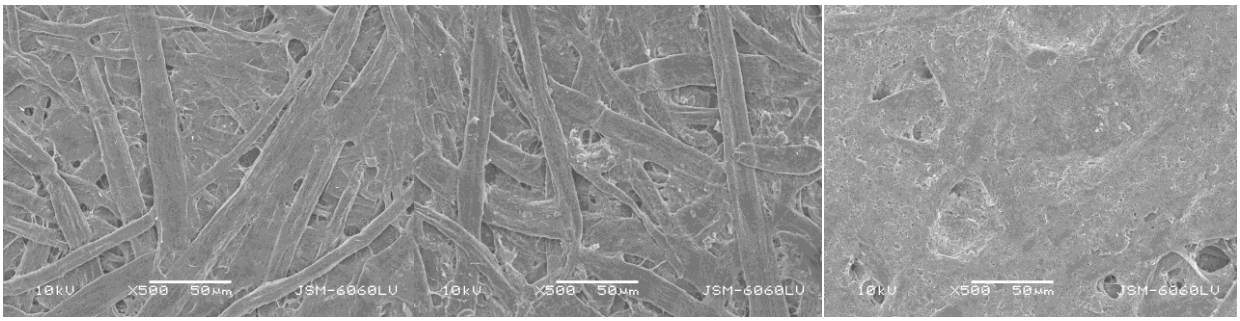

Paper 1 ***Paper 2*** ***Paper 3***

Figure 1: SEM images (500× magnification) of the surfaces of the base papers.

The basic properties as well as SEM images of the paper's surface offer the important insight for understanding further evaluation of applied coatings on the paper samples.

After the coating application, water vapor transmission rate (WVTR) was determined on starch coated (EVO 280) and starch with CNF (EVO 280 + VTT24, EVO 280 + VTT20) coated samples (Figure 2). The application of EVO 280 starch alone significantly decreased WVTR across all paper substrates, confirming its effectiveness as a moisture barrier under both humidity conditions. While the addition of CNF in the coating did not result in substantial further improvements at 50% RH, enhancements were observed under more challenging conditions at 85% RH. Notably, Paper 3, which contains fillers and precoat, exhibited the greatest improvement when combined with unbleached CNF (VTT20), suggesting synergistic effects between the filler and CNF in enhancing the moisture barrier. Furthermore, a marked difference in performance was observed between the two CNFs tested: bleached VTT24 showed limited benefit, whereas unbleached VTT20 significantly improved the barrier properties—reducing WVTR on Paper 3 from 310 g/m²/24h (starch EVO 280 only) to approximately 200 g/m²/24h (EVO 280 + VTT20).

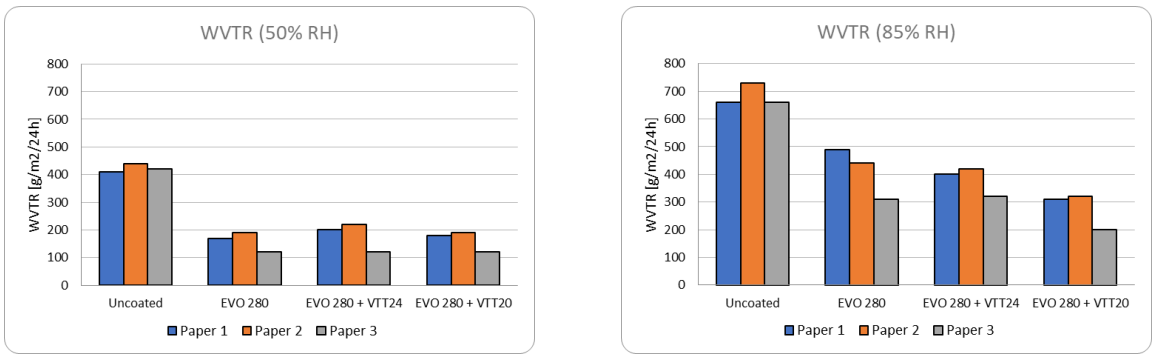

Figure 2: WVTR of uncoated and coated paper samples at 50% RH and 85% RH.

Similarly, the influence of coating on grease resistance is obvious when the samples were coated with starch only (from KIT 0 to KIT 4 on Paper 1 and KIT 7 on Paper 2 and Paper 3), however with addition of CNF into the coating solutions, the grease resistance increases significantly. From Figure one can observe that on Paper 1, that has no filler and precoat, the maximum KIT value 9 is achieved when bleached CNF was added to the starch coating. Filler in Paper 2 improved grease resistance, while with addition of bleached or unbleached CNF increase KIT value to 11. The best grease resistance was achieved on Paper 3, where KIT value increased from KIT 7 (starch coating) to KIT 12, when (bleached or unbleached) CNF was added into the coating solution.

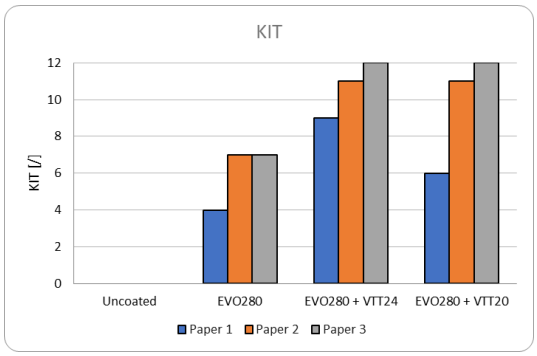

Figure 3: KIT values of uncoated and coated paper samples.

The tensile properties of the samples are presented in Figure 4 and Table 2. The stress–strain curves provide insight into the mechanical response under loading, while the Table 2 parameters summarize the elongation and stress at break. The uncoated Paper 1 showed the highest strength, with maximum stresses at break among uncoated papers (58.93 MPa) together with a moderate elongation at break of 2.57%. Paper 2 presented intermediate behaviour while Paper 3 was the weakest substrate, with stresses at break around 40 MPa, and elongation of 1.67%. These results of mechanical evaluation of the uncoated samples reflect the composition of the base papers (Paper 1 as the mechanically strongest, Paper 2 as intermediate, and Paper 3 as the weakest substrate). Starch coating improved the tensile performance of all papers. In the stress–strain curves, the coated papers generally followed the shape of the uncoated ones, but reached higher forces at a given strain. Paper 1 increased elongation from 2.57% to 3.56%, while Paper 2 improved from 1.53% to 1.89% elongation. Paper 3 showed the strongest relative response, with elongation increasing from 1.67% to 2.22%. Stronger substrate (Paper 1), shows only marginal improvement with addition of CNF, while weaker substrate (Paper 3) benefit substantially from the reinforcement, particularly with the bleached CNF (VTT24). Starch coating consistently improves all papers, mainly by increasing elongation, while CNF provides additional strength and stiffness, with VTT20 being more effective for Paper 2 and VTT24 for Paper 3.

These findings are in line with the results of Lengowski et al. (2023), who also observed improved tensile performance when applying CNF coatings, particularly in substrates with lower initial strength. The addition of CNF to starch further modified the tensile response. In Paper 1, both coatings slightly increased elongation compared to the uncoated substrate (3.20–3.36%). Paper 2, in contrast, benefited more from the nanocellulose addition: EVO280+VTT20 yielded the best performance, with stress at break above 40 MPa, exceeding both the uncoated and starch-only conditions. For Paper 3, the weakest substrate, EVO280+VTT24 increased stress at break from 40 to 41 MPa, as well as showing enhanced strength in the force–strain curves, especially beyond 1% strain. These results confirm that the effectiveness of the coatings is substrate-dependent and align well with Lyytikäinen et al. (2025), who reported that multilayered cellulose-based coatings, particularly those including modified CNF, exhibited strong barrier and reinforcement effects under challenging environmental conditions.

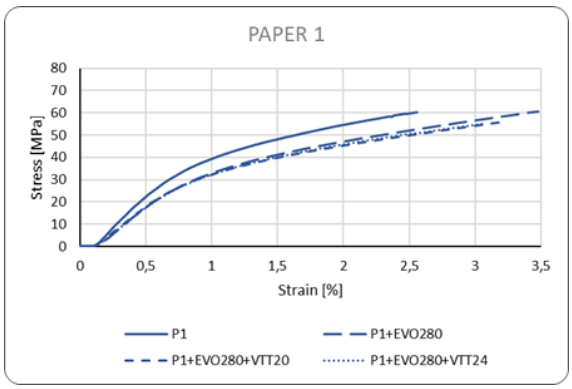

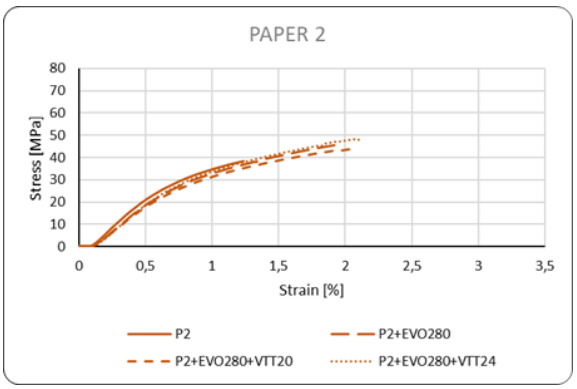

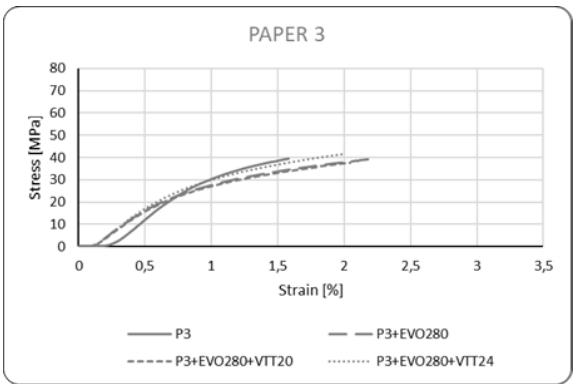

Figure 4: Tensile stress/strain curves of uncoated and coated samples on three papers

Table 2: Tensile properties of papers without and with coatings

	Paper 1	*Paper1 + EVO280*	*Paper1 +EVO280 +VTT20*	*Paper1 +EVO280 +VTT24*	*Paper 2*	*Paper2 +EVO280*	*Paper2 +EVO280 +VTT20*	*Paper2 +EVO280 +VTT24*	*Paper 3*	*Paper3 +EVO280*	*Paper3 +EVO280 +VTT20*	*Paper3 +EVO280 +VTT24*
Strain [%]	*2.57*	*3.56*	*3.36*	*3.20*	*1.53*	*1.89*	*1.99*	*2.04*	*1.67*	*2.22*	*2.15*	*2.09*
Stress at break [MPa]	*58.93*	*60.50*	*56.33*	*55.53*	*41.07*	*43.96*	*43.53*	*46.71*	*40.02*	*38.89*	*37.28*	*40.99*

4 CONCLUSIONS

This study confirmed that bio-based coatings provide improvements to both barrier and mechanical properties of paper substrates, supporting their potential as sustainable alternatives to plastic laminates in food packaging. Starch alone enhanced tensile strength, elongation, and barrier properties across all substrates, while the addition of bark-based CNF further reinforced the papers in a substrate-dependent manner. Unbleached bark-based CNF (VTT20) proved most effective for Paper 2, whereas bleached CNF (VTT24) gave the strongest reinforcement in the weakest substrate Paper 3. The highest influence on barrier properties was achieved with starch coating alone, however, the influence of addition of bark-based CNF on WVTR at 85% RH was promising and additionally improved barrier (especially on Paper 3). Similar influence of bark-based CNF was observed also with grease resistance, where CNF evidently increase the KIT value. The highest grease barrier (KIT 12) on Paper 3 was achieved solely due to the addition of bark-based CNF into the starch coating. These results are consistent with previous research on CNF coatings and demonstrate that tailoring coating formulations to the characteristics of the base paper is essential for achieving optimal performance. Overall, starch (with addition of nanocellulose) coatings represent a promising strategy to advance bio-based and biodegradable paper packaging solutions.

Acknowledgments: *The SuperBark project (grant agreement No. 101112447) is supported by the Circular Bio-based Europe Joint Undertaking and its members.*

Funded by the European Union. Views and opinions expressed are however those of the author(s) only and do not necessarily reflect those of the European Union or CBE JU. Neither the European Union nor the CBE JU can be held responsible for them.

5 REFERENCES

Asim, N., Badiei, M., & Mohammad, M. (2022). Recent advances in cellulose-based hydrophobic food packaging. In Emergent Materials (Vol. 5, Issue 3, pp. 703–718). Springer Nature. https://doi.org/10.1007/s42247-021-00314-2

Hamdani, S. S., Li, Z., Sirinakbumrung, N., & Rabnawaz, M. (2020). Zein and PVOH-Based Bilayer Approach for Plastic-Free, Repulpable and Biodegradable Oil- And Water-Resistant Paper as a Replacement for Single-Use Plastics. Industrial and Engineering Chemistry Research, 59(40), 17856–17866. https://doi.org/10.1021/acs.iecr.0c02967

Lengowski, E. C., Bonfatti Júnior, E. A., Coelho Simon, L., de Muniz, G. I., de Andrade, A., Neves Leite, A., & de Miranda Leite, E. L. (2023). Nanocellulose Coating on Kraft Paper. Coatings, 13(10). https://doi.org/10.3390/coatings13101705

Lyytikäinen, J., Koljonen, K., & Leminen, V. (2025). Effects of multilayered cellulose-based coatings on the barrier properties of paperboard. Cellulose, 32(4), 2617–2628. https://doi.org/10.1007/s10570-025-06416-y

Mazega, A., Tarrés, Q., Aguado, R., Pèlach, M. À., Mutjé, P., Ferreira, P. J. T., & Delgado-Aguilar, M. (2022). Improving the Barrier Properties of Paper to Moisture, Air, and Grease with Nanocellulose-Based Coating Suspensions. Nanomaterials, 12(20). https://doi.org/10.3390/nano12203675

Zheng, Y., Oguzlu, H., Baldelli, A., Zhu, Y., Song, M., Pratap-Singh, A., & Jiang, F. (2022). Sprayable cellulose nanofibrils stabilized phase change material Pickering emulsion for spray coating application. Carbohydrate Polymers, 291. https://doi.org/10.1016/j.carbpol.2022.119583

BIOPLASTICS BASED ON POTATO AND COFFEE BY-PRODUCTS FOR ACTIVE CARDBOARD COATING

Gabriela Campos, E. M. T. Gonçalves, P. Ferreira, I. Gonçalves

Aveiro Institute of Materials, Department of Materials and Ceramic Engineering, University of Aveiro, Aveiro, Portugal

doi: 10.5281/zenodo.17294721
gabrielacampos@ua.pt

Abstract: *Cardboard is widely used in packaging due to its biodegradability, lightness, and recyclability. However, its hydrophilic nature and porous fibre network limit water vapor barrier properties and compromise mechanical strength, particularly under humid conditions. To overcome these limitations, cardboard is often coated with synthetic polymers or aluminium. However, these coatings decrease biodegradability and recyclability, undermining the environmental benefits of fibre-based packaging. Sustainable alternatives based on agri-food by-products have gained attention as environmentally compatible coatings. As part of the BIOCOATING project, this work focuses on the development of biodegradable active coatings for cardboard, using thermoplastic starch obtained from potato washing slurries and enriched with coffee industry by-products, intended for use in paper-based packaging systems. Coffee silverskin (CS) and spent coffee grounds (SCG) were selected for their content in bioactive compounds, including lignin, cellulose, caffeine, and phenolics, which positively influence the performance of the coatings by enhancing antioxidant activity, reducing water vapor permeability, and contributing to mechanical reinforcement. The starch extracted from potato washing residues acts as a biodegradable matrix with good film-forming properties. The coatings were produced by thermomechanical blending and applied onto cardboard substrates through hot-pressing. The resulting coated cardboard is expected to exhibit natural pigmentation, enhanced water resistance, and antioxidant activity. By valorising low-value residues from the agri-food sector, this work supports the development of eco-friendly and functionally enhanced cardboard-based packaging materials aligned with circular economy principles.*

Acknowledgements: *This work was developed within the scope of the project CICECO-Aveiro Institute of Materials, UIDB/50011/2020 (DOI 10.54499/UIDB/50011/2020), UIDP/50011/2020 (DOI 10.54499/UIDP/50011/2020) & LA/P/0006/2020 (DOI 10.54499/LA/P/0006/2020), financed by national funds through the FCT/MCTES (PIDDAC). G.J. Campos and E.M.T. Gonçalves acknowledge the BIOCOATING project (COMPETE2030-FEDER-00590400), funded by Compete 2030, Portugal 2030, and the European Union, for the research grants. The authors also thank Isolago Europe (project leader), as well as A Saloinha and FEB Cafés, for kindly providing the agri-food by-products used in this study. I. Gonçalves acknowledges funding from FCT through the Individual Call to Scientific Employment Stimulus (https://doi.org/10.54499/CEECIND/00430/2017/CP1459/CT0032).*

AVOCADO SEED-DERIVED BIOPLASTICS AS ACTIVE COATINGS FOR CARDBOARD

P. B. C. Vicent[1], E. M. T. Gonçalves[2], G. J. Campos[2], Ana. F. R. Cerqueira[2], P. A. R. Fernandes[1], M. A. Coimbra[1], P. Ferreira[2], I. Gonçalves[2]

[1]LAQV-REQUIMTEs, Department of Chemistry, University of Aveiro, 3810-193 Aveiro, Portugal;
[2]CICECO–Aveiro Institute of Materials, Department of Materials and Ceramic Engineering, University of Aveiro, Aveiro, Portugal

doi: 10.5281/zenodo.17294812
pedrobcvicente@ua.pt

Abstract: *Cardboard is widely used in packaging due to its biodegradability, recyclability, and compatibility with circular economy systems. However, its porous and hydrophilic structure limits barrier performance, especially against moisture and oxygen, restricting its use in food packaging without additional layers. Conventional coatings often use synthetic polymers or metals, which compromise recyclability and biodegradability. Environmental concerns over fossil-based plastics have increased demand for sustainable alternatives, such as bioplastics from industrial agri-food waste, promoting by-product valorization and supporting the circular economy. These wastes, rich in bioactive compounds and nutrients, can yield materials with valuable properties, such as moisture-wicking and antioxidant activity. As part of the BIOCOATING project, this study developed avocado seed-derived bioplastics as active coatings for cardboard to enhance functionality while maintaining circularity. Avocado seeds, an underused agri-food residue, were utilized as a source of bioactive compounds and starch-rich fractions suitable for thermoplastic processing. The research followed five stages: (i) preparation and characterization of avocado seed; (ii) production of thermobioplastic granulates; (iii) development and analysis of bioplastic films; (iv) hot stamping of films onto cardboard; and (v) evaluation of coated samples. The films showed a brown color, flexibility, and demonstrated moisture-wicking and antioxidant properties. Once applied via hot stamping, the coatings adhered well and formed a continuous layer. These findings show that avocado seed-derived bioplastics can give cardboard packaging active and protective functions, supporting circular design by reducing dependence on fossil-based plastics and enabling waste valorization.*

Keywords: polysaccharides; agri-food waste; biodegradability; circular economy; functional properties; environmental sustainability

Acknowledgements: *This work was developed within the scope of the project CICECO-Aveiro Institute of Materials, UIDB/50011/2020 (DOI 10.54499/UIDB/50011/2020), UIDP/50011/2020 (DOI 10.54499/UIDP/50011/2020) & LA/P/0006/2020 (DOI 10.54499/LA/P/0006/2020) and UID/50006 - Laboratório Associado para a Química Verde - Tecnologias e Processos Limpos, financed by national funds through the FCT/MCTES (PIDDAC). G.J. Campos and E.M.T. Gonçalves acknowledge the BIOCOATING project (COMPETE2030-FEDER-00590400), funded by Compete 2030, Portugal 2030, and the European Union, for the research grants. The authors also thank Isolago Europe (project leader), as well as A Saloinha and FEB Cafés, for kindly providing the agri-food by-products used in this study. I.*

Gonçalves acknowledges funding from FCT through the Individual Call to Scientific Employment Stimulus (https://doi.org/10.54499/CEECIND/00430/2017/CP1459/CT0032).

THERMALLY CONDUCTIVE CELLULOSE-BASED SUBSTRATES FOR FLEXIBLE ELECTRONICS

Vanja Kokol[1], Vera Vivod[2], Katja Klinar[3]

[1] Faculty of Mechanical Engineering, Univeristy of Maribor, Maribor, Slovenia
[2] Faculty of Mechanical Engineering, University of Ljubljanja, Ljubljana, Slovenia

doi: 10.5281/zenodo.17294975
vanja.kokol@um.si

Abstract: *The use of renewable biopolymers in advanced (opto)electronics and wearable sensor devices has attained extensive attention recently, above all, to replace non-biodegradable dielectric thermoplastic polymers (e.g. polyimide/PI, polyethylene/PE, and polyvinylidene fluoride/PVDF) while maintaining the device's flexibility and increasing their recyclability. Nanocellulose/NC has gained particular attention due to its inherent biocompatibility, cost-effectiveness, and film-forming properties.* However, all of these substrates are thermal insulators, while attached electronic components produce heat by Joule (resistive) effect during operation, *thus affecting their function adversely,* while also softening the thermoplastics*. The thermal diffusivity of NC films can be obtained by reducing the thermal resistance at the interface between the cellulose fibrils/crystals with an increased interaction through their highly aligned anisotropic structure and/or introduced thermally-conductive 2D nanofillers. In this work, the films have been prepared from semi-crystalline cellulose nanofibrils (CNF) and the addition of 2D hexagonal boron nitrides (hBNs) of different lateral sizes (100 nm to 150 µm) by pressure-filtration to examine their impact on the films' morphological and thermal dissipation (through-plane, in-plane) properties. In the next stage, the up-scalable slot-die coating technology was used to study the coatability of the most promising formulations onto the paper substrate. A uniform and relatively high coat weight (19 g/m^2) was achieved by using CNC-hBN suspensions, leading to good coverage of the paper's surface and an improved thermal conductivity in both substrate directions, through- and in-plane.*

Keywords: nanocellulose, 2D hBN, films, slot-die coating, heat dissipation.

1 INTRODUCTION

Thin, light and flexible dielectric substrates are typically still made from fossil/fuel-based thermoplastic polymers (Zhao et al. 2023) due their advantage of a smooth surface suitable for (opto)electronics device fabrication, high thermal stability (>500 °C), mechanical toughness, chemical resistance, as well as excellent electrical insulation properties (dielectric constant of 3-4) and inherently low coefficient of thermal expansion (CTE 3-6 x 10^{-5} 1/K). However, they are thermal insulators, while on such a substrate attached electronic components like integrated circuits produce heat by Joule (resistive) effect during operation (Uyor et al. 2023) that becomes even more serious by being more miniaturized and complicated. If the heat dissipated is not discarded (or converted into the other one), it accumulates and affects the performance and reliability of electronic devices, while also softening the polymeric dielectric substrate. Flexible substrates with high enough thermal conductivity are thus urgently needed to improve thermal management and reach new applications, including active/intelligent packaging, healthcare (medical instruments, wearable devices), intelligent (robots,

industrial machinery), and automotive industries (electronics), smart cities (consumer electronics), and space/military systems (Baruh et al. 2023).

The nanocomposite films have attracted much attention recently by adding a small amount of highly thermally-conductive 2D layered nanofillers (like hexagonal boron nitrides / h-BN with ~600 W/mK in-plane and ~30 W/mK through-plane TC of a monolayer, density of ~2.2 g/cm^3, elastic constant of 220–510 N/m and Young's modulus of 1 TPa) (Falin et al. 2017) through the specific structure construction (Uyor et al. 2023), thus combining the advantages of heat dissipation, light weight, high flexibility, and good processing performance (Wu et al. 2017). The added hBNs can also improve mechanical strength, electrical insulation (dielectric constant of ~6.9 at 1 MHz), and flame retardancy (temperature resistance above 700 °C) (Wu et al. 2022), allowing them to be applied in harsh environments.

By introduction of hBNs (loading up to 50 wt%) to CNF-based films, the in-plane TC of CNF can thus be increase from about 0.6 - 2 W/mK (Uetani K & Hatori 2017) up to ~12 W/mK (Xu et al. 2022), at loading below 50 wt%. Since phonon transport (and thus TC) is affected by the functional groups on the surfaces of the CNF, the lateral dimension of hBN sheets as well as their interactions and distribution into the CNF matrix, which all influence on inter-sheets thermal resistance, the TC of CNF/hBNs can be increased further by improving the bulk structuring and using differently large hBNs.

In this work, TC properties of TEMPO-oxidized CNF (CNF) films prepared by an up-scalable pressure filtration method were studied over a broad temperature (30 – 120 °C) range. Various weight percentages of few-layered hBNs of different (100 nm - 150 µm) lateral sizes were included, to verify the impact of CNF on their self-assembly and interphase arrangement in such a composite films, and, consequently, through-plane and in-plane heat dissipation capacity. In the next stage, the up-scalable slot-die coating technology was used to study the coatability of the most promising formulations onto the paper substrate and its TC properties.

2 MATERIALS AND METHODS

2.1 Materials

TEMPO-oxidized CNFs with chain-like structures, diameter of the 10-30 nm and length of a few (1–3) µm, were prepared from bleached softwood pulp at the Stockholm University, Department of Chemistry (Sweden). The few-layered 2D hexagonal boron nitride (hBN) powders of low density (~2.2 g/cm^3), high surface area (3-4 m^2/g) and purity (>99%), and different lateral sizes were purchased from Nanografi (Ankara, Turkey) and Henze BNP AG (Lauben, Germany, respectively, and used as received. The isopropyl alcohol (IPA) was purchased from Sigma-Aldrich GmbH (Germany). The pigment pre-treated paper (grammage of 51±2 g/m^2, thickness of 78±3 µm) was obtained from Papirnica Vevče d.o.o. (Slovenia).

2.2 Preparation of pristine and composite films

For the preparation of the films, the initial 1.1 wt% CNF suspended in milli-Q water was diluted to 0.4 wt% by using a homogenizer Ultra-Turrax T18 (IKA-Werke GmbH & Co.KG, Germany). At the same time, various quantities of hBN were overnight pre-hydrated in few mL of IPA by magnetic stirring. Finally, different volumes of IPA-wetted hBNs were mixed with different volumes of the water-suspended TCNF by ultrasonic processor (VCX 750, Sonics & Materials, Inc., USA) for few min at 20% amplitude to get homogeneous CNF-hBN dispersions with a final 0.4-0.2 wt% of CNF and 0.1-1.2 wt% of hBN, containing 10 vol% or 50 vol% of IPA. The as prepared CNF/hBN dispersions were pressure filtered through a PVDF filter with a pore size of 0.22 µm at 5 bars pressure by the dead-end mode using the HP4750 stirred cell (Sterlitech Co., USA) and 2.24 cm^2 of effective surface area to get wetted densely packed gel films (Fig. 1) with homogenously distributed and parallelly aligned structure. The films were then left to dry at room temperature, removed from the filter paper, conditioned at 23 ºC and 60% RH

for 24 h before being cold pressed for 24 h and 100 bars by a Perkin Elmer laboratory hydraulic press (Scientific Instruments, USA). The composite films were designated according to the weight percentage of CNF and hBN used, recalculated related to the total volume (generally 50 mL).

2.3 Slot-die coating of CNf-hBN suspension

A Challanger 175, semi-pilot & fully automated Sheet-to-Sheet (S2S) coating unit (Norbert Schläfli nsm AG, Switzerland) with an inline integrated 190 mm wide slot-die (TSE Troller AG, Switzerland) and NIR drying unit with 180 Ws/cm^2 of energy density (NIR252-125 Adphos GmbH, Germany) was used to control the coating speed (10 m/min), wet thickness deposition (40 µm), the drying speed (1 m/min) and power/time (40%, 120-180 sec); as shown on Fig. 2. A slot-die shim of 165 µm thickness was used, while the distance between the substrate and the slot lips was set to 100 µm.

2.4 Characterization

The thickness of the substrates was measured using a dial thickness gauge, F1000/30 (Käfer Messuhrenfabrik GmbH & Co. KG, Germany). The volumetric density (g/cm^3) was calculated from the weight mass, diameter and thickness of the samples. The presented results are the arithmetic mean values and the Standard Deviations of at least two independent measurements, obtained after cold pressing. Scanning electron microscopy (SEM) imaging of sample surfaces and cross-sections were performed by using a low-vacuum scanning electron microscope, FEI Quanta 200 3D (Thermo Fisher Scientific Inc, USA). The thermal diffusivity in both through-plane and in-plane configuration was measured by the laser flash method using an LFA 467 HyperFlash (Netzsch Holding, Germany) at different temperatures (30 °C, 60 °C, 90 °C and 120 °C). At least three laser pulses (xenon of 10 J/pulse) for 20 µs were performed at each temperature. The samples were spray coated with graphene before the analysis. The thermal conductivity (TK, W/mK) was calculated as $TK = \alpha \times \rho \times Cp$, where α and ρ are the thermal diffusivity (TD, mm^2/s) and density (g/cm^3) of the substrate for each temperature, and Cp is the specific heat capacity (J/gK) measured with the classic sapphire method according to the standard procedure (User Com 7, Mettler Toledo GmbH, Schwerzenbach, Switzerland, 1998) using a differential scanning calorimeter Mettler Toledo DSC1 (Switzerland). For both TK and C_p determination samples were pre-heated to 140 °C, left for 15 min so that the adsorbed moisture was evaporated, then cooled to 5 °C, and thermostated at this temperature for 15 min before the dynamic measurement was performed at a rate of 10 K/min up to 120 °C; thus to determine the C_p of dried samples. Up to three measurements were made per each sample, and the results were given as an average value with a Standard Deviation.

3 RESULTS AND DISCUSSION

The effect of the hBN size and content on the morphology and thermal conductive (TC) properties of the CNF/hBN composite films are shown in Fig. 1. As shown in the SEM images, the micro-large hBNs has a typical plate-like morphology, consisting of a few nm thick nanosheets, stacked together in a multi-layered structure. The smoother surface, but randomly interwoven arranged cellulose fibrils, are visible in the cross-section of film containing the smallest (100 nm) and slightly aggregated hBNs, resulting in a relative high density (~2.2 g/cm^3) without any impact on the improvement of TC compared to the reference film (prepared without hBN). By the addition of a larger and more homogenosuly distrubuted hBNs the fibrils and hBN platelest become more longitudinally oriented, but the film less densely structured (to ~2.0 g/cm^3 for 20 µm hBN, to ~1.8 g/cm^3 for 45 µm hBN and to ~1.6 g/cm^3 for even larger 150 µm hBN) while given significant increse in both through-plane (for ~350%, to ~3.2 W/mK) and in-plane (for ~120%, to ~13.3 W/mK) TC (analysed by isotropic model) for film containing 150 µm hBN at the same weight ratio. By threefold addition of medium sized hBN (20 µm), the TC of such a composite film also incresed from ~10.12 to ~13.8 W/mK, but with a significant deterioration of its bending properties (the film become more brittle). The slot-die coated CNf-hBN suspansions with the same weight ratio (1:1) resultet to ~19 g/m2 of coating weight, but paper

thickness increased from ~8.5 to ~14 µm (and density from ~0.75 to ~0.92 g/cm^3) by using larger hBNs (150 µm), and, as expected, given more surface deposited and in-plane oriented platelets (Fig. 2). Although the coating weight and its density was relatively much lower than those used in the films, the in-plane TC of the paper improved by 77% (isotropically, to ~8.4 W/mK) with the addition of better distributed 45 µm large particles at nd 30ºC; this effect increased linearly with increasing temperature which is attributed to the longer mean free path of phonon transport in such a hybrid structure.

Cellulose aggregates contain a lot of interfaces; the lower interfacial thermal resistance between semi-crastyline cellulose fibrils is thus derived from the strong surface interactions, such as hydrogen bonding and van der Waals forces. Such a molecular arrangement constrains the phonon transfer within the fibrils, thus resulting to lower TC as compared to composite structures containing hBNs. However, hydrophobic interactions between CNFs and hBNs also affect phonon transport not only in the axial direction (through-plane), but also in the radial direction (in-plane). The phonon mean free path, which is larger than the lateral size of hBN (and cellulose crystals), is also limited by boundary scattering of phonons on crystal grains; as a result, higher values of TC evaluated by the isotropic model than the anisotropic is evident, and the effect further increases with increasing the temperature. The presence of disorder and high density, which are more pronounced when using laterally smaller hBNs (both in films and paper-based coatings), further weaken phonon transport and the overall temperature dependence in such structures.

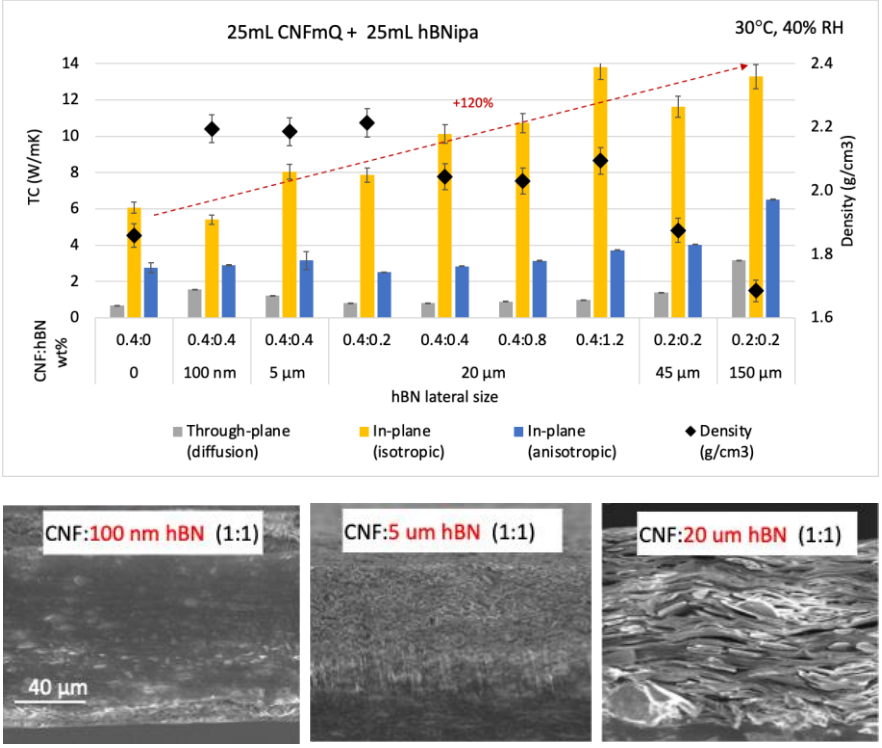

Figure 1: Morphology and thermal conductivity of CNF-hBN composite films.

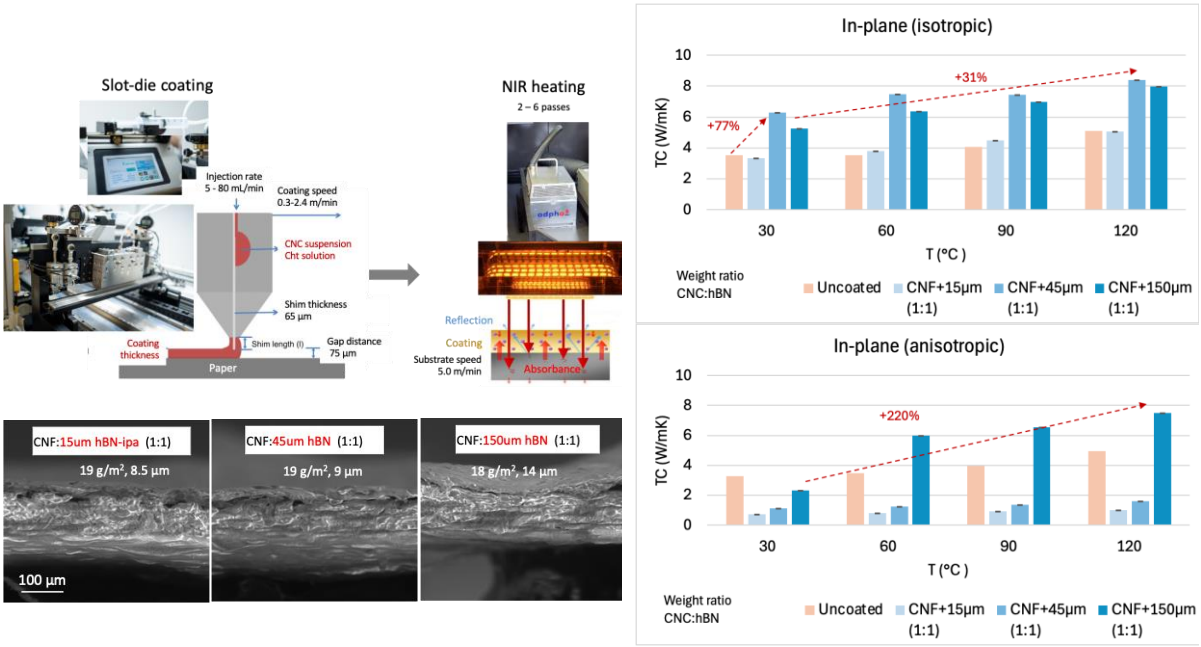

Figure 2: Schematic presentation of the slot-die coating deposition with the morphology and in-plane thermal conductivity of the CNF-hBN coated paper.

4 CONCLUSIONS

The TC properties of CNF-hBN composite films as well as coted paper are highly affected by the arrangement of both the cellulose fibrils and hBNs within the matrix, their interactions and alignment. By using laterally larger hBNs, the anistropic in-plane TC properties of such a substrates are thus the higest among all tested formulations an both models used in their evaluation. This is particularly important as it allows for further improvement of the TC performance of such substrates with predefined heat dissipation properties required for specific applications, as printed electronic to ensure its optimal performance and reliability. On the other hand, substrates with randomly oriented composition exhibit higher isotropic TC (up to 14 W/mK at 30ºC) similar to those obtained by other studies.

Acknowledgments: *The authors would like to thank the Slovenian Research and Innovation Agency (J2-60048, P2-0424), and the Ministry of High Education, Science and Innovation (Flag-Era 2D-PAPER) for financing this research work.*

5 REFERENCES

Baruah R.K., Yoo H., Lee E.K. (2023) Interconnection technologies for flexible electronics: materials, fabrications, and applications. *Micromachines*, 14(6), pp. 1131.

Falin A., Cai Q., Santos E.J.G., Scullion D., Qian D., Zhang R., Yang Z., Huang S., et.al. (2017). Mechanical properties of atomically thin boron nitride and the role of interlayer interactions. Nat Commun., 22(8), pp. 15815.

Uetani K., Hatori K. (2017) Thermal conductivity analysis and applications of nanocellulose materials. Sci. Technol. Adv. Mater., 18, pp. 877.

Uyor U.O., Popoola A.P.I., Popoola O.M. (2023) Flexible dielectric polymer nanocomposites with improved thermal energy management for energy-power applications. Front. Energy Res., 11, pp. 1114512.

Zhao C., Li Y., Liu Y., Xie H., Yu W. (2023) A critical review of the preparation strategies of thermally conductive and electrically insulating polymeric materials and their applications in heat dissipation of electronic devices. Adv. Compos. Hybrid. Mater., 6(1), pp. 27.

Xu Y., Chen X., Zhang C. et al. (2022) Enhancing thermal conductivity and toughness of cellulose nanofibril/boron nitride nanosheet composites. Carbohydr. Polym., 296, pp 119938.

Wu Y.P., Xue Y., Qin S., et al. (2017) BN nanosheet/polymer films with highly anisotropic thermal conductivity for thermal management applications. ACS Appl. Mater. Interfaces, 9/49, pp. 43163.

Wu M., Zhou Y., Zhang H., Liao W. (2022) 2D boron nitride nanosheets for smart thermal management and advanced dielectrics. Adv. Mater. Interfaces, 9/25, pp. 2200610.

A NOVEL CHARACTERIZATION OF THE MECHANICAL PROPERTIES OF PAPER-BASED MATERIALS

Gregor Čepon[1], Gregor Ševerkar[1],Aleš Mihelič[2]

[1]University of Ljubljana, Faculty of Mechanical Engineering, Aškerčeva 6, 1000 Ljubljana, Slovenia
[2]Gorenje d. o. o., Velenje, Slovenia

doi: 10.5281/zenodo.17294999
gregor.cepon@fs.uni-lj.si

Abstract: *This study presents a novel approach to characterizing the mechanical behavior of paper-based materials with a focus on their cushioning performance. By analyzing cushioning curves obtained through controlled compression tests, the energy absorp tion capacity and deformation characteristics of various paper structures were evaluated. The results demonstrate how material composition, layering, and structural design influence the cushioning response. These findings offer valuable insights for optimizing paper-based packaging solutions as sustainable alternatives to traditional foams and plastics.*

Keywords: coushening, paper, packaging, drop test

1 INTRODUCTION

Commercial goods are commonly encased in packaging buffers to protect them from damage due to vibration and impact shock during handling and transportation (G. Kun). The materials used to fabricate protective packaging are usually plastic foam such as EPS with good cushioning performance and cost-effective but not friendly to the environment (L. Andena). The growing trend towards the use of environmentally friendly packaging has led to an increase in the research and use of alternative biobased packaging solutions. Considering this paper-based packaging (molded pulp, honeycomb paper, etc.) already offers established sustainable packaging solutions that is recyclable, biodegradable and compliant with ISO 14000 and European Green Dot standards (S. W. Lye). Usually, the paper packaging solution are implemented for protection of lightweight structures such as small domestic appliances, electronic components, food products, etc.

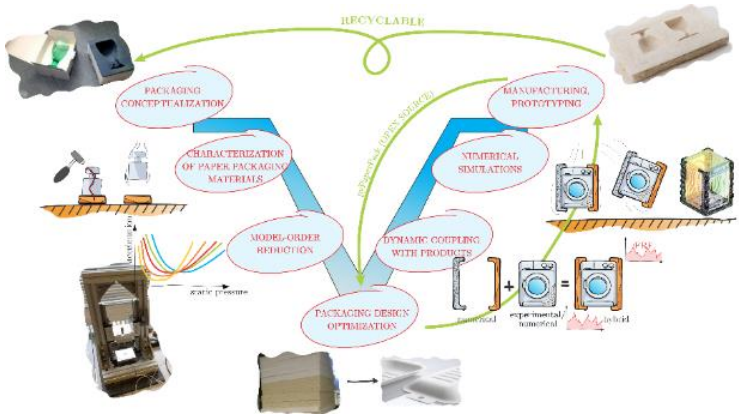

Figure 1: Sustainable design of protective packaging using experimental-numerical approach

Although the paper-packaging materials and corresponding numerical design methods are already well established, they cannot be readily used to design packaging of heavy and complex home appliances for several reasons (G. Kun,). Firstly, these materials exhibit high stiffness before plastic deformation which makes them far from being regarded as an ideal cushioning material. Moreover, the established paper packaging solutions have comparable cushioning performance to EPS only at low static loads and low drop heights (G. Kun). Therefore, to improve the cushioning performance, the design of the paper packaging relay on the numerical structural optimization to reduce vibration transmissibility and to increase shock absorption in the case of single and multiple impacts (T. Fadiji).

2 EXPERIMENTAL INVESTIGATION OF HONEYCOMB-PAPER CUSHIONING PROPERTIES.

Cushioning of packaging materials is typically evaluated in terms of the maximum deceleration versus the static stress for a specific drop height and cushion thickness. This enables one to obtain cushioning curve that defines minimum cushioning area to obtain best shock absorption. These standard methods provide a general guidance to the evaluation of cushioning performance. Here the standard impact-based test facility is proposed as shown in Fig. 2.

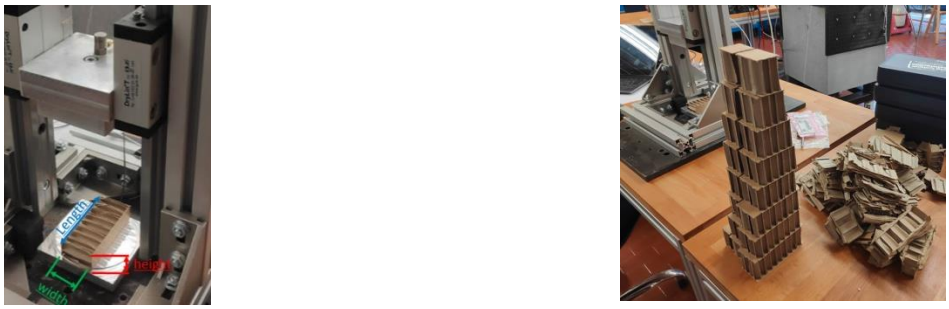

a) b)

Figure 2: Experimental determination of honeycomb cushioning characteristics; a) Experimental test rig, b) Specimen before and after testing.

In Fig. 3 the cushioning curves obtained by measuring honeycomb panels with 20mm thickness are presented. The curves were obtained by performing the measurement with test samples of different cross-sections and considering multiple successive impacts. It can be observed that the cushioning curves change significantly in the event of consecutive impacts. The reason for this is that the honeycomb structure is deformed and as a result loses its cushioning ability, especially at high static contact pressures.

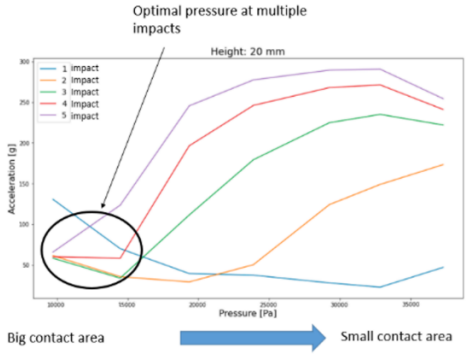

Figure 3: Measured cushioning curves for honeycomb panel of height 20mm at multiple subsequent impacts.

The optimal static pressure for analyzed honeycomb panels (thickness 20mm) is between 10kPa and 15kPa.

3 PAPER-BASED PACKAGING DESIGN METHODOLOGY

The paper-based packaging design methodology is demonstrated on the packaging design of the tumble dryer as shown in Fig. 4a. The entire packaging concept is based on folding through V-groove cuts without gluing. The principle of packaging folding can be clearly demonstrated by the unfolded and folded configuration of packaging corner (Fig. 4b).

a) b)

Figure 4: Design concept of the paper honeycomb packaging for Gorenje tumble dryer; a) The packaging together with appliance, b) Folding concept.

To enhance the packaging protective performance, a static analysis was firstly carried out to deduce the contact pressures due to the weight of the appliance (Fig. 5a). The calculated stresses on the bottom part of packaging are presented in Fig. 5b. The contact areas are deduced in such a way that they are close to the optimal pressure of 15kPa to achieve the best cushioning performance. The static pressure analysis is carried out for both for the vertical impact and the impact from the side of the appliance.

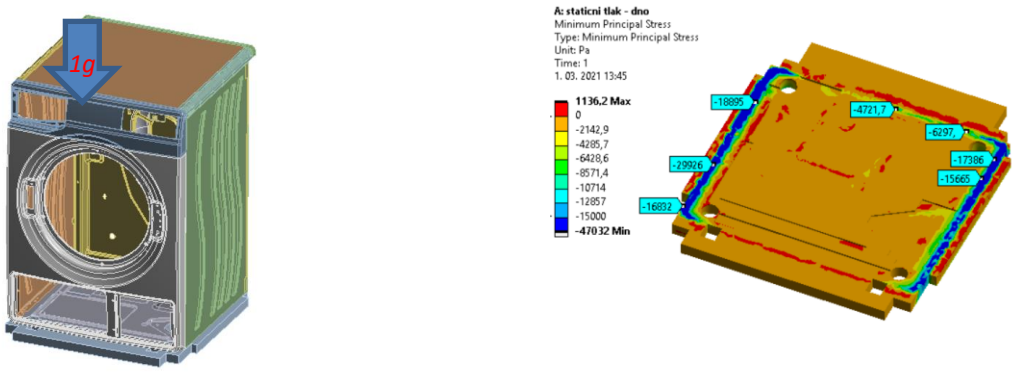

a) *b)*

Figure 5: Calculation of static loads on the packaging; a) Application of gravitational load, b) Calculated static pressures on the bottom part of the packaging.

With an optimized packaging design, the simulation of loads caused by impacts during transport is then carried out. These loads are usually determined based on the acceleration measurements during standard transportations tests. This includes the drop test and the side impact test, also known as the slope test. In Fig. 6 the loads applied to the sidewall during the slope test are presented along with induced stresses on the appliance. These simulations make it possible to identify stresses that could potentially lead to plastic deformation and breakage of an appliance.

a) *b)*

Figure 6: The simulation of impact on the sidewall during slope test; a) Application of acceleration loads, b) Stresses on the appliance during impact.

Based on the numerical simulations, the final concept of the packaging design is deduced and the prototypes of the packaging are produced as shown in Fig. 7. With the prototype packaging, it is then possible to conduct an actual transportation test and in that way finally validate the proposed concept of packaging design.

4 CONCLUSIONS

The proposed approach for paper packaging design is based on an interdisciplinary research that integrates the state-of-the-art dynamics simulation methods with the latest advances in paper material technology. It is demonstrated that suitable geometric design of honeycomb packaging makes it possible to improve the paper packaging cushioning characteristics even at multiple transportation shock loads. The presented design methodology enables development of a sustainable and recyclable packaging solutions even for heavy home appliances. This will allow GORENJE to expand its sales on markets that have already taken significant regulations towards sustainability and recyclability.

a) *b)*

Figure 7: The actual prototype of paper honeycomb packaging; a) Packaged appliance in cardboard box, b) Inner view of packaging design.

5 REFERENCES

G. Kun, W. Xi, Design and Analysis of Cushioning Packaging for Home Appliances, Procedia Engineering, 174, 2017

L. Andena, F. Caimmi, L. Leonardi, Compression of polystyrene and polypropylene foams for energy absorption applications: A combined mechanical and microstructural study, Journal of Cellular Plastics, 55, 2018

S. W. Lye, S. G. Lee, B. H. Chew, Virtual design and testing of protective buffers, Computers in industry, 54, 2004

T. Fadiji, C. J. Coetzee, T. M. Berry, A. Ambaw, U. L. Opara, The efficacy of finite element analysis (FEA) as a design tool for food packaging: A review, Biosystems Engineering, 174, 2018

A NOVEL TEST METHOD FOR EVALUATING DEWATERING OF FIBER MIXTURES USED FOR MOLDED PULP PACKAGING PRODUCTION

Chiara Czibula[1], Ulrich Hirn[2]

[1]Wood K plus - Kompetenzzentrum Holz GmbH, Veit an der Glan, Austria
[2]Institute of Bioproducts and Paper Technology, Graz University of Technology, Inffeldgasse 23, 8010 Graz, Austria

doi: 10.5281/zenodo.17295025
c.czibula@wood-kplus.at, ulrich.hirn@tugraz.at

Abstract: *The shift toward sustainable and circular materials in packaging has intensified interest in molded pulp products as eco-friendly alternatives to plastics. Since multiple factors affect the efficiency of the pulp molding process, it is essential to understand each step in detail and to evaluate how process parameters can be influenced by fiber type, blends, or additives. Among these, dewatering behavior during the forming process is one of the most critical parameters for product quality and production efficiency. To investigate this, a custom-built laboratory device was developed to analyze fiber mixtures under vacuum-assisted drainage conditions. The device measures two primary parameters in real time: applied vacuum pressure and cumulative water mass drained. The obtained data enable the characterization of drainage dynamics in fiber suspensions and provide a practical framework for comparing the dewatering efficiency of different raw material blends. In this study, the first results of the dewatering tests with the lab-testing device, together with the main fiber properties of the investigated material mixtures, are presented and discussed. The work focuses on mixtures composed mainly of recycled paper and fresh fibers – materials commonly used in molded pulp applications. The results contribute to a deeper process understanding and support future improvements in sustainable packaging production.*

Keywords: molded pulp, packaging technology, test method, dewatering efficiency, cellulosic material

1 INTRODUCTION

Molded pulp packaging—produced by shaping recycled paper fibers into protective forms—is increasingly recognized as a sustainable alternative to plastic and Styrofoam. The market for molded pulp packaging is growing rapidly, fueled by rising consumer demand for eco-friendly solutions and stricter regulations on single-use plastics (Semple et al., 2022; Singh et al., 2022; Su et al., 2018). Today, molded pulp products are generally classified by their manufacturing methods. According to the International Molded Fiber Association (IMFA), they fall into four categories: (1) thick wall, (2) transfer, (3) thermoformed, and (4) processed (Dey et al., 2020; Didone et al., 2017; Freville et al., 2024; Su et al., 2018).

1. Thermoforming – This method is a very widely applied manufacturing technique in industry. The process generally consists of four stages: the material is first shaped within a cold mold, then compacted in a heated mold, further densified, and finally dried. A key benefit of thermoforming is that it eliminates the need for an additional drying step in an oven. The resulting products exhibit high dimensional quality, smooth surface finishes, and wall thicknesses typically between 2 and 4 mm, sometimes even down to 1 mm.

2. Transfer molding – This approach requires both a forming mold and a transfer (or take-off) mold, in addition to a drying oven. The products manufactured through transfer molding usually possess uniform surfaces on both sides and wall thicknesses ranging from 3 to 5 mm.
3. Thick-wall molding – In this process, an open mold is employed, and the molded pieces are subsequently dried in an oven. The feedstock often includes Kraft fibers combined with recycled paper. The finished products show a contrast in surface texture: the inner surface is comparatively smooth, while the outer surface remains coarse. Typical wall thicknesses vary between 5 and 10 mm.
4. Processed molding – This category covers molded pulp products that undergo post-processing treatments, such as coating, printing, or the incorporation of functional additives (Didone et al., 2017).

For nearly 30 years molded pulp products were mainly used for egg trays, but today their applications have become more diverse (Gavazzo et al., 2005). Molded pulp packaging type is already widely used across sectors such as food, transportation, construction, healthcare, and household goods. The applications of this packaging type depend on whether it is required solely to protect products from external influences or also to provide cushioning. However, the effects of additives, material blends, and process parameters on production efficiency and product quality are not yet fully understood, which limits technical advancements in pulp molding. To address this gap, the present work introduces initial results from dewatering tests using a new method designed to evaluate the dewatering efficiency of material mixtures, aiming to reflect their behavior in molded pulp production.

2 MATERIALS & METHODS

2.1 Raw materials

The raw materials employed in this study are already used industrially for producing molded pulp packaging via the thermoforming process. For the initial trials, two pulp suspensions were prepared. Mixture 1 consisted of unused corrugated board (class 4.01.02) combined with ECF-bleached long-fiber sulphate pulp. Mixture 2 contained the same pulp in combination with GC1, a pigment-coated virgin mechanical pulp board with a white reverse side.

2.2 Fiber analysis

To characterize the different kinds of raw materials, morphological Fiber Tester measurements were conducted to know the fiber shape (curl), the fines content and the average fiber length. For this, the L&W Fiber Tester Plus device from ABB (Zürich, Switzerland) was used to analyze fiber dimensions, as well as the fiber form, from which the mean kink-index and kink-angle were acquired.

2.3 Freeness of pulp (Canadian standard method)

The Canadian Standard Freeness (CSF) test, performed in accordance with TAPPI T 227, was used to evaluate the drainage rate of dilute pulp suspensions. This method measures the volume of water discharged from a standardized freeness tester after a 3 g/L pulp suspension drains through a perforated screen under controlled conditions.

2.4 Lab-testing device

A laboratory-scale drainage test bench (see Figure 1) was developed to replicate the forming station of pulp molding machines, excluding the 3D-formed mold at this stage. This setup enables small-scale testing, thereby avoiding the high energy and material costs associated with full-scale TPM machinery. The system consists of two primary containers: a vacuum container (1), where the required vacuum is generated, and an intermediate container (2) with a removable sieve structure, which is connected to an upper attachment where the pulp suspension is introduced (3). To simulate the vacuum drainage process seen in industrial machines while maintaining a decoupled and controllable laboratory setup, a pneumatic ball valve (4) is installed between the vacuum and intermediate containers. This valve, connected via a hose (5), allows controlled initiation of the vacuum suction. Additionally, a pressure sensor (6) is integrated into the vacuum container to record the vacuum profile during each test. A scale (7) located beneath the entire apparatus continuously logs the mass change, providing a time-resolved drainage curve.

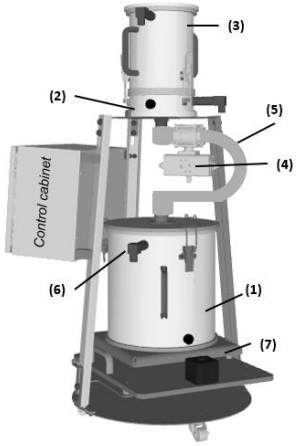

Figure 3: Scheme of the lab-testing device for the dewatering measurements. (1) vacuum container; (2) intermediate container with removable sieve structure; (3) upper container for adding the pulp suspension; (4) pneumatic valve with the connecting hose (5); (6) pressure sensor; (7) scale.

3 RESULTS AND DISCUSSION

Before starting the measurements with the lab-testing device, the fiber properties of the material mixtures were analyzed. Of particular interest are the fiber length distribution (length-weighted) and the Canadian Standard Freeness (CSF) values. These parameters provide an initial estimation of how the raw material suspension will behave—first in the forming station of the pulp molding machines, and second during the dewatering test with the self-built dewatering device.

Table 1 summarizes the fiber properties, including the CSF values of the investigated raw material mixtures. The fiber length distribution (length-weighted) is illustrated in Figure 2. By combining these results, it becomes evident that mixture 1 should dewater more slowly than mixture 2, which can be attributed to its higher CSF value despite the measured fines content was slightly lower in mixture 1.

Table 5: Summary of the fiber properties of mixture 1 and mixture 2.

sample	mixture 1	mixture 2
Fiber length numeric Ln [mm]	0.779	0.825
Fiber length (length weighted) Lw [mm]	1.4	1.4
Fiber length (weight weighted) Lz [mm]	2.205	2.176
Fiber width [µm]	24.2	24.4
Fine content (length weighted) Lw [%]	46.75	47.73
Kink index [-]	1.463	1.498
Kink angle [°]	50.7	50.1
CSF	617	744
Fine percentage [%]	97.3	97.5

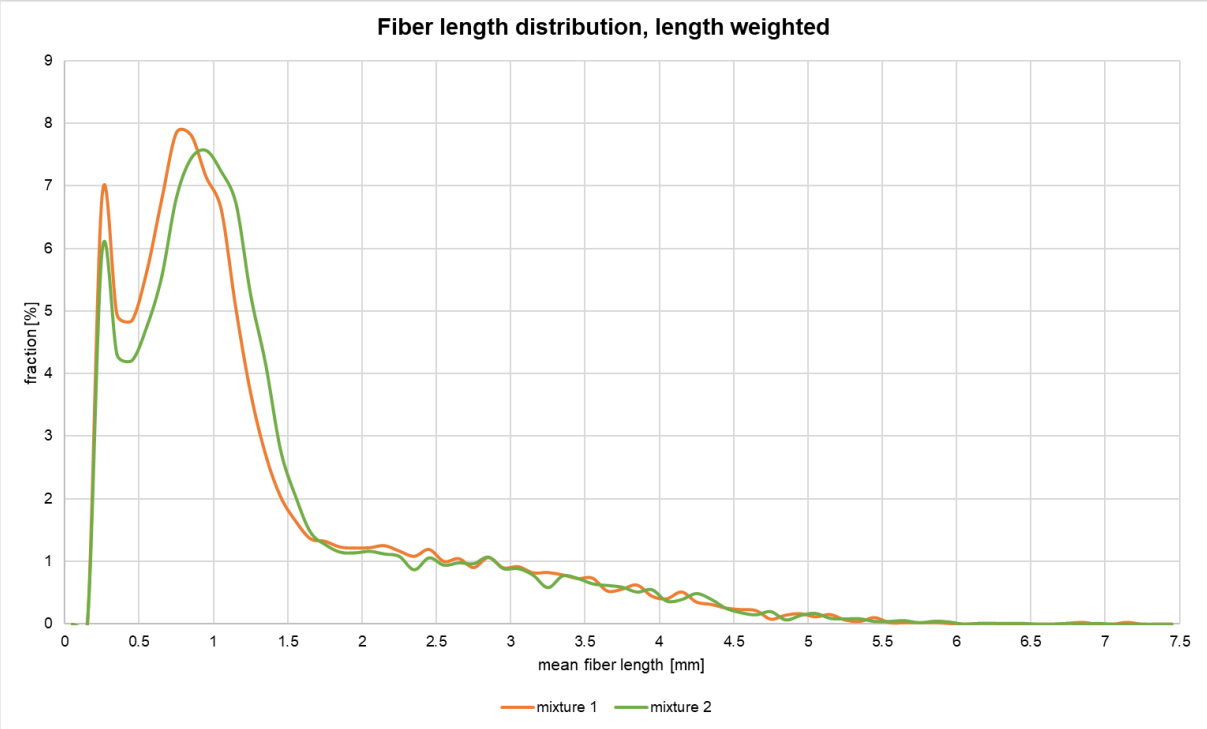

Figure 4: Length weighted fiber distribution of the two used pulp suspensions

After the fiber properties of the material mixtures had been analyzed, dewatering tests of the two mixtures with the same concentrations were carried out on the new lab-testing device, as it was shown in Figure 1. For these measurements a concentration of 5g o.d. fibers in 2L was used (see Figure 3).

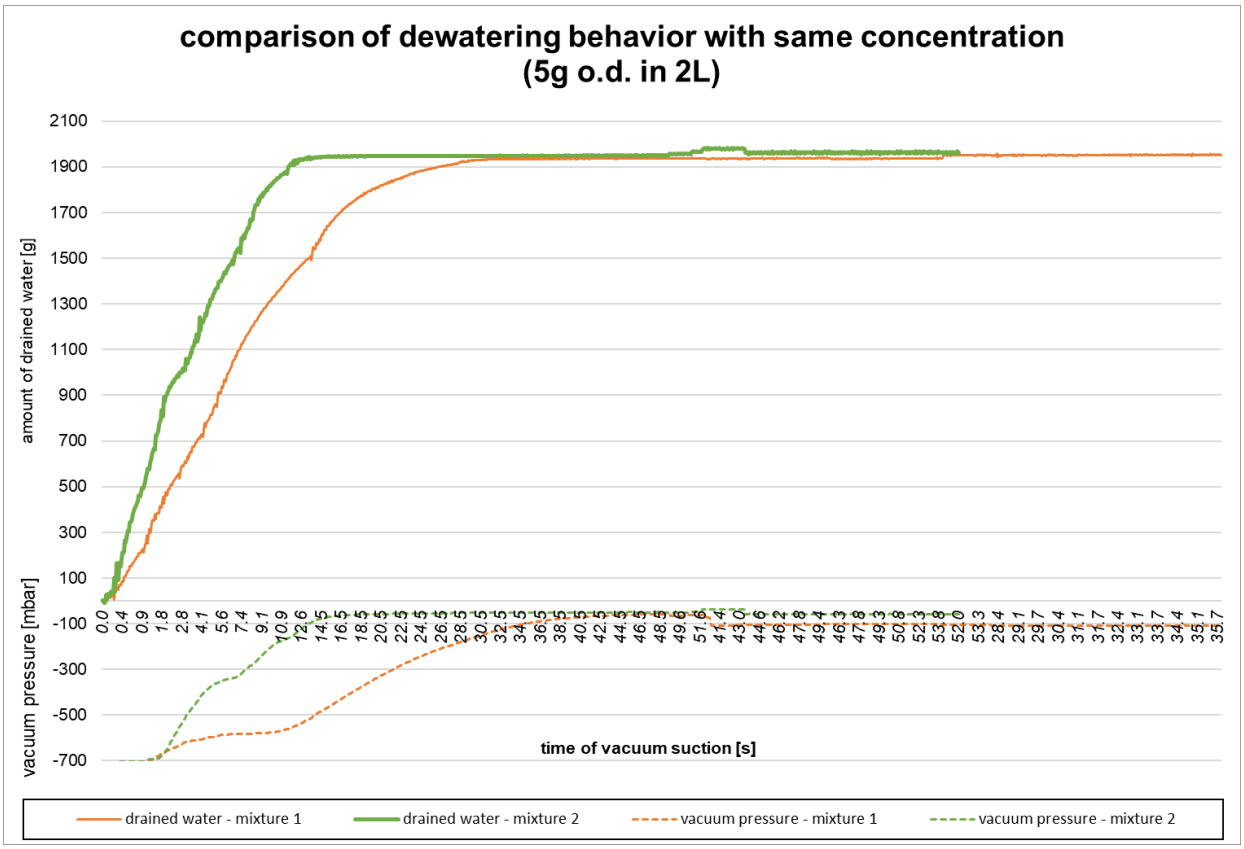

Figure 5: Comparison of dewatering behavior of the two mixtures with the lab-testing device. Dotted lines show the progress of the vacuum pressure, while the continuous lines represent the mass of the drained water during the measurements.

The conducted measurements, presented in Figure 3, confirmed the expected trend: mixture 1, characterized by a lower CSF value, exhibited slower dewatering compared to mixture 2, which had a higher CSF value. This behavior is consistent with observations in pulp molding machines, supporting the conclusion that the laboratory testing device yields reliable data.

4 CONCLUSIONS

In this work, a novel test method for investigating the behavior of different material mixtures and raw materials during dewatering with applied vacuum was presented. Combined with the characterization of fiber properties, this approach should provide a better understanding of the dewatering step in the forming station of pulp molding machines.

The first measurements yielded promising results: the same trends observed in pulp molding machines could be reproduced in the lab-testing device. In particular, the fiber properties—especially the CSF value—correlated well with the measured dewatering behavior. Future measurements will be carried out using different sieve structures, concentrations and additives.

Overall, the results demonstrate that the developed test method can improve process understanding in pulp molding and support practical advancements in sustainable packaging production, contributing to more efficient manufacturing practices.

5 REFERENCES

Dey, A., Sengupta, P., Pramanik, N.K., Alam, T., 2020. Paper and other pulp based eco-friendly moulded materials for food packaging applications : a review. J. Postharvest Technol. 08, 1–21.

Didone, M., Saxena, P., Brilhuis-Meijer, E., Tosello, G., Bissacco, G., Mcaloone, T.C., Pigosso, D.C.A., Howard, T.J., 2017. Moulded Pulp Manufacturing: Overview and Prospects for the Process Technology. Packag. Technol. Sci. 30, 231–249. https://doi.org/10.1002/pts.2289

Freville, E., Sergienko, J.P., Mujica, R., Rey, C., Bras, J., 2024. Novel technologies for producing tridimensional cellulosic materials for packaging: A review. Carbohydr. Polym. 342, 122413. https://doi.org/10.1016/j.carbpol.2024.122413

Gavazzo, G.B., Lanouette, R., Valade, J.L., 2005. Production of molded pulp at laboratory scale. Prog. Pap. Recycl. 14, 20–25.

Semple, K.E., Zhou, C., Rojas, O.J., Nkeuwa, W.N., Dai, C., 2022. Moulded pulp fibers for disposable food packaging: A state-of-the-art review. Food Packag. Shelf Life 33, 100908. https://doi.org/10.1016/j.fpsl.2022.100908

Singh, A.K., Itkor, P., Lee, M., Shin, J., Lee, Y.S., 2022. Promoting sustainable packaging applications in the circular economy by exploring and advancing molded pulp materials for food products: a review. Crit. Rev. Food Sci. Nutr. 0, 1–16. https://doi.org/10.1080/10408398.2022.2088686

Su, Y., Yang, B., Liu, J., Sun, B., Cao, C., Zou, X., Lutes, R., He, Z., 2018. Prospects for Replacement of Some Plastics in Packaging with Lignocellulose Materials: A Brief Review. BioResources 13, 4550–4576. https://doi.org/10.15376/BIORES.13.2.SU

UPCYCLED CARDBOARD BY-PRODUCTS AS FUNCTIONAL ADDITIVES IN THERMOPLASTIC STARCH-BASED BIOPLASTICS

Idalina Gonçalves, G. J. Campos, E. M. T. Gonçalves, M. Pinho, A. M. Ferreira, F.H. B. Sosa, P. Ferreira

Aveiro Institute of Materials, Department of Materials and Ceramic Engineering, University of Aveiro, Aveiro, Portugal

doi: 10.5281/zenodo.17295091
idalina@ua.pt

Abstract: *The growing demand for sustainable materials has driven research into circular strategies that valorize packaging waste. In this context, cardboard production trims, an abundant by-product of packaging manufacturing, were explored as a source of cellulose-rich nanostructures to be used as additives in thermoplastic starch (TPS)-based bioplastics. Within the scope of the BIOCOATING project, various chemical pre-treatments were evaluated to disintegrate and upcycle these cardboard residues. NaOH/urea aqueous systems and ionic liquids were applied under controlled temperature and mixing conditions to dissolve the fiber matrix and generate gel-like suspensions rich in cellulose. The resulting gels were purified, dried, and incorporated into TPS formulations developed using starch recovered from potato washing slurries. The incorporation of upcycled cardboard fractions into the TPS matrix aims to enhance film-forming ability, moisture barrier performance, and mechanical resistance, while preserving biodegradability. Preliminary results indicate that ionic liquids show a promising balance between processing efficiency and functional enhancement. This approach demonstrates a double valorization strategy, integrating cellulosic packaging waste and food processing residues into a single, biodegradable material platform for packaging applications. Upcycled cardboard-derived structures thus offer a renewable alternative to synthetic fillers and support the design of packaging materials aligned with circular economy principles.*

Acknowledgements: *This work was developed within the scope of the project CICECO-Aveiro Institute of Materials, UIDB/50011/2020 (DOI 10.54499/UIDB/50011/2020), UIDP/50011/2020 (DOI 10.54499/UIDP/50011/2020) & LA/P/0006/2020 (DOI 10.54499/LA/P/0006/2020), financed by national funds through the FCT/MCTES (PIDDAC). G.J. Campos and E.M.T. Gonçalves acknowledge the BIOCOATING project (COMPETE2030-FEDER-00590400), funded by Compete 2030, Portugal 2030, and the European Union, for the research grants. The authors also thank Isolago Europe (project leader), as well as A Saloinha and FEB Cafés, for kindly providing the agri-food by-products used in this study. I. Gonçalves acknowledges funding from FCT through the Individual Call to Scientific Employment Stimulus (https://doi.org/10.54499/CEECIND/00430/2017/CP1459/CT0032).*

SAFETY ASSESSMENT OF CHEMICALLY MODIFIED LIGNIN FOR FOOD PACKAGING APPLICATIONS

Francisco AG Soares Silva[1], Sristhi Singh[1], Joel Pereira[1,3], Tomás Duarte[2], Fátima Poças[1 3]

[1]Universidade Católica Portuguesa, CBQF - Centro de Biotecnologia e Química Fina - Laboratório Associado, Escola Superior de Biotecnologia, Porto, Portugal.
[2]RAIZ – Instituto de Investigação da Floresta e do Papel, Quinta de S. Francisco, Portugal
[3]CINATE – Escola Superior de Biotecnologia, Universidade Católica Portuguesa, Portugal

doi: 10.5281/zenodo.17295117
fpocas@ucp.pt

Abstract: *This study evaluates the safety implications of propionic acid–mediated lignin esterification intended to improve hydrophobicity and polymer compatibility. Lignin was esterified using propionic acid with sulfuric acid as catalyzer. FTIR and NMR confirmed successful ester bond formation through the appearance of characteristic carbonyl and alkyl signals, alongside reduction of hydroxyl-related peaks. Gas chromatography–mass spectrometry (GC-MS) was employed to identify volatile and semi-volatile compounds in unmodified and esterified lignin, with toxicity classification via Cramer's Decision Tree. Esterification altered lignin's chemical profile, introducing new esters and transforming guaiacol-derived phenolics while degrading some volatiles. Most detected compounds belonged to Cramer Class I (low toxicity), but certain Class III substances, including diethyl sulfate (IARC 2A carcinogen), emerged after modification, likely due to acid-catalyzed side reactions.*

Keywords: food packaging, lignin, safety, barrier, coatings

1 INTRODUCTION

One promising candidate to be used as additive in food packaging applications is lignin, a natural aromatic macromolecule derived from lignocellulosic biomass. Its structure, however, varies across biomass types (softwoods, hardwoods, grasses), with differences in monolignol composition and linkages influencing reactivity and compatibility (Zhang et al. 2022). Lignin has attracted attention as a bio-based additive for coatings and films due to its antioxidant, antimicrobial, and hydrophobic characteristics, with potential enhancer of the functional performance of biopolymer-based coatings (Camargos et al. 2022), (Boarino e Klok 2023). Lignin can reduce oxygen and water vapor transmission, especially when the base material is hydrophilic, as lignin's chemical structure contains hydrophobic groups, such as aromatic rings and methoxy (-OCH_3) groups, that repel water. However, lignin also contains hydrophilic groups, such as hydroxyl (-OH) and carboxyl (-COOH) groups(Marques et al. 2025; Zadeh et al. 2018). In hydrophilic matrices, these groups facilitate compatibility; however, for hydrophobic materials such as PBAT (which contains terephthalate units, aliphatic methylene groups, and ester bonds), the hydrophilic groups in lignin may hinder compatibility, necessitating lignin modification or the use of compatibilizing additives to improve compatibility (Boarino e Klok 2023). Several strategies can be employed to improve lignin compatibility on hydrophobic matrices, including esterification (Liu et al. 2019), acetylation (Sameni et al. 2017), grafting (Eraghi Kazzaz et al. 2019), compatibilizers (Han e Wu 2019), and physical modifications such as particle size reduction (Camargos

et al. 2022). These strategies have been shown to improve compatibility with hydrophobic matrices; however, many involve toxic reagents such as acid chlorides or anhydrides. Emerging strategies, such as esterification with organic acids offer safer, simple and sustainable alternatives (Liu et al. 2019). These modifications are considered less hazardous, although esterification may still introduce additional safety concerns, which are addressed in this study. This study investigates safety risks associated with esterification byproducts through chemical migration analysis using gas chromatography–mass spectrometry (GC-MS).

2 MATERIALS AND METHODS

2.1 Lignin esterification and characterization

Esterification was adapted from Liu et al. (2019). Kraft alkali lignin (CAS 8068-05-1) was reacted with propionic acid at a 1:7 lignin-to-acid ratio, with 10% (v/v) acetone to aid dispersion, and 5% (w/w) sulfuric acid relative to lignin as catalyst. The suspension was stirred for 3 h, then thermally treated in an autoclave at 121 °C for 4 h. The reaction mixture was washed repeatedly with distilled water and centrifuged at 4000 rpm until neutral pH, air-dried, and milled. Approximately 90% of the propionic acid was recovered by rotary evaporation and re-used for subsequent esterifications.

Fourier-Transform Infrared Spectroscopy (FTIR) - FTIR analysis of Lignin and E.lignin was carried out in a Bruker FTIR spectrometer ALPHA II (Bruker Corporation, Billerica, MA, USA) in transmission mode, operating at a resolution of 4 cm-1. The spectra were taken between 4000 and 300 cm-1 by averaging 60 scans for each spectrum. All samples were scanned twice for verification purposes.

Nuclear magnetic resonance (NMR) - NMR analysis of Lignin and E.lignin was carried out. 1H–13C of cross-polarization/rotation at the magic angle (CP/MAS NMR) was obtained in a Bruker Avance III spectrometer of 9.4 T wide bore, with Larmor frequency of 400 MHz for 1H. A 4 mm dual-resonance MAS probe was used, operating at 400.1 MHz for 1H and 100.6 MHz for 13C.

Gas chromatography mass spectrometry analysis - Lignin and esterified lignin were analysed through GC-MS, to detect volatile compounds from these samples. Two extraction methods were used, h*eadspace and Liquid method*. Through headspace, about 25 mg of lignin and E.lignin were thermally treated at 200°C for 1 hour. Analysis was performed using a Zebron 5ms plus column (30 m × 0.25 mm ID × 0.25 µm), with a 1 mL injection volume. The injector was set to 250°C (split 1:10). The oven was programmed from 40 °C (5 min), ramped at 10 °C/min to 320°C. Mass spectrometry was conducted with electron ionization (EI) at 70 eV, scanning m/z 33–350. Compounds were identified using the NIST 2020, Version 2.4 library. In the *liquid Extraction Method* volatile compounds of lignin and E.lignin were extracted in 3 mL ethanol for 24 hours at 60 °C. A 1 µL aliquot was injected into the Zebron 5ms plus column under splitless mode (injector at 320°C, 0.75 min). The oven was programmed from 50 °C (3 min), ramped at 10°C/min to 320 °C, and held for 15 min. MS detection was carried out using EI at 70 eV, with full scan range 33–700 m/z. Identification was performed using the NIST 2020, Version 2.4 library.

3 RESULTS AND DISCUSSION

Lignin esterification

Esterification of lignin was performed to enhance its compatibility with the hydrophobic matrices. The process involved treating kraft alkali lignin with propionic acid under controlled heat (90–120 °C) to introduce ester functional groups. The reaction led to structural modifications, confirmed by FTIR (Figure 1). The first spectral change was the appearance of a strong absorption band around 1722 cm^{-1}, corresponding to C=O stretching in ester groups. This band is absent in native lignin and confirms the successful formation of ester bonds (Zhao et al. 2017). Additionally, bands observed at 2918 cm^{-1} and 2850 cm^{-1} represent asymmetric and symmetric C–H stretching, respectively, associated with the presence of propionyl alkyl groups (Sangeetha et al. 2022). Further changes were noted in the 1000–1300 cm^{-1} region, where alterations in C–O and C–O–C stretching vibrations were observed (Figure 1).

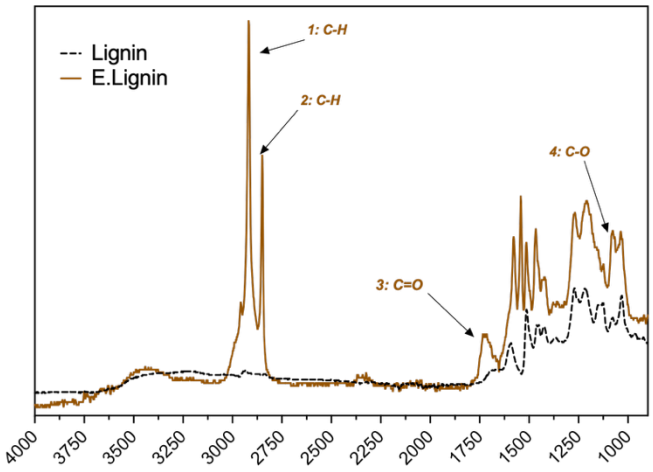

number	*Peak/Change*	*Indication*
1	*2918 cm^{-1}*	*Propionyl alkyl group.*
2	*2850 cm^{-1}*	*Propionyl alkyl group.*
3	*1722 cm^{-1}*	*Ester bond formation.*
4	*1128 and 1030 cm^{-1}*	*Loss of hydroxyl groups.*

Figure 1: FTIR spectrum of lignin and esterified lignin

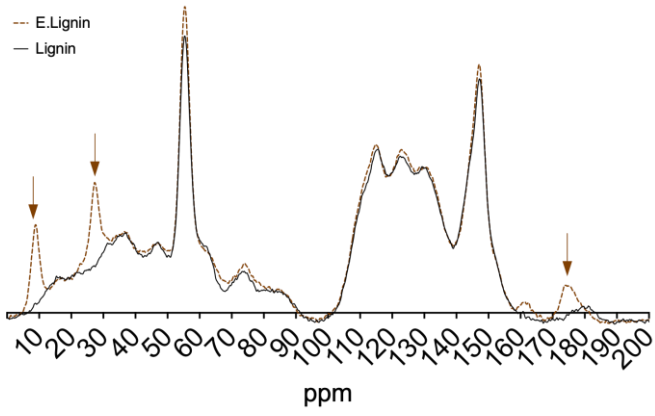

Figure 2: 13C CP/MAS NMR spectra of lignin and esterified lignin

The NMR spectra allowed detailed analysis of structural changes in lignin before and after esterification. Significant differences were observed in regions associated with aliphatic and carbonyl carbons, confirming the formation of ester groups. New resonances appeared at δ = 180–170 ppm,

corresponding to aliphatic ester carbonyl carbons, and at δ = 28–26 ppm and δ = 10–8 ppm, corresponding to aliphatic carbon chains of the propionate groups. The aromatic region was unaffected, thus esterification mainly affecting aliphatic hydroxyl groups (Boarino e Klok 2023; L.-Y. Liu, Hua, e Renneckar 2019). As confirmed by both FTIR and NMR, lignin was successfully esterified using propionic acid. While absolute quantification was not possible with NMR, the significant reduction of signal intensity in the δ = 60–80 ppm region (associated with aliphatic –OH carbons) indicates substantial esterification.

Safety of Lignin & E.Lignin

As observed above, esterification modifies the lignin structure, which can introduce chemical changes. For materials intended for food-contact applications, such modifications raise critical questions about the potential migration of toxic or uncharacterized substances into food (EFSA Panel on Food Contact Materials, Enzymes, Flavourings and Processing Aids (CEF) 2016). Therefore, a thorough chemical safety assessment of E.lignin is essential to evaluate its suitability and regulatory compliance for use in sustainable food packaging. GC-MS analysis of lignin and E.lignin identified several compounds, which were classified according to their toxicity using Cramer's Decision Tree classification (Roberts et al. 2015). This system categorizes compounds into Class I (low toxicity), Class II (moderate toxicity), and Class III (high toxicity) based on their chemical structure.

Table 1: Major Compounds found in Lignin (GC-MS) and their toxic classification according to Cramer

Compounds	***CAS***	***Chem class***	***Cramer***	***Peak change***	***Obs***
4-Acetoxy-3-methoxyphenethyl alcohol, acetate	*32022-28-9*	*Ester*	*Class I*	*Appeared*	*Ester formed*
1,2,3-Propanetriol, tripropanoate	*139-45-7*				
Propanoic acid, ethyl ester	*105-37-3*				
Propanoic acid	*79-09-4*	*Organic acid*			
3-(4-Allyl-2-methoxyphenoxy)-1,2-propanediol	*398-58-3*	*Phenylpropanoid*			*Esterification of guaiacol*
4-Acetoxy-3-methoxyphenethyl alcohol, acetate	*32022-28-9*	*Phenol and benzoate ester*			*Esterified phenolic compound*
Naphthalene, 2,3-dimethoxy-	*10103-06-7*	*Polycyclic aromatic ether*			*Detectable after esterification*
Phenol, 4-(2-propenyl)- (4 Allyphenol)	*501-92-8*	*Phenylpropanoid*			
1-Hydroxy-2-butanone	*5077-67-8*	*Hydroxyketone*			
2,3-Bis[(4-hydroxy-3-methoxyphenyl)methyl]butane-1,4-diol, tetraacetate	*41025-80-3*	*Phenylpropanoid*			*Conversion of coniferyl alcholol*
3-Penten-2-one, 4-methyl-	*141-79-7*	*Olefinic compound*			*Stable olefinic structure unaffected by esterification.*
4-Penten-2-one, 4-methyl-	*3744-02-3*				
Diethyl sulfate	*64-67-5*	*Ester*	*Class III*		*Formed on the presence of sulfuric acid*
Methanesulfonic acid, methyl ester	*66-27-3*				
Dimethyl sulfone	*67-71-0*	*Sulfone*			
Furfural	*98-01-1*	*Furan derivative*			*Thermal degradation during esterification*
2,5-Furandione, 3-methyl-	*616-02-4*	*Cyclic anhydride*			
Furfural, 5-methyl-	*620-02-0*	*Furan derivative*			

Propanamide	*79-05-0*	*monocarboxylic acid amide*			*Formed via condensation*
Guaiacol	*90-05-1*	*Phenol*	*Class I*	*Decreased*	*Partially reacted to form 3-(4-Allyl-2-methoxyphenoxy)-1,2-propanediol*
2-Methoxy-4-vinyphenol	*7786-61-0*				
Benzenepropanol, 4-hydroxy-3-methoxy-	*2305-13-7*				
Phenol, 4-ethyl-2-methoxy-	*2785-89-9*				
Vanillin	*121-33-5*	*Benzaldehydes*			*Possibly converted into 3,4-Divanillyltetrahydrofuran*
(E)-3,3'-Dimethoxy-4,4'-dihydroxystilbene	*7329-69-3*	*Stilbenol*			*Partially reacted to form 2,3-Bis[(4-hydroxy-3-methoxyphenyl)methyl]butane-1,4-diol, tetraacetate*
Apocynin	*498-02-2*	*Aromatic ketone*			*Esterified*
Phenol, 2,6-dimethoxy-	*91-10-1*	*Phenol*			*Possible conversion of phenolic OH during esterification.*
trans-isoeugenol	*5932-68-3*	*Essential oil*			*Reactivity of its allyl and phenolic groups.*
2-Cyclopenten-1-one, 3-ethyl-2-hydroxy-	*21835-01-8*	*Cyclic ketone*	*Class III*		*Partial esterification of the hydroxy group.*
2-Cyclohexen-1-one, 2-hydroxy-3-methyl-6-(1-methylethyl)-	*490-03-9*				
1,4-Benzenediol, 2,5-dimethyl-	*615-90-7*	*Hydroquinone*	*Class I*	*Disapeared*	*Volatilized or decomposed*
Coniferyl Alcohol ((E)-4-(3-Hydroxyprop-1-en-1-yl)-2-methoxyphenol)	*32811-40-8*	*Phenylpropanoid*			*Conversion to 2,3-Bis[(4-hydroxy-3-methoxyphenyl)methyl]butane-1,4-diol, tetraacetate*
2-Hydroxy-gamma-butyrolactone	*19444-84-9*	*Furan derivative*			*Esterified*
Octanal	*124-13-0*	*Fatty aldehyde*			*Volatilized or decomposed*
1H-Pyrrole-2-carboxaldehyde	*1003-29-8*	*Pyrrole and Aldehyde*	*Class II*		*Volatilized or decomposed*
Cyclohexanone, 2-acetyl-	*874-23-7*	*Cyclic ketone*			*Conversion or reactivity of the ketone group during esterification.*
Benzonitrile, 4-hydroxy-3-methoxy- (Dehydrodieugenol)	*4421-08-3*	*Biphenyls*	*Class III*		*Reduced volatility or interaction during esterification*
3,4-Divanillyltetrahydrofuran	*34730-78-4*	*Furan derivative*	*Class I*	*Increased*	
Dehydroabietic acid	*1740-19-8*	*Abietane diterpenoid*	*Class III*		*Conversion of abietic acid into its dehydrogenated form.*

Esterification of lignin markedly altered its chemical composition, forming new esters (e.g., diethyl sulfate, propanoic acid ethyl ester), transforming guaiacol-derived compounds, and degrading certain volatiles (Table 2). Guaiacol derivatives partially reacted to yield complex structures such as 3-(4-allyl-2-methoxyphenoxy)-1,2-propanediol, while coniferyl alcohol formed higher-molecular-weight phenylpropanoids. Thermal degradation produced furfural and other furan derivatives. Some phenolic

and guaiacol-based compounds decreased or disappeared, indicating esterification or volatilization (e.g., vanillin → 3,4-divanillyltetrahydrofuran; hydroquinone and coniferyl alcohol decomposed). Conversely, compounds like dehydroabietic acid increased, suggesting oxidative transformations. Most lignin compounds belonged to low-toxicity Class I, including vanillin, eugenol, creosol, benzenepropanol derivatives, and trans-13-octadecenoic acid, consistent with previous reports (Takada et al., 2004; Ehara et al., 2005; Lucejko et al., 2020). New Class III compounds—diethyl sulfate, methanesulfonic acid methyl ester, dimethyl sulfone, furfural, and 5-methylfurfural—appeared only in esterified lignin, indicating potential health concerns and the need for purification before food-contact use. Diethyl sulfate is classified as a Group 2A carcinogen (IARC, 1999). While esterified lignin is only 1% of PBAT coatings, migration studies are required to assess safety.

4 CONCLUSIONS

Lignin esterification with propionic acid successfully improved its hydrophobic character and as confirmed by FTIR and NMR. However, GC-MS analysis revealed that the modification altered lignin's chemical composition, generating new esters and transforming phenolic constituents. While most detected substances were classified as low toxicity (Cramer Class I), certain high-toxicity Class III compounds, including diethyl sulfate, were formed during esterification. These byproducts underscore the necessity for additional purification steps to ensure compliance with food-contact safety requirements. Overall, this study demonstrates that propionic acid–based esterification can be a viable route to enhance lignin performance in hydrophobic bio based coatings, after addressing the main safety concerns found.

5 REFERENCES

Boarino, Alice, e Harm-Anton Klok. 2023. «Opportunities and Challenges for Lignin Valorization in Food Packaging, Antimicrobial, and Agricultural Applications». Biomacromolecules 24 (3): 1065–77. https://doi.org/10.1021/acs.biomac.2c01385.

Camargos, Camilla H. M., Giovanna Poggi, David Chelazzi, Piero Baglioni, e Camila A. Rezende. 2022. «Protective Coatings Based on Cellulose Nanofibrils, Cellulose Nanocrystals, and Lignin Nanoparticles for the Conservation of Cellulosic Artifacts». ACS Applied Nano Materials 5 (9): 13245–59. https://doi.org/10.1021/acsanm.2c02968.

Eraghi Kazzaz, Armin, Zahra Hosseinpour Feizi, e Pedram Fatehi. 2019. «Grafting Strategies for Hydroxy Groups of Lignin for Producing Materials». Green Chemistry 21 (21): 5714–52. https://doi.org/10.1039/C9GC02598G.

Han, Buxing, e Tianbin Wu, eds. 2019. Green Chemistry and Chemical Engineering. Springer New York. https://doi.org/10.1007/978-1-4939-9060-3.

Liu, Li-Yang, Qi Hua, e Scott Renneckar. 2019. «A Simple Route to Synthesize Esterified Lignin Derivatives». Green Chemistry 21 (13): 3682–92. https://doi.org/10.1039/C9GC00844F.

Marques, Clara Suprani, Tarsila Rodrigues Arruda, Karoline Ferreira Silva, e Taíla Veloso de Oliveira. 2025. «Lignin in Food Packaging». Em Handbook of Lignin, editado por Mohammad Jawaid, Akil Ahmad, e Aatikah Meraj. Springer Nature Singapore. https://doi.org/10.1007/978-981-97-2664-6_62-1.

Sameni, Javad, Sally Krigstin, e Mohini Sain. 2017. «Solubility of Lignin and Acetylated Lignin in Organic Solvents». BioResources 12 (1): 1548–65. https://doi.org/10.15376/biores.12.1.1548-1565.

Zadeh, Elham Mohammad, Sean F. O'Keefe, e Young-Teck Kim. 2018. «Utilization of Lignin in Biopolymeric Packaging Films». ACS Omega 3 (7): 7388–98. https://doi.org/10.1021/acsomega.7b01341.

Zhang, Liming, Anette Larsson, Annelie Moldin, e Ulrica Edlund. 2022. «Comparison of Lignin Distribution, Structure, and Morphology in Wheat Straw and Wood». Industrial Crops and Products 187 (novembro): 115432. https://doi.org/10.1016/j.indcrop.2022.115432.

CIRCULAR MODELS, POLICY, AND CONSUMER INSIGHTS

COMPARATIVE ANALYSIS OF LIFE CYCLE IMPACT ASSESSMENT METHODS FOR PACKAGING PRODUCTS

Gregor Radonjič, Matjaž Denac

University of Maribor, Faculty of Economics and Business, Department for Technology and Entrepreneurial Environment Protection, Maribor, Slovenia

doi: 10.5281/zenodo.17295142
gregor.radonjic@um.si

Abstract: *In assessing environmental impacts of packaging, it is necessary to use modern software tools, supported by verifiable databases based on the environmental life cycles of products. There are several software solutions that differ greatly from each other in terms of the complexity of life cycle modeling, accessibility to databases, LCIA methods used to determine environmental impacts, and the dynamics of database updating. The aim of this paper is to conduct LCA study for the case of a two-layered polymeric film made from low density polyethylene (PE-LD) and polyamide-6 (PA-6) laminated plastic packaging film using several LCIA methods to compare and comment the final LCA results in terms of the life-cycle environmental impacts. Results clearly show that the choice of LCIA method for evaluating environmental impacts within LCA study has a very large impact on the final result.*

Keywords: packaging, life cycle assessment, LCIA methods, environmental impacts.

1 INTRODUCTION

Without any doubt, environmental sustainability issues have become a leading trend regarding packaging development and use. Unfortunately, the simplistic view that packaging is ''environmentally friendly'' still prevails if it can be recycled, or if it is produced from recycled materials, still often prevails in companies and environmental NGOs. However, the environmental impacts of packaging are much more complex (Radonjič 2008; Radonjič 2014; Verghese 2012). They occur throughout the supply chain, during use phase and during waste processing. Therefore, a more holistic thinking has been established in the European Union and elsewhere in the world when assessing the environmental impacts of packaging and packaged products, based on environmental life cycle assessments (LCA), especially since there are numerous design options of packaging products on the market produced from different materials combinations (Kan 2022; Sinnko 2024).

To determine which environmental impacts are the most harmful, or which environmental categories are the most influential and in which phase of the life cycle they occur, it is necessary to use quantitative tools for their calculation. The most popular and methodologically most sophisticated is certainly the LCA method. This complex analytical method determines the impacts of products throughout their entire life cycles, which include the extraction of raw materials, the extraction of energy sources, the production and distribution of the required energy, the production of semi-finished products, products and by-products, transport and distribution, effects during use and alternative options for handling product wastes after use.

Nowadays, many different packaging options exist on food, cosmetic and other markets. A thin flexible multilayered plastic film packaging is widely use but it is rarely suitable for recycling because it consists

of several layers of different polymeric materials which cannot be easily technically separated in an economically feasible way. However, their environmental benefits can be expressed for example through much lower use of primary resources and energy consumption among others (Bukowski 2018). However, such environmental benefits must be carefully calculated within their entire life cycle for every individual case and not generalized, especially when compared to other packaging materials options like paper, aluminium or a thicker single-material plastic options. With this regards, LCA is a powerful tool for such comparisons of environmental impacts of this typs of packaging (Siracusa 2014; Tunçok-Çeşme 2024; Mousania 2025).

However, the results of LCA studies are highly dependent of different life cycle model assumptions, cut-off criteria, allocation and other aspects including the choice of the environmental impact assessment method employed in a study. This was confirmed by our own findings as well as findings from other authors which suggest that different life cycle impact assessment (LCIA) methods can lead to clearly different final results (Reap 2008; Owsianiak 2014; Tascione 2024; Bher 2024).

The aim of this paper is to conduct LCA study for the case of a laminated plastic packaging film using several LCIA methods to compare and comment the final LCA results in terms of the life-cycle environmental impacts.

2 LIFE CYCLE ASSESSMENT IMPACT METHODS

The determination of the environmental impacts of products in LCA studies is based on four steps (phases) defined by standard ISO 14040 (ISO 2006): goal and scope definition, inventory analysis, impact assessment and interpretaion.

More than 40 different LCIA methods are available for the implementation of the third phase, among which there are many significant differences both in terms of the scientific basis for calculating complex environmental impacts and in terms of the number of environmental categories included in the final results of the LCA analysis (PRé Consultants, 2020). The following methods are among the most well-known in practice: Ecoindicator 99 (EI99), ReCiPe 2016 and the EU Environmental Footprint (EF), which also represent stages in the development of LCIA methods. They have some common features, but also significant differences, such as the number of harmful substances and the number of environmental categories taken into account (11 for the Ecoindicator 99 method, 22 for the ReCiPe 2016 method and 27 for Environmental Footprint). Newer methods such as ReCiPe and EF are also based on better models of the action of harmful substances in the environment and in organisms, which increases their credibility or. accuracy of calculations (PRé Consultants, 2020). The ReCiPe 2016 and EF methods additionally includes water consumption and other pollution categories in the calculation, which is an important parameter for wood products. They also differ how biogenic CO2 is considered.

What all three LCIA methods have in common is that the calculated environmental impacts can be weighted with predefined environmental weights, which allows them to be aggregated and the results presented as so-called ecopoint. Without such a calculation procedure, it would be impossible to combine different environmental categories since they are expressed in different units.. Here, 1 ecopoint represents one thousandth of the environmental burden of one EU (or world, depending on the method used) citizen in one year. Thus, an ecopoint is not an absolute value of a product's impact on the environment, but only a relative measure of the damage caused to the environment and it should be understood as a quantitative guideline for planners who want to analyze and minimize the environmental burden of their products and compare them with each other.

3 CASE STUDY

3.1 Description of packaging under study

Due to the reasons described in Introduction, two-layered polymeric film made from low density polyethylene (PE-LD) and polyamide-6 (PA-6) which is used for food packaging with the process of vacuum packing or packing in the modified atmosphere was chosen as a case for conducting LCA analysis with the aim of using different LCIA methods to study their influence on final results. Thickness of PE-LD layer is 60 µm and 30 µm for PA-6 layer.

3.2 Description of PE-LD/PA film life cycle

The LCA analysis includes the environmental impacts of oil extraction, production of organic compounds (ethylene, ε-caprolactam), polymerization of both polymers, film extrusion, lamination of multilayer film, welding and waste processing (Figure 1). The environmental impacts of adhesive production are also taken into account. Transport between all the aforementioned life cycle phases is included. PE-LD production takes place in Slovakia, while PA-6 production takes place in Germany. Plastic granulate is transported from both chemical industry plants to Milan to the film manufacturer, where lamination also takes place. From Milan, the laminated PE-LD/PA-6 film is transported to Ljubljana, where packaging bags are produced by heat welding. The average EU waste scenario for plastic packaging wastes was taken into consideration for determination of environmental impacts of PE-LD/PA wastes treatment.

3.2 LCA methodological aspects

The functional unit is 1m^2 of laminate foil, ready for package of food. Due to the limited scope of the paper, we present only part of the 'cradle-to-grave' LCA analysis, which covers the life cycle of packaging from the extraction of raw materials to the production of the packaging product.

Three different methods of life cycle impact assessment (LCIA) were used: the Econdicator 99 (H) method, which is the oldest, the ReCiPe 2016 (H), and the Environmental Footprint (EF) method. The EF method was developed as an official LCIA method to measure and communicate the life cycle environmental performance of products and organisations (European Commission 2024). On the other hand, the Econdicator 99 method is no longer being updated and is actually outdated, but surprisingly some Slovenian LCA study practitioners still use it, so we included it in the calculations for comparison. Other characterstics of LCIA methods used are given in Chapter 2.

The environmental impacts of the PE-LD/PA film were calculated using the SimaPro Analyst software tool, version 9.5.0.2 based on data on materials and processes from the internationally verified Ecoinvent database. Regarding production and consumption of electrical energy, energy mix for Slovenia was used in calculations.

4 RESULTS AND DISCUSSION

A comparative analysis of different LCIA methods showed significant differences in the environmental impact results of PE-LD/PA packaging film (Table 1, Figure 2). The environmental impacts of PA-6 production are higher than those of PE-LD production regardless of the LCIA method used. The key difference between the LCIA methods is evident when comparing the impact of films extrusion with the impacts of the production of both polymer materials.

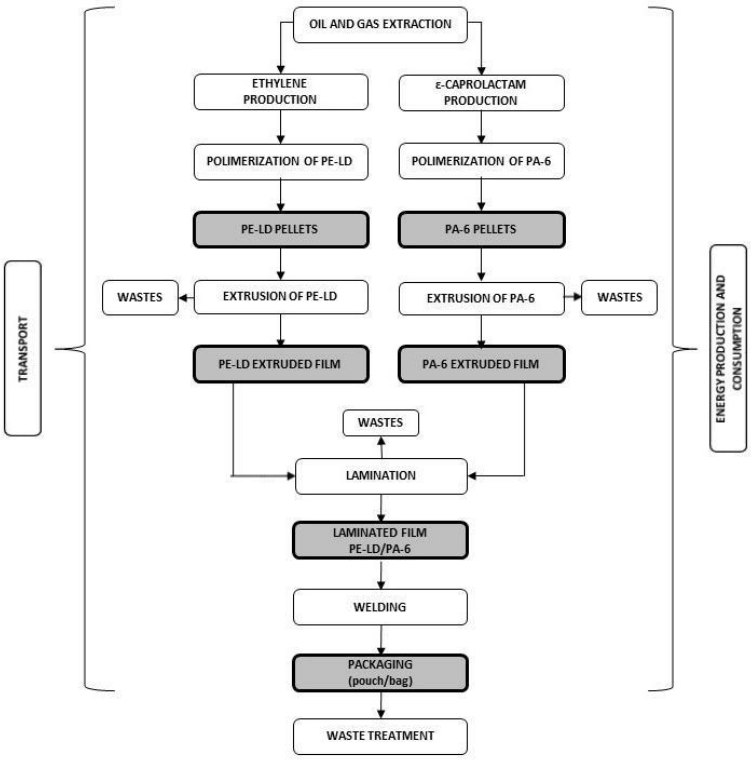

Figure 1: Schematic representation of PE-LD/PA packaging life cycle

Both recent LCIA methods (ReCiPe 2016, EF) calculate significantly higher environmental impact of the film extrusion phase compared to the environmental impacts of the production of PE-LD and PA-6. In addition, the environmental impacts of the extrusion process vary greatly depending on the LCIA method used. Very obvious differences in the calculated environmental impacts using different LCIA methods are also evident in electricity production. End-of-life phase (waste treatment and processing) was also included in LCA calculations. It was found that its contribution to the overall environmental impact of PE-LD/PA film was negligible and consequently it is not presented in Figure 2.

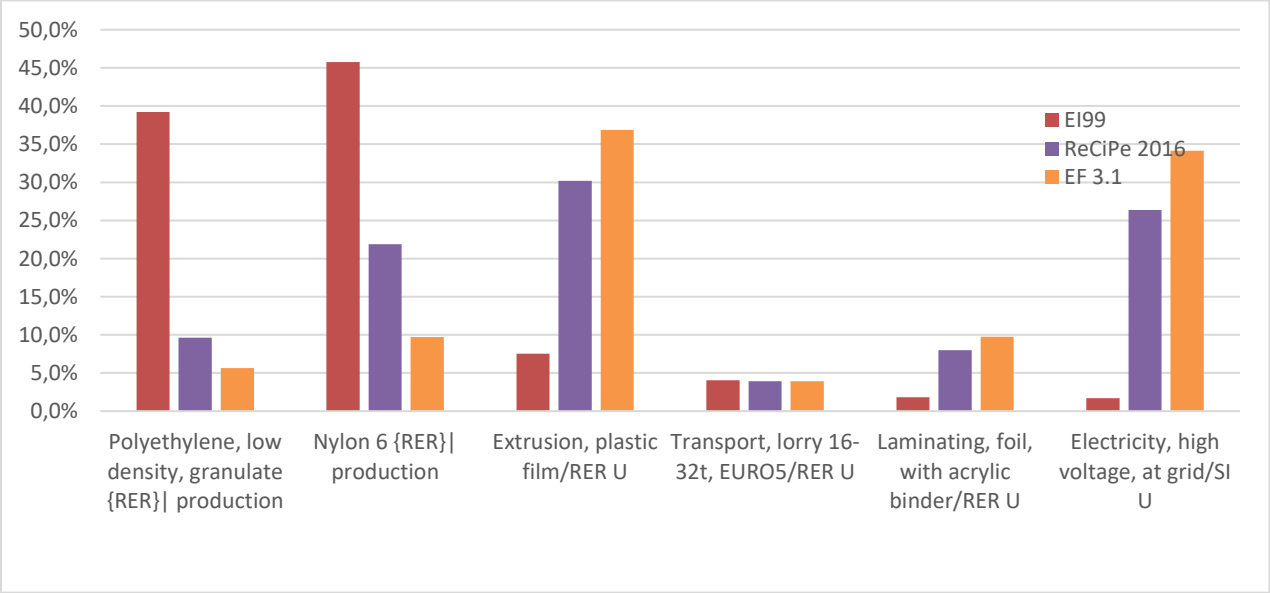

Figure2: Comparison of environmental impact results (in %) calculated with different LCIA methods.

Table 1: Life cycle stages of PE/PA-6 packaging and results of comparative environmental impact analysis calculated with different LCIA methods

Materials/processes	***EI99 (mPt)***	***EI99 (%)***	***ReCiPe 2016 (mPt)***	***ReCiPe 2016 (%)***	***EF 3.1 (mPt)***	***EF 3.1 (%)***
Polyethylene production	*19,758*	*39,2*	*4,137*	*9,6*	*0,014*	*5,6*
Nylon 6 production	*23,058*	*45,7*	*9,380*	*21,9*	*0,024*	*9,7*
Extrusion plastic film	*3,790*	*7,5*	*12,962*	*30,2*	*0,092*	*36,9*
Transport lorry	*2,029*	*4,0*	*1,688*	*3,9*	*0,010*	*3,9*
Laminating foil	*0,921*	*1,8*	*3,429*	*8,0*	*0,024*	*9,8*
Electricity high voltage	*0,849*	*1,7*	*11,310*	*26,4*	*0,085*	*34,1*
Total	***50,405***	***100***	***42,906***	***100***	***0,249***	***100***

5 CONCLUSIONS

To assess the environmental impacts of packaging, it is necessary to use modern analytical software tools, supported by verifiable databases. There are several software solutions available on the market, which differ greatly in terms of the complexity of product life cycle modeling, accessibility to databases, methods used to determine environmental impacts, and the dynamics of database updates.

LCA method is a poweful tool for assesing environmental impacts of packaging to obtain more objective picture whether a certain packaging option is more environmentally friendly or not. It is of particular importance in the case of more complex packaging products, which can include thin multilayer (laminated) plastic packaging.

Results of LCA study presented in this paper clearly show that the choice of LCIA method for evaluating environmental impacts within LCA study has a very large impact on the final result. Developers, designers and managers must be aware of this important fact interpreting LCA results and when considering the environmental suitability of packaging option.

The promotion of more environmentally friendly packaging must be based on credible data on environmental impacts of entire life cycles. Therefore, for the credibility of promotional and marketing materials, it is necessary to use results that have been calculated using the most modern methods and tools. For assessing the environmental impacts of packaging, we suggest using the latest LCIA methods such as the ReCiPe and/or EU Environmental Footprint method instead of the Ecoindicator 99 method.

6 REFERENCES

Bher A., Auras R. Life cycle assessment of packaging systems: A meta-analysis to evaluate the root of consistencies and discrepancies. J. Clean. Prod. 2024, 476, 143785.

Bukowski T., Richmond M. A. Holistic View of the Role of Flexible Packaging in a Sustainable World. PTIS, Flexible Packaging Association, Annapolis. 2018.

European Commission. Environmental Footprint Methods – Calculating the Environmental Impact of Products and Services. 2024. Available: https://green-forum.ec.europa.eu/green-business/environmental-footprint-methods_en (21.8.2025).

ISO 14040:2006. Environmental Management – Life Cycle Assessment – Principles and Framework, ISO standard.

Kan M., Miller S. A. Environmental impacts of plastic packaging of food products. Res. Cons. Recycl. 2022, 180, 106156.

Mousania Z., Atkinson, J.D. A Cradle-to-grave life cycle assessment of multilayer plastic film food packaging materials, comparing to a paper-based alternative. Waste Manag. 2025, 200, 114747.

Owsianiak M., Laurent A., Bjorn A., Hauschild M. Z. IMPACT 2002+, ReCiPe 2008 and ILCD's recommended practice for characterization modelling in life cycle assessment: a case study-based comparison. Int. J. LCA. 2014, 19, 1007 – 1021.

PRé Consultants. SimaPro Database Manuel. Methods Library. 2020. Available: https://simapro.com/wp-content/uploads/2020/10/DatabaseManualMethods.pdf (6.10.2022).

Radonjič G. Embalaža in varstvo okolja – Zahteve, smernice in podjetniške priložnosti. Založba Pivec, Maribor, 2008.

Radonjič G. Oblikovanje in razvoj okolju primernejše embalaže. Fakulteta za kemijo in kemijsko tehnologijo Maribor, 2014.

Reap J., Roman F., Duncan S., Beas B. A survey of unsolved problems in life cycle assessment. Part 2: Impact Assessment and Interpretation. Int. J. LCA. 2008, 13, 5, 374-388.

Sinnko T., Amadei A., Venturelli S., Ardente F. Exploring environmental performance of alternative food packaging products in the European Union. Life cycle impacts of single-use and multiple-use packaging. Joint Research Centre. Luxemburg: Publishing Office of the European Union, 2024.

Siracusa V., Ingrao C., Lo Guidice A., Mbohwa C., Environmental assessment of a multilayer polymer bagfor food packaging and preservation: An LCA approach. Food Res. Int. 2014, 62, 151-161.

Tascione V., Simboli A., Taddeo R., Del Grosso M., Raggi A., A comparative analysis of recent life cycle guidelines and frameworks: Methodological evidence from the packaging industry. Env. Impact Assess. Review. 2024, 108, 107590.

Tunçok-Çeşme B., Yildiz-Geyhan E., Çiftçioglu G. A. Environmental life cycle assessment of two types of flexible plastic packaging under a sustainable circular economy approach. Sustainability. 2024, 16, 3149.

Verghese K., Lewis H., Fitzpatrick L. Packaging for Sustainability. 2012. Springer.

EXTENDED PRODUCER RESPONSIBILITY FOR PACKAGING– INDUSTRY PERSPECTIVE FROM A GLOBAL COMPANY

Igor Karlovits[1,2]

[1]Danfoss Power Solutions, Danfoss Trata doo, Ljubljana, Slovenia
[2]National Institute of Chemistry, Ljubljana, Slovenia

doi: 10.5281/zenodo.17295166
Igor.karlovits@danfoss.com

Abstract: *This paper provides a global manufacturing company's perspective (with more than 100 business units in almost all continents) on Extended Producer Responsibility (EPR) for packaging, focusing on the implications of its implementation and outcomes in the United States and the European Union, and some other countries introducing EPR schemes. EPR schemes shift the financial and/or operational responsibility for the end-of-life management of products, including packaging, from municipalities to producers. For a global company, this policy instrument (taxes and fees) aims to incentivize the design of more sustainable products, reduce waste generation, and increase recycling rates across diverse markets. On the other hand, the overly complex policy landscape with non-harmonized requirements poses a challenge in terms of designing, reporting, and policy compliance. The paper summarizes the requirements that would enable a more systemic approach to the EPR schemes for different states/countries. Also, company strategies are presented through systemic design choices based on sustainability and regulatory requirements through eco-modulation and eco-design of the products.*

Keywords: Extended Producer Responsibility, compliance, eco modulation

1 INTRODUCTION

Extended producer responsibility (EPR) is another economic tool (like the plastic taxes) whose aim is to incentivise behaviour change by changing the market and legal requirements of stakeholders. EPR is basically a policy approach that makes producers responsible for their products along the entire lifecycle, including at the post-consumer stage. By doing so, it helps achieve environmental goals such as recycling targets. At the same time, EPR generates funding from producers that help to pay for the collection, sorting, and recycling of waste products, as well as generates detailed information on production, products, waste generation, and treatment (OECD, 2016).In the last few years in many cases, it is also been a tool mainly aimed to contain plastic pollution in with developed and developing countries (UNEP, 2022).

Effectively, EPR has two principal environmental goals:

- To provide incentives for manufacturers to design resource-efficient and low-impact products (through eco design incentives or so-called eco modulation fees or bonus/malus systems).
- To ensure effective end-of-life collection, the environmentally sound treatment of collected products, and improved rates of reuse and recycling (through collective additional funds

through fees to scale up infrastructure, which would receive materials suitable for recycling – based on the first goal).

The origins of EPR systems stem from the early 1990s in the EU. The Packaging and Packaging Waste Directive (94/62/EC) (PPWD) in 1994 marked the first major legislative application, requiring producers to finance or organize the recovery and recycling of packaging waste. In its early form, the focus of EPR in the EU was end-of-life waste management, and implementation was largely voluntary or industry-led. (Michaelis, 2025). Two other crucial EU documents have paved the way for the EPR schemes in the EU: first the Green Deal from 2019 and the Circular Economy Action Plan in 2020 (CEAP), which explicitly defines EPR as a central policy instrument, and lays out concrete actions to expand and harmonize it. EPR was set up as a driver of sustainable design, circularity, and green innovation, not just waste handling. The extent of the EPR adaptation in the EU is summarized in Figure 1. (Webster, 2025).

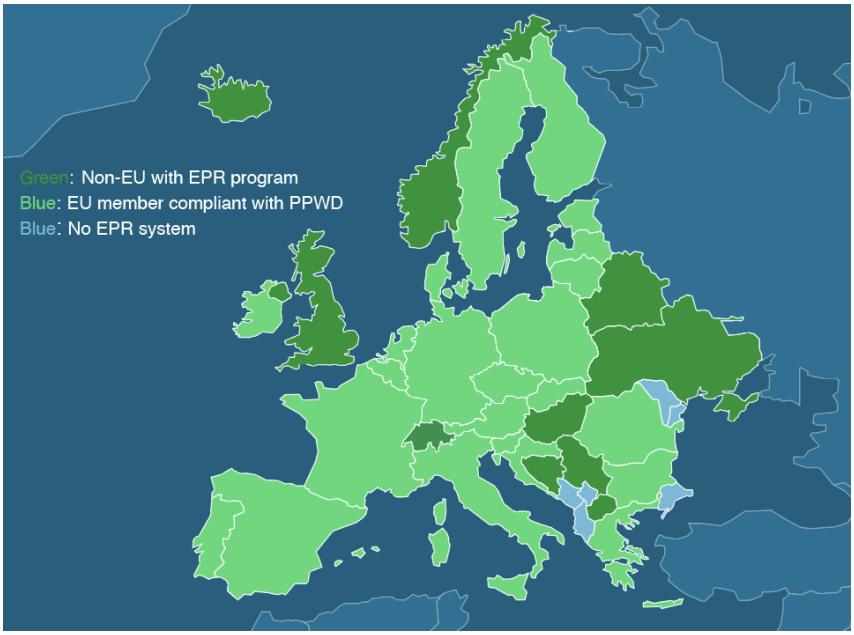

Figure 1: EPR systems in Europe (Webster, 2024)

Nations that fall under the PPWD (indicated in light green) include EU member states:Austria, Belgium, Bulgaria, Croatia, Republic of Cyprus, Czech Republic, Denmark, Estonia, Finland, France, Germany, Greece, Hungary, Ireland, Italy, Latvia, Lithuania, Luxembourg, Malta, Netherlands, Poland, Portugal, Romania, Slovakia, Slovenia, Spain, Sweden. Countries that are not in the European Union have also developed their own approaches to EPR, many of which align with the European Union's Directive. These countries are marked in dark green on the map, including the United Kingdom, Iceland, Serbia, Belarus, North Macedonia, Bosnia and Herzegovina, Norway, Switzerland, and Ukraine. The UK has its own system.

So, from the overview, we can see the European landscape is quite complex with many different solutions, and combining state level plastic tax variations makes the single market difficult to navigate. One recent court decision from the Court of Justice of the EU (CJEU) has issued a final ruling in favor of Slovenia's new Extended Producer Responsibility (EPR) scheme in the case INTERZERO and Others v Državni zbor Republike Slovenije (Case C-254/23). This court ruling is important not just for Slovenia but also can trigger changes again in countries with competing PROs if policymakers see that the Single PRO setup is more beneficial. While this does not directly concern producers, more pressure is on the profit loss of waste management companies – the additional changes can cause potential problems due to changes and adaptations.

The extent to which EPR has spread to other countries and continents is well presented by Figure 2. This gives a global overview of the EPR schemes (Webster, 2024).

Figure 2. EPR systems in place (Webster, 2024)

From different overviews by (Clarity, 2024), (Bünemann et al., 2020), we can see that in the Americas, for example, the United States, EPR laws and programs currently operate at a state-by-state basis, with no federal program in existence. There is a common Producer Responsible Organization (PRO) collecting the fees and dealing with reporting. There are currently 6 states who have running EPR schemes in place (Maine, Oregon, Colorado, California, Maryland, and Minnesota) and several other states with EPR schemes in perspective in the near future. While the reporting is through one PRO, the Circular Alliance, the requirements differ from state to state. Canada also has several EPR schemes and Similar to the US approach, the establishment of EPR programs are managed by individual provinces, not federally (Alberta, British Columbia, Manitoba, New Brunswick, Nova Scotia,Ontario, Quebec, Saskatchewan, and Yukon). In Central and South America (Dominican Republic, Costa Rica) and Colombia, Venezuela, Chile, Brazil, Peru, and Uruguay have EPR installed.

In Asia, Russia, China, Taiwan, Singapore, India, Saudi Arabia, South Korea, Japan, Vietnam, Philippines, Indonesia, Kazakhstan have EPR systems, and in Oceania Australia, New Zealand lead the way with implemented EPR systems.

All these systems have their specific rules and fees, which makes requirements from a global company producing and placing into different markets a huge effort in compliance with the local EPR schemes. It is important to note that Danfoss is a manufacturing company, and the largest number of EPR schemes are focused on consumer level packaging, so due to specific rules these types of companies are exempt from many EPR schemes. But nevertheless, such companies are in scope in some of the companies, so the knowledge and oversight of all requirements are still needed. In our cases, due to complex business structures, we have some segments producing also business to customers and some just business to business to which just adds to the complexity for these type of companies. While exact global ratios are not consistently published, based on regulatory coverage:

- B2C packaging likely accounts for 70–85%of the EPR scope globally.
- B2B packaging makes up the remaining 15–30%, depending on national definitions and exemptions.

2 ECO MODULATION AND ECO DESIGN

Eco-modulation adjusts EPR fees based on the environmental performance of packaging:

- Lower fees for packaging that aligns with eco-design principles
- Higher fees for packaging that is hard to recycle, contains toxic materials, or generates more waste

While the factors considered in eco-modulation vary from law to law, in the packaging context, the factors usually fall under end-of-life factors and life cycle factors.End-of-Life Characteristics include: Recyclability,Compostability,Presence of hazardous substances, Clear consumer labelling; while Life Cycle Characteristics include: use of renewable or recycled materials, Reusability, Greenhouse gas emissions during production. (Sayegh, 2025) France (and some other EU countries) use the Bonus/malus system, where producers receive reductions in fees (the bonus) for using packaging that is recyclable, contains post-consumer recycled (PCR) content, or is reusable. Conversely,fee increases (maluses)apply to packaging with harmful substances or poor recyclability. As a result, producers can receive a deduction of up to 24% of the amount due or, in contrast, be penalised by paying more than 100% of the basic fee (EU Comission, 2016). Paper companies pay 10% less (bonus) if they use packaging with more recyclable material, but 5% more (malus) if they use unsustainable fibres or introduce materials, like ink or glue, into the recycling system. Lower Fees also include packaging made from mono-materials that are easily recyclable, use of certified compostable materials, and inclusion of >30% PCR content. Higher fees are induced for:multi-layer plastic films,packaging with carbon black (hard to sort), or, for example, Use of PVC or other non-recyclable plastics and can bring up tp 100% extra fee. The exact amount is calculated based on Theexact malus ratedepends on the packaging weight, number of packaging units, placement (closures, films, containers), and the industrial sector. The Danish system is planned to have three levels (green, yellow, and red) with a malus of 35%on top of their calculated operational costs for waste management of all packaging in the red category. A workflow of how this system works is presented in Figure 3 (Vana, 2025).

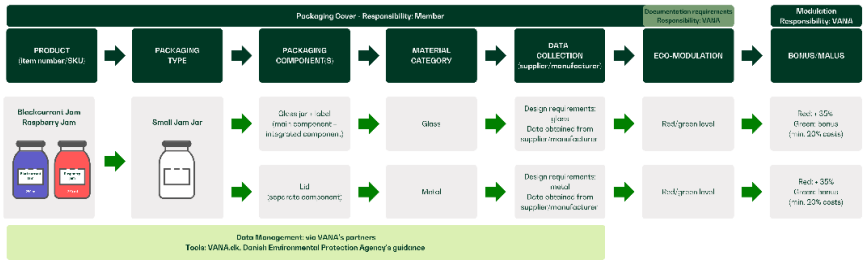

Figure 3: Danish EPR determination for bonus/malus (Vana, 2025)

Similar characteristics are also considered in US states which introduced EPR (Piece, 2025) is presented in Figure 3.

STATE-BY-STATE ECO-MODULATION FACTORS CONSIDERED

FACTOR	CALIFORNIA	COLORADO	MAINE	MINNESOTA	OREGON
RECYCLING RATE	x				x
PCR	x	x	x	x	x
REUSE	x	x	x	x	
LIGHT-WEIGHTING	x	x		x	
RECYCLA-BILITY	x	x	x	x	
RENEWABLE SOURCING	x			x	
TOXICS	x		x	x	
LABELING	x		x		
COMPOSTING	x			x	
REDUCTION	x	x	x		
PACKAGE TO PRODUCT RATIO					x
LIFE CYCLE ASSESSMENT					x
MATERIAL CHOICE					x

Figure 4: Danish EPR determination for bonus/malus (Vana, 2025)

3 OUR SOLUTION

To achieve the multi level requirements (compliance, quality, decarbonization efforts, production efficiency) a packaging framework is used which is presented in Figure 5.

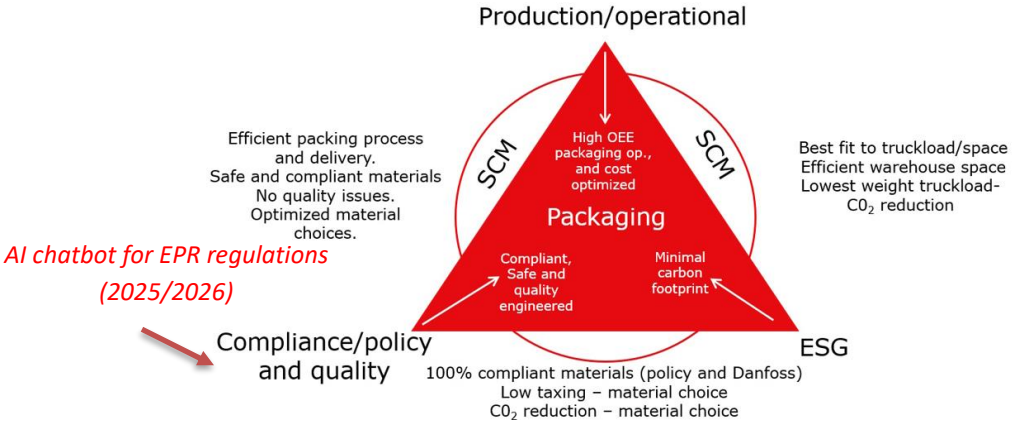

Figure 5: Danfoss Power Solutions packaging framework

The DPS packaging framework uses company packaging standards, which defines the preferred materials that are updated every second year. Operational efficiency is calculated through the mechanical characteristics of the required materials to achieve efficient production, picking, and packing. Sustainability is cross-checked with an internal Sustainable Packaging Assessment Tool or a full LCA analysis to decide if one-way or returnable packaging is the best option. Here, we aim for the minimization of eC02 of the whole packaging material and lifecycle with the highest possible recycled content of materials. The compliance and quality requirements were mostly manually checked through consultation with companies. With the implementation of artificial intelligence and internal chatbots throughout the company, similar technology is planned to cover the EPR/legal requirements regarding packaging. By feeding into the system all the legal documents and eco modulation materials, we are expecting to at least decrease the time needed to get the most efficient solution with the lowerst eC02 and the lowest fees with maximum bonuses for most of the countries where we place our products.

4 CONCLUSIONS

Based on the current EPR landscape and compliance requirements and the upcoming PPWR regulation in the EU, as a company, we are introducing EPR awareness already in the design and procurement

stage through the combination of internal tools, the packaging framework, and an AI chatbot to guide us through regulatory requirements. For industry stakeholders, the most challenging things are the patchwork of global regulations, the need for clear definitions and harmonized standards like “recyclable” or “compostable” (by the definition of the local legal jurisdiction), and the immense reporting and transparency verification requirements. Regulatory bodies often require detailed documentation and may implement verification processes to substantiate claims related to a reduction in material amount used, PCR content, product reuse, recyclability, or composability. Businesses need to invest in ERP systems to establish robust data collection and extra tracking systems just for packaging to meet these reporting obligations.Also, technological innovations make this market very dynamic, so newly developed materials that can fall under eco-modulation bonuses need to be constantly monitored and implemented in stages when they are ready for upscaling. In times of economic uncertainty (tarrifss, global conflicts) together with environmental changes which are reshaping supply chains, companies need to be very focused on choosing the right solutions which will enable the most sustainable solutions with minimal economic costs, including AI technologies.

5 REFERENCES

Bünemann, A., Brinkmann, J., Löhle, S. and Bartnik, S. (2020). EPR Toolbox | Know-how to enable Extended Producer Responsibility for packaging. [online] https://prevent-waste.net/epr-toolbox/#factsheets. Bonn: Deutsche Gesellschaft für Internationale Zusammenarbeit (GIZ) GmbH PREVENT Waste Alliance. Available at: https://prevent-waste.net/wp-content/uploads/2024/03/PREVENT-Toolbox-interactivePDF_2024.pdf [Accessed 27 Aug. 2025].

Clarity. (2024). EU EPR for Packaging Rollouts: A State-by-State Guide | Clarity. [online] Available at: https://clarity.eco/knowledge/a-state-by-state-guide-to-the-rollout-of-packaging-epr-approaches-across-eu-member-countries/.

Daniela Michaelis (2025). The Evolution of EPR in the EU: From Waste Policy to Circular Economy Driver | 3E. [online] Available at: https://www.3eco.com/article/the-evolution-of-epr-in-the-eu/.

EU Commission (2016.). Eco-Emballages (France) | Green Best Practice Community. [online] Available at: https://greenbestpractice.jrc.ec.europa.eu/node/193.

Mitch Webster. (2024). Extended Producer Responsibility Laws for Packaging Around The World. [online] Available at: https://packagingschool.com/lessons/extended-producer-responsibility-laws-for-packaging-around-the-world.

OECD (2016). Extended Producer Responsibility - Guidance for efficient waste management. [online] OECD. Available at: https://www.oecd.org/en/topics/extended-producer-responsibility-and-economic-instruments.html [Accessed 27 Aug. 2025].

Piece, L. (2025). Extended Producer Responsibility (EPR) Eco-modulation Overview. [online] https://sustainablepackaging.org/. Sustainable Packaging Coalition i. Available at: https://sustainablepackaging.org/wp-content/uploads/2025/04/SPC-Mini-EPR-Eco-Modulation-Final.pdf [Accessed 27 Aug. 2025].

Pravin Kumar Mallick, Kim Bang Salling, Daniela C.A. Pigosso and McAloone, T.C. (2024). Designing and operationalising extended producer responsibility under the EU Green Deal. Environmental challenges, 16, pp.100977–100977. doi:https://doi.org/10.1016/j.envc.2024.100977.

Sayegh, C. (2025). Eco-Modulation & EPR: Lower Packaging Fees & Boost Sustainability | H2 Compliance. [online] H2 Compliance. Available at: https://h2compliance.com/the-rise-of-eco-modulation-a-deep-dive-into-how-fees-are-driving-greener-packaging/ [Accessed 27 Aug. 2025].

UNEP (2022). Reducing Plastic Pollution through the Extended Producer Responsibility. [online] UNEP - UN Environment Programme. Available at: https://www.unep.org/reducing-plastic-pollution-through-extended-producer-responsibility.

Vana. (2025). Eco-modulated fees. [online] Available at: https://www.vana.dk/en/producer-responsibility/eco-modulated-fees/ [Accessed 27 Aug. 2025

CONSUMER PERCEPTION AND ACCEPTANCE OF BIO-BASED PACKAGING: INSIGHTS FROM A QUALITATIVE STUDY

Isabelle Sauter[1], Mara Strenger[1], Elisa Liebscher[1], Anna Sadzik[1], Corinna Hempel[1], Markus Schmid[1], Andrea Maier-Nöth[1]

[1]Faculty of Life Sciences, Albstadt-Sigmaringen University, Sigmaringen, Germany

doi: 10.5281/zenodo.17295214
strenger@hs-albsig.de

Abstract: *In the face of growing resource scarcity and socio-environmental concerns, more sustainable packaging solutions are becoming increasingly important, especially under the European Green Deal and the new Packaging Waste Regulation (PPWR). Although consumers are showing a growing interest in recycling and environmentally friendly packaging, they often find it difficult to properly assess sustainability. Most of them cannot distinguish between materials such as recycled, biodegradable, and bio-based plastics, because they are not always visually recognizable. This qualitative study, namely focus group discussions, investigates consumer perception and acceptance of bio-based packaging, underlining the importance of acceptance for successful market introduction. An extensive literature review was carried out to develop the discussion guideline and to identify keywords, which were used as anchor points for the analysis. In addition, product samples were presented to the participants to assess their perception of sustainable packaging. The results show that consumers evaluate sustainable packaging mainly based on color and material. Although they appreciate sustainability claims, consumers want them to be easy to understand. The design should not be too novel and should align with brand recognition, as well as price and quality of the product. Overall, consumers are still reluctant to pay significantly more for sustainable packaging. This is why clearly communicating the added value is essential for achieving wider acceptance. Based on these findings, the study provides recommendations for design and consumer communication to foster acceptance of bio-based packaging and support a successful market launch.*

Keywords: consumer perceptions, qualitative consumer research, consumer decision criteria for sustainable packaging, focus group discussion, bio-based packaging

1 INTRODUCTION

In view of resource scarcity, stricter regulatory requirements, and growing socio-ecological challenges, the development of more sustainable packaging solutions is becoming increasingly important, as emphasized by the European Green Deal and the new EU Packaging and PPWR (European Commission, 2019; European Parliament and Council, 2025). At the same time, consumer awareness is rising, reflected in a significant increase in interest in recycling and sustainably produced materials (Rietz and Kremel, 2023; Herbes, Beuthner and Ramme, 2018). In this context, it is imperative to understand consumer acceptance of sustainable packaging, as despite the growing interest and significant efforts from academia and industry, a gap persists between interest and the actual acceptance of sustainable alternatives. Based on authors` experience, transparent cellulose-based film packaging is often not

considered to be more sustainable than plastic-based film packaging. Consumers often find it challenging to distinguish between recycled and biodegradable materials and to assess the sustainability of packaging. Even bio-based plastic, which can have the potential to be less impactful on the environment than fossil-based plastic, is not always identifiable as such (Magnier and Schoormans, 2017). Whilst features, such as natural colours (e.g. green or brown), rough textures (Otto et al., 2021), images of animals or flowers (for cosmetics and household care products), and labels referencing nature and ecological sustainability (Robertson, 2013), are noticed, the ecological added value of alternative packaging remains unclear to consumers. Consequently, conventional packaging is often preferred. Against this backdrop, research into the acceptance of sustainable packaging solutions, particularly bio-based ones, and their design options, is becoming increasingly important.

The EU project BioSupPack aims to demonstrate a process for the production and enzymatic recycling of environmentally safe, superior, and versatile polyhydroxyalkanoate-based rigid packaging solutions by plasma integration in the value chain. BioSupPack's purpose is to upscale innovative, economically convenient and highly-performing bio-based rigid packaging solutions which are also suitable for being recycled and recovered. The results of this qualitative consumer study will be taken into account in the development of innovative packaging in order to increase market acceptance. The project encompasses a diverse range of applications, including food and household packaging. In addition to the functional, ecological, social and economic aspects, the consumer perception is considered, given that acceptance is one of the key factors in the success of packaging innovations. This study assesses consumer understanding of sustainability, focusing on consumers' expectations on circular bio-based packaging. The focus is on the following questions:(1) Which selection criteria do consumers use and which information needs do they have regarding sustainable packaging in the cosmetics, household goods, food and beverages product groups? (2) How do consumers evaluate the new bio-based packaging in comparison to non-bio-based benchmark packaging?

2 MATERIALS AND METHODS

In February 2025, four focus group discussions were conducted to investigate how consumers perceive and accept new bio-based packaging compared to non-bio-based reference packaging. This method was chosen because focus group discussions allow for the collection of in-depth insights into consumer attitudes and perceptions that would not emerge in standardized surveys or individual interviews. The discussions took place in the designated test area at Mangold`s Video Observation Laboratory of the University Albstadt-Sigmaringen, which complies with ISO 8589 standards, ensuring a controlled and professional environment. Each discussion lasted approximately 90 minutes. Recruitment was carried out using convenience sampling method, a non-random sampling method whereby participants were selected because they were available at the time. Only consumers aged 18 to 70, who regularly purchase conventional products and are interested in the topics of packaging, transparency, and sustainability, were considered. People, who do not deal with packaged products, as well as professionals from the packaging industry or related fields, were excluded. In total, 16 consumers participated in the four focus group discussions. The focus group discussions were audio- and video-recorded and were transcribed using an AI-supported transcription system (AI based transcription in Mangold INTERACT and descript). The structuring of the focus group discussions was based on keywords. Building on previous research (e.g., Otto et al., 2021), a comprehensive literature review was conducted, from which the most relevant keywords for the study were identified and selected. This resulted in a set of keywords (i.e., credibility, transparency, individuality, relevance, the novelty factor, sustainability, packaging, price, and bio-based materials) that served as a common thread throughout the discussion and as anchor points for the analysis. The participants in the study were not given an explicit definition of the individual key words to not influence their perception and interpretation.

The text material was analyzed qualitatively using a predefined evaluation scheme. The evaluation process consisted of manually identifying the most important information from the discussions. The procedure contains fixed criteria for identifying key sentences containing the keywords and is shown in Figure 1.

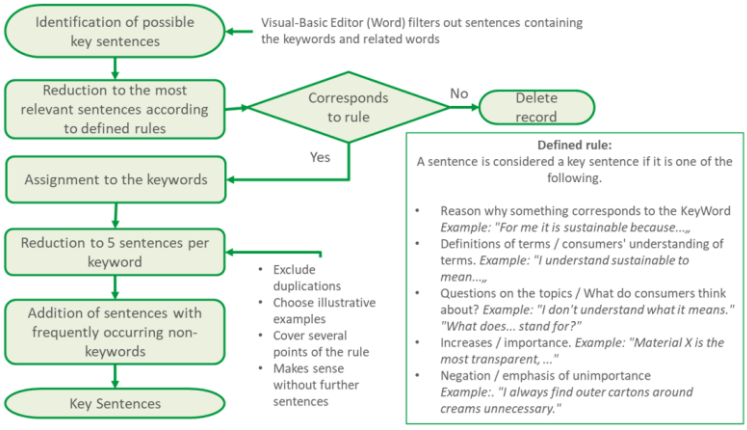

Figure 1: Procedure for identifying key sentences within qualitative consumer research.

In addition to generating text material, image material was also collected within the study to determine which visual and haptic criteria are relevant to consumers. To this end, two sorting tasks were carried out at the beginning of the focus group discussions to gather initial assessments of the packaging to sustainability from the four categories. First, participants were separated in two small groups, in which each was asked to select two packages from a mixed set of prototypes and commercially available packaging. Group 1 had to select the two packages perceived to be the most sustainable, while Group 2 had to select the two perceived to be the least sustainable. Then, the four selected packages were discussed and ranked together on a scale from “less sustainable” to “sustainable”. In a second sorting process, participants select packages within a product group (food, beverages, cosmetics, or household goods) to capture context-specific differences, with the sorting again ranging from “sustainable” to “less sustainable”. For the purpose of evaluation, the packaging that was rated as particularly sustainable or particularly unsustainable by all groups was compared with each other in order to identify possible similarities (see figure 3).

3 RESULTS AND DISCUSSION

*On the one hand, the manual analysis of key sentences reveals that consumers tend to prefer unique and individual designs for c*osmetics packaging. On the other hand, food, household goods, and beverages should be packaged more simply with easily recognizable sustainability features. The findings demonstrate that consumers have a desire to be able to identify and purchase their customary products. Packaging should enable consumers to easily recognize products, among other things, to facilitate product selection (Robertson, 2013). The product is more important than the packaging, as evidenced by the fact that some participants said that “different-looking packaging signals a change, but the most important thing is that the contents remain the same.” Furthermore, unconventional designs have the potential to attract consumers' attention, yet they may also perplex consumers and potentially dissuade them from making a purchase (Bauer et al., 2023). Regarding packaging size, large packages are perceived as more sustainable than single servings, according to the results of the focus group discussion. For example, participants in the focus group discussions explained that “if there is little product inside, it is likely to be used up more quickly and you have to buy another package soon,” so this result contradicts the findings presented in the study of Bauer et al. (2023). The discrepancy in the results may be due to the fact that the comparable study focused on food waste, whereas our study focused on the use of packaging materials in relation to the product. Sustainability can be

assessed differently depending on the perspective. Studies by Tapiola et al. (2023) and Bauer et al. (2023) show, that although packaging size is a selection criterion, oversized packaging is considered less sustainable because it can lead to food waste (Tapiola et al., 2023; Bauer et al., 2023).

Furthermore, the focus group discussions revealed that the term "bio-based" is relatively unknown and plays only a minor role in purchasing decisions. Many consumers are not aware of the ecological benefits of bio-based materials, highlighting the importance of clear communication. Future communication measures should therefore convey the term “bio-based” clearly and simply through short explanatory texts, illustrative symbols, or examples directly on the packaging. This can help prevent misunderstandings and build trust. Furthermore, the study by Uehara et al. (2023) shows that acquiring basic knowledge influences consumers’ preferences for certain attributes (Uehara et al., 2023). Informational materials can thus help consumers recognize the added value of “bio-based” more quickly and guide their purchasing decisions toward more sustainable products. During the discussion, participants brought up the topic of recycling. It became apparent that information on the recyclability printed directly on the packaging helps consumers perceive the packaging as more sustainable, as “this term is now widely understood”, according to one participant. Information on waste separation on packaging is desirable, but it is important that the information on the packaging is easy to understand and strikes a balance between price, quality, and clarity (Hoogland et al., 2007).

In addition to consumers’ visual preferences (e.g., colors, uniqueness of design) and the provision of information on the packaging, the material itself also plays a decisive role: regardless of its bio-based origin, plastic is generally perceived as unsustainable. Studies, e.g Lignou et al. (2021) and Uehara et al. (2023), confirms that it has a negative environmental image compared to other packaging materials (Lignou & Oloyede, 2021; Uehara et al., 2023). This assessment is often based on a general aversion to plastic rather than on sound knowledge of the ecological balance of individual materials. As a result, a potential advantage of bio-based plastics for consumers often remains invisible. This limited perception makes price an even more critical factor in purchasing decisions. A more precise segmentation of participants, for example into “early adopters” or “price-sensitive shoppers”, as described in Otto et al. (2021) (Otto et al., 2021) , could therefore provide valuable insights into how price sensitivity interacts with the recognition of sustainable packaging benefits. For adoption to increase, it is essential that consumers both clearly perceive the added value of more sustainable packaging and find it reasonably priced.

Figure 2 shows an example of the results of the sorting process conducted by the participants, in which bio-based packaging was assessed in terms of sustainability compared to non-bio-based reference packaging and was then classified into categories ranging from “less sustainable” to “sustainable”.

Figure 2: An example of the sorting based on the “Household products” category: new bio-based packaging (prototypes) compared to non-bio-based reference packaging in terms of their sustainability.

Packaging classified as "less sustainable" often has common characteristics. It is mostly small, disposable packaging made of multiple materials, such as plastic and metal, and it features striking

colors, such as pink, orange, and black, for example a cleaning agent bottle that is recognizable as being made of three different materials (bottle body, spout attachment, cap), which are conspicuously colored, and whose bottle body is also labeled. In contrast, packaging rated as "more sustainable" has a simple design and uses a single material consistently. These packages are also characterized by natural colors, such as white, green, or cream/brown, for example a a paper cup with a paper lid made of brown cardboard. These results correspond with the findings of Otto et al. (2021) (Otto et al., 2021). Green and brown are associated with sustainable products and low emissions, as are rough textures, like those found in cardboard or paper. Consumers are given the impression of purchasing an environmentally friendly product when labels evoke a connection to nature. This finding is consistent with Bauer et al. (2023), who show that color significantly influences how consumers perceive products (Bauer et al., 2023). To illustrate these observations more concretely, Figure 3 shows the new bio-based packaging (prototypes) rated as most and least sustainable compared to non-bio-based reference packaging.

Figure 3: Summary of all sorting results for the new bio-based packaging (prototypes) and the non-bio-based reference products, showing only the most extreme ratings: packaging rated by participants as less sustainable (left) or most sustainable (right).

The results provide recommendations for increasing the acceptance of new bio-based packaging. The most important recommendations for sustainable labeling of bio-based packaging are a clear explanation of the term "bio-based" and the provision of comprehensive information to consumers. Furthermore, consumers evaluate packaging differently depending on the product group: For cosmetics, design, individuality, and appearance are paramount, while for food, beverages, and household goods, simplicity, functionality, and clearly identifiable sustainability features are most relevant. To increase general acceptance, the price should be comparable to that of conventional packaging.

4 CONCLUSIONS

The study concludes that ecological sustainability must be communicated to consumers clearly and credibly, ideally through a combination of appropriate packaging design and clear labeling. While design elements such as colors or materials can support the intuitive perception of environmental friendliness, clear information on e.g. $CO_{2eq.}$ values, recyclability, or recycled content, as required by the new PPWR, is essential to ensure transparency and avoid misunderstandings. For example, clear and simple communication through labels, symbols, or short explanatory texts can be crucial for making the term “bio-based” understandable and enhancing consumer acceptance. Furthermore, careful material selection plays a central role, ideally in the form of recyclable mono-materials, while packaging design is equally important. Consumer expectations and perception patterns must be

specifically addressed. Simple designs, natural colors (e.g., white, green, or cream/brown), and a needs-based selection of packaging sizes (e.g., single vs. family sizes) can positively influence the perception of sustainability. However, this is also the limitation of the study, as it is particularly difficult to separate aesthetic preferences (e.g., colors, design) from the assessment of sustainability, since consumers often intuitively associate visual characteristics with ecological aspects. This overlap should be examined more closely in future studies in order to draw more reliable conclusions. The biggest challenge in the future will be making sustainable packaging recognizable to consumers at first glance. To validate the qualitative findings, a quantitative study will follow, including a 10-minute online survey in Germany, Greece, and Spain, followed by a 15-minute qualitative survey with 10% of participants (n = 15). This study is expected to provide more comprehensive insights into consumer price sensitivity and a deeper understanding of which packaging design features consumers notice and which influence their decision to purchase the product at the point of sale. The study seeks to answer whether consumers truly prefer purchasing products with more sustainable packaging and under which conditions this preference is expressed.

Acknowledgments: *We acknowledge the support of this work by the project BioSupPack which received funding from the Bio-Based Industries Joint Undertaking (JU) under grant agreement No 101023685. The JU receives support from the European Union's Horizon 2020 research and innovation program and the Bio-Based Industries Consortium.*

5 REFERENCES

Bauer, A.-S., Dörnyei, K.R. & Krauter, V., 2023. Consumer complaints about food packaging. Frontiers in Sustainable Food Systems, 7.

Bearth, A., Miesler, L. & Siegrist, M., 2017. Consumers' risk perception of household cleaning and washing products. Risk Analysis, 37(4), pp.647–660.

Europäische Kommission, 2019. Mitteilung der Kommission an das europäische Parlament, den europäischen Rat, den Rat, den europäischen Wirtschafts- und Sozialausschuss und den Ausschuss der Regionen. Der europäische Grüne Deal. [online] Available at: https://eur-lex.europa.eu/resource.html?uri=cellar:b828d165-1c22-11ea-8c1f-01aa75ed71a1.0021.02/DOC_1&format=PDF [Accessed 22 Sep. 2025].

Europäisches Parlament & Rat der Europäischen Union, 2025. Regulation (EU) 2025/40 of the European Parliament and of the Council of 19 December 2024 on packaging and packaging waste. [online] Available at: https://eur-lex.europa.eu/eli/reg/2025/40/oj [Accessed 22 Sep. 2025].

Herbes, C., Beuthner, C. & Ramme, I., 2018. Consumer attitudes towards biobased packaging – A cross-cultural comparative study. Journal of Cleaner Production, 194(6), pp.203–218.

Hoogland, C.T., Boer, J. de & Boersema, J.J., 2007. Food and sustainability: do consumers recognize, understand and value on-package information on production standards? Appetite, 49(1), pp.47–57.

Lignou, S. & Oloyede, O.O., 2021. Consumer acceptability and sensory profile of sustainable paper-based packaging. Foods, 10(5).

Magnier, L. & Schoormans, J., 2017. How do packaging material, colour and environmental claim influence package, brand and product evaluations? Packaging Technology and Science, 11, pp.735–751.

Otto, S., Strenger, M., Maier-Nöth, A. & Schmid, M., 2021. Food packaging and sustainability – Consumer perception vs. correlated scientific facts: A review. Journal of Cleaner Production, 298, 126733.

Rietz, S.D. & Kremel, A., 2023. Consumer Behavior as a Challenge and Opportunity for Circular Food Packaging – a Systematic Literature Review. Circular Economy and Sustainability.

Robertson, G.L., 2013. Food Packaging: Principles and Practice. 3rd ed. Boca Raton: CRC Press.

Tapiola, T., Varho, V. & Soini, K., 2023. Exploring visions and vision clusters of sustainable food packaging – The case of Finland. Futures.

Uehara, T., Nakatani, J., Tsuge, T. & Asari, M., 2023. Consumer preferences and understanding of bio-based and biodegradable plastics. Journal of Cleaner Production, 417, 137979. [online] Available at: https://www.sciencedirect.com/science/article/pii/S0959652623021376 [Accessed 22 Sep. 2025].

SUSTAINABLE PACKAGING ASSESSMENT – A MORE HOLISTIC METHODOLOGY FOR SUSTAINABILITY ASSESSMENT OF FOOD PACKAGING

Mara Strenger[1], Alina Siebler[1], Markus Schmid[1]

[1]Sustainable Packaging Institute SPI, Faculty of Life Sciences, Albstadt-Sigmaringen University, Sigmaringen, Germany

doi: 10.5281/zenodo.17301376
strenger@hs-albsig.de

Abstract: *Current packaging sustainability assessment methods do not consider packaging functionality in terms of packaging-related food loss and waste (food wastage) in a standardised way. However, packaging functionality should be considered when conducting a more holistic sustainability assessment, as food constitutes higher proportion of total resource consumption and consequently exerts a greater impact on sustainability in comparison to its packaging. Consequently, a more holistic sustainability assessment method for food packaging along its life cycle is needed. The present paper assesses the packaging functionality in relation to its dimensions, as outlined in ISO 18602:2013. Consequently, it is necessary to give due consideration to the distinct barrier requirements of specific food products, whilst seeking to minimise impacts on sustainability arising from packaging that is either oversized or undersized. To operationalise this balance, the Fit-for-Purpose Indicator (FFPI) has been developed, representing methodological progress compared to previous approaches. The FFPI facilitates a systematic assessment of whether a packaging concept adequately fulfils food-specific requirements without excessive material usage. This, in turn, supports both sustainability and food product protection agendas. The objective of the present paper is to facilitate a more holistic sustainability assessment, encompassing considerations of packaging functionality and ecological, economic and social sustainability aspects. To this end, the paper identifies and aligns suitable ecological, economic, and social assessment frameworks and combines them with the new FFPI. This approach is intended to ensure consistency and comparability across dimensions, thereby emphasising the importance of interpretable results, ideally via aggregated indicators such as single scores.*

Keywords: sustainability assessment method, food packaging, packaging-related food wastage, fit-for-purpose indicator

1 INTRODUCTION

Packaging, particularly for food, fulfils a variety of functions *Wohner, 2021*, the most important being product protection *(Dörnyei et al., 2023; Singh et al., 2017; Verghese et al., 2012)*. Adequate product protection impacts the amount of food wastage *(Gruber et al., 2016; Pauer et al., 2019; Wikström & Williams, 2010; Williams & Wikström, 2011)*, for example by extending the shelf life *(Wohner et al., 2019)*. Food wastage refers to any food lost by deterioration or disposal. Thus, the term “wastage” encompasses both food loss and food waste (Food and Agriculture Organization, 2013; Uhlig et al., 2025). The product protection and the shelf-life depend on packaging functionality such as barrier and mechanical properties *(Lindh et al., 2016; Sasaki et al., 2021*). Given that globally around one third of

all food produced is not consumed *(Gustavsson et al., 2011)* and that avoiding food wastage could potentially reduce climate impact by up to 8 % *(Food and Agriculture Organization, 2013;* E*coplus et al., 2020*), it is necessary to realign the sustainability assessment of food packaging, taking into account packaging functionality and its influence on food wastage. Moreover, most resources in the packaging concept are usually linked to the food itself rather than the packaging*(Wohner, 2021; Wikström & Williams, 2010; Silvenius et al., 2013)*. Since the protective function of packaging has a proportional impact on the amount of food wastage *(Gruber et al., 2016; Pauer et al., 2019; Wikström & Williams, 2010; Williams & Wikström, 2011)*, it should be given top priority in reducing resource waste and potential environmental impacts of the food packaging concept.

Several studies have addressed this issue and integrate (packaging-related) food wastage into packaging life cycle assessment (LCA) and/or provide approaches how to do it. For instance Grant et al. (2015) propose a theoretical system expansion to include packaging-related food wastage, but without details on implementation or quantification *(Grant et al., 2015)*. Heller et al. (2019) model 13 food packaging concepts to illustrate how food wastage affects the potential environmental impact of packaging concepts *(Heller et al., 2019)*, while Manfredi et al. (2015) assess the impact of an antimicrobial packaging coating for milk packaging, focusing on shelf-life extension and reduced food wastage *(Manfredi et al., 2015)*. However, these studies rely on generic waste rates rather than packaging-specific data. Wikström and Williams (2010) introduce a formula to include food wastage in packaging LCA but leave practical aspects of quantification unaddressed (Wikström & Williams, 2010). In contrast, Wohner et al. (2020) provide a more concrete example by measuring residual emptiability of ketchup packaging and incorporating the resulting food wastage into the LCA and economic assessment of the packaging *(Wohner et al., 2020*). Similarly, Silvenius et al. (2011) cosider the effect of packaging size on food wastage using consumer survey data *(Silvenius et al., 2011)*, and Yokokawa et al. (2018) explore consumer-related food losses from a behavioural perspective (Yokokawa et al., 2018). Conte et al. (2015) estimate food wastage for sheep's milk products by modelling waste probability based on shelf-life changes due to different packaging concepts, though the model relies heavily on assumptions and limited empirical data (*Conte et al., 2015*). In conclusion, these approaches highlight the importance of incorporating packaging functionality, although they remain largely theoretical or specific to individual cases. They highlight the challenges of systematically supplementing with packaging functionality and, by extension, the holistic sustainability assessment of packaging. Since sustainability is not only a question of potential environmental impacts but also economic and social aspects, a holistic sustainability assessment of food packaging should consider all these dimensions as well as the packaging functionality.

The aim of this research is to address the challenges that have been encountered to date and to develop an indicator that considers the functionality of packaging. The intention is to provide a standardised method for a more holistic assessment of food packaging that considers ecological, economic and social factors, as well as packaging functionality.

2 MATERIALS AND METHODS

In the following section 2.1, the assessment of the packaging functionality is first presented as a broadly applicable and practice-orientated implementation and represents the core of this paper. Subsequently, in section 2.2., the assessment of the ecological, economic and social dimensions of sustainability is briefly presented.

2.1 Assessment of packaging functionality

Packaging functionality, such as the barrier properties against gases and water vapour, have a strong influence on food safety and quality and therefore on the shelf life of the food *(Lindh et al., 2016)*. Different foods also pose different demands on the barrier properties of packaging (Figure 6). For

example, sensitive products such as meat require high barriers against oxygen and, in some cases, light barriers to prevent light-induced autoxidation. On the other hand, respiring foods such as fruit and vegetables require a certain degree of gas exchange.

In addition to product-specific requirements, the functionality of packaging is assessed in accordance with the optimised packaging concept, as defined in ISO 18602:2013 *(ISO, 2013)*. The ISO 18602:2013 approach is intended to balance the environmental impacts of overdimensioning (excessive material use) against those of underdimensioning (potential food wastage). In the light of these considerations, the objective of this paper is to assess the packaging functionality based on the optimal dimensioning in terms of fulfilment of food-specific requirements. Even though Figure 7 concentrates on the environmental impacts, analogous relations can also be observed for the economic and social impacts.

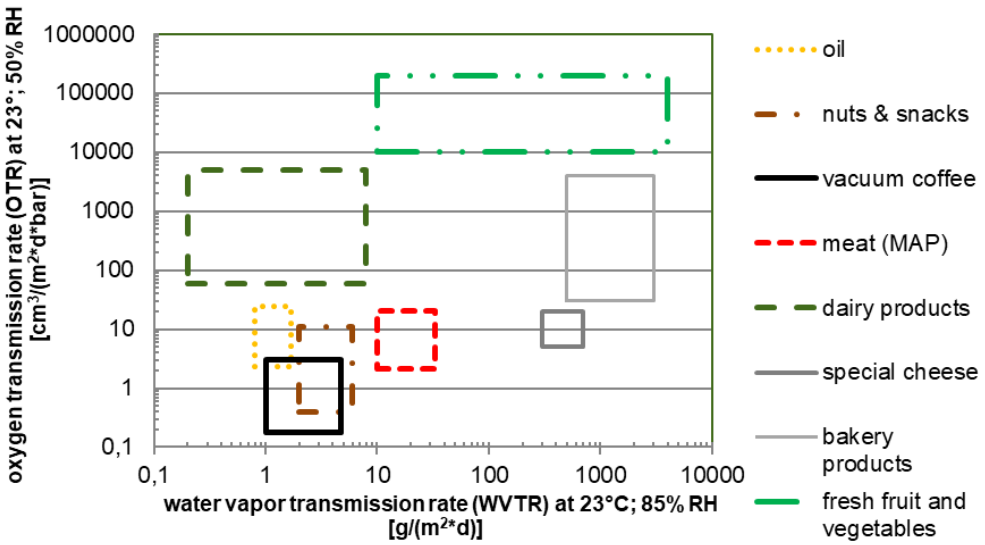

Figure 6: Specific barrier requirements of food products to their packaging, expressed as oxygen transmission rate and water vapour transmission rate, relevant to ensure product quality and shelf life. Translated from (Detzel et al., 2018).

2.2 Sustainability assessment frameworks and methods

For the sustainability assessment, suitable standards and methods are selected to ensure that the ecological, economic and social dimensions can be assessed in a maximally consistent and comparable manner. In accordance with this aim, the approaches for e.g. data collection, system boundaries, functional unit and implementation across the three dimensions are aligned as closely as possible. Moreover, it is imperative for the practical applicability of the results that they are as straightforward to interpret and communicate across all dimensions as possible, for example using aggregated indicators such as single scores per sustainability dimension. Although the aggregation of results simplifies communication, it also poses challenges. For instance, to ensure transparency, the weighting factors utilised must be disclosed. Caution should be paid to ensure that discrepancies in individual impact categories are not obscured and that relevant trade-offs, for example between different environmental impact categories or sustainability dimensions, remain visible.

3 RESULTS AND DISCUSSION

3.1 Assessment of packaging functionality – Fit-for-Purpose Indicator

The assessment of packaging functionality in terms of optimum fulfilment of the food-related requirements is based on the developed Fit-for-Purpose-Indicator (FFPI). The FFPI is calculated from

the ratio of the food-related requirements for the barrier against oxygen and water vapour of the packaging and the actual barrier of the packaging (equation 1):

$$FFPI = \frac{Optimal\ transmission\ rate\ food}{Transmission\ rate\ packaging} \qquad (1)$$

The food-specific requirements can be derived from existing literature values (see Figure 6) or from primary data in the form of manufacturer specifications. Subsequently, these values are then compared with the measured or calculated permeation properties (indicated as transmission rates) of the packaging to be assessed. Optimally dimensioned packaging results in an FFPI value of 1. Under-dimensioned packaging results in an FFPI value of less than 1. Over-dimensioned packaging results in an FFPI value of greater than 1. As a case example, minced meat (pork and beef) packaged in a flow pack under modified atmosphere (MAP) with a PP/EVOH/PA structure was assessed. The oxygen transmission rate of the packaging was 3.57 cm^3/m^2 day, which lies within the food-specific requirement range of 2–20 $cm^3/m^2 \cdot day$ (see Figure 6). This results in an FFPI value of 1. In contrast, the water vapour transmission rate of 1.92 $g/m^2 \cdot day$ was below the requirement range of 10–30 $g/m^2 \cdot day$ (see Figure 6), leading to an FFPI value of 5.21. Thus, while the packaging can be considered optimally dimensioned regarding oxygen permeability, it is over-dimensioned with respect to water vapour permeability.

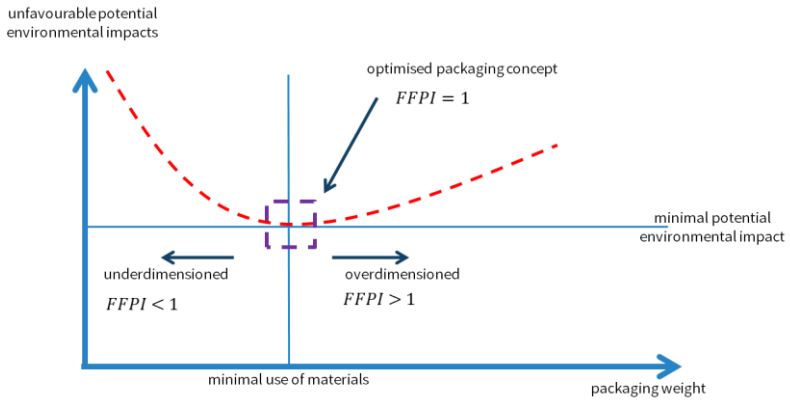

Figure 7: Approach to the general conceptualization of an optimised packaging concept based on ISO 18602:2013 supplemented with the developed Fit-for-Purpose Indicator (FFPI) for optimally dimensioned packaging concepts regarding their functionality in terms of barrier properties.

3.2 More holistic Sustainability assessment of food packaging

Table 6 provides an overview of how ecology, economy and social aspects as well as packaging functionality are evaluated in the sustainability assessment methodology.

Table 6: Overview of the consideration and evaluation of the ecological, economic and social sustainability aspects of food packaging as well as the packaging functionality.

Packaging functionality	***Ecological sustainability***	***Economic sustainability***	***Social sustainability***
Assessment of fulfilment of the required product protection measured by the Fit for Purpose Indicator (FFPI)	*Life Cycle Assessment (LCA) of packaging based on ISO 14040/44:2021 and EU Recommendation 2021/2279*	*Life Cycle Costing (LCC) of packaging with costs of all material and energy flows*	*Social Life Cycle Assessment (sLCA) of packaging based on ISO 14075:2024*

3.3 Discussion

The proposed approach offers the opportunity to assess the sustainability of food packaging in a more holistic way by integrating environmental, economic, social and functional packaging aspects. Notwithstanding this integrative perspective, the approach still has potential for improvement.

The FFPI does not account for the magnitude of impact resulting from over- or under-dimensioning in relation to the resource-intensity of the packaged food product. In this context, from an ecological and economic standpoint, overdimensioning may be regarded as more acceptable for resource-intensive food products than for those with a lower resource footprint. This is because the overall resource balance is more heavily weighted toward the food itself *(Wohner et al., 2021; Wikström & Williams, 2010; Silvenius et al., 2013)*. Conversely, from a social ethics perspective, it cannot be determined that food requiring fewer resources should not be granted the requisite protection. The prevention of all manner of food wastage is of paramount importance, irrespective of the resource intensity, which is why it should be accorded a high degree of priority. Despite this, the differing resource intensity of various foodstuffs results in varied break-even points for the effects of packaging-related food wastage and packaging itself. To illustrate this point, one may consider the relative sustainability impact of a marginal increase in packaging input within the broader context of food packaging, particularly in the context of resource-intensive food products. Nevertheless, this differentiation has not yet been incorporated into the current application of the FFPI. To adequately reflect the resource intensity of the packaged food in sustainability assessments, packaging-related food wastage must be systematically integrated into LCA, LCC, and sLCA.

4 CONCLUSIONS

This paper presents an integrative approach for a more holistic sustainability assessment of food packaging by combining ecological, economic, and social assessment with a functionality-based assessment via the developed Fit-for-Purpose Indicator (FFPI). The approach enables to include the contribution of packaging to the preservation of food quality and safety as a significant factor influencing the sustainability of packaging. A limitation of the present approach that remains to be addressed is the integration of the four individual results (FFPI, ecological, economic and social assessment) into a single overall result. Notwithstanding, the approach offers a structured basis for identifying under- or overdimensioned packaging solutions regarding product protection. However, the current FFPI does not yet reflect the resource intensity of the packaged food. In order to more accurately reflect this, future developments should incorporate a consistent integration of packaging-related food wastage into the sustainability assessment of packaging. This would facilitate for a more differentiated, product-specific assessment of packaging concepts. Existing studies have addressed this issue in a case-specific manner. Nonetheless, there is an absence of consistent and systematic quantification of packaging-related food wastage across product categories. The authors of this paper are currently developing a methodological approach to close this gap and enable a more holistic and differentiated sustainability assessment of food packaging concepts.

Acknowledgments: *This work was supported by the Deutsche Bundesstiftung Umwelt [AZ 37233_01]. The authors would also like to thank the project partners from the Institute for Acoustics and Building Physics of the University of Stuttgart and the German Agricultural Society, who made a significant contribution to the project from which this publication emerged.*

5 REFERENCES

Conte, A., Cappelletti, G.M., Nicoletti, G.M., Russo, C. & Del Nobile, M.A., 2015. Environmental implications of food loss probability in packaging design. Food Research International, 78, pp.11–17.

Detzel, A., Bodrogi, F., Kauertz, B., Bick, C., Welle, F., Schmid, M., Schmitz, K., Müller, K. & Käb, H., 2018. Biobasierte Kunststoffe als Verpackung von Lebensmitteln.

Dörnyei, K.R., Uysal-Unalan, I., Krauter, V., Weinrich, R., Incarnato, L., Karlovits, I., Colelli, G., Chrysochou, P., Fenech, M.C., Pettersen, M.K., Arranz, E., Marcos, B., Frigerio, V., Apicella, A., Yildirim, S., Poças, F., Dekker, M., Johanna, L., Coma, V. & Corredig, M., 2023. Sustainable food packaging: An updated definition following a holistic approach. Frontiers in Sustainable Food Systems, 7.

ecoplus, BOKU, denkstatt & OFI, 2020. Food Packaging Sustainability: A guide for packaging manufacturers, food processors, retailers, political institutions & NGOs.

Food and Agriculture Organization, 2013. Food wastage footprint: Impacts on natural resources - Summary report.

Grant, T., Barichello, V. & Fitzpatrick, L., 2015. Accounting the impacts of waste product in package design. Procedia CIRP, 29, pp.568–572.

Gustavsson, J., Cederberg, C. & Sonesson, U., 2011. Global food losses and food waste: Extent, causes and prevention; study conducted for the International Congress Save Food! at Interpack 2011, [16–17 May], Düsseldorf, Germany. Rome: Food and Agriculture Organization of the United Nations.

Heller, M.C., Selke, S.E.M. & Keoleian, G.A., 2019. Mapping the influence of food waste in food packaging environmental performance assessments. Journal of Industrial Ecology, 23(2), pp.480–495.

International Organization for Standardization, 2013. Packaging and the environment — Optimization of the packaging system; ICS 55.020, 13.020.01 (18602). Best Beuth Standards Collection.

Lindh, H., Williams, H., Olsson, A. & Wikström, F., 2016. Elucidating the indirect contributions of packaging to sustainable development: A terminology of packaging functions and features. Packaging Technology and Science, 29(4–5), pp.225–246.

Manfredi, M., Fantin, V., Vignali, G. & Gavara, R., 2015. Environmental assessment of antimicrobial coatings for packaged fresh milk. Journal of Cleaner Production, 95, pp.291–300.

Pauer, E., Wohner, B., Heinrich, V. & Tacker, M., 2019. Assessing the environmental sustainability of food packaging: An extended life cycle assessment including packaging-related food losses and waste and circularity assessment. Sustainability, 11(3), 925.

Sasaki, Y., Orikasa, T., Nakamura, N., Hayashi, K., Yasaka, Y., Makino, N., Shobatake, K., Koide, S. & Shiina, T., 2021. Life cycle assessment of peach transportation considering trade-off between food loss and environmental impact. International Journal of Life Cycle Assessment, 26(4), pp.822–837.

Singh, P., Langowski, H.-C. & Wani, A.A., 2017. Food Packaging Materials: Testing & Qand. CRC Press.

Silvenius, F., Grönman, K., Katajajuuri, J.-M., Soukka, R., Koivupuro, H.-K. & Virtanen, Y., 2013. The role of household food waste in comparing environmental impacts of packaging alternatives. Packaging Technology and Science, 27(4), pp.277–292.

Silvenius, F., Katajajuuri, J.-M., Grönman, K., Soukka, R., Koivupuro, H.-K. & Virtanen, Y., 2011. Role of packaging in LCA of food products. In: M. Finkbeiner, ed. Towards Life Cycle Sustainability Management. Dordrecht: Springer Netherlands, pp.359–370.

Social Hotspot Database, 2025. For more information. Available at: http://www.socialhotspot.org/for-more-information.html [Accessed 20 March 2025].

Uhlig, E., Sadzik, A., Strenger, M., Schneider, A.-M. & Schmid, M., 2025. Food wastage along the global food supply chain and the impact of food packaging. Journal of Consumer Protection and Food Safety.

Verghese, K., Lewis, H. & Fitzpatrick, L., 2012. Packaging for sustainability. London: Springer.

Wikström, F. & Williams, H., 2010. Potential environmental gains from reducing food losses through development of new packaging - a life-cycle model. Packaging Technology and Science, 23(7), pp.403–411.

Williams, H. & Wikström, F., 2011. Environmental impact of packaging and food losses in a life cycle perspective: A comparative analysis of five food items. Journal of Cleaner Production, 19(1), pp.43–48.

Wohner, B., 2021. Nachhaltigkeitsbewertung von Verpackungen: Eine Empfehlung der ECR Austria Arbeitsgruppe "Nachhaltigkeitsbewertung".

Wohner, B., Gabriel, V.H., Krenn, B., Krauter, V. & Tacker, M., 2020. Environmental and economic assessment of food-packaging systems with a focus on food waste. Case study on tomato ketchup. Science of the Total Environment, 738, 139846.

Wohner, B., Kladnik, V., 2021. Nachhaltigkeitsbewertung von Verpackungen: Eine Empfehlung der ECR Austria Arbeitsgruppe "Nachhaltigkeitsbewertung" 2021.

Wohner, B., Pauer, E., Heinrich, V. & Tacker, M., 2019. Packaging-related food losses and waste: An overview of drivers and issues. Sustainability, 11(1), 264.

Yokokawa, N., Kikuchi-Uehara, E., Sugiyama, H. & Hirao, M., 2018. Framework for analyzing the effects of packaging on food loss reduction by considering consumer behavior. Journal of Cleaner Production, 174, pp.26–34.

TOWARDS A CIRCULAR ECONOMY: A COMPREHENSIVE REVIEW OF CIRCULAR BUSINESS MODELS

Natasha Daniloska[1], Tatjana Petkovska Mirchevska[1], Diana Boshkovska[1]

[1] Institute of Economics - Skopje at Ss. Cyril and Methodius University in Skopje, R.N Macedonia

doi: 10.5281/zenodo.17301440
natasha.daniloska@ek-inst.ukim.edu.mk
tatjana@ek-inst.ukim.edu.mk
diana@ek-inst.ukim.edu.mk

Abstract: *The transition to a circular economy (CE) requires innovative business models that move beyond traditional linear practices. This paper systematically reviews Circular Business Models (CBMs) using the PRISMA methodology, analysing 42 peer-reviewed publications[1]. Two complementary classification perspectives are identified: The* ***Strategic Focus Classification*** *(design, use, recovery-focused, and hybrid models) and the* ***Operational Typology*** *(product, service, resource, and design-innovation CBMs). Together, these frameworks clarify both the rationale for circularity and its practical implementation. Key findings highlight significant challenges, including regulatory gaps, high upfront costs, organizational resistance, and digital infrastructure needs. The review underscores the importance of standardized frameworks and cross-sectoral collaboration to advance CBM adoption and support sustainable economic transitions.*

Keywords: circular business models (CBMs), circular economy (CE), sustainability, systematic literature review PRISMA methodology, business model innovation

1 INTRODUCTION

The CE addresses the ecological and economic limitations of the linear model by promoting reuse, repair, remanufacturing, and recycling (Geissdoerfer et al., 2020). At its core are CBMs, which reshape value creation and capture to support resource circularity (Hofmann, 2019). Yet research on CBMs remains fragmented, with diverse definitions and approaches limiting clarity and adoption. While many earlier reviews have specific focus, this paper offers a broader synthesis that integrates strategic intent and operational architecture across sectors. It addresses this gap through a systematic literature review that traces the evolution of CBM definitions, synthesizes key conceptual categories, and introduces a dual classification, Strategic Focus and Operational Typology, that explains both the rationale for circularity and its implementation. The framework enables cross-sectoral comparison and offers a conceptual foundation for future CBM research and application.

[1] Funded by the project *"The Republic of North Macedonia's Transition Towards a Circular Economy: Prospects and Challenges"*, University of Ss. Cyril and Methodius, Skopje, RNM (NIP.UKIM.24-25.19).

2 MATERIALS AND METHODS

The literature search was conducted between April and May 2025, focusing on peer-reviewed articles published between 2010 and 2025. It was carried out across major scientific databases, including Google Scholar, Scopus, Web of Science, Copernicus, and EBSCO. The search strategy combined keywords such as “Circular Business Models”, “Circular Economy”, “Sustainability” and “Business Model Innovation”. The analysis focused on two objectives: (1) tracing the historical evolution and definitional variations of CBMs; and (2) classifying conceptual models based on strategic focus and operational characteristics. The selection and screening of publications followed the PRISMA (Preferred Reporting Items for Systematic Reviews and Meta-Analyses) guidelines to ensure a structured and transparent review process.

2.1 Sample

From 234 records initially identified, 9 were removed as duplicates or irrelevant. In title&abstract and full-text screening, 42 studies were excluded for superficial coverage of CBMs, 32 for addressing isolated sustainability topics, and 37 for being overly context or product-specific. The final sample included 42 publications offering conceptual or theoretical insights on CBMs. Thematic categories were derived inductively, based on their relevance to CBM theory and practice.

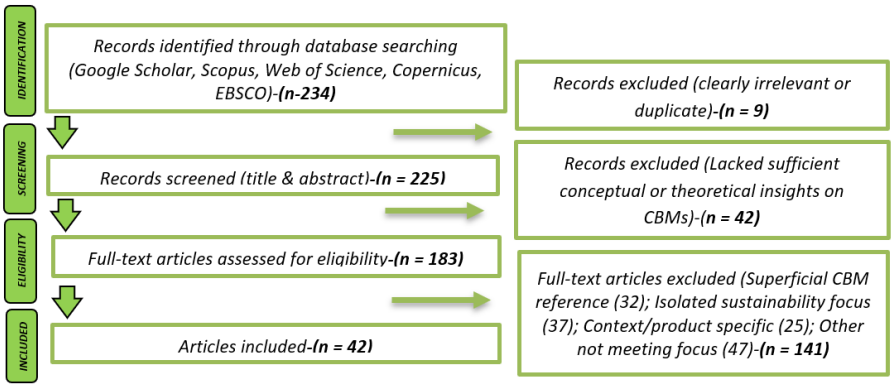

Figure 1: PRISMA DIAGRAM

(Limitation: Using specific keywords may have excluded studies addressing CBMs indirectly, though the sample remains sufficient for analyzing their evolution and strategic implications.)

3 RESULTS AND DISCUSSION

CBMs have evolved from early eco-innovation efforts into structured approaches supporting reuse, repair, remanufacturing, and recycling, which is essential for transitioning beyond the limitations of linear systems. (Zafar et al., 2021). This review identifies four dominant definitional categories, each aligned with distinct business model configurations. The resulting classification framework reflects recurring patterns across the analysed literature and is grounded in the following dominant definitional approaches:

- **Strategy-Oriented Definitions**-emphasize long-term competitiveness and value retention through closed-loop systems (Puglieri et al., 2022; Konietzko et al., 2020) and next-generation sustainable business models leveraging circular principles (Rosa et al., 2019).

- **Activity-Based Definitions**-emphasize actions like product-as-a-service and reverse logistics (Urbinati et al., 2017), with reverse logistics noted as a strong marketing strategy (Lahti et al., 2018; Guillén et al., 2023).

- **Value-Focused Definitions**-stress the shift from linear to shared or regenerative value (Bocken et al., 2018), with frameworks proposing CBMs that realign value creation to circular principles (Kirchherr et al., 2017).

- **Hybrid (or Holistic) Definitions**-provide integrated perspectives that transcend sector-specific models, supporting wider adoption of CE concepts (Sjödin et al., 2023). For example, a finance-marketing hybrid based on customer lifetime value shows how circular strategies can enhance market equity (Awan & Sroufe, 2022).

The variety of definitions reflects disciplinary differences: while engineering and environmental sciences focus on technical processes, business and management studies emphasize value configuration and strategic orientation. This disciplinary divergence has created challenges in forming a unified definition. However, several researchers (Kirchherr et al., 2023) advocate for hybrid approaches that integrate ecological, economic, and systemic dimensions.

The definitional review shaped the classification framework by revealing recurring patterns that conceptually distinguish strategic from operational CBM typologies.

The implementation of a viable business model is critical to achieving the goals of a CE. Literature on CBMs reveals a wide spectrum of approaches, generally focusing on strategic goals, value creation mechanisms, and business model components. Two complementary classification perspectives are identified: **Strategic Focus Classification** and **Operational Typology** based on business model (BM) architecture.

Strategic Focus Classification is based on the primary logic for achieving circularity, emphasizing distinct approaches to value creation, delivery, and capture:

a) *Design-Focused CBMs*-rely on eco-design to extend lifecycles, reduce inputs, and enable modularity. Strategies include repair, reuse, remanufacturing, and recycling (Lüdeke-Freund et al., 2019). Key archetypes are design for longevity (Lee & Sicklinger, 2024), disassembly (Den Hollander et al., 2017; Rosa et al., 2019), and reuse (Schulte, 2013; Ferasso, 2020).
b) *Use-Focused CBMs*-promote access over ownership through Product-Service Systems, leasing, and sharing platforms, reducing idle capacity (Yang et al., 2017; Loon, 2020).
c) *Recovery-Focused CBMs*-close loops through remanufacturing, recycling, and take-back schemes, enhancing both cost efficiency and consumer participation (Schwanholz et al., 2020; Nußholz, 2018; De Keyser & Mathijs, 2023)
d) *Hybrid and Emerging CBMs*-integrate design, use, and recovery logics, exemplified by emerging archetypes such as waste-based and platform-based start-ups (Marvin et al., 2019).

Operational Typology is based on BM Architecture and is focusing on business model elements such as value proposition, customer interface, and supply chain design:
a) *Product-Oriented CBMs*-extend lifecycles through reuse and remanufacturing, common in electronics and machinery (Ertz et al., 2019; Whalen, 2019).
b) *Service-Oriented CBMs*-emphasize access over ownership, particularly in mobility and fashion, via leasing and sharing models (Heyes et al., 2017; Coscieme et al., 2022).
c) *Resource-Oriented CBMs-f*ocus on input substitution and industrial symbiosis in bio-based and agricultural sectors (Donner et al., 2020; Carraresi & Bröring, 2021)
d) *Design-Innovation CBMs-e*mbed circularity at the design stage, enabling modularity and repair (Santa-Maria et al., 2022; Scholtysik et al., 2023).

Despite their potential, CBMs face persistent challenges: limited regulatory incentives (Fraccascia et al., 2019), high upfront costs and uncertain returns (Vermunt et al., 2019), organizational resistance to shifting from linear models (Linder & Williander 2015), and infrastructure demands for digital technologies such as IoT and analytics (Sjödin et al., 2023).

Together, the two classifications provide a holistic framework. The strategic perspective clarifies *why* circularity is pursued, while the operational perspective shows *how* it is implemented. This dual lens highlights both overarching logics and practical architectures, while the diversity of classifications underscores the need for greater coherence and standardized frameworks to guide adoption (Frishammar & Parida, 2018). Strategically, CBMs range from incremental innovations that enhance efficiency and recycling, to transformational models that redesign entire value systems through systemic solutions such as closed-loop supply chains and cross-sectoral collaboration (Palmié et al., 2021; Averina et al., 2021). Their application spans firm-level strategies by reducing material dependency and meeting regulatory demands (Moggi & Dameri, 2021;), to broader initiatives like industrial symbiosis and circular ecosystems, reinforcing their role as drivers of sustainable transitions (Angelis, 2022; Geissdoerfer, 2022).

4 CONCLUSIONS

This review confirms that CBMs are central to advancing the circular economy by enabling extended product lifecycles, resource optimization, and material regeneration. Based on a PRISMA-guided synthesis of the literature, this paper introduces a dual typology, *Strategic Focus* and *Operational Architecture*, that clarifies both the intent and implementation of CBMs. This typology offers a conceptual framework for interpreting and applying CBMs across sectors, allowing organizations to align model selection with their specific goals and contexts. In doing so, it enhances the likelihood of reconciling ecological objectives with economic feasibility. Despite their promise, different CBM types face distinct implementation challenges. Strategic models often struggle with systemic inertia, misaligned incentives, and insufficient policy support, while operational models confront infrastructure demands, limited digital capabilities, and scaling difficulties. Understanding these barriers through the lens of typology enables more targeted, type-specific interventions-regulatory, financial, or technological. The proposed framework provides a structured approach for navigating the fragmented CBM literature and supports cross-sectoral comparison and practical application. As interest in circular strategies continues to grow, such integrative typologies will be essential for bridging academic insight with real-world implementation in the transition towards a sustainable CE.

5 REFERENCES

Angelis, Roberta. (2022). Circular economy business models as resilient complex adaptive systems. Business Strategy and the Environment. 31. 2245-2255.

Averina, Elizaveta & Frishammar, Johan & Parida, Vinit. (2021). Assessing sustainability opportunities for circular business models. Business Strategy and the Environment. 31.

Awan, U., & Sroufe, R. (2022). Sustainability in the Circular Economy: Insights and Dynamics of Designing Circular Business Models. *Applied Sciences*, *12*(3), 1521.

Bocken, Nancy & Schuit, Cheyenne & Kraaijenhagen, Christiaan. (2018). Experimenting with a circular business model: Lessons from eight cases. Environmental Innovation and Societal Transitions. 28.

Carraresi, Laura & Bröring, Stefanie. (2021). How does business model redesign foster resilience in emerging circular value chains?. Journal of Cleaner Production. 289.

Coscieme, Luca & Manshoven, Saskia & Gillabel, Jeroen & Grossi, Francesca & Mortensen, Lars. (2022). A framework of circular business models for fashion and textiles: the role of business-model, technical, and social innovation. Sustainability: Science, Practice and Policy. 18. 451-462.

De Keyser Erika, Mathijs Erik. (2023). A typology of sustainable circular business models with applications in the bioeconomy, Frontiers in Sustainable Food Systems, Vol. 6-2022.

Den Hollander, Marcel & Bakker, C.A. & Hultink, Erik. (2017). Product Design in a Circular Economy: Development of a Typology of Key Concepts and Terms: Key Concepts and Terms for Circular Product Design. Journal of Industrial Ecology. 21.

Ertz, Myriam & Leblanc-Proulx, Sébastien & Sarigollu, Emine & Morin, Vincent. (2019). Advancing quantitative rigor in the circular economy literature: New methodology for product lifetime extension business models. Resources Conservation and Recycling. 150. 1-12.

Ferasso, Marcos & Beliaeva, Tatiana & Kraus, Sascha & Clauß, Thomas & Ribeiro-Soriano, Domingo. (2020). Circular economy business models: The state of research and avenues ahead. Business Strategy and the Environment. 29. 3006-3024.

Florian Hofmann. (2019). Circular business models: Business approach as driver or obstructer of sustainability transitions?, Journal of Cleaner Production, Volume 224.

Fraccascia, Luca & Giannoccaro, Ilaria & Agarwal, Abhishek & Hansen, Erik. (2019). Business models for the circular economy: Opportunities and challenges. Business Strategy and the Environment. 28.

Frishammar, Johan & Parida, Vinit. (2018). Circular Business Model Transformation: A Roadmap for Incumbent Firms. California Management Review. 61.

Geissdoerfer, Martin & Pieroni, Marina & Pigosso, Daniela & Soufani, Khaled. (2020). Circular business models: A review. Journal of Cleaner Production. 277. 123741.

Geissdoerfer, Martin & Santa-Maria, Tomas & Kirchherr, Julian & Pelzeter, Carla. (2022). Drivers and barriers for circular business model innovation. Business Strategy and the Environment. 32. 3814-3832. 10.1002/bse.3339.

Henry, Marvin & Bauwens, Thomas & Hekkert, M.P. & Kirchherr, Julian. (2019). A Typology of Circular Start-Ups: An Analysis of 128 Circular Business Models. Journal of Cleaner Production. 118528.

Heyes, Graeme & Sharmina, Maria & F. Mendoza, Joan Manuel & Gallego Schmid, Alejandro & Azapagic, Adisa. (2017). Developing and implementing circular economy business models in service-oriented technology companies. Journal of Cleaner Production. 177. 621-632.

Katherine A. Whalen, (2019). Three circular business models that extend product value and their contribution to resource efficiency, Journal of Cleaner Production, Volume 226, pp. 1128-1137.

Kirchherr Julian, Nan-Hua Nadja Yang, Frederik Schulze-Spüntrup, Maarten J. Heerink, Kris Hartley, (2023). Conceptualizing the Circular Economy (Revisited): An Analysis of 221 Definitions, Resources, Conservation and Recycling, Volume 194.

Kirchherr, Julian & Reike, Denise & Hekkert, M.P. (2017). Conceptualizing the Circular Economy: An Analysis of 114 Definitions. SSRN Electronic Journal. 127. 10.2139/ssrn.3037579.

Konietzko, Jan & Baldassarre, Brian & Brown, Phil & Bocken, Nancy & Hultink, Erik. (2020). Circular business model experimentation: Demystifying assumptions. Journal of Cleaner Production. 277.

Lahti, Tom & Wincent, Joakim & Parida, Vinit. (2018). A Definition and Theoretical Review of the Circular Economy, Value Creation, and Sustainable Business Models: Where Are We Now and Where Should Research Move in the Future? Sustainability.

Lara Guillén, Jorge & Jimenez-Zarco, Ana & Méndez-Aparicio, M Dolores. (2023). Reverse Logistics and Marketing as Tools for Sustainability.

Lee, Sheng-Hung & Sicklinger, Andreas. (2024). Design for Longevity: People, Process, and Platform. diid. 1.

Linder, Marcus & Williander, Mats. (2015). Circular Business Model Innovation: Inherent Uncertainties. Business Strategy and the Environment.

Loon, Patricia & Diener, Derek & Harris, Steve. (2020). Circular products and business models and environmental impact reductions: Current knowledge and knowledge gaps. Journal of Cleaner Production. 288. 125627.

Lüdeke-Freund, Florian & Gold, Stefan & Bocken, Nancy. (2019). A Review and Typology of Circular Economy Business Model Patterns. Journal of Industrial Ecology. 23. 36-61.

Mechthild Donner, Romane Gohier, Hugo de Vries, (2020). A new circular business model typology for creating value from agro-waste, Science of The Total Environment, Volume 716.

Moggi, S., & Dameri, R. P. (2021). Circular business model evolution: Stakeholder matters for a self-sufficient ecosystem. Business Strategy and the Envi, 30(6), 2830–2842.

Nußholz, J. L. K. (2018). A Circular Business Model Mapping Tool for Creating Value from Prolonged Product Lifetime and Closed Material Loops. Journal of Cleaner Production, 197, 185-194.

Palmié, Maximilian & Böhm, Jonas & Lekkas, Charlotte-Katharina & Parida, Vinit & Wincent, Joakim & Gassmann, Oliver. (2021). Circular business model implementation: Design choices, orchestration strategies, and transition pathways for resource-sharing solutions. Journal of Cleaner Production. 280.

Puglieri, Fabio & Salvador, Rodrigo & Romero-Hernandez, Omar & Filho, Edmundo & Piekarski, Cassiano & Francisco, Antonio & Ometto, Aldo. (2022). Strategic planning oriented to circular business models: A decision framework to promote sustainable development. Business Strategy and the Environment. 31. 3254-3273.

Rosa, Paolo & Sassanelli, Claudio & Terzi, Sergio. (2019). Towards Circular Business Models: A systematic literature review on classification frameworks and archetypes. Journal of Cleaner Production. 236. 117696.

Scholtysik, Michel & Rohde, Malte & Koldewey, Christian & Dumitrescu, Roman. (2023). DESIGNING BUSINESS MODELS FOR A CIRCULAR ECONOMY. Proceedings of the Design Society. 3. 1347-1356.

Schulte, Uwe. (2013). New business models for a radical change in resource efficiency. Environmental Innovation and Societal Transitions. 9. 43–47.

Schwanholz, Julia & Leipold, Sina. (2020). Sharing for a circular economy? an analysis of digital sharing platforms' principles and business models. Journal of Cleaner Production. 269. 122327.

Sjödin, David & Parida, Vinit & Kohtamäki, Marko. (2023). Artificial intelligence enabling circular business model innovation in digital servitization: Conceptualizing dynamic capabilities, AI capacities, business models and effects. Technological Forecasting and Social Change. 197. 122903.

Urbinati, Andrea & Chiaroni, Davide & Chiesa, Vittorio. (2017). Towards a New Taxonomy of Circular Economy Business Models. Journal of Cleaner Production. 168. 487-498.

Yang, Miying & Smart, Palie & Kumar, Mukesh & Jolly, Mark & Evans, Steve. (2017). Product-service system business models for circular supply chains. Production Planning and Control.

Vermunt, Dorith & Negro, S.O. & Verweij, P.A. & Kuppens, D.V. & Hekkert, M.P.. (2019). Exploring barriers to implementing different circular business models. Journal of Cleaner Production. 222.

Zafar, U., Maqbool, A., Haleem, A., Pathak, R., & Samson, D. (2021). Analyzing the business models for circular economy implementation: A fuzzy TOPSIS approach. *Operations Management Research*, 14(3), 256–271.

BRAILLE AND DIGITAL PRINTING IN PACKAGING AND ACCESSIBLE DESIGN

Nemanja Kašiković, Gojko Vladić, Sandra Dedijer, Saša Petrović, Željko Zeljković, Katarina Maričić

University of Novi Sad, Faculty of technical sciences, Department of graphic engineering and design, Serbia

doi: 10.5281/zenodo.17301488
knemanja@uns.ac.rs

Abstract: *The integration of Braille with digital printing enhances accessibility for visually impaired individuals by enabling the production of tactile and readable materials. Advanced digital printing technologies facilitate precise embossing and layering techniques, ensuring both high-quality print and effective tactile communication. This innovation plays a crucial role in packaging, allowing product information to be accessible to all consumers, while also being applied to business cards, labels, and informational materials. The combination of digital printing and Braille improves inclusivity, regulatory compliance, and user experience in various industries.*

ADVANCES IN SUSTAINABLE POLYMERS

MECHANICAL PROPERTIES OF BINARY POLYESTER BLENDS

Aleksandra Nešić, Ksenija Ilić, Branka Pilić

Faculty of Technology Novi Sad, Novi Sad, Serbia

doi: 10.5281/zenodo.17301520
alexm@uns.ac.rs

Abstract: *Poly(lactide) is the most widely used polyester from the biobased and biodegradable group of polymers. It is available and the price is affordable for high-volume applications. The main disadvantage of PLA is brittleness, thus, PLA is a low-impact polymer. For certain applications that require tailored mechanical properties, it is necessary to blend PLA with other polymers or modify it by adding plasticizers. In this work, PLA was blended with poly(butylene succinate) (PBS) and poly(butylene adipate terephthalate) (PBAT), where PBS or PBAT were added in amounts of 10, 20 and 30%, and thin films were produced using flat die extrusion. Those ratios were chosen because of the transparency of the films obtained from blended materials, since PLA is the most transparent of all alternative materials, and the addition of PBS or PBAT significantly affects it. Examination of mechanical properties resulted in a very high deviation of values within one sample, which indicates the immiscibility of PLA with other polyesters. Due to this fact, there were two approaches as the solution to the problem: the addition of a plasticizer/modifier and two-step processing, which gave better compatibility results.*

BEYOND OBJECT-BASED SORTING: WHY HETEROGENEOUS RIGID PP PACKAGING REQUIRES SYSTEMIC SOLUTIONS

Moritz Mager[1], Nikolai Kuhn[2], Joerg Fischer[1]

[1]Johannes Kepler University Linz, Institute of Polymeric Materials and Testing & LIT Factory, Linz, Austria

[2]Montanuniversitaet Leoben, Waste Processing and Waste Management, Department of Environmental and Energy Process Engineering, Leoben, Austria

doi: 10.5281/zenodo.17301595
moritz.mager@jku.at

Abstract: *The Packaging and Packaging Waste Regulation (PPWR) of the European Parliament and of the Council sets ambitious targets for the incorporation of recycled content in rigid polypropylene (PP) packaging, requiring 10 % in contact-sensitive applications and 35 % in all other packaging by 2030. Meeting these goals demands not only an expansion of recycling capacity but also significant improvements in recyclate quality. A key challenge lies in the inherent heterogeneity of post-consumer rigid PP waste, which comprises products with diverse processing methods, polymer grades, additives, and fillers. This study analyzes 19 representative rigid PP packaging products collected from an Austrian material recovery facility, covering bottles, trays, cups, tubs, and pails. Melt flow rate, tensile modulus, and Charpy notched impact strength were determined to evaluate material diversity and its implications for sorting strategies. The results reveal significantly higher melt flow rates for injection molded products compared to blow-molded and thermoformed packaging. Moreover, substantial variation in stiffness and impact strength due to PP types and application-specific requirements were found. To avoid mixed and intermediate recyclate properties, eco-efficient sorting strategies need to be developed, relying both on object- and flake-sorting. Object-based sorting can isolate distinct product categories and is indispensable for producing high-purity streams, such as those intended for food-contact recycling. However, its effectiveness is constrained by recognition limitations, unknown material formulations and product properties, multi-component designs, and contamination. Property-based flake sorting offers complementary advantages, including a higher spectral quality after pre-treatment and the potential for more accurate property-based separation, but requires robust prediction models linking spectral data to mechanical properties. Due to the scarcity in this field, future research should aim to close this gap. It can be concluded that neither sorting approach alone can deliver the range of recyclate properties needed to meet market demands. Instead, a systemic combination of object-based and flake-based sorting, supported by advanced property-prediction capabilities, is essential for developing a diversified PP recyclate portfolio in a resource-efficient manner.*

Keywords: mechanical recycling, property-based sorting, rigid polypropylene, post-consumer packaging

1 INTRODUCTION

The Packaging and Packaging Waste Regulation (PPWR) of the European Parliament and of the Council sets ambitious targets for the incorporation of recycled materials in plastic packaging. For polypropylene (PP), one of the most widely used rigid packaging plastics in the EU27 + 3 region, the recycling content shall be at 10 % for contact-sensitive packaging and at 35 % for all other packaging by 2030 (European Parliament and the Council, 2025). Meeting these goals will necessitate not only expanded recycling capacities, but also substantial improvements in recyclate quality to fulfill diverse and demanding product specifications (Plastics Recyclers Europe, 2023).

Achieving a closed-loop for rigid PP packaging is significantly complicated by the complexity of the waste stream, which contains a fluctuating mix of products with specifically tailored material formulations of all major processing methods (Eriksen et al., 2019; Geier et al., 2024a, Mager et al., 2023). Therefore, the challenge in PP recycling is to convert its heterogeneous feedstock into a diversified recyclate portfolio. In pursuit of enhanced quality, sensor-based sorting is considered to be a critical point for intervention, which is already implemented at multiple stages of the recycling process (Kroell et al., 2022). Advanced object-based sorting offers distinct advantages compared to flake-based sorting, such as the isolation of food contact materials (AIM – European Brands Association, 2025). However, significantly reducing the feedstock heterogeneity from a material property perspective on object-level may not be feasible under ecoefficiency constraints (Van Camp et al., 2024).

Since specific grades and formulations (including additives and fillers) are not disclosed by manufacturers and material degradation during the production and use phase is unspecified, an initial property screening of post-consumer PP packaging waste was conducted in this study. Based on the obtained product-property matrix of nineteen different PP packaging products from the Austrian PP waste, limitations of advanced object-based sorting and advantages of flake-based sorting were identified.

2 MATERIALS AND METHODS

2.1 Materials

Sample collection was conducted at an Austrian material recovery facility (MRF), where sorting of separately collected post-consumer lightweight packaging is conducted. The light-colored rigid PP stream was targeted, which was accessible at a conveyor belt prior to baling. The selection of suitable products for this study was limited to frequently occurring white and transparent packaging, so that the collection of a specific product (distinct brand and type in terms of, e.g., aroma or design) was feasible in sufficient quantities within a moderate time frame. Moreover, the product selection was aimed to cover all major applications of rigid PP packaging, as at least 2 kg of products from the categories bottles, trays, cups, tubs, and pails could be collected. However, no representative samples for lids, caps, and closures were obtained, primarily due to the abundant product variety and the low weight of certain products. Furthermore, a scarcity of caps and closures prevailed, as they were predominantly still attached to the primary packaging (e.g., high-density polyethylene bottles). A list of the investigated products is depicted in Table 1, including the processing method, color, and filling volume.

Table 1: Overview on investigated post-consumer rigid PP packaging products collected from the light-colored PP stream at an Austrian material recovery facility

Bottles		***Trays***		***Cups***		***Tubs***		***Pails***	
Product	***Details***	***Product***	***Details***	***Product***	***Details***	***Product***	***Details***	***Product***	***Details***
Bottle-A	*blow molding, clear, 0.24 L*	***Tray-A***	*thermo-forming, clear, 0.20 L*	***Cup-A***	*thermo-forming, white, 0.20 L*	***Tub-A***	*injection molding, white, 0.20 L*	***Pail-A***	*injection molding, white, 1.00 L*
Bottle-B	*blow molding, clear, 0.25 L*	***Tray-B***	*thermo-forming, clear, 0.20 L*	***Cup-B***	*injection molding, white, 0.23 L*	***Tub-B***	*injection molding, clear, 0.50 L*	***Pail-B***	*injection molding, white, 1.00 L*
Bottle-C	*blow molding, clear, 3.75 L*	***Tray-C***	*injection-molding, white, 5.00 L*	***Cup-C***	*injection molding, white, 0.23 L*	***Tub-C***	*injection molding, white, 1.00 L*	***Pail-C***	*injection molding, white, 10.00 L*
Bottle-D	*blow molding, white, 4.50 L*			***Cup-D***	*thermo-forming, clear, 0.50 L*	***Tub-D***	*injection molding, clear, 1.00 L*	***Pail-D***	*injection molding, white, 10.00 L*

2.2 Wet-mechanical treatment and sample preparation

In a first step, all removable parts (i.e., lids, labels, sealing film) were separated from the main PP body. The products were then pre-washed with cold water for 5 min in a PW 818 washing machine (Miele & Cie. KG, Gütersloh, Germany) with the addition of 0.5 % sodium hydroxide (NaOH) to reduce the overall contamination load. Subsequently, the products were coarsely shredded in a SM300 cutting mill (Retsch GmbH, Haan, Germany) with a screen size of 20 mm. The following washing process consisted of a hot-washing step (60 °C, 2 % NaOH, 10 min) and a rinsing step (20 °C, 5 min). After drying for 8 h at 60 °C (LUXOR A, motan holding GmbH, Konstanz, Germany), the flake-size was reduced to 8 mm (SM 300, Retsch GmbH, Haan, Germany), in order to facilitate direct injection molding. Multipurpose specimens and Type 1 specimens were produced according to ISO 19069-2:2024 via injection molding (Victory 60, ENGEL AUSTRIA GmbH, Schwertberg, Austria).

2.3 Characterization methods

Melt flow rate (MFR) measurements were conducted with an Aflow melt flow indexer (ZwickRoell, Ulm, Germany) according to ISO 1133-1:2022. Tests were performed using flakes at 230 °C with a load of 2.16 kg. Within one measurement, six cut-offs were made. Young's modulus was determined in tensile tests using an AllroundLine Z005 universal testing machine equipped with multi-extensometers (ZwickRoell, Ulm, Germany). According to ISO 527-1:2019 and ISO 527-2:2025, the traverse speed was set to 1 mm/min for the determination of the Young's modulus and 50 mm/min until failure. Five specimens were tested per material. Charpy notched impact strength (nIS) was obtained on an HIT25P pendulum impact tester (ZwickRoell, Ulm, Germany) equipped with a 2 J pendulum according to ISO 179-1:2023. Ten specimens were notched and tested in edgewise blow direction.

3 RESULTS AND DISCUSSION

3.1 Properties of investigated PP packaging products

Since the data presented in this work is limited to three material parameters, a three-dimensional graphical display would be feasible. However, two separate graphs were chosen due to an enhanced visibility, with the MFR being the common feature in both, as it allows the grouping of the main

processing methods at certain MFR ranges. Thus, the correlation between tensile modulus and MFR is displayed in Figure 1, while the correlation between Charpy notched impact strength is depicted in Figure 2. Blow molding products are found to have the lowest melt flow rates (2.1 – 4.9 g/10 min), followed by thermoformed products (6.6 – 8.4 g/10 min). Even though the investigated sample set does not show overlaps between blow-molded and thermoformed products in terms of MFR, it can be assumed that there would be overlaps to a certain extent in a larger sample set. Contrary to these low-MFR products, injection molding grades in rigid PP packaging were found to have significantly higher melt flow rates, which were measured between 56.1 g/10 min and 90.4 g/10 min.

The analysis of tensile modulus and Charpy nIS sheds light on the usage of homo- and copolymers in the investigated products, which are required to fulfill demanding product specifications. Especially the reduction of material in packaging necessitates optimized material properties, so that, e.g., a lower wall thickness is compensated by a higher stiffness of the material. In that case, nucleated homopolymers with an enhanced stiffness are a frequent choice. This becomes evident for Cup-A and Cup-D, which are both thermoformed cups without a specialized design for increased stability, exhibiting tensile moduli of 1990 MPa and 1710 MPa, respectively. In contrast, the lowest tensile moduli were obtained for the investigated bottles (800 – 1040 MPa), for which random copolymers are commonly used. Their advantage of having a high impact strength (6.8 – 10.5 kJ/m^2) comes at the cost of having a lower tensile modulus. For trays, tubs, and injection molded cups intermediate tensile modulus values were obtained, yet covering a significantly large range from 1220 MPa to 1610 MPa. In general, clear products exhibit a lower tensile modulus, which is in accordance with Kuhn et al. (2025), and can be explained by a higher probability of random copolymers. The results of Charpy impact testing apart from bottles show that the majority of products lies in the range of 4.0 kJ/m^2 to 7.0 kJ/m^2. Notable exceptions are Cup-A and Tub-D, with 3.4 kJ/m^2 and 9.3 kJ/m^2, respectively. Since Cup-A is most likely a highly-stiff homopolymer, the low impact strength is not surprising. Tub-D, on the other hand, is an ice cream packaging, which explains the high impact strength, as it is required for sub-zero temperatures to maintain product safety. A balance of stiffness and increased impact strength is commonly only achieved with block copolymers, which Tub-D can be attributed to.

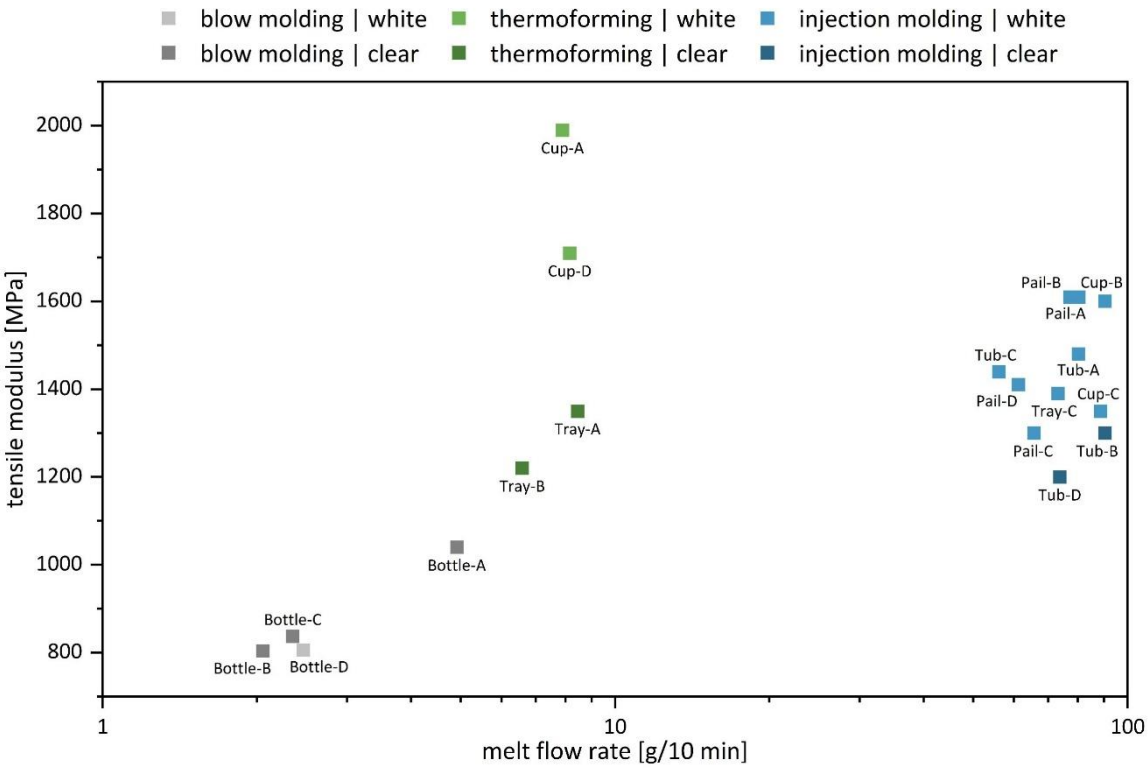

Figure 1: Tensile modulus over melt flow rate of the investigated rigid PP packaging products.

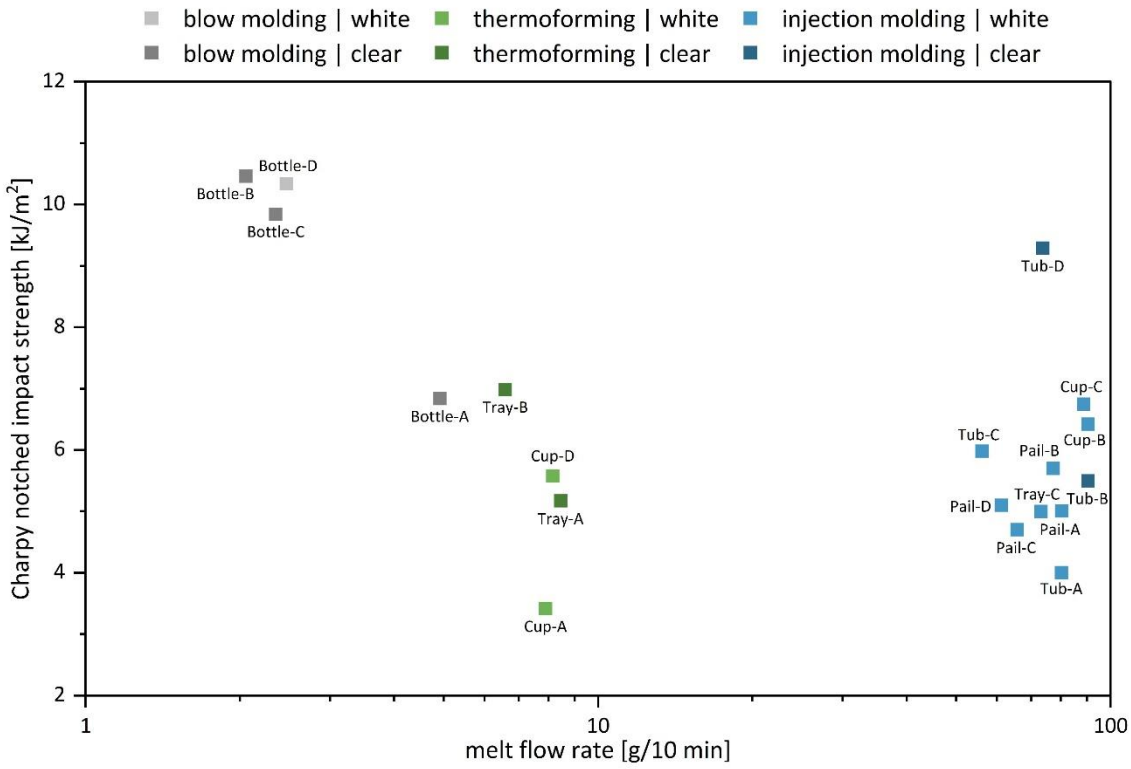

Figure 2: Charpy notched impact strength over melt flow rate for the investigated rigid PP packaging products.

3.2 Towards systemic solutions for enhancing PP recyclate quality through improved sorting

The material characteristics of the investigated packaging products clearly underline the diversity of grades and formulations that are present in the post-consumer rigid PP waste stream. To avoid mixed and intermediate recyclate properties, eco-efficient sorting strategies need to be developed, relying both on object- and flake-sorting.

Enhancing the sorting depth on an object-level bears the potential to isolate distinct products of the waste stream. This can either be implemented to exclude sources of severe contamination (e.g., silicon cartridges), or to generate a feedstock of defined products. Especially for obtaining highly-pure streams intended for food-contact recycling, sorting on object-level is indispensable. Furthermore, the potential of creating specified recyclates by object recognition could be demonstrated by Geier et al. (2024b), who obtained a low-MFR by sorting out blow-molded bottles. However, AI recognition is mainly limited to the products the system was trained on, and the recognition can be impeded by contamination, fragmentation, and agglomeration. In recent years, digital watermarks and the use of tracers have gained attention to enhance the accuracy in object recognition. While these systems are promising in theory, a comprehensive and unanimous application would be a prerequisite, which the authors consider unlikely without appropriate incentives or legislation. Moreover, the exact material properties of a product will predominantly be unknown, as they are not disclosed by the manufacturer, and non-separated multi-component products (e.g., injection-molded tub with thermoformed lid) will inevitably be sorted incorrectly from a property perspective. Finally, other potential disadvantages of splitting the rigid PP waste stream at object-level are separate logistics and wet-mechanical treatment for each fraction. Hence, either a batch process with intermediate bunkers or parallel washing lines are required.

As a fitting counterpart, property-based flake-sorting would allow for the feedstock to be processed as a whole in wet-mechanical treatment. Therefore, the throughput can be maximized and the reduced bulk density after shredding would be beneficial if intermediate bunker systems are required.

Nevertheless, a clear verdict regarding the preferred sorting option for a resource-efficient wet-mechanical treatment is not possible, since the appropriate setup and its scaling can be adjusted accordingly. The main challenge in effectively using flake-sorting for the diversification of recyclate properties is the correlation of spectral data and the corresponding material characteristics. While there are already approaches to determine MFR and density for polyethylene high-density, comparable research for PP is scarce. Therefore, future research should aim to close this gap by developing robust prediction models for material properties from spectral data. Flake-sorting has the upside that the overall spectral quality is significantly higher due to the removal of contaminants, films, labels, and also printing inks. Additionally, the scattering of flakes and the potentially higher spectral resolution in flake-sorting contribute to the data quality. Contrary to conventional flake-sorting, where the efficiency is highest if only a small percentage of contamination needs to be removed, spectral sorting according to direct material properties may require the positive sorting of a larger percentage of flakes, as well as multiple sorting steps. Hence, the setup will likely involve a flake sorter cascade, aimed to diversify PP recyclates in a resource-efficient manner.

4 CONCLUSIONS

Based on the investigated post-consumer products, the diversity of material grades that prevail in the rigid PP packaging stream could be demonstrated. The assessed product parameters lie the foundation for the development of robust property prediction models from spectral data, which are required to implement flake-sorting as a key technology for the diversification of PP recyclates. Once such prediction models become available, cost-efficient strategies for clustering materials by property profile will be needed, considering the practical limitation of simultaneous sorting fractions.

Meeting the PPWR targets for recycled content will require PP recyclates tailored to demanding applications, including food-contact packaging. The results presented here underline that this goal can only be achieved through a systemic combination of object-based and flake-based sorting, leveraging the specific strengths of each approach. Object-sorting ensures the removal or isolation of defined product categories, while flake-sorting enables refined property-based separation at scale.

Acknowledgments: *This work was funded by the Austrian Federal Ministry of Climate Action, Environment, Energy, Mobility, Innovation (BMK) and Austrian Research Promotion Agency (FFG) within the program "Energy of the Future. Circular Economy 2021 (KP)" under project circPLAST-mr (grant no 889843). Additionally, we would kindly thank TriPlast GmbH for giving us access to the waste stream, as well as our colleagues who significantly contributed in waste treatment and data acquirement.*

5 REFERENCES

AIM – European Brands Association (2025). Holy Grail 2.0. https://www.digitalwatermarks.eu/ (last accessed: 30.07.2025)

European Parliament and the Council (2025). Regulation (EU) 2025/40 of the European Parliament and of the Council of 19 December 2024 on packaging and packaging waste, amending Regulation (EU) 2019/1020 and Directive (EU) 2019/904, and repealing Directive 94/62/EC. https://eur-lex.europa.eu/eli/reg/2025/40 (last accessed: 30.07.2025)

Eriksen, M. K., Christiansen, J. D., Daugaard, A. E., & Astrup, T. F. (2019). Closing the loop for PET, PE and PP waste from households: Influence of material properties and product design for plastic recycling. Waste Management, 96, 75-85. https://doi.org/10.1016/j.wasman.2019.07.005

Geier, J., Bredács, M., Witschnigg, A., Vollprecht, D., Oreski, G. (2024a). Analysis of different polypropylene waste bales: Evaluation of the source material for PP recycling. Waste Management & Research, 42(9), 767-775. https://doi.org/10.1177/0734242X241227369

Geier, J., Barretta, C., Hinczica, J., Haar, B., Bredács, M., Witschnigg, A., Mayrbäurl, E., & Oreski, G. (2024b). Feasibility study on the production of low melt flow rate recycled polypropylene from postconsumer waste. Journal of Applied Polymer Science, 141(30), Article e55694. https://doi.org/10.1002/app.55694

Kroell, N., Chen, X., Greiff, K., Feil, A. (2022). Optical sensors and machine learning algorithms in sensor-based material flow characterization for mechanical recycling processes: A systematic literature review. Waste Management, 149, 259-290. https://doi.org/10.1016/j.wasman.2022.05.015

Kuhn, N., Mager, M., Fischer, J., Koinig, G., & Tischberger-Aldrian, A. (2025). Increasing the PP-recyclate quality by enhanced mechanical processing of post-consumer packaging waste. Resources, Conservation and Recycling, 223, 108494. https://doi.org/10.1016/j.resconrec.2025.108494

Mager, M., Berghofer, M., & Fischer, J. (2023). Polyolefin Recyclates for Rigid Packaging Applications: The Influence of Input Stream Composition on Recyclate Quality. Polymers, 15(13), 2776. https://doi.org/10.3390/polym15132776

Plastics Recyclers Europe (2023). HDPE & PP Rigids Market in Europe: State of play, data 2023. https://www.plasticsrecyclers.eu/publications/ (last accessed: 30.07.2025)

Van Camp, N., Lase, I. S., De Meester, S., Hoozée, S., & Ragaert, K. (2024). Exposing the pitfalls of plastics mechanical recycling through cost calculation. Waste Management, 189, 300–313. https://doi.org/10.1016/j.wasman.2024.08.017

CLOSING THE LOOP: MIXED PET AND PLA WASTE TO BLENDS WITH IMPROVED RECYCLING POTENTIAL

Rebeka Lorber[1], Aleksandra Nešić[2], Silvester Bolka[1], Branka Pilić[2], Blaž Nardin[1]
[1]Faculty of Polymer Technology, Slovenj Gradec, Slovenia
[2]Faculty of Technology Novi Sad, University of Novi Sad, Novi Sad, Serbia

doi: 10.5281/zenodo.17301728
rebeka.lorber@ftpo.eu

Abstract: *Blending PLA with mixed PET/PLA waste offers a direct recycling route. Separating these plastics is hard due to similar uses. Even small PLA amounts degrade PET's thermal and mechanical properties, hindering its recycling. However, adding PET improves PLA. This study used PET as a benchmark and created three PLA/PET blends in varying ratios. These blends underwent 10 mechanical recycling cycles (injection molding and milling), with property checks after each. The blends maintained processability and most mechanical properties. In contrast, PET degraded significantly in toughness, strength, and processability after just 7 cycles.*

Keywords: PET, PLA, blends, mechanical recycling, mixed waste

1 INTRODUCTION

The increasing demand and consumption of polymers in a wide range of applications has led to an increase in plastic waste in recent years. To reduce the impact on the environment, it is necessary to manage waste efficiently, making closing the loop in circular economy even more import. The basic approach to the circular economy consists of the 5R rule: refuse, reduce, reuse, repurpose and recycle (Dorigato, 2021; Schyns and Shaver, 2021). Recycling can be divided into four categories: primary, secondary, tertiary, and quaternary recycling, where primary means mechanical recycling of pre-consumer waste, secondary means mechanical recycling of post-consumer waste, tertiary means chemical recycling, and quaternary means energy recovery. Mechanical recycling of pre-consumer waste is easy and very cost-effective because the source of the waste is known, while recycling of post-consumer waste is more challenging. The first and biggest challenge is the collection and proper separation of the material, on which the resulting material depends the most (Worrell and Reuter, 2014; Volfand, 2019). In terms of efficiency of separation methods, there is still much to be done, as many polymers are difficult and expensive to separate. For example, in the beverage industry, bottles as well as other similar products in packaging industry are mainly made from PET and more recently PLA as a bio-based and biodegradable alternative. Separation of these materials is challenging because the most common method based on density - the floating-sink test with water - is not efficient enough because the materials have similar densities (1.25 g/cm^3 of PLA and about 1.35 g/cm^3 of PET), which is higher than that of water (Harper, 2006; González-López *et al.*, 2019). PLA and PET can be separated by NIR spectroscopy, which is less economical and has been reported to result in 86 % - 99 % separation accuracy, which is hardly accurate enough for bottle-to-bottle recycling because PLA degrades at the temperatures required to process PET, resulting in yellowing and other defects in the recycled products (Gent *et al.*, 2009; La Mantia *et al.*, 2011; Alaerts, Augustinus and Van Acker, 2018; Gere and Czigany, 2020). The contamination of PET with PLA is a fairly well-researched topic, mainly revealing how much even small amounts of contamination negatively affect the rheological and

mechanical properties of the recycled material (Chen, Pyda and Cebe, 2009; Xia *et al.*, 2014; McLauchlin and Ghita, 2016; Topkanlo, Ahmadi and Taromi, 2018; Plavec *et al.*, 2020).
Considering the above and poor mechanical and thermal properties of recycled biomaterials compared to fossil-based polymers, this study addresses the challenge from the other side by exploring ways to improve the properties of recycled PLA, which include reactive reprocessing, the use of nanoparticles, and mixing PLA with other polymers (Hopmann, Schippers and Höfs, 2015; Badia and Amparo, 2016). Blending PET with PLA represents a simple way to treat post-consumer waste that is difficult to separate with an option to up-scale PLA in terms of mechanical and thermal behaviour, i.e., poor toughness, low impact strength, poor crystallisation behaviour, and especially thermal degradability of the recycled material. Since many studies have shown negative effects of mechanical recycling on PLA (Beltrán *et al.*, 2017; Schyns and Shaver, 2021), the prepared blends were mechanically recycled to evaluate their recycling prospects.

2 EXPERIMENTAL

2.1 Materials

Ground PLA and PET pre-consumer bottles supplied by Stramex PET d.o.o. (Podplat, SLO) were used to make the blends. The ground material consisted of various particle shapes and sizes ranging from fine dust to 3 mm in diameter, with the average shifted towards the upper limit. Ground supplied materials were injection moulded and their properties evaluated. Determined properties are presented in Table 1.

Table 1: Determined properties of base materials.

Property	***rPLA***	***rPET***
Tensile Modulus (GPa)	*2.62 ± 0.23*	*3.53 ± 0.47*
Tensile Strength (MPa)	*68.20 ± 2.72*	*59.80 ± 0.48*
Impact toughness (kJ/m^2)	*15.34 ± 2.80*	*- (no break)*
T_g (°C)	*59.26*	*80.76*
T_m (°C)	*148.79*	*248.16*
T_d (°C)	*369.03*	*441.76*
Storage modulus (GPa)	*2.86*	*2.15*
Tanδ peak (-)	*1.942 at 66.96 °C*	*1.590 at 85.84 °C*

2.2 Blend preparation and processing

The ground PLA and PET were dried in the Memmert 100-800 hot-air drying oven until the moisture content, determined with the Mettler Toledo HX204 moisture analyser, was below 0.025 % before mixing and compounding with the LabTech 20-44 co-rotating twin-screw extruder with a screw diameter of 20 mm and an L/D ratio of 44. Rotation speed was 800 rpm^{-1}, and temperatures increased from 165 °C at the hopper to 200 °C at the die. PLA/PET blends were produced in three different ratios: 95/5 (5 wt.% PET), 90/10 (10 wt.% PET), and 85/15 (15 wt.% PET) without any additives. The extruded filament was transferred at through a water bath into the Scheer SGS 25-E4 pelletizer. The prepared granules were dried before injection moulding (Arburg Allrounder 320 C 500-100 Golden Edition with a screw diameter of 20 mm) into test specimens with the shape according to the standards ISO 527 (type 1BA), ISO 178 and ISO 179. The temperature profile was set to increase from 185 °C to 200 °C on the die, the screw rotated at 100 rpm^{-1} at a backpressure of 30 bar, the injection speed was 50 mm/s, the holding pressure was set to 320 bar for 5 s, and the cooling was set to 25 °C for 20 s. Last forty samples from each series were analysed for their properties, while the rest were milled using the

Wanner C13.20 s mill for thermoplastics, and re-injected. Mechanical recycling, consisting of milling and injection moulding, was repeated 10 times.

2.3 Characterization

The thermal and mechanical properties of the specimens were evaluated after each processing cycle, however for more straight forward presentation the results of 1st, 3rd, 5th, 7th, and 10th cycles of reprocessing are presented. For thermal properties, differential scanning calorimetry (DSC) and thermogravimetric analysis (TGA) were performed. Samples for DSC (DSC 2, Mettler Toledo) weighing between 5 mg and 10 mg were prepared in aluminium crucibles. The temperature regime of the analysis consisted of a 5 min isothermal section at 0 °C followed by heating from 0 °C to 280 °C at 10 °C/min, at 280 °C there was a 5 min isothermal section followed by cooling at 10 °C/min, in two cycles, and the entire measurement was performed in nitrogen atmosphere with a gas flow of 20 mL/min. TGA analyses were performed using a Mettler Toledo TGA/DSC 3+. Samples of approximately 10 mg prepared in an alumina crucible were heated from 40 °C to 600 °C in a nitrogen atmosphere with a gas flow of 20 mL/min, followed by heating from 600 °C to 700 °C at 10 °C/min in an oxygen atmosphere (20 mL/min). Dynamic mechanical analysis (DMA) was performed using a Perkin Elmer DMA 8000 dynamic mechanical analyser in dual cantilever mode. Samples were heated at 2 °C/min from room temperature to 170 °C in an air atmosphere and dynamically loaded at a frequency of 1 Hz and an amplitude of 20 µm.

Mechanical evaluation included tensile, flexural, and impact tests on notched specimens using the Charpy method. Tensile and flexural properties were determined using the Shimadzu AG-X plus universal testing machine equipped with a 10 kN load cell and an optical strain gauge. The tensile test was performed according to ISO 527-1 and the flexural test according to ISO 178. Impact strength was tested according to ISO 179 standard using Dongguan Liyi LY-JJD5 impact strength tester. Notched specimens were tested using a 1 J pendulum. The results of tensile and flexural tests represent the average of 5 specimen measurements each, while 10 specimens were submitted to impact toughness testing.

3 RESULTS AND DISCUSSION

3.1 Thermal properties

Figure 1 shows the DSC thermograms for the second heating cycle of prepared blends. The glass transition of PLA was recorded at about 58 °C, followed by its cold crystallisation in the range of 125 °C ± 5 °C and melting at 147.5 °C ± 2 °C for all samples studied, while the melting of PET was recorded in the range between 243.5 °C and 247.9 °C. No significant differences were detected between the tested blends by DSC, even between the 1st and the last recycling series of each blend. Due to the inhomogeneity of the samples taken out of injection moulded specimen, it was not possible to determine the effect of blend composition or recycling on the degree of crystallinity.

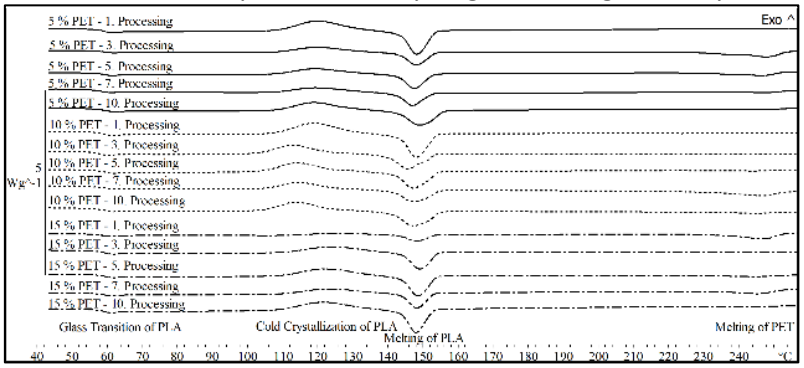

Figure 1. DSC thermographs of second heating recorded for blends

Similarly, the samples for TGA with comparable compositions could not be taken from injection moulded samples because the PET particles in PLA were not uniformly distributed. However, the degradation temperatures for the first decomposition (PLA) could be determined for all samples. The highest and lowest degradation temperatures were measured for the blend with 5 % PET after the 1st and 10th injection moulding of the blends, and the degradation temperature dropped from 368.6 °C to 360.4 °C. All other degradation temperatures of the other blends were in between. The content of PET does not seem to affect the degradation temperature uniformly across the different processing cycles, while overall consideration of the degradation temperatures seems to point to slightly decreasing trend from the 1st to the 10th recycling cycle, as shown in Figure 2. The general expectation was that the trend would be significantly decreasing, however due to better compatibility of the PLA and PET chains, which have shortened due to degradation resulting from multiple processing the decrease is probably suppressed (Worrell and Reuter, 2014).

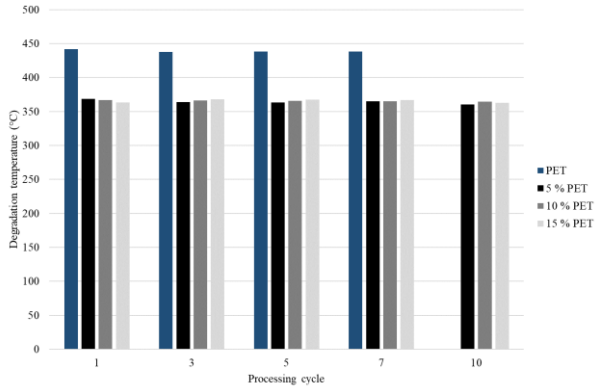

Figure 2. Degradation temperatures determined by TGA

Considering the glass transition temperature (T_g), which is determined as the maximum of the loss factor measured by DMA, presented in Figure 3 *(left)*, rPET has higher temperature of the transition compared to blends due to main material of the sample having higher T_g, however over multiple reprocessing cycles the temperature decreases while with blends increasing trends are observed, presumably due to the shortening of the PET backbone by the induced thermal and shear degradation and the resulting improved interactions with PLA. Furthermore, higher PET content in the blend seems to increase the retention of mechanical properties up to higher temperatures, as blends with 10 % and 15 % PET show higher T_g than blends with 5 % PET. *Right side of* Figure *3* presents loss factor values at peak temperatures. Loss factor of rPET over multiple reprocessing cycles decreases to less than a third of initial value, indicating stiffer and less damping behaviour. Blends are in terms of loss factor comparable after initial processing, however with reprocessing their dampening behaviour and suppleness are even increasing indicating the interactions between the components.

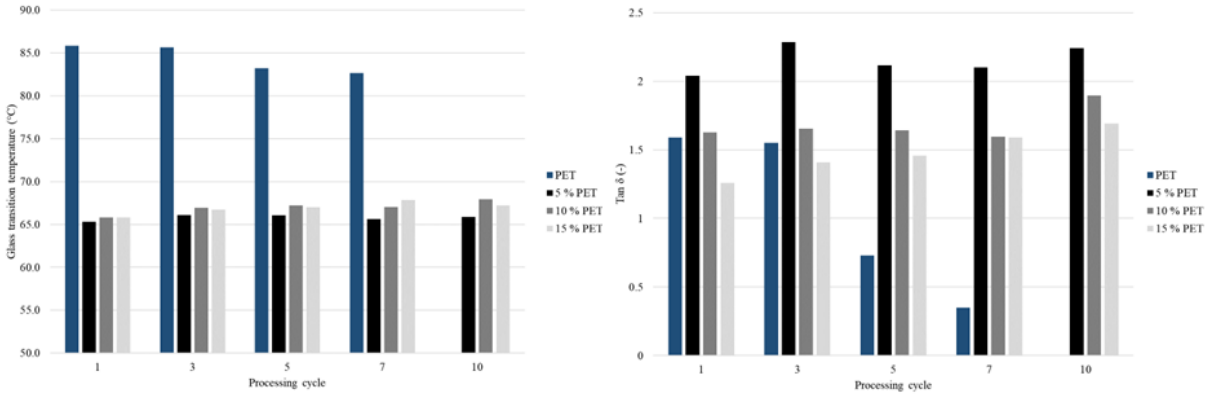

Figure 3. Glass transitions (left) and loss factor values at peak (right) determined by DMA

3.2 Mechanical properties

Tensile moduli of rPET and blends a function of cycles of mechanical recycling are shown in Figure 5. Moduli of rPET is in the similar range as 5 % PET blend, and it decreases with the increase of the amount of PET. After initial processing moduli of rPET decreases and stays in the range of standard deviation as long as it retains the processability. However, the multiple mechanical processing has no influence on the blends since most of the values obtained from the 1st to the 10th cycle stay in the range of standard deviation of each blend, yet again demonstrating the reprocessability of the blends.
Moreover, the tensile strength was not influenced by the PLA/PET ratio or by the multiple processing, but the tensile strength of PET from near 60 MPa at initial processing fell to almost 20 MPa after 7th reprocessing cycle. The determined tensile strengths are presented in Figure 6.

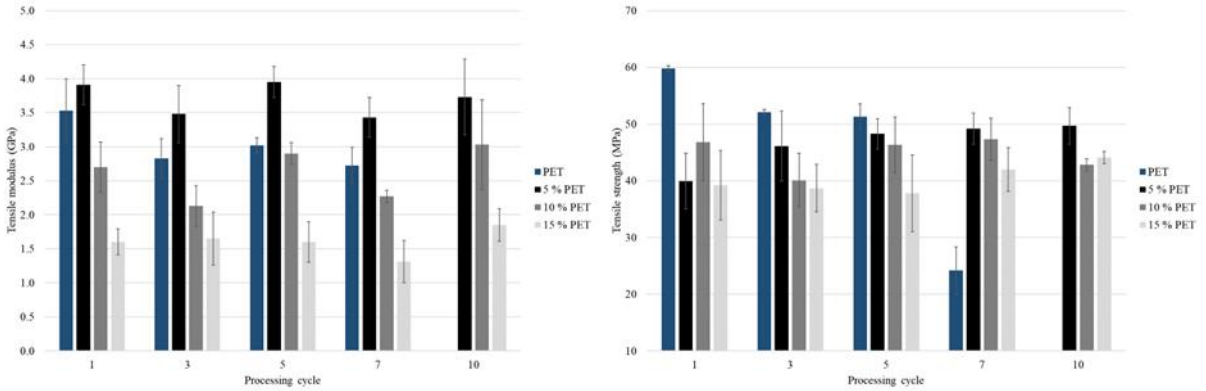

Figure 4. Tensile moduli (left) and strengths (right)

Figure 5 shows the results of the notched impact strength tests. PET loses significant proportion of its original impact strength each two cycles, while interestingly with blends no significant differences could be identified in dependence of PET content as well as loss of strength from initial up to 10th reprocessing cycle.

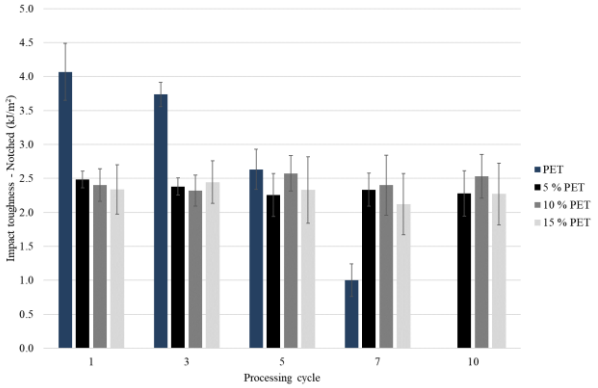

Figure 5. Notched Charpy impact toughness

4 CONCLUSIONS

European Union directives, such as 94/62/EC, in the field of packaging materials have become stricter in recent years, as have the expectations of society, which seeks a more environmentally friendly use of resources and a circular economy (The European Parliament and the Council of the European Union, 1994). One of these strategies is the use of more environmentally friendly alternatives, bio-based and biodegradable polymers such as PLA, wherever possible. However, there are some disadvantages compared to petroleum-based polymers, such as lower performance and contamination of waste streams. Paper investigated potential solutions and recycling prospects for hard-to-separate packaging waste. Three blends were made from ground bottles and mechanically recycled 10 times. The results of the thermal tests showed no significant effects of the composition of the blend or the different

processing cycles on the first and second order thermal transitions. While the trend of a slight decrease in the temperature of thermal degradation as a function of the number of recycling cycles was observed, the difference between maximum and minimum for the blend with the lowest PET content was below 3 %, indicating a positive influence of higher PET contents on thermal stability in blends. Similarly, the retention of mechanical properties at higher temperatures was observed when considering the glass transition temperature, as increasing trends were observed as a function of increasing processing cycles as well as increasing PET content. As far as mechanical properties are concerned, decreasing stiffness was observed only for tensile modulus as a function of PET content. Surprisingly, other mechanical properties such as tensile strength, flexural modulus, and strength as well as impact strength did not change significantly as a function of composition or recycling. From a structural point of view, this makes the blends a perfect material for multiple recycling. Moreover, thermal, and mechanical properties of blends are compared to neat rPLA and rPET on competitive level, making them suitable material for various applications, as well as reprocesing since they rented the processability at least 3 reprocessing cycles more than rPET.
Overall, the investigated properties of blends did not change significantly even after 10 cycles of mechanical recycling, showing an enormous recycling potential, which could be further improved by using powdered PET particles to improve the homogeneity of the material, coupling agents to improve compatibility of materials, nucleating agents to tailor the morphology, antioxidants to prevent oxidative degradation and chain extenders to keep the length of polymer chains.

Acknowledgements: *We would like to kindly thank the company Stramex PET d.o.o. for providing the material for the study.*

5 REFERENCES

Alaerts, L., Augustinus, M. and Van Acker, K. (2018) 'Impact of Bio-Based Plastics on Current Recycling of Plastics', Sustainability, 10(5). doi: 10.3390/su10051487.

Badia, J. D. and Amparo, R. (2016) 'Mechanical recycling of polylactide, upgrading trends and combination of valorization techniques', European Polymer Journal, 84. doi: 10.1016/j.eurpolymj.2016.09.005.

Beltrán, F. R. et al. (2017) 'Mechanical recycling of polylactide: improvement of the properties of the recycled material', Polymers, Characterization and Applications Research Group.

Chen, H., Pyda, M. and Cebe, P. (2009) 'Non-isothermal crystallization of PET/PLA blends', Thermochimica Acta, 492(1–2), pp. 61–66. doi: 10.1016/j.tca.2009.04.023.

Dorigato, A. (2021) 'Recycling of polymer blends', Advanced Industrial and Engineering Polymer Research. Elsevier Ltd, 4(2), pp. 53–69. doi: 10.1016/j.aiepr.2021.02.005.

Gent, M. R. et al. (2009) 'Recycling of plastic waste by density separation: Prospects for optimization', Waste Management and Research, 27(2), pp. 175 – 187. doi: 10.1177/0734242X08096950.

Gere, D. and Czigany, T. (2020) 'Future trends of plastic bottle recycling: Compatibilization of PET and PLA', Polymer Testing. Elsevier Ltd, 81(July), p. 106160. doi: 10.1016/j.polymertesting.2019.106160.

González-López, M. E. et al. (2019) 'Effect of Maleated PLA on the Properties of Rotomolded PLA-Agave Fiber Biocomposites', Journal of Polymers and the Environment. Springer US, 27(1), pp. 61–73. doi: 10.1007/s10924-018-1308-2.

Harper, C. A. (2006) 'Handbook of plastics technologies', IEEE Electrical Insulation Magazine, p. 53. doi: 10.1109/MEI.2006.253437.

Hopmann, C., Schippers, S. and Höfs, C. (2015) 'Influence of recycling of poly(lactic acid) on packaging relevant properties', Journal of Applied Polymer Science, 132(9). doi: https://doi.org/10.1002/app.41532.

La Mantia, F. P. et al. (2011) 'Effect of small amounts of poly(lactic acid) on the recycling of poly(ethylene terephthalate) bottles', Polymer Degradation and Stability, 97(1), pp. 21–24. doi: 10.1016/j.polymdegradstab.2011.10.017.

McLauchlin, A. R. and Ghita, O. R. (2016) 'Studies on the thermal and mechanical behavior of PLA-PET blends', Journal of Applied Polymer Science, 133(43), pp. 1–11. doi: 10.1002/app.44147.

Plavec, R. et al. (2020) 'Recycling possibilities of bioplastics based on PLA/PHB blends', Polymer Testing, 92(September). doi: 10.1016/j.polymertesting.2020.106880.

Schyns, Z. O. G. and Shaver, M. P. (2021) 'Mechanical Recycling of Packaging Plastics: A Review', Macromolecular Rapid Communications, 42(3), pp. 1–27. doi: 10.1002/marc.202000415.

The European Parliament and the Council of the European Union (1994) 'European Parliament and Council Directive 94/62/EC', (1990), pp. 38–59.

Topkanlo, H. A., Ahmadi, Z. and Taromi, F. A. (2018) 'An in-depth study on crystallization kinetics of PET/PLA blends', Iranian Polymer Journal (English Edition). Springer Berlin Heidelberg, 27(1), pp. 13–22. doi: 10.1007/s13726-017-0582-5.

Volfand, J. (ed.) (2019) Razvoj embalaže v krožnem gospodarstvu: priročnik. Fit media.

Worrell, E. and Reuter, M. A. (2014) Handbook of Recycling: State-of-the-art for Practitioners, Analysts, and Scientists, Handbook of Recycling: State-of-the-art for Practitioners, Analysts, and Scientists. doi: 10.1016/C2011-0-07046-1.

Xia, X. L. et al. (2014) 'Degradation behaviors, thermostability and mechanical properties of poly (ethylene terephthalate)/polylactic acid blends', Journal of Central South University, 21(5), pp. 1725–1732. doi: 10.1007/s11771-014-2116-z.

ASSESSMENT OF MATERIAL COMPOSITION AND COLOR DISTRIBUTION IN POST-CONSUMER POLYPROPYLENE BALES

Hannah Zeilinger, Joerg Fischer

Johannes Kepler University Linz, Institute of Polymeric Materials and Testing & LIT Factory, Linz, Austria

doi: 10.5281/zenodo.17302001
hannah.zeilinger@jku.at

Abstract: *In order to meet the recycling targets according to the Packaging and Packaging Waste Regulation (PPWR) within a circular economy framework, a comprehensive understanding of the input stream is essential. The input stream for plastic waste recycling, commonly delivered as compressed plastic bales, vary in composition and quality due to the heterogeneous composition of the stream. These bales contain the targeted polymer fraction as well as amounts of foreign polymer contaminants and non-plastic contaminants that significantly influence the recycling process and recyclate quality. This study focused on rigid post-consumer polypropylene (PP) bales, assessing both material composition and color. PP is one of the most commonly used polymers in consumer packaging. The bales consist of food packaging, such as yoghurt cups, ice cream, or butter containers as well as non-food packaging, such as flower pots. The input materials, processed into shredded flakes, were sorted by material type using a portable near-infrared (NIR) sensor. The flakes were divided into rigid polymers, including PP, polyethylene, polystyrene, and polyamide as well as flexible polymers, aluminum, non-detectable components (e.g., black particles), and other materials (e.g., wood). Moreover, the rigid PP fraction was manually classified by color (transparent, white, red, green, and blue). The study showed that 80-90% of the investigated input samples consist of rigid polypropylene. Color sorting revealed that approximately 40 % of the rigid PP fraction was transparent. White rigid PP comprised around 30%. A detailed analysis of the plastic input stream enables an optimized recycling process that leads to an improved recyclate quality and reduced material loss. This supports regulatory compliance and enhances overall recycling efficiency and sustainability.*

Keywords: plastic waste, polypropylene, mechanical recycling, sorting, material composition, color

1 INTRODUCTION

The growing demand for sustainability and circular economy concepts to achieve the recycling targets have intensified the focus on viable end-of-life strategies for post-consumer plastics. The largest end-use market for plastics in the EU27+3 is represented by packaging, accounting for nearly 60 % of the total plastic waste. Polypropylene is the second most used plastic after polyethylene for packaging applications (Plastics Europe, 2022; European Commission, 2018). A common method to recycle plastic waste is mechanical recycling. Typical mechanical recycling steps include sorting, shredding, washing, drying, and extrusion of the collected plastic waste into recyclates (Friedrich, 2019; Brouwer, 2020). The quality of the input waste stream plays a crucial role in effective recycling processes. Quality differences and inconsistencies like a heterogeneous composition and contamination of the input waste streams limit the processability and the subsequent applications of mechanically recycled

materials. The presence of even small amounts of foreign polymers or non-plastic contaminants can significantly impair the performance and appearance of recyclates. Therefore, sorting and separation is an essential step to generate a homogenous and clear input to produce high-quality recyclates (Al-Salem, 2009). Sorting can be done on object-level and on flake-level, based on different criteria such as material composition, shape, density, color, size, or application. Common sorting techniques include manual sorting, and automated sorting (e.g., near-infrared (NIR) spectrometry, wind sifting, and density separation). Near-infrared is one of the most widely used methods for sorting plastics. However, NIR has a few limitations. As it is an optical surface technique, any obstruction - such as labels, sleeves, overlapping products, or dirt - can cause false readings. Furthermore, multilayered plastics, flexibles (i.e., films) or black particles cannot be accurately identified or are not at all identifiable by NIR (Ragaert, 2017; Akhras, 2024; Hahladakis, 2019). Although plastic films (two-dimensional (2D)) are recyclable, their low bulk density limits the efficiency in sorting and mechanical reprocessing compared to rigid, three-dimensional (3D), plastics (e.g., hollow bodies) (Hahladakis, 2019; Feil, 2020). Sorting by material composition is important to remove foreign polymeric and non-polymeric contaminations, as their presence can lead to immiscibility and incompatibility issues affecting the mechanical and thermal properties of the recycled products. Furthermore, color sorting is essential, since colorants can also cause problems during plastics recycling and influence aesthetic, mechanical, and thermal properties. No color sorting usually results in dark green, brown, or grey colored products with a lower quality, limiting further applications (Akhras, 2024; Cucuzza, 2023). This study focuses on the analysis of rigid post-consumer polypropylene waste bales on flake-level to gain insight into the composition and color distribution of the input stream. These two indicators should provide an estimation of the quality of a rigid post-consumer polypropylene waste stream used in an industrial polypropylene mechanical recycling plant.

2 MATERIALS AND METHODS

2.1 Materials and pre-treatment

Pre-sorted rigid PP bales, containing post-consumer food and non-food packaging waste, were provided by PreZero Polymers Austria GmbH. Among others, the bales included yoghurt cups, ice cream, butter/margarine pots, meat packages, microwave-proof containers, and flower pots. As a first step, the bales were mechanically shredded into flakes and used as input material for a mechanical recycling process of the industrial mechanical recycling plant. To gain representative insight into the composition of the input stream, a total of six samples were taken post-shredding from the recycling line at intervals of approximately 30 minutes. The flakes were washed at 20 °C for 15 min using an industrial washing machine (Miele & Cie. KG, Gütersloh, Germany). Additionally, a separation from higher-density materials via a swim-sink tank with water at room temperature was done. After the washing and separation step, the samples were dried at 60 °C for 3 h in a drying chamber (Binder GmbH, Tuttlingen, Germany). Furthermore, the flakes were sieved with a vibration sieve shaker (Retsch GmbH, Haan, Germany) to remove all particles with a size of 1 mm or smaller. Pre-treatment of the flakes was necessary to replicate key steps of the washing process during mechanical recycling in order to remove surface contaminants to enable a more accurate analysis.

2.2 Methods

Material-based sorting of the pre-treated flakes was conducted to determine the composition of the six samples. Flake classification was carried out using a portable NIR hand-sensor (trinamiX GmbH, Ludwigshafen, Germany) to assign them to distinct material categories. The flakes were sorted into rigid polymers (3D), specifically PP, polyethylene (PE), polystyrene (PS), and polyamide (PA). Further categories included films, aluminum, non-detectable flakes (primarily black particles), and other materials (e.g., wood). Due to the above-mentioned limitations of NIR regarding multilayered plastics and flexibles, no classification of the film fraction was done. Each material category was weighed and expressed as a percentage of the total mass of the corresponding sample. The rigid PP fraction was

additionally analyzed to evaluate the color distribution. For this purpose, five color categories (transparent, white, red, green, and blue) were defined and the PP flakes were manually sorted based on these classifications. The individual color fractions were also weighed and expressed in mass percent.

3 RESULTS AND DISCUSSION

3.1 Material composition

The material composition of the flake samples of the six investigated input fractions is depicted in Figure 1 and the exact percentages of the composition analysis are summarized in Table 1. As expected, the PP content dominates in all samples analyzed.

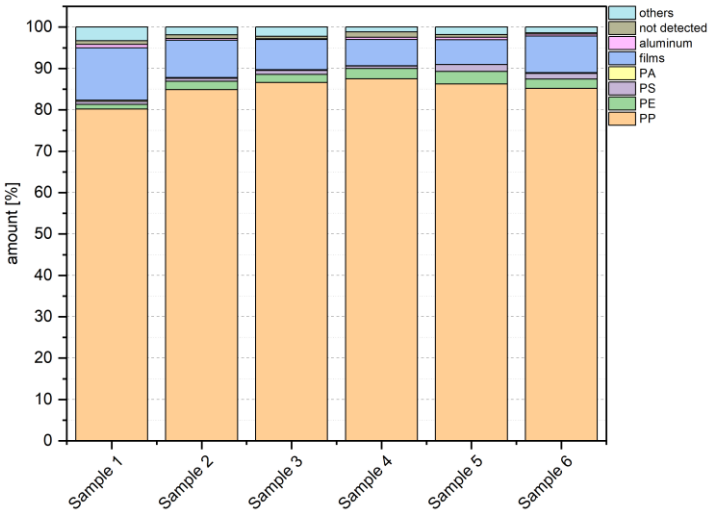

Figure 8: Material composition of the investigated post-consumer rigid PP bales.

The results displayed that rigid PP comprises between 80 and 90% of the total flake mass in all six samples. Minor fractions of PE, PS, and PA are also present, albeit in significantly lower portions. PE constantly contributes approximately 1-3 %, with PS and PA being even less abundant. These polymers can be considered as impurities in PP dominant streams. Films represent the second highest share in the compositions ranging from 6% to nearly 13%. Flexibles also impede plastics recycling and lower the quality of the end-products. Aluminum and materials labeled as "not detected" and "others" constitute very small percentages of the overall sample composition. The presence of all these contaminants impacts the processability and quality of the recycled material if not removed. The non-PP fractions, although in small amounts, highlight the need for effective sorting before entering the recycling process and separation during the process to ensure high-quality PP recyclates.

Table 7: Overview on the detailed material composition of the investigated post-consumer rigid PP bales

	PP [%]	***PE [%]***	***PS [%]***	***PA [%]***	***Films [%]***	***Aluminum [%]***	***not detected [%]***	***Others [%]***
Sample 1	*80.2*	*1.1*	*0.7*	*0.3*	*12.7*	*0.8*	*0.9*	*3.3*
Sample 2	*84.9*	*2.2*	*0.7*	*0.2*	*9.1*	*0.4*	*0.9*	*1.9*
Sample 3	*86.6*	*2.0*	*1.0*	*0.1*	*7.3*	*0.2*	*0.6*	*2.2*
Sample 4	*87.5*	*2.5*	*0.6*	*0.1*	*6.3*	*0.5*	*1.3*	*1.2*
Sample 5	*86.3*	*3.0*	*1.7*	*0.0*	*6.0*	*0.6*	*0.7*	*1.8*
Sample 6	*85.2*	*2.2*	*1.4*	*0.2*	*8.9*	*0.4*	*0.3*	*1.4*

3.2 Color distribution

Figure 2 illustrates the color distribution of the six rigid PP flake samples, which is a crucial parameter for evaluating the functional and aesthetic suitability of recyclates in high-quality applications. Across all samples, two color categories dominate: transparent and white.

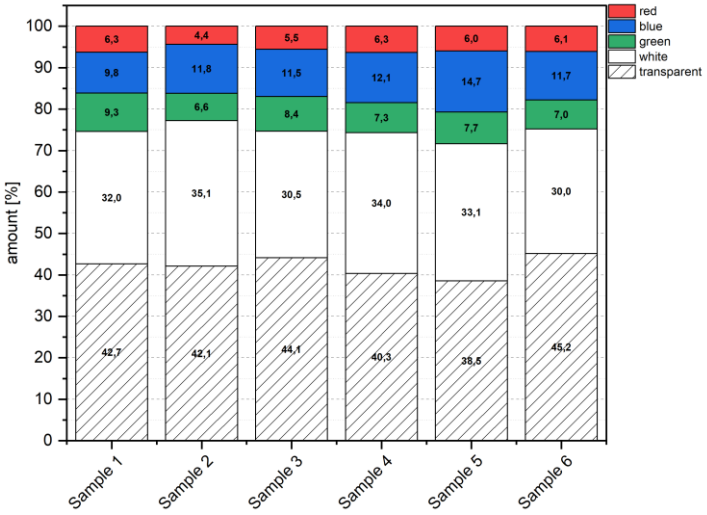

Figure 9: Color distribution of the investigated post-consumer rigid PP fraction.

Transparent flakes consistently contribute the largest fraction, ranging from roughly 38% to slightly over 45%. White flakes represent the second most abundant category, accounting for approximately 30-35%. Together, these two categories comprise more than 70 % of the total flake volume in all samples. Colored flakes appear in smaller, yet non-negligible, proportions. Green flakes range from 6.6% to 9.3%. Blue flakes contribute between 9.8% and nearly 15.0%, with sample 5 showing the highest share. Red flakes make up the smallest share, with percentages between 4.4% and 6.3%. Transparent and white flakes are favorable for recycling processes since they enable a broader range of recoloring or direct reuse in higher-performance products. In contrast, strongly pigmented flakes limit the recycling and aesthetic flexibility of the recyclates and restrict end-use options.

4 CONCLUSIONS

The analysis of a rigid polypropylene input waste stream revealed that even though PP is the dominant polymer in the sample set, minor fractions of other polymers and non-polymeric contaminants were present. These non-PP fractions, even in small amounts, negatively influence the processability and recyclate properties, if not eliminated during mechanical recycling using sorting and separation techniques. The level and distribution of foreign polymeric and non-polymeric contaminants can vary due to seasonal fluctuations or suppliers. Although material composition and color distribution may vary within a single supplier, greater variability is expected when sourcing from multiple suppliers. Color sorting showed transparent and white flakes make up the largest share, but their desirable advantages are diminished by the presence of colored flakes. This color variability not only results in a darker end-color and a restricted reusability of the recycled material but also downgrades recyclability, mechanical and thermal properties and complicates sorting processes due to poor detectability of dark pigment with NIR spectroscopy. The results underline that accurate knowledge of the input stream is important for tailoring and optimizing the mechanical recycling process. This study highlights the necessity of thorough sorting of post-consumer plastic waste to ensure a consistent and homogenous input stream for mechanical recycling. The production of high-quality secondary raw materials requires

sorting not only by material but also by color, combining object-based sorting with flake-based sorting. Material and color purities contribute significantly to the economic and functional viability of recycled plastic and are crucial for realizing the PPWR recycling targets.

Acknowledgments: *The authors acknowledge financial support from the COMET Centre CHASE, funded within the COMET – Competence Centers for Excellent Technologies program by the BMIMI, the BMWET and the Federal Provinces of Upper Austria and Vienna. The COMET program is managed by the Austrian Research Promotion Agency (FFG). Additionally, we would like to thank PreZero Polymers Austria GmbH for the support and for providing the materials used in this study.*

5 REFERENCES

Akhras, M.H., Fischer, J. (2024) Influence of color sorting on the property profile of polyethylene recyclates. AIP Conf. Proc., 3158, 120001. https://doi.org/10.1063/5.0207901.

Al-Salem, S.M, Lettieri, P., Baeyens, J. (2009) Recycling and recovery routes of plastic solid waste (PSW): a review. Waste Management, 29, 2625-2643. https://doi.org/10.1016/j.wasman.2009.06.004.

Brouwer, M.T., Thoden van Velzen, E.U., Ragaert, K, ten Klooster, R. (2020) Technical limits in circularity for plastic packages. Sustainability, 12(23), 10021. https://doi.org/10.3390/su122310021.

Cucuzza, P., Serranti, S., Capabianco, G., Bonifazi, G. (2023) Multi-level color classification of post-consumer plastic packaging flakes by hyperspectral imaging for optimizing the recycling process. Spectrochimica Acta Part A: Molecular and Biomolecular Spectroscopy, 302, 123157. https://doi.org/10.1016/j.saa.2023.123157.

European Commission (2018) A European Strategy for Plastics in a Circular Economy. EUR-Lex - 52018DC0028 - EN - EUR-Lex (last accessed: 06.08.2025).

Feil, A., Pretz, T. (2020) Mechanical recycling of packaging waste. Plastic Waste and Recycling, chapter 11, 283-319. https://doi.org/10.1016/B978-0-12-817880-5.00011-6.

Friedrich, K., Möllnitz, S., Holzschuster, S., Pomberger, R., Sarc, R. (2019) Benchmark analysis for plastic recyclates in Austrian waste management. Detritus, 9, 105-112. https://doi.org/10.31025/2611-4135/2019.13869.

Hahladakis, J.N., Iacovidou, E. (2019) An overview of the challenges and trade-offs in closing the loop of post-consumer plastic waste (PCPW): focus on recycling. Journal of Hazardous Materials, 380, 120887. https://doi.org/10.1016/j.jhazmat.2019.120887.

Plastics Europe (2022) Plastics - the Facts 2022. https://plastic seurope.org/knowledge-hub/plastics-the-facts-2022/ (last accessed: 07.08.2025).

Ragaert, K., Delva, L., Van Geem, K. (2017) Mechanical and chemical recycling of solid plastic waste. Waste Management, 69, 24-58. http://dx.doi.org/10.1016/j.wasman.2017.07.044.

A CIRCULAR APPROACH TO HYDROPONICS: UPCYCLED POLYPROPYLENE AND COCONUT FIBER WASTE AS SUSTAINABLE MATERIAL FOR HYDROPONIC GROWTH POTS

Marko Verčkovnik[1], Natalija Štumpfl[2], Silvester Bolka[1], Blaž Nardin[1], Primož Mlačnik[2], Sebastjan Zaverla[1], Rajko Bobovnik[1]

[1]Faculty of polymer technology, Slovenj Gradec, Slovenia
[2]KO-SI d.o.o., Slovenj Gradec, Slovenia

doi: 10.5281/zenodo.17302103
marko.verckovnik@ftpo.eu

Abstract: *Plant fibres are considered to have great potential for use as reinforcment in the production of value-added recycled plastic composites. Unfortunately, only a small portion of waste plant fibres is utilized as secondary raw materials, while the majority ends up being randomly incinerated or disposed of in landfills. From a materials perspective to achieve sustainable development, the solution lies in moving toward more environmentally friendly trends, which have led to the rise of so-called "biocomposites." Biocomposites are a class of materials formed by blending natural fibres with a matrix material. The natural fibres used in biocomposite production can be derived from various sources, including flax, coconut, hemp, jute, sisal, and bamboo. The matrix material used in biocomposites can varie from biodegradable, non-biodegradable, synthetic to recycled. In this paper, the use of waste polypropylene combined with waste coconut fibres is presented for the production of a low-density pot that enables hydroponic plant cultivation. At the Faculty of Polymer Technology, waste packing belts from the company KO-SI were used in the form of recycled polypropylene, which was ground and mixed with ground waste coconut fibres—an industrial waste product from the company KO-SI. To achieve proper bonding between the matrix and the fibres, a suitable compatibilizer was added. This ensured good interfacial interactions between the waste coconut fibres and the recycled polypropylene matrix. Using computer-aided design (CAD) with Siemens NX 12 software, a 3D model of a pot suitable for hydroponic plant cultivation was first created. This was followed by the construction of a thermoforming tool, which was printed using fused filament fabrication (FFF) technology. With the help of a press, sheets were produced from the prepared composite material. These sheets were then shaped into hydroponic plant pots using a thermoforming machine and the 3D-printed tool.*

Keywords: biocomposites, natural fiber reinforcement, coconut fiber, prototyping

1 INTRODUCTION

Industrial waste is generally better separated from municipal waste and is often much less polluted. This consequently means that additional sorting and washing of industrial waste is not necessary. Recycling of industrial waste is therefore much easier (Ragaert et al., 2017). The main advantage of thermoplastic composites is that the combination of matrix and waste reinforcing fibers produce excellent properties, while at the same time reduce production costs (Zhidan et al., 2011).

Recently, PP recycling has been a very important topic, mainly due to the increasing amount of PP. A large part of the packaging is made of PP. Polypropylene grafted with maleic anhydride as a compatibilizer in the composition of waste coconut fibers and polypropylene matrix allows for better dispersion of waste coconut fibers in the PP matrix. In addition, the use of this compatibilizer improves the interfacial adhesion of waste PP with natural fibers. Waste composite has increased stiffness compared to recycled polypropylene (Zhidan et al., 2011), (Di Bella et al., 2012).

The aim of this study was to ensure sufficient stiffness of the composite material and maintain a sufficiently low density, which in addition to buoyancy, ensures the floating capability of the final product. In addition, the aim was to prepare a functional product from industrial waste materials. As part of the study, it was necessary to design a thermoforming tool and adapt it to the composite material. This is precisely why we chose FFF technology to manufacture these prototype tools. The versions of the thermoforming tool thus differ in geometry to achieve the thermoforming for the simplest production of pots for hydroponics.

2 MATERIALS AND METHODS

In the experimental part of the study which was based on previous research on composites reinforced with waste coconut fibers, we prepared two versions of the material with different ratio of additives.

2.1 Sample

In the study, we used industrial waste from the company KO-SI d.o.o. We used coconut fibers from the company KO-SI, which represent industrial waste for which the company is looking for innovative solutions for use and applications in various products. We also received the company's waste packing belts made of polypropylene. For proper bonding, we used the compatibilizer PP-g-MAH (Graftabond 02025A CA). Two versions of the composite material were produced, in the first we used 20 wt.% waste coconut fibers in combination with the addition of 5 wt.% compatibilizer PP-g-MAH (Graftabond 02025A CA) and 75 wt.% rPP. We also produced a version of the material, where we used 30 wt.% waste coconut fibers with the addition of 5 wt.% compatibilizer PP-g-MAH (Graftabond 02025A CA) and 65 wt.% rPP (Table 1).

Table 1: Basic material characteristics of the used invasive plants for packaging

Sample	***rPP (wt.%)***	***Coconut fiber (wt.%)***	***PP-g-MAH (wt.%)***
0	*100*	*/*	*/*
1	*75*	*20*	*5*
2	*65*	*30*	*5*

Before compounding, the coconut waste fibers were grinded and than dried to a moisture content below 0.1 wt.%. After compounding, the biocomposite was also dried to a moisture content below 0.1 wt.%. All samples were first compounded on a Labtech LTE 20-44 twin-screw extruder. The screw diameter was 20 mm, the L/D ratio was 44:1, the screw speed was 300 min^{-1}, and the barrel temperature ranged from 165 °C at the inlet to 190 °C at the nozzle. The nozzle had two 4 mm diameter openings. The filaments were fed through a water bath (15 °C) into a Scheer granulator, where the filaments were cut to a length of about 5 mm. All three samples were extruded and granulated into pellets.

Using a press, we produced sheets for thermoforming. The samples were prepared with a Baopin BP-8170-B press. Before thermoforming, the material was evenly distributed between the metal plates. The composite material was then inserted into the heated press with the plates. The temperature of the upper and lower heating plates of the press was 185 °C. First, a profile with a lower pre-pressing pressure of 0.25 MPa was used, which lasted 90 s. The pressure was then increased to 2 MPa for 60 s. This was followed by cooling the heating plates to a plate temperature of 60 °C, after which the press

opened. The composite sheet was then left between two metal plates until it cooled. Figure 1 shows the used materials and the produced products.

Figure 1: PP packing belts (top left), waste coconut fiber (top middle), biocomposite granulate with 20 wt.% waste coconut fiber (top right), samples cut from the sheet used for laboratory tests (bottom left) and composite sheet (bottom right)

2.2 Laboratory tests

The tensile test was performed on a Shimadzu AG-X plus 10 kN tensile testing machine. This was performed in accordance with ISO 527. The distance between the clapming assembley was 115 mm, the testing speed to 0.25 % elongation was 1 mm/min, and above 0.25 % was 50 mm/min.

Thermogravimetric analysis (TGA) was performed on a Perkin Elmer TGA 4000 instrument. The sample was heated from 40 °C to 550 °C, with a heating rate of 10 °C/min, in a nitrogen atmosphere (20 mL/min), and then held isothermally at 550 °C for 5 min in an oxygen atmosphere (20 mL/min).

Differential scanning calorimetry (DSC) was performed on a Mettler Toledo DSC 2 calorimeter according to ISO 11357. The heating and cooling rate was 10 °C/min. The samples were heated from -50 °C to 200 °C, followed by an isothermal segment at 200 °C for 5 min. They were then cooled from 200 °C to - 50 °C, followed by an isothermal segment at - 50 °C for 5 min. Then all steps were repeated once more.

2.3 Procedure of making pots for hydroponics

We used Siemens NX 12 CAD program to model the pot and the tool. First, we drew a 3D model of a pot suitable for growing plants with hydroponics. This was followed by the construction of a thermoforming tool based on the pot. Different versions of the tool were also prepared. These versions of the thermoforming tools were printed using FFF 3D printing technology, using polyethylene terephthalate glycol (PETG) manufactured by Plastika Trček. For 3D printing, we used a Tumaker Bigfoot 500 Pro Dual 3D printer. Thermoforming was done with FormBox FBA 180123EU. Prepared composite sheets were clamped into the thermoforming machine and heated up. The thermoforming tool was then inserted into the thermoforming machine. With the assistance of vacuum, sheets were thermoformed into pots. Based on the thermoforming results the optimal tool and optimal material version were used to produce a larger quantity of hydroponic pots. We could not produce pots with material sample 2, due to the higher content of coconut fibers that resulted in processing issues because of the brittleness of produced sheets. Therefore, measurements were made only on samples 0 and 1.

3 RESULTS AND DISCUSSION

Laboratory tests were performed on a version of the material that proved to be more suitable for thermoforming (sample 1). The use of waste coconut fibers in combination with a compatibilizer in the rPP matrix in sample 1 increases the tensile E modulus (E). From Figure 2, the tensile strength (σ_m) is slightly reduced compared to the tensile strength of rPP (sample 0). The elongation at tensile strength (ε_m) and the elongation at break (ε_b) are significantly reduced (Figure 3).

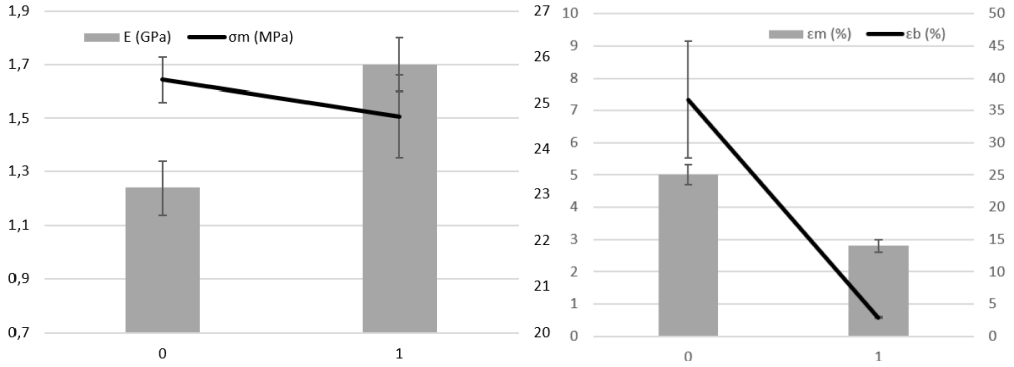

Figure 2: Tensile E-modulus and tensile strength (left figure) and elongation at tensile strength and elongation at break (right figure)

As a result of good interfacial interactions between waste coconut fibers and rPP due to the compatibilizer PP-g-MA, we can observe an increase in tensile stiffness by 68 wt.%. We can also observe a decrease in tensile strength by 6 wt.%, which can be concluded that this occurs because the length of coconut fibers is smaller than the critical length of coconut fibers. We can also observe that the standard deviation of the tensile strength of sample 1 increases to the extent that it is in the range of the tensile strength of sample 0. We can conclude that PP-g-MA is a good compatibilizer, since the tensile stiffness increases significantly, but due to the smaller length of coconut fibers, a slightly lower tensile strength can be observed.

TGA analysis shows a one-step decomposition of the sample. From Table 2, we can see that the composite with added waste coconut fibers undergoes a two-step decomposition. The first decomposition at a lower temperature is the decomposition of the coconut fibers in composite, the second at a higher temperature is the decomposition of the rPP matrix with additives, compared to sample 0 we can see that sample 1 has a higher degradation temperature of matrix, which may be a result of a higher degree of crystallinity due to the addition of coconut fibers. We can also observe 6.8 wt.% inorganic fillers, which are a result of mineral substances in natural fibers (Table 2).

Table 2: TGA analysis results

Sample	***T_{d1} (°C)***	***T_{d1} (°C)***	***Residue (wt.%)***
0	*/*	*437.7*	*0.00*
1	*337.8*	*464.4*	*6.83*

The addition of waste coconut fibers does not affect the melting point of the rPP biocomposite. The glass transition is at -11.9 °C, the melting point is at 166 °C. From Table 3, the glass transition temperature is slightly reduced due to the added coconut fibers, which act as nucleation agent and enable a higher degree of crystallinity to be achieved.

Table 3: DSC analysis results

Sample	***T_g (°C)***	***T_c (°C)***	***ΔH_c (J/g)***	***T_m (°C)***	***ΔH_m (J/g)***	***X_c (%)***
0	*-3.9*	*123.8*	*58.46*	*165.7*	*64.33*	*31*
1	*-11.9*	*125.4*	*49.09*	*166.0*	*55.60*	*38*

In Figure 4, we can see a cross-section of the pot model based on this geometry.

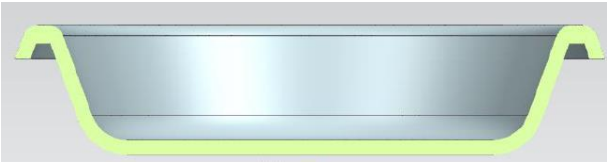

Figure 4: Cross-section of the crucible model

In the model of the pot itself, we considered the direction of thermoforming, we also tried to avoid sudden changes in the geometry in the thermoforming direction of the composite sheet. That is why on the model we can see an angle of 110 ° and a radius of 7 mm in the inner part of the pot. Based on this geometry of the pot the first version of the thermoforming tool was modeled (Figure 5). First a male version of the tool was modeled to produce a greater thickness in the middle of the product. For the usage of vacuum during termoformig small holes with a diameter of 1 mm in the direction of transformation were implemented.

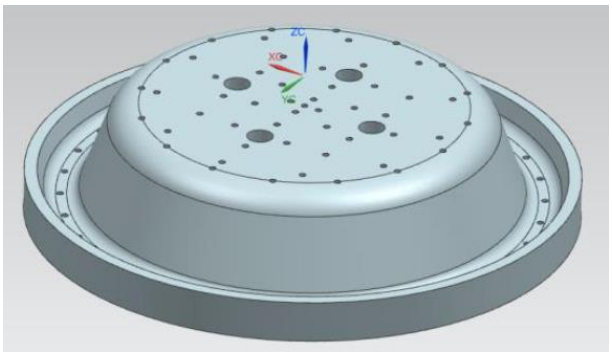

Figure 5: Male version of the cup thermoforming tool

Because of the localized sagging during heating we decided to model a second female version of the tool. We also considered the less efficient vacuum application from the first version. For this reason, holes with initial diameter of 2 mm were made. The diameter was then reduced to 1 mm in the last 3 mm of the hole length. To produce this part easier with printing, a 3 mm chamfer was used in the transition of the hole from 2 mm to 1 mm (Figure 6).

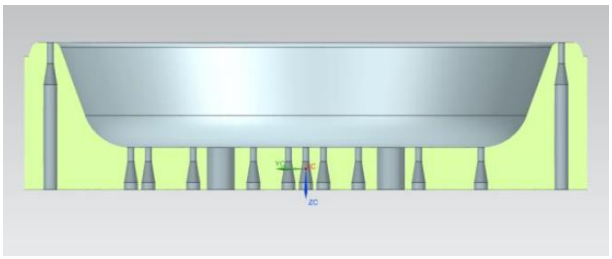

Figure 6: Male version of the cup thermoforming tool

It turned out that the change in shape had a significant impact on the quality of the pots produced. The final female version of the tool can be seen in Figure 7.

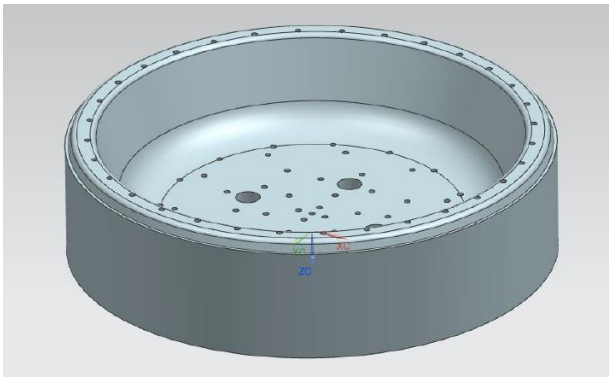

Figure 7: Female version of the cup thermoforming tool

4 CONCLUSIONS

As part of the research, we tested a biocomposite prepared from rPP, waste coconut fibers and with the addition of the compatibilizer PP-g-MA. The stiffness of the biocomposite with waste coconut fibers and PP-g-MA is significantly higher compared to rPP. The strength of the biocomposite with waste coconut fibers and PP-g-MA is slightly lower compared to rPP, this could be due to the length of the used coconut fibers, which might be shorter than the critical length of coconut fibers. The higher stiffness and slightly lower strength confirm good interactions between the components of the biocomposite due to the compatibilizer PP-g-MA. The thermal stability of biocomposite with waste coconut fibers is higher compared to rPP. The melting point and crystallization temperature of biocomposites with waste coconut fibers do not change compared to rPP. The degree of crystallinity of biocomposites is higher compared to rPP. The glass transition temperature is in the case of biocomposite shifts to a slightly lower temperature, which is because of higher degree of crystallinity of the biocomposite. The higher degree of crystallinity occurs due to coconut fibers in the matrix, which act as nucleating agents. This also improved mechanical and thermal properties of the biocomposite.

As part of the research, we also developed the optimal shape of the pot and, based on the product and properties of the composite material, the shape of the tool. This shape enables easier production of pots for growing plants with hydroponics. In addition, we managed to prepare a material from waste materials with the help of an appropriate compatibilizer that can be transformed into a functional product. As part of the study, we also demonstrated the use of FFF technology for the rapid production of prototype tools (Figure 8).

Figure 8: Male version of the tool (top right), female version of the tool (top left), and pot for growing plants with hydroponics (bottom middle)

5 REFERENCES

Di Bella, G., Fiore, V., and Alavanza, A., Natural Fibre Reinforced Composites, Chapter 2, 2012. https://www.researchgate.net/publication/233991603.

Ragaert, K., Delva, L., Van Geem, K.: Mechanical and chemical recycling of solid plastic waste. Waste Management. 2017; 69: 24–58.

Zhidan, L., Chao, C., Zixian, G., Shaozao, T., Xiuju, Z.: A Compatibilized Composite of Recycled Polypropylene Filled with Cellulosic Fiber from Recycled Corrugated Paper Board: Mechanical Properties, Morphology, and Thermal Behavior, Journal of Applied Polymer Science, Vol. 122 (2011) No.4, pp. 2789-2797.

FORMULATION AND ENVIRONMENTAL IMPACT EVALUATION OF SUSTAINABLE PHBV/PBAT/RICE STRAW COMPOSITES

Laura Andrea Cabrera-Villamizar[1], Eugenia Núñez[1], Erlantz Lizundia[2], Amparo López-Rubio[1], María José Fabra[1]

[1]Food Safety and Preservation Department, Institute of Agrochemistry and Food Technology (IATA-CSIC), Carrer del Catedràtic Agustín Escardino Benlloch, Spain
[2]Life Cycle Thinking Group, Department of Graphic Design and Engineering Projects, Faculty of Engineering in Bilbao. University of the Basque Country (UPV/EHU), Bilbao, Spain. BCMaterials, Basque Center for Materials, Applications and Nanostructures, UPV/EHU Science Park, Leioa, Spain.

doi: 10.5281/zenodo.17302158
la.cabrera10@iata.csic.es

Abstract: *As an alternative to conventional plastics, the formulation of biopolymeric composites, including biomass fillers, has gained attention in recent years (Phiri et al., 2023). This study focuses on formulating and characterizing biopolymeric composites, incorporating fillers obtained from residual biomasses as a potentially sustainable alternative to conventional plastics. Specifically, it showed novel composite materials that utilize rice straw (RS) as a filler in blends of poly(3-hydroxybutyrate-co-3-valerate) (PHBV) and polybutylene adipate terephthalate (PBAT). In addition to evaluating the physicochemical properties of these composites, the environmental impact (disintegration in soil, biodegradability, and life-cycle assessment (LCA)) was evaluated, contributing to the advancement of sustainable materials in the circular packaging sector. The research addresses the increasing demand for eco-friendly packaging solutions by exploring the use of agricultural waste as a functional filler in biopolymer composites.*

Composites were prepared by melt compounding followed by compression molding, with variations in PHBV:PBAT ratios (80:20, 50:50 and 20:80), RS particle size ($\leqslant$ 250 µm and $\leqslant$ 500 µm), and RS concentration (20, 30, and 40%). The resulting materials were physicochemically characterized, showing that the polymer ratio and the RS concentration influenced the mechanical properties of the composites. In addition, the RS content results in significant color changes when using different particle sizes. FTIR analysis indicated that RS incorporation did not alter the chemical structure of the base polymers, suggesting a physical dispersion of the filler without forming new chemical interactions.

Thermal analysis (TGA and DSC) showed that RS incorporation generally decreased the thermal stability while the crystallization behavior was altered. Microstructural analysis revealed varying RS dispersion depending on the PHBV:PBAT ratio, with the 50:50 blend exhibiting a porous structure and poor dispersion. The water vapor permeability of the composites increased significantly in the 50:50 blend with the RS addition.

Biodegradability assessments included disintegration tests and biodegradation tests under industrial composting conditions. Only the 80:20 blends met ISO 20200:2016 standards for disintegration. Interestingly, biodegradation tests revealed lower biodegradation percentages for RS-containing 80:20 blends than the control. This discrepancy highlights the complex influence of environmental conditions and microbial communities on the degradation of RS-incorporated polymer blends. LCA was conducted to quantify the environmental impact of these novel materials. The cradle-to-grave analysis revealed a climate change potential for the composite films below the impact of commercial plastics based on fossil resources, underscoring the potential environmental benefits of these biodegradable composites.

This study highlights the potential of RS as a sustainable filler in biodegradable polymer composites for packaging applications. The results demonstrate that RS incorporation enhances mechanical properties while significantly reducing environmental impacts compared to conventional plastics. This research paves the way for valorizing agricultural waste in high-value applications, supporting circular economy principles, and promoting the transition to more sustainable packaging solutions.

REFERENCES

Phiri, R., Rangappa, S.M., Siengchin, S., Oladijo, O.P. and Dhakal, H.N., 2023. Development of sustainable biopolymer-based composites for lightweight applications from agricultural waste biomass: A review. Advanced Industrial and Engineering Polymer Research, 6(4), pp.436–450.

ELECTRONIC PACKAGING MOVEMENT SENSOR IN AN INTELLIGENT PACKAGING SYSTEM

Gojko Vladić[1], Marko Ađin[1], Nemanja Kašiković[1], Gordana Bošnjaković[1], Magdolna Pal[1]

[1]University of Novi Sad, Faculty of technical sciences, Novi Sad, Serbia

doi: 10.5281/zenodo.17302246
vladicg@uns.ac.rs

Abstract: *Intelligent packaging systems utilize technology to enhance traditional packaging functions, usually in order to enhance customer experience by improving quality, safety, and integrity during transit. One of the potential applications is to track the movement of packages along a supply chain by incorporating movement-sensing technologies, which can monitor the state of a package, the environment around it, and interactions between them. Packaging movement sensors are primarily used to track the physical movement of packages, providing real-time information about their location and conditions during transit. This paper presents the steps in the development and practical application of a packaging movement sensor based on commonly used electronic components. In contrast to drop/tip and tell sensors, an accelerometer-based sensor can actively detect and log movement and changes in position during transport as 3-axis data for later analysis, offering valuable information not only for the user's benefit but also for the improvement of the packaging design.*

Keywords: packaging, movement sensor, intelligent packaging, mishandling.

1 INTRODUCTION

The growing demand for enhanced product quality, safety, and consumer engagement has driven rapid advancements in the field of smart packaging. Unlike traditional packaging, which primarily serves a protective and informational role, smart packaging integrates innovative technologies that actively monitor, communicate, and sometimes even respond to changes in the product or its environment. Smart packaging can have a variety of features or uses, but overall, it has two categories, namely active packaging and intelligent packaging (Young et al., 2020). Active packaging interacts with the product/environment (e.g., moisture absorbers, oxygen scavengers), preventing the growth of pathogens and destructive microorganisms, preventing the transport of pollutants, and extending the shelf-life while preserving the safety and quality of the product. Intelligent packaging monitors, senses, and communicates information through electronic, mechanical, chemical, electrical, or online technologies (e.g., sensors, indicators, data tags) (Ozcan, 2020).

Intelligent packaging systems are focused on improving packaging functions in order to meet increasing regulatory requirements regarding waste reduction, safety, reliability, and also growing consumer demands. This aligns with the broader Industry 4.0 trends, where digitalization and sensor technologies are increasingly applied and integrated into product supply chains (Punia et al., 2023). In order to support all the requirements wide range of intelligent packaging technologies are being developed, such as time and temperature indicators, freshness sensors, movement sensors, and interactive digital labels.

Movement sensors have emerged as a promising solution for addressing specific packaging challenges related to product safety, authenticity, and logistics. The integration of movement sensors into

packaging enables the detection and recording of physical handling events, including shocks, vibrations, tilting, and unauthorized opening. Such functionality is particularly relevant for sensitive products like pharmaceuticals, perishable foods, and high-value consumer goods, where inappropriate handling can lead to quality degradation, reduced efficacy, or economic losses.

Applications for movement-sensor-based packaging extend beyond product protection. They provide valuable data for logistics optimization, supply chain transparency, and consumer trust. For example, by recording irregular handling during transportation, stakeholders can identify weak points in distribution networks, enforce accountability, and enhance overall efficiency. Furthermore, consumers benefit from real-time access to information regarding the handling history of products, which strengthens confidence in brand integrity and safety (Osmólska et al., 2022).

Adoption of movement sensors in packaging still faces challenges, including cost-efficiency, sensor miniaturization, energy consumption, and integration with existing supply chain systems. Ongoing research therefore focuses on the development of low-power sensor platforms, wireless data transmission, and smart materials that can seamlessly incorporate sensing elements.

1.1. Overview of movement sensors applicable in intelligent packaging

Movement sensors applicable in intelligent packaging can be divided into two groups: electronic movement sensors and analog movement sensors. Electronic sensors are digital/semiconductor-based and allow direct data logging, integration with microcontrollers or wireless modules. They offer precision, miniaturization, and connectivity options. In practice, electronic sensors are used in high-value goods packaging (pharmaceuticals, electronics, and luxury items) because of their relatively high price per unit (Unander, 2011).

Electronic movement sensors can be grouped by their construction into:

- accelerometers (3-axis MEMS digital accelerometer),
- gyroscopes (MEMS gyroscope for measuring angular velocity),
- inertial measurement units (combines 3-axis accelerometer and 3-axis gyroscope, 9-axis IMU with built-in sensor fusion),
- vibration sensors (piezoelectric vibration sensors, MEMS vibration sensors), and
- tilt/orientation sensors (MEMS tilt sensors, capacitive inclination sensors).

Analog movement sensors are simpler, can be passive, and respond to physical motion without requiring digital processing. They are lower-cost compared to the electronic sensors and are more common in low-cost logistics packaging. Less precise and most often indicate one time movement over certain threshold, their design prioritizes simplicity and disposability more than data logging.

Analog movement sensors can be grouped by … into:

- mercury tilt switches (obsolete in most applications due to toxicity),
- ball tilt sensors (contain a small conductive ball that rolls inside a cylinder, making or breaking an electrical connection),
- spring vibration/shock sensors (small springs inside a casing that close a circuit when jolted),
- piezoelectric discs (generate voltage in response to vibration or bending), and

- mechanical impact indicators (purely mechanical, irreversible color-changing labels that indicate when a package has been dropped, mishandled or tilted beyond a set angle).

Table 1: Comparison of motion sensors for Intelligent Packaging

Sensor Type	***Precision***	***Cost***	***Power Requirement***	***Suitability for Packaging***
MEMS Accelerometer	*High*	*Medium*	*Low*	*Best for active monitoring*
Gyroscope	*Very High*	*Higher*	*Medium*	*Advanced applications*
Piezoelectric Vibration	*Medium*	*Low*	*Passive or low*	*Good for shock detection*
Ball Tilt Sensor	*Very Low*	*Very Low*	*Passive*	*Simple tilt/tamper detection*
Mechanical Shock/Tilt Indicators	*Low*	*Very Low*	*Passive*	*One-time-use, low-cost*

This paper aims to contribute to a deeper understanding of how electronic movement-sensing technologies can enhance packaging functionality and support sustainable, transparent, and consumer-centric supply chains. Development of the motion sensor prototype, applicable mainly to high-value consumer goods, was used in order to explore the role of movement sensors in intelligent packaging, emphasizing their principles of operation, potential applications across industries, and the challenges that must be overcome for widespread implementation. In this context, the present study explores the application of movement sensors in intelligent packaging, with particular emphasis on the use of the ADXL345 accelerometer as a practical and cost-effective solution.

2 MATERIALS AND METHODS

The intelligent packaging prototype was developed using the common low cost electronic components. Movement sensor selected for this study was ADXL345 Accelerometer, as it is a small, low-power, three-axis digital accelerometer capable of measuring acceleration in the range of ±2 g to ±16 g. It provides high-resolution (13-bit) output data and is optimized for applications where low power consumption and high sensitivity are required. Its digital output is available via both I^2C and SPI interfaces, making it suitable for integration with a wide range of microcontrollers and wireless modules. ESP32 CH340C with USB-C Microcontroller unit for data acquisition and processing. WROOM-32 Wireless communication module (Bluetooth or Wi-Fi) for transmitting sensor data to an external device. Power source (lithium polymer battery 602040, 500 mAh) optimized for low-energy operation with TP4056 constant-current/constant-voltage linear charger. Casing (custom 3D printed PLA polymer container) in which the sensor unit was embedded.

System Architecture:

• accelerometer ADXL345,

• microcontroller unit ESP32 CH340C,

• wireless communication module WROOM-32, and

• power source (602040, 500 mAh) & TP4056.

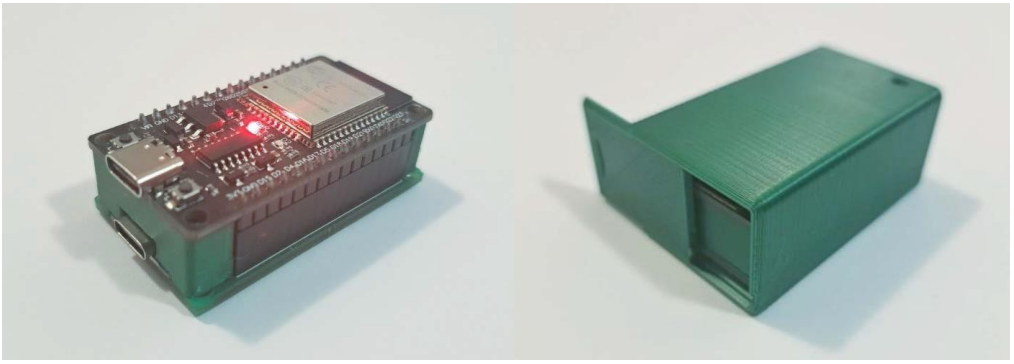

Figure 1: Final assembly of the packaging motion sensor prototype

Sensor ADXL345 was mounted on a small, printed circuit board via a pin header for added modularity and placed in the 3D printed casing, which was fixed to the packaging inner wall. Initial calibration was performed to establish baseline acceleration values when the package was at rest. Data acquisition was done by MCU, which collected real-time data from the accelerometer at a sampling rate of 100 Hz. Motion data were transmitted wirelessly to a central monitoring unit using Serial Bluetooth Terminal software by Kai Morich, the collected data, as shown in Figure 2, was transferred to the PC for further analysis using Microsoft Excel.

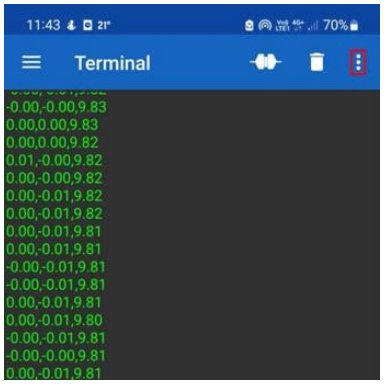

Figure 2. Raw data transferred from the device

3 RESULTS AND DISCUSSION

Collected data was analyzed to assess the frequency and intensity of movement during transportation. Threshold-based algorithms were implemented to identify abnormal events such as impacts (a sharp spike in acceleration magnitude, 2-3 g above gravity, spike duration less than 100 ms to distinguish from longer), drops (free fall net acceleration ≈ 0 g, followed by a sudden impact spike, within a 200 ms), there was possibility for detection of prolonged vibrations (repetitive oscillations around gravity) but it was not tested. In order to capture overall motion and reduce orientation dependency, vector magnitude can be calculated. To reduce false positives minimum time separation between events was required and axis dominance was monitored. Figure 3 shows three independent identified drop events where the vertical Z-axis is represented by green color. Noticeable changes in vertical direction are present as expected in the drop scenario. Significantly less movement is detected in X and Y directions as they represent the initial shock and stabilization of the packaging after the fall.

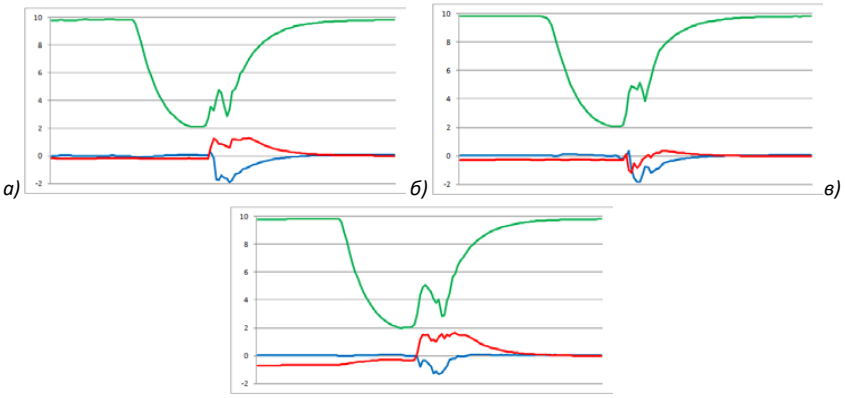

Figure 3. Three drop events where vertical Z-axis is green, X-axis is blue and Y-axis is red

The results from the test where the packaging was dropped from approximately the same height three times, shown in Figure 4, indicate that three lines representing the Z-axis are similar, inferring repeatability of measurements.

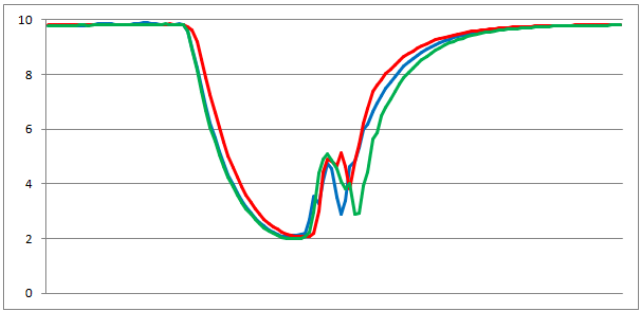

Figure 4. Comparison of Z-axis measurements for three similar drops

The results from the prototype system demonstrate that the ADXL345 accelerometer is capable of effectively detecting and quantifying movement events within intelligent packaging applications, and the selectable measurement ranges provided flexibility for monitoring.

One of the major advantages of the ADXL345 is its low power consumption, which extends battery life and makes it suitable for long-duration shipments. This could be further enhanced with additional modularity of the system regarding the memory and battery capacity. The digital communication interface simplifies communication with microcontrollers and wireless modules, facilitating the development of cost-effective solutions, especially in the case of multi-use packaging.

However, several potential limitations were observed. Battery capacity remains a challenge, especially for extended monitoring in global supply chains, shipping first and foremost. Threshold-based algorithms are efficient in experimental conditions. With additional machine learning techniques, they may be able to capture complex handling patterns far more efficiently. The reliability of wireless communication may decrease in environments with significant electromagnetic interference, so reliable internal data storage may be needed as backup, which can be a problem for extended monitoring.

Despite these challenges, the integration of electronic movement sensors into intelligent packaging provides a significant improvement in mishandling diagnostics over analog movement sensors and traditional passive packaging. By enabling real-time packaging monitoring and data logging, researchers could provide valuable information for the packaging designers alongside ensuring enhanced transparency, accountability, and trust in the supply chain.

4 CONCLUSIONS

This study demonstrates the feasibility and potential of using the ADXL345 accelerometer as a core component of intelligent packaging solutions. The sensor enables accurate monitoring of product handling through wireless data communication for remote supervision. These features make intelligent packaging with movement sensors a promising tool for industries where product integrity and safety are critical, as well as provide valuable information for packaging designers to improve product protection features of the packaging. Future work should focus on integrating machine learning algorithms for advanced event classification and scaling the system for industrial deployment.

Acknowledgments: *This research has been supported by the Ministry of Science, Technological Development and Innovation through Contract No. 451-03-136/2025- 03/200156.*

5 REFERENCES

Impactograph (2025) How Impact Sensor Technology and Shock Data Loggers Prevent Shipping Damage, https://impactograph.com/how-impact-sensor-technology-and-shock-data-loggers-prevent-shipping-damage, Accessed on 15.08.2025.

Osmólska, E., Stoma, M., Starek-Wójcicka, A. (2022) Application of Biosensors, Sensors, and Tags in Intelligent Packaging Used for Food Products—A Review. Sensors, 22, 9956.

Ozcan A., (2020) New approaches in smart packaging technologies, 10th International Symposium on Graphic Engineering and Design GRID 2020, pp. 21-37.

Punia Bungar S., Sharma N., Trif M. and Adeel M. (2023) Editorial: Emerging active, smart and intelligent packaging solutions in the fourth phase of the industrial revolution (Industry 4.0). Front. Nutr. 10.

Theengineeringprojects (2025) ADXL345 3-Axis Digital Accelerometer https://www.theengineeringprojects.com/2025/02/adxl345-3-axis-digital-accelerometer.html Accessed on 15.08.2025.

Unander, T., (2011) System integration of electronic functionality in packaging application, https://www.diva-portal.org/smash/get/diva2:434473/FULLTEXT01.pdf, Accessed on 15.08.2025.

Young, E., Mirosa, M., Bremer, P. (2020) A Systematic Review of Consumer Perceptions of Smart Packaging Technologies for Food. Front. Sustain. Food Syst. 4.

BE-UP: EU-FUNDED PROJECT TO DRIVE INNOVATION IN SUSTAINABLE PACKAGING

Irena Pulko[1], Kaja Kupnik[1], Patricija Skrivarnik[1]

[1]Faculty of Polymer Technology, Slovenj Gradec, Slovenia

doi: 10.5281/zenodo.17347216
irena.pulko@ftpo.eu

Abstract: *The Be-UP project, funded by the Horizon Europe programme, represents a step forward in the pursuit of a more sustainable future for the packaging industry. By uniting 17 partners from 9 countries, the project's main objective is to accelerate the industrial uptake of biodegradable polymers across Europe. Officially launched on May 1st, 2025, and coordinated by the Spanish technology centre ITENE, the project focuses on developing innovative aliphatic-aromatic biopolyesters with a high content of renewable raw materials, thereby directly contributing to the goals of the European Green Deal. At the core of the Be-UP project is the development of new synthesis and processing methods for biopolymers. This includes the use of bio-based building blocks in combination with advanced catalysts and additives. A key role is played by advanced digital modelling tools, such as the Kinetic Monte Carlo (kMC) method, which enable the optimization of synthesis and polymerization processes. The resulting biopolyesters will be blended with established commercial biopolymers like PLA, PBAT, and PHA, as well as bio-based chain extenders and mineral fillers. Through advanced techniques such as innovative screw design and inline rheology measurements, the Be-UP project will strive to create high-performance bioplastic materials that meet specific technical, sustainability, and biodegradability targets. The project places special emphasis on transferring its results into industrial practice, focusing on key processes in the packaging industry, namely blown film extrusion, injection moulding, and thermoforming. Packaging product prototypes, such as films, containers, and closures, will be manufactured to a Technology Readiness Level of TRL7. These prototypes will serve to validate the developed materials under real-world conditions. A crucial part of the project is the assessment of the materials' biodegradability in various end-of-life scenarios, including open environments and controlled conditions. The findings from these tests will be essential for understanding the materials' behaviour beyond standard laboratory testing. The main expected outcomes of the Be-UP project include guidelines and tools for circular design based on the Safe and Sustainable by Design (SSbD) framework; evidence-based improvements to the regulatory framework for testing and labelling packaging materials; and the development of circular business models for the industrial-scale production of bio-based and biodegradable packaging materials. Ultimately, the Be-UP project will make a concrete contribution to the implementation of several key European strategies and directives, including the Plastics Strategy, the Single-Use Plastics Directive, the Circular Economy Action Plan, and the Packaging and Packaging Waste Regulation. By developing innovative, sustainable, and competitive solutions, Be-UP is laying the groundwork for a greener and more circular future for the European packaging industry.*

Keywords: biopolyester, PLA, PBAT, PHA, packaging

DS Smith

Redefining Packaging for a Changing World

Packaging is more than just a box.
It's our vision for a better world.

www.dssmith.com/sl